Thermal-Hydraulics in Nuclear Systems

Henryk Anglart

Thermal-Hydraulics in Nuclear Systems

This textbook is intended to be an introduction to selected thermal-hydraulic topics for students of nuclear engineering and applied sciences as well as for professionals working in the nuclear engineering field. The basic aspects of thermal-hydraulics in nuclear systems are presented with a goal to demonstrate how to solve practical problems. This 'hands-on' approach is supported with numerous examples and exercises provided throughout the book. In addition, the book is accompanied with computational software, implemented in the Scilab (www.scilab.org) environment. The software is available for downloading at www.sh2701.blogspot.se and is shortly described in Appendices D and E.

I C O N K E Y	
🗁	Note Corner
✐	Examples
💻	Computer Program
📖	More Reading

The textbook is organized into five chapters dealing with rudiments of thermodynamics, fluid mechanics and heat transfer, as well as presenting selected applications related to nuclear power plants. Parts in the book of special interest are designed with dedicated icons, as indicated in the table above. The "Note Corner" icon indicates a section with additional relevant information, not directly related to the topics covered by the book, but which could be of interest to the reader. All examples are marked with a pencil icon. Special icons are also used to mark sections containing computer programs and suggesting additional literature to the reader.

The first chapter describes general thermal-hydraulic processes taking place in nuclear systems. In particular, various sources of thermal energy and their distributions in nuclear reactor cores are discussed. The second chapter contains an introduction to thermodynamics, covered at the level which is necessary to understand the material presented in Chapter 3 (fluid mechanics) and Chapter 4 (heat transfer). The chapter can be omitted by readers who are acquainted with thermodynamics at the level typical for technical universities. The last chapter contains analyses of several applications of practical concern such as critical flows of gases, critical flows of two-phase mixtures, as well as fluid-structure interactions, including the waterhammer phenomenon. The last section is devoted to analyses of selected plant components.

CONTENTS

1. Introduction

T he energy released in nuclear fission reactions has different forms, as indicated in TABLE 1.1. During the operation of a nuclear reactor, the energy is transformed from its primary form into the heat accumulated in the reactor fuel elements. Part of the energy is deposited outside of the nuclear fuel, or even lost from the reactor, due to radiation.

TABLE 1.1. Approximate distribution of energy per fission of ^{235}U.

	$pJ\ [10^{-12}\ J]^{1)}$	$MeV^{2)}$
Kinetic energy of fission products	26.9	168
Instantaneous gamma-ray energy	1.1	7
Kinetic energy of fission neutrons	0.8	5
Beta particles from fission products	1.1	7
Gamma-rays from fission products	1.0	6
Neutrinos	1.6	10
Total fission energy	32	200

[1)] pico-Joule, [2)] megaelectronvolt

The heat must be removed from the reactor core structure in the same rate as it is generated due to fissions to avoid the core damage. Usually the cooling of the reactor core is provided by forcing a working fluid – so called coolant – through it. The heat accumulated in the coolant is then used for various goals, according to the purpose of the nuclear reactor. In nuclear power reactors, the heat is transformed into electricity using the standard steam cycles. In nuclear propulsion reactors the heat is used to create the thrust. Whatever the purpose of the reactor is, various aspects of heat transfer and fluid flow are present. The branch of nuclear engineering which is dealing with these aspects is called the nuclear reactor thermal-hydraulics.

One of the major objectives of the reactor thermal-hydraulics is to predict the temperature distributions in various parts of the reactor. The most important part of the nuclear reactor is the reactor core, where heat is released and the highest temperatures are present. Such temperatures must be predicted for various reactor

operation conditions. To assure a safe reactor operation it is necessary that the temperatures are below specific limit values for various construction and fuel materials.

Another important objective of the reactor thermal-hydraulics is to predict forces exerted by the flowing coolant onto internal structures of the reactor. Too high or persistent oscillatory forces may cause mechanical failures of the structures. Thus, the thermal-hydraulic analysis provides information about the mechanical loads in the nuclear reactor, which in turn is used in the structure-mechanics analysis to investigate the system integrity. Very often such analyses have to include the effect of temperature distributions as well, especially when thermal stresses are significant.

Even though thermal-hydraulics analyses of nuclear reactors can be performed as stand-alone tasks, they are usually performed in a chain with other types of analyses, such as the reactor-physics analysis and the structure-mechanics analysis (FIGURE 1-1).
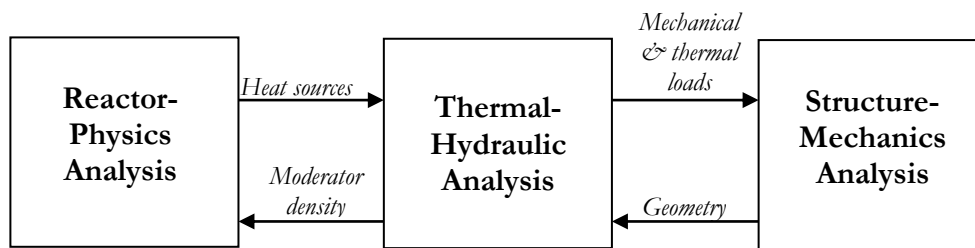
FIGURE 1-1. Thermal-hydraulics as a part of the nuclear reactor analysis chain.

As indicated in FIGURE 1-1, the thermal-hydraulic analysis provides input data (the moderator density and other nuclear data not specified here) to the reactor-physics analysis, whereas the latter gives information about the distribution of heat sources, which is needed to perform the thermal-hydraulic analysis. The strong coupling between the two types of analyses causes that iterative approaches have to be used. There is also a coupling between the thermal-hydraulic and structure-mechanics analyses; however, it is less strong. The mechanical and thermal loads obtained from the thermal-hydraulics analysis are used to predict the structure displacements and thus the actual geometry under consideration. Usually the displacements are small and can be neglected. Thus, the design geometry can be used while performing the thermal-hydraulics analysis.

The coupled analysis of nuclear reactors is a subject of the nuclear reactor design process and is beyond the scope of the present book. Instead, the goal of this book is to cover purely thermal-hydraulics topics. For that purpose, typical thermal-hydraulic processes taking place in nuclear reactors are considered. Such processes are shortly described in the following sections.

1.1 Thermal-Hydraulic Processes in Nuclear Reactors

The kinetic energy of fission products in nuclear reactors is eventually transformed into an enthalpy increase of the coolant. This transformation is realized in several

steps, as shown in FIGURE 1-2. The figure depicts thermal processes inside a nuclear reactor pressure vessel and is valid for a Boiling Water Reactor (BWR).

```
┌─────────────────┐    ┌─────────────────┐    ┌─────────────────┐
│ Release of       │    │ Conduction       │    │ Heat transfer    │
│ fission-          │──▶│ through fuel     │──▶│ across fuel-clad │
│ product energy in │    │ and radiation    │    │ gas gap          │
│ fissile material │    │                  │    │                  │
└─────────────────┘    └─────────────────┘    └─────────────────┘
                                                        │
                                                        ▼
┌─────────────────┐    ┌─────────────────┐    ┌─────────────────┐
│ Forced convection│    │ Heat transfer    │    │ Heat conduction  │
│ to coolant in fuel│◀─│ from clad to     │◀─│ across clad      │
│ assemblies       │    │ coolant          │    │                  │
└─────────────────┘    └─────────────────┘    └─────────────────┘
        │
        ▼
┌─────────────────┐    ┌─────────────────┐    ┌─────────────────┐
│ Steam generation │    │ Steam            │    │ Steam expansion  │
│ due to boiling   │──▶│ separation from  │──▶│ in turbine and   │
│                  │    │ moisture         │    │ performing work  │
└─────────────────┘    └─────────────────┘    └─────────────────┘
```
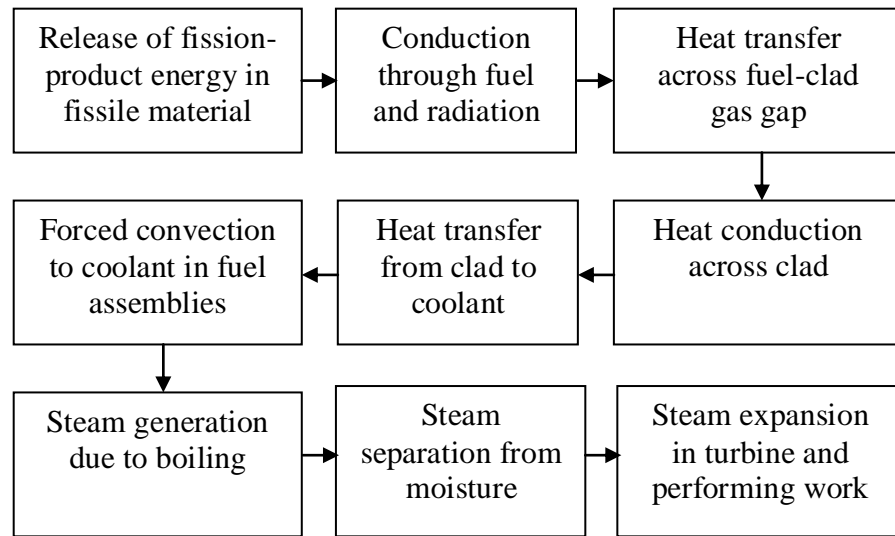
FIGURE 1-2. Thermal energy cycles in a BWR nuclear power plant.

The thermal energy is generated in the reactor core, where the coolant enthalpy increases due to heat transfer from the surface of fuel rods. In BWRs, the two-phase mixture that exits the core is separated into water and wet steam. The steam is further dried in steam dryers and finally exits through steam lines to turbines. After passing through turbines and condensing in a condenser, it turns into condensate and then feedwater which is pumped by the feedwater pumps back to the reactor pressure vessel. A schematic of a primary loop in a nuclear power plant with BWR is shown in FIGURE 1-3.
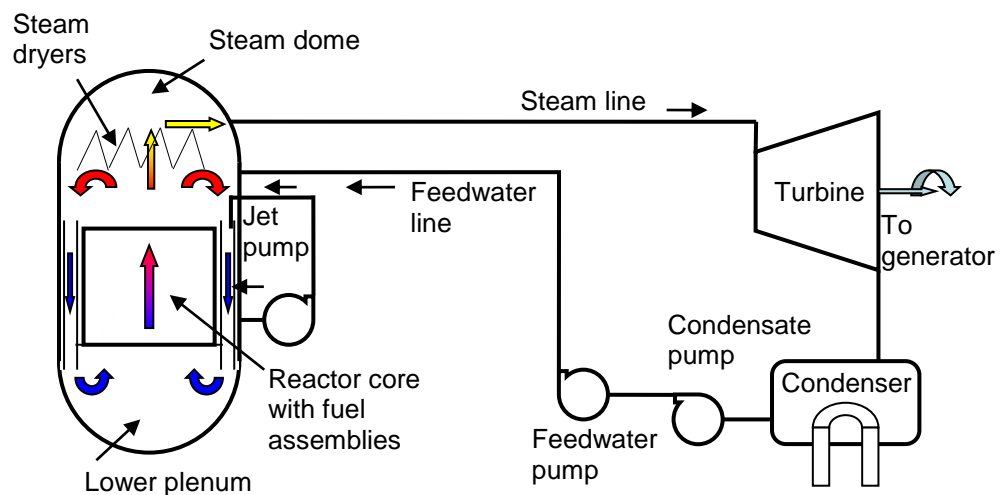
FIGURE 1-3. Schematic of the primary loop in nuclear power plant with BWR.

A nuclear power reactor is designed to generate heat that can be used to produce electricity, typically by way of an associated steam thermal cycle. One of the unusual features of nuclear reactors is that the rate of energy release can be very high. From the reactor-physics point of view, a nuclear reactor can operate at (almost) any power level.

The limit on the upper power level is determined by the properties of nuclear and construction materials and their capability to withstand high temperatures. Due to that the thermal-hydraulic analysis of nuclear reactors plays a very important role in the reactor core design. In fact, the design of nuclear reactor depends as much on thermal as on nuclear considerations. This is because the core must be designed in such a way that ensures a safe and economic production of the thermal power, which can be further used to generate electricity.

There are several existing reactor types in which heat transfer solutions depend on particular design concepts and on the choice of coolant. Although each reactor design has its own specific thermal-hydraulic issues, the solution of these issues can be approached in standard engineering manners that involve the fluid flow and heat transfer analyses. The effort to integrate the heat transfer and fluid mechanics principles to accomplish the desired rate of heat removal from the reactor fuel is the essence of the thermal-hydraulic design of a nuclear reactor.

An important difference between nuclear power plants and conventional power plants is that in the latter the temperature is limited to that resulting from combustion of fossil fuel, whereas it can increase continuously in a nuclear reactor in which the rate of heat removal is less than the rate of heat generation. Such situation could lead to serious core damages. This feature requires accommodation of safe and reliable systems that provide continuous and reliable cooling of nuclear reactor cores.

For a given reactor design, the maximum operating power is limited by the maximum allowable temperature in the system. There are several possible factors that will set the limit temperature (and thus the maximum reactor power) such as: property changes of some construction material in the reactor, allowable thermal stresses or influence of temperature on corrosion. Thus the maximum temperature in a nuclear reactor core must be definitely established under normal reactor operation and this is one of the goals of the thermal-hydraulic design and analysis of nuclear reactor cores.

In nuclear reactors the construction materials must be chosen not only on the basis of the thermo-mechanical performance, but also (and often exclusively) on the basis of the nuclear properties. Beryllium metal, for example, is an excellent material for use as moderator and reflector, but it is relatively brittle. Austenitic stainless steels are used as the cladding for fast reactor fuels, but they tend to swell as a result of exposure at high temperatures to fast neutrons.

Another peculiarity (and factor that adds problems) of nuclear reactors is that the power densities (e.g. power generated per unit volume) are very high. This is required by economic considerations, which lead to power densities of approximately 100 MWt/m^3 in PWRs and 55 MWt/m^3 in BWRs. A typical sodium-cooled commercial fast breeder reactor has a power density as high as 500 MWt/m^3. In conventional power plants the maximum power density is of the order of 10 MWt/m^3.

1.2 Power Generation in Nuclear Reactors

The energy released in nuclear fission reaction is distributed among a variety of reaction products characterized by different range and time delays (see TABLE 1.1). In thermal design of nuclear reactors, the energy deposition distributed over the coolant and structural materials is frequently reassigned to the fuel in order to simplify the

thermal analysis of the core. The volumetric fission heat source in the core can be found in a general case as,

$$(1\text{-}1) \qquad q'''(\mathbf{r}) = \sum_i w_f^{(i)} N_i(\mathbf{r}) \int_0^\infty dE \, \sigma_f^{(i)}(E) \phi(\mathbf{r}, E).$$

Here $w_f^{(i)}$ is the recoverable energy released per fission event of i-th fissile material, N_i is the number density of i-th fissile material, $\phi(\mathbf{r}, E)$ is the neutron flux, $\mathbf{r}$ is the spatial position vector and $\sigma_f^i(E)$ is its microscopic fission cross section for neutrons with energy E. Since the neutron flux and the number density of the fuel vary across the reactor core, there will be a corresponding variation in the fission heat source. Further details concerning Eq. (1-1) are provided in relevant reactor physics books[1-1] and are not discussed here. In the following, some special cases of heat transfer distribution in nuclear reactors are given.

The simplest model of fission heat distribution would correspond to a bare, cylindrical, homogeneous core (that is a reactor core without a reflector and consisting of a homogeneous mixture of fuel, moderator and construction materials). The one-group neutron flux distribution for such reactor is given as,

$$(1\text{-}2) \qquad \phi(r, z) = \phi_0 J_0\left(\frac{2.405r}{\tilde{R}}\right) \cos\left(\frac{\pi z}{\tilde{H}}\right),$$

and the corresponding heat source density with a single fuel type is given as,

$$(1\text{-}3) \qquad q'''(r, z) = w_f \Sigma_f \phi(r, z).$$

Here J_0 is the Bessel function of the first kind and zero order (see Appendix B), ϕ_0 is the neutron flux at the centre of the core, w_f is the recoverable energy released per fission, Σ_f is the macroscopic cross-section for the fission reaction and $\tilde{R}$ and $\tilde{H}$ are effective (extrapolated) core dimensions that include extrapolation lengths. In case of a reflected core (that is a core with a surrounding material that bounces the escaping neutron back to the core), this length includes an adjustment to account for a reflected core as well. Thus, the effective dimensions are as follows,

$$(1\text{-}4) \qquad \tilde{H} = H + 2d, \quad \tilde{R} = R + d,$$

where H and R are the physical dimensions of the cylindrical core and d is the extrapolation length, derived on the basis of the reactor-physics considerations. Expressions for spatial distributions of the volumetric heat source in nuclear reactors with various shapes are given in FIGURE 1-4. These expressions have been obtained from analytical solutions of equations for the neutron flux distributions in reactors without reflectors. Such equations can be used as first approximations for heat source distributions, however, the actual distributions may significantly deviate from the theoretical ones. This is mainly due to the presence of reflectors and due to non-homogeneity of the core material.

Cylindrical reactor

$$q'''(r,z) = q_0''' J_0\left(\frac{2.405r}{\tilde{R}}\right)\cos\left(\frac{\pi z}{\tilde{H}}\right)$$

Spherical reactor

$$q'''(r) = q_0'''\left(\frac{\tilde{R}}{\pi}\right)\frac{\sin\frac{\pi r}{\tilde{R}}}{r}$$

parallele-pipoidal reactor

$$q'''(x,y,z) = q_0'''\cos\left(\frac{\pi x}{\tilde{a}}\right)\cos\left(\frac{\pi y}{\tilde{b}}\right)\cos\left(\frac{\pi z}{\tilde{c}}\right)$$
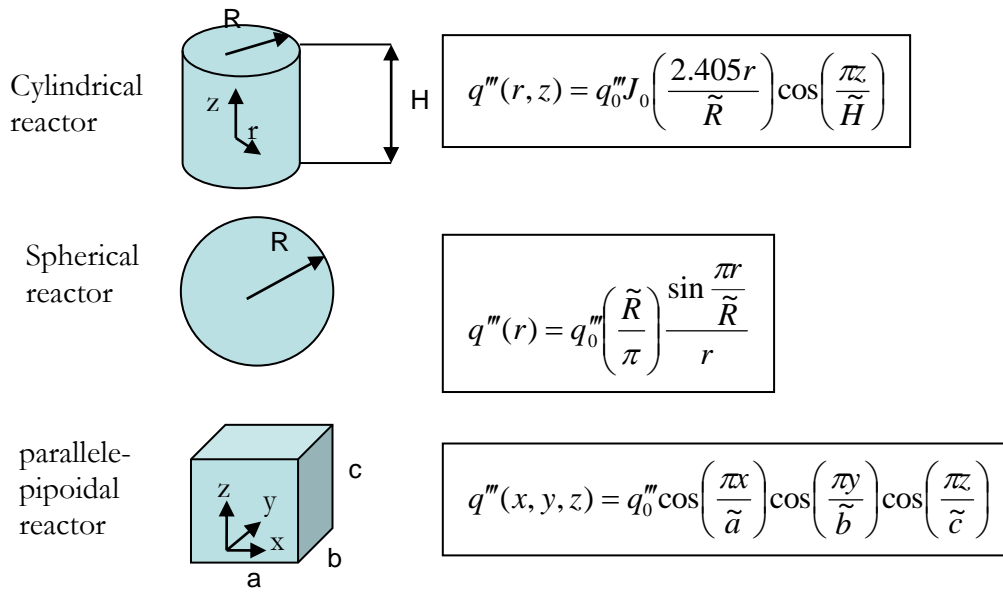
FIGURE 1-4. Spatial power distribution in reactors with various shapes.

Having a fuel rod located at $r = r_f$ distance from the centreline of a cylindrical core (see FIGURE 1-5), the volumetric fission heat source becomes a function of the axial coordinate, z, only,

$$(1\text{-}5)\qquad q'''(z) = w_f \Sigma_f \phi_0 J_0\left(\frac{2.405r_f}{\tilde{R}}\right)\cos\left(\frac{\pi z}{\tilde{H}}\right) = q_0''' J_0\left(\frac{2.405r_f}{\tilde{R}}\right)\cos\left(\frac{\pi z}{\tilde{H}}\right).$$
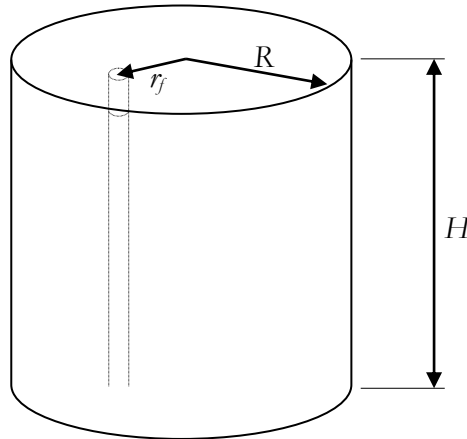
FIGURE 1-5. Cylindrical core with a fuel rod located at r_f distance from the centreline.

There are numerous factors that perturb the power distribution of the reactor core, and the above equations for the spatial power distributions will not be valid. For example the nuclear fuel is usually not loaded with a uniform enrichment in uranium 235. At the beginning of the fuel cycle, a high-enrichment fuel is loaded towards the edge of the core in order to flatten the power distribution. Other factors include the influence of the control rods and variation of the coolant density.

All these power perturbations will cause a corresponding variation of the temperature distribution in the core. A usual technique to take care of these variations is to estimate the local working conditions (power level, coolant flow, etc.) which are the closest to the thermal limitations. Such part of the core is called the **hot channel** and the working conditions are related with so-called **hot channel factors**.

One common approach to define the hot channel is to choose the channel where the core heat flux and the coolant enthalpy rise are at the maximum. Working conditions in the hot channel are defined by several ratios of local conditions to core-averaged conditions. These ratios, termed the hot channel factors or power peaking factors are discussed in more detail in the course of nuclear reactor technology. However, it should be mentioned here that the basic initial plant thermal design relay on these factors.
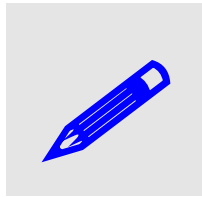
EXAMPLE 1-1. Calculate the power peaking factor for a cylindrical core.
SOLUTION: The power peaking factor is defined as,

$$f = \frac{q_0'''}{\overline{q'''}},$$

where the mean heat flux is found as,

$$\overline{q'''} = \frac{1}{\pi R^2 H} \int_0^R \int_{-\frac{H}{2}}^{\frac{H}{2}} q_0''' J_0\left(2.405\frac{r}{\tilde{R}}\right)\cos\frac{\pi z}{\tilde{H}} 2\pi r dr dz = \quad .$$

$$q_0''' \frac{1}{\pi R^2}\int_0^R J_0\left(2.405\frac{r}{\tilde{R}}\right)2\pi r dr \frac{1}{H}\int_{-\frac{H}{2}}^{\frac{H}{2}}\cos\frac{\pi z}{\tilde{H}} dz = \frac{q_0'''}{f_R f_H}$$

Here,

$$f_R = \frac{2.405R}{2\tilde{R}J_1\left(\dfrac{2.405R}{\tilde{R}}\right)}, \qquad f_H = \frac{\pi H}{2\tilde{H}\sin\left(\dfrac{\pi H}{2\tilde{H}}\right)};$$

where J_1 is the Bessel function of the first kind and the first order. The peaking factor is then obtained as,

$$f = f_R f_H.$$

As can be seen, the peaking factor depends on the ratio of the physical dimensions of the reactor to the extrapolated ones and it increases with increasing ratios. The maximum peaking factor is obtained when the extrapolated dimensions are equal to the physical ones (the ratios are then equal to 1) and is equal to $f = f_R * f_H = 2.32 * 1.57 = 3.64$.

In thermal reactors it can be assumed that 90% of the fission total energy is liberated in fuel elements, whereas the remaining 10% is equally distributed between moderator (which in LWRs is also a coolant) and reflector/shields. However, as already mentioned, as a first approximation, one can assign the whole energy to the fuel. With this assumption, more conservative (that is more pessimistic) results will be obtained in terms of the maximum fuel temperature, which is usually desirable in the preliminary reactor design stage.

R E F E R E N C E S

[1-1]   Duderstadt, J.J. and Hamilton, L.J. Nuclear Reactor Analysis, John Wiley & Sons, New York, 1979.

E X E R C I S E S

EXERCISE 1-1. A cylindrical core has the extrapolated height and extrapolated radius equal to 3.8 m and 3.1 m, respectively, and the extrapolation length is $d = 0.06$ m. Calculate the volumetric heat source ratio between the point located in the middle of the central fuel assembly and the point located in a fuel assembly with a distance $r_j = 1.9$ m from the core centre and at $z = 2.5$ m from the beginning of the heated length of the assembly.

EXERCISE 1-2. A cylindrical reactor core has physical dimensions $H = 3.65$ m and $R = 3.25$ m and the extrapolation length is $d = 0.05$ m. The total core power is 3000 MW. Calculate the ration of the local power density at the centre of the core to the mean-in-core power density.

EXERCISE 1-3. A reactor core with the same shape and dimensions as in EXERCISE 1-2 has to be divided into two radial zones with the same total power each. Calculate the dimensions of each of the zones.

EXERCISE 1-4. A fuel assembly with quadratic cross-section and side length 140 mm is located in a reactor core as shown in the figure below. The core has physical dimensions $H = 3.70$ m and $R = 3.30$ m and the extrapolation length is $d = 0.075$ m. The total core power is 3300 MW. Estimate the total power of the assembly. Discuss the approximation errors in the calculations.

1250 mm

Fuel assembly 140 mm x 140 mm
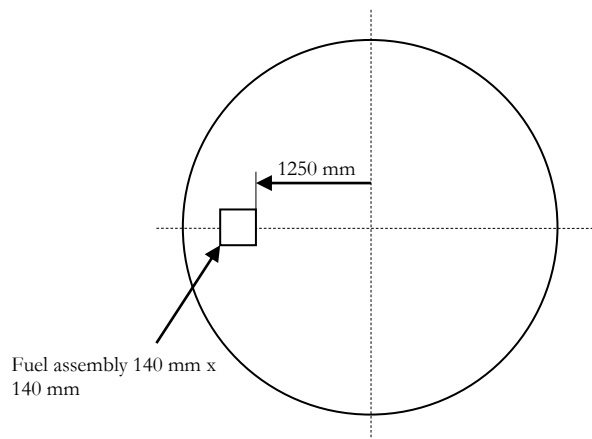
EXERCISE 1-5. A cylindrical core of a Gas Cooled Reactor (GCR) with total thermal power 300 MW and 1150 fuel assemblies has dimensions $R = 4.5$ m and $H = 9$ m. Assuming the extrapolation length $d = 0.55$ m, calculate: (a) the mean power density in the core, (b) the maximum power density in the core.

EXERCISE 1-6. A cylindrical core ($R=6.3$ m, $H=7.9$m) of a graphite-moderated gas-cooled reactor has the total thermal power equal to 700 MW, from which 95% is released in the fuel material contained in 2940 fuel assemblies. Assuming the extrapolation length $d = 0.52$ m, calculate: (a) the mean, the highest and the lowest power in fuel assemblies, (b) the power of the fuel assembly located at $r=R/2$ distance from the core centreline.

2. Thermodynamics

T
hermodynamics is a branch of engineering science that deals with the nature of heat and its transformations to other energy forms. A fundamental role in thermodynamics is played by so-called laws of thermodynamics, which have been formulated to reflect the empirical observations of processes where heat transformations are involved. In a macroscopic world, where all matter is treated as a continuum, the laws can be considered as axioms that constitute the rules according to which such equipment as turbines, compressors and heat exchangers operate. Their efficiency and performance can be then evaluated using such macroscopic quantities as volume, pressure and temperature. Thus, one of the most important objectives of this chapter is to give an introduction to thermodynamic laws and cycles, that are relevant to energy transformations in nuclear power plants. However, before going to the description of laws of thermodynamics and to analysis of thermodynamic cycles, some fundamental quantities, such as temperature and enthalpy, will be defined.

Temperature is a physical property that is probably best known from the everyday experience which says that something hotter has greater temperature. Temperature arises from the random microscopic motions of atoms in matter. Its SI unit is 1 K (Kelvin). Other temperature units still used in nuclear engineering are 1 °C (Celsius centigrade) and 1 °F (Fahrenheit). The temperature in different units is expressed as,

T [K] = t [°C] + 273.15,

t [°F] = 1.8 t [°C] + 32,

t [°C] = 5/9 (t [°F] – 32).

The **internal energy** E_I of a thermodynamic system is the total of the kinetic energy due to the motion of molecules and other types of energy related to the molecular structure of a system. It does not include the kinetic and potential energy of the system as a whole. Strictly speaking, the internal energy of a system cannot be precisely measured; however, the changes in the internal energy can be measured.

Entropy is a physical property that describes a thermodynamic system. It is often related to as a measure of disorder. Its symbol is S and SI unit is J K^{-1}.

The thermodynamic property – **enthalpy** - is the sum of the internal energy of a thermodynamic system and the energy associated with work done by the system on the surroundings which is the product of the pressure times the volume. Thus the enthalpy is given as,

(2-1) $I = E_I + pV$,

where I is the enthalpy [J], E_I is the internal energy [J], p is the pressure of the system [Pa] and V is the volume [m³].

All properties mentioned above and designed with capital letters are so-called **extensive properties** which values depend on the amount of the substance for which they are measured. If a property is expressed per unit mass, it becomes a so called **Intensive property**, that is $e_I = E_I / m$, $i = I/m$, $s = S/m$ are intensive properties and represent specific internal energy, specific enthalpy and specific entropy, respectively.

The state of thermodynamic systems is described by so-called **state variables**. State variables are single-valued, precisely measurable physical properties that characterize the state of a system. Examples of state variables are pressure p, volume V and temperature T.

2.1 Laws of Thermodynamics

There are four laws of thermodynamics. The numbering starts from zero, since the "zero-th law" was established long after the three others were in wide use.

2.1.1   Zero-th Law of Thermodynamics

The **zero-th law of thermodynamics** states that "if two thermodynamic systems are in thermal equilibrium with a third, they are also in thermal equilibrium with each other". With this formulation the zero-th law can be viewed as an equivalence relation. The zero-th law is visualized in FIGURE 2-1.
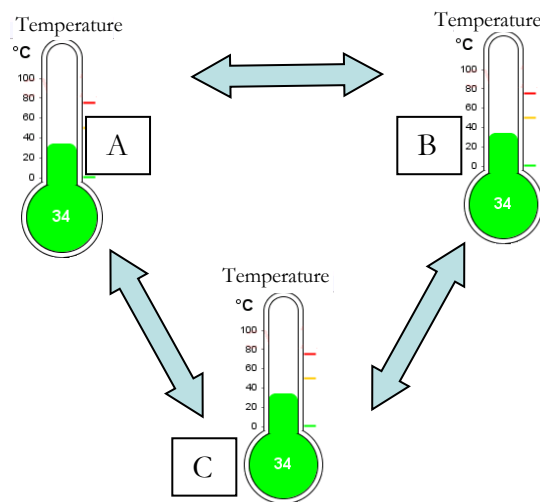
FIGURE 2-1. Zero-th law of thermodynamics. If systems *A* and *B* are in equilibrium with system *C*, then they are in equilibrium with each other.

Systems in equilibrium have the same temperature. If two systems with different temperatures are put into a thermal contact, heat flows from the hotter system to the colder one.

2.1.2   First Law of Thermodynamics

The **first law of thermodynamics** states that "the increase in the energy of a system is equal to the amount of energy added by heating the system, minus the amount lost as a result of work done by the system on its surroundings". Often the first law of thermodynamics is formulated as "the energy conservation law". It is expressed as,

(2-2) $\Delta E_I = Q - L$,

where Q is the heat added to the system, L is the work done by the system on its surroundings and ΔE_I is the change in the internal energy.

In the differential form, the first law of thermodynamics is written as,

(2-3) $dE_I = \delta Q - \delta L$,

where dE_I is the differential increase of the internal energy, δQ is the heat added to the system and δL is the work performed by the system on surroundings. Note that δ symbolizes here the inexact differential, since Q and L are not state functions and cannot be differentiated. The internal energy E_I is a state function and it can be differentiated. The picture shown in FIGURE 2-2 illustrates the fundamental difference between the internal energy and the energy in transit (heat and/or work).

Heat, δQ

System S_1 with internal energy E_I

Work, δL

System S_2 with internal energy $E_I + dE_I$
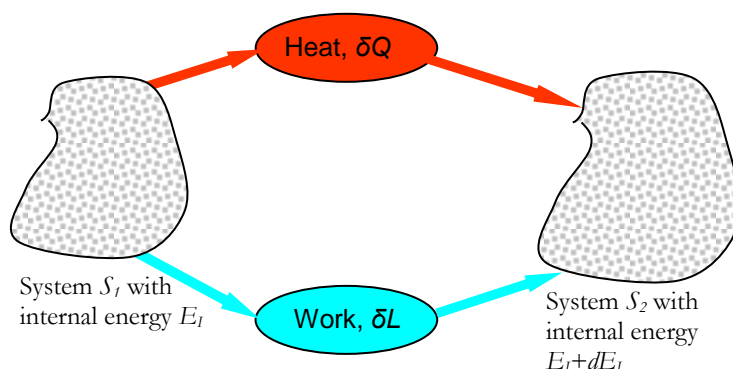
FIGURE 2-2. Relations between internal energy, heat and work.

The energy conservation principle can be expressed per unit mass of substance as,

(2-4) $\Delta e_I = \hat{Q} - l$,

where $\hat{Q}$ is the heat per unit mass. Work is such an energetic interaction between two closed systems that energy change of each of the systems can be totally used to change the potential energy of the system. A graphical representation of work using the $p\text{-}V$ coordinates is shown in FIGURE 2-3.

$$L = \int_{V_1}^{V_2} p\,dV$$
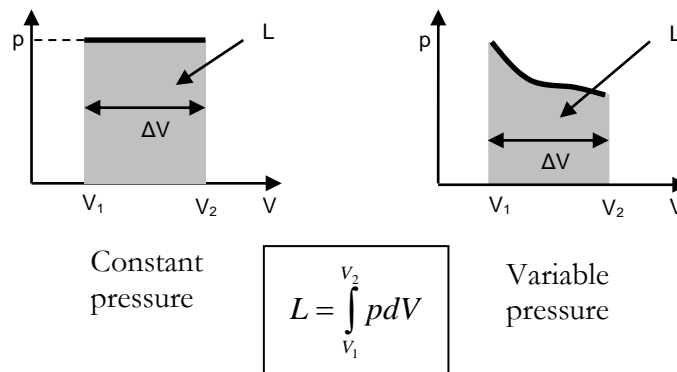
FIGURE 2-3. Work represented on the *p-V* plane.

Another form of transferring energy between systems is heat. However, heat can be transferred only when the interacting systems have different temperatures. Moreover, energy supplied as heat cannot be totally used to change the potential energy of the system.

Consider an open system through which a certain working fluid is passing with a constant rate, as shown in FIGURE 2-4. Such systems could represent a compressor or a turbine, and are usually involved in exchanging work *L* with the surroundings.
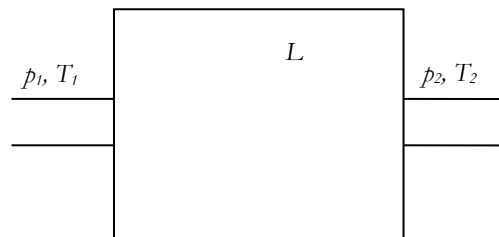
FIGURE 2-4. An open thermodynamic system.

The total work which is performed in the system consists of three parts:

1. (positive) work done by fluid entering to the system equal to p_1V_1

2. (negative) work that needs to be added to fluid exiting the system equal to p_2V_2

3. external work resulting from a change of the volume: $L = \int_1^2 p\,dV$

The sum of the three components is called the **technical work** and is equal to:

$$L_{t1,2} = p_1V_1 - p_2V_2 + \int_1^2 pdV = -\int_1^2 d(pV) + \int_1^2 pdV =$$

(2-5)

$$\int_1^2 (pdV - pdV - Vdp) = -\int_1^2 Vdp$$

For a unit mass of the working fluid the technical work is given as,

(2-6) $\quad l_{t1,2} = -\int_1^2 vdp$.

It should be noted that the first principle of thermodynamics can be applied to an open system as well. However, in that case the work needed to introduce the fluid into the system must be taken into account as well. Assume that the internal energy of the system shown in FIGURE 2-4 is E_I. If amount of mass Δm_1 of the working fluid with internal energy per unit mass $e_{I,1}$, pressure p_1 and specific volume v_1 is introduced into the system, then the internal energy of the system will increase as,

(2-7) $\quad \Delta E_I = (e_{I,1} + p_1v_1)\Delta m_1 + Q - L_t'$,

where Q and L_t' are the heat and the work exchanged with the surroundings. Quantity $e_I + pv$ appearing in Eq. (2-7) is recognized as **specific enthalpy** i, [J/kg], and, as already mentioned, plays an important role in technical applications. Thus the first law of thermodynamics for open systems can be written as,

(2-8) $\quad \Delta E_I = \Delta I_1 + Q - L_t'$.

In general, if there are many inflows and outflows to the system, its internal energy is given as,

(2-9) $\quad \Delta E_I = \sum_i \Delta I_i + Q - L_t'$.

If the mass flow rates of the working fluid are constant and equal on inlets and outlets, the first law of thermodynamics yields,

(2-10) $\quad I_2 - I_1 = Q_{1,2} - L_{t1,2}$

where now L_t' becomes equal to the technical work $L_{t1,2}$ given by Eq. (2-5).
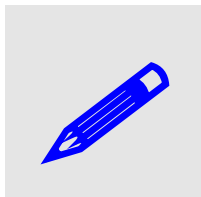
EXAMPLE 2-1. Calculate the work performed in a closed system, which internal energy has changed from $E_{I,1} = 5$ MJ to $E_{I,2} = 4$ MJ and to which heat was added equal to $Q_{t,2} = 6$ MJ. SOLUTION: From Eq. (2-10) one gets: $L_{t1,2} = E_{I,1} - E_{I,2} + Q_{1,2} =$ 5 MJ – 4 MJ + 6 MJ = 7 MJ. Since the sign of the work is positive, it was performed by the system on surroundings.

The internal energy and the enthalpy are examples of so-called **thermodynamic potentials**. A thermodynamic potential is a scalar function that describes the thermodynamic state of a system. Other examples of the thermodynamic potentials are the **Gibbs free energy**, G, and the **Helmholtz free energy**, F.

The Gibbs free energy is defined as,

$$(2\text{-}11) \quad G = E_I + pV - TS = I - TS \, ,$$

and the Helmholtz free energy is given as,

$$(2\text{-}12) \quad F = E_I - TS \, .$$

The term TS appearing in the expressions for the Gibbs and Helmholtz free energy represents the amount of energy that can be obtained by the system from the surroundings. Thus the Gibbs free energy can be interpreted as the enthalpy of the system minus the energy that can be obtained from the surroundings. In a similar way, the Helmholtz free energy is equal to the internal energy of the system minus the energy that can be obtained from the surroundings. All forms of thermodynamic potentials are frequently used to describe non-cyclic processes.

2.1.3   Second Law of Thermodynamics

The **second law of thermodynamics** states that "there is no process that, operating in cycle, produces no other effect than the subtraction of a positive amount of heat from a reservoir and a production of an equal amount of work". This formal statement (known as the **Kelvin-Plank statement**) says nothing more than that the energy systems have a tendency to increase their entropy (chaos) rather than to decrease it. The constraints resulting from the second law of thermodynamics are depicted in FIGURE 2-5.
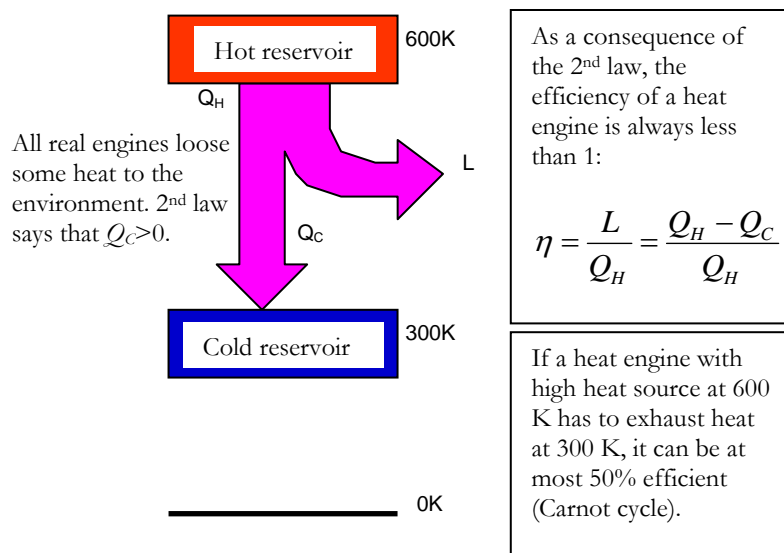
FIGURE 2-5. Consequences of the 2nd law of thermodynamics.

The most general expression for a change of the internal energy is given by the **Gibbs equation**,

$$(2\text{-}13) \qquad dE_I = TdS - pdV + \sum_i \mu_i dm_i ,$$

where dS is a change of entropy, dV is a change of volume, μ_i is the chemical potential of species i and dm_i is an exchange of mass of the system for species "i" with its surroundings. For a closed system without chemical reactions, the Gibbs equation becomes,

$$(2\text{-}14) \qquad dE_I = TdS - pdV .$$

The differential dE_I in Eq. (2-14) can be replaced with the value obtained from Eq. (2-1):

$$dI = dE_I + pdV + Vdp ,$$

which yields,

$$(2\text{-}15) \qquad TdS = dI - Vdp .$$

For 1 kg of substance, the equation becomes,

$$(2\text{-}16) \qquad Tds = di - vdp = de_I + pdv .$$

A thermodynamic engine cannot transform into work the whole introduced heat but only a part of it. From the economical point of view it is essential to know how much of the supplied heat can be transformed into work, since the heat is generated through burning fuel and the cost of the work depends on the amount of the consumed fuel. Due to that an important parameter is the **efficiency of a heat engine**, defined as,

$$(2\text{-}17) \qquad \eta = \frac{L_c}{Q} ,$$

where L_c is the cycle work and Q is the supplied heat to the cycle. According to what was mentioned earlier, this efficiency is always less than 1.

An equivalent formulation of the second law of thermodynamics can be given as follows: a thermodynamic engine cannot work without subtracting heat from a "hot reservoir" and releasing heat to a "cold reservoir".

2.1.4　Maximum Work and Exergy
In technical applications, an important question concerns the amount of work that can be performed by a system, and in particular, the following question: what is the maximum work possible? The maximum work results from the first law of thermodynamics and depends on the amount of heat exchanged with surroundings, $\Delta Q = T_0 \Delta S$, and the change of the internal energy, $\Delta E_I = E_{I,1} - E_{I,2}$,

$$(2\text{-}18) \qquad L_{\max} = E_{I,1} - E_{I,2} + T_0 (S_2 - S_1).$$

A special case is considered when the system surroundings are the environment at standard conditions (temperature and pressure). For that purpose one defines **exergy** of a substance as the maximum work that this substance can perform in a reversible process, in which the surroundings is treated as a source of useless substance and heat, and at the end of the process all substances taking part in it are in a thermodynamic equilibrium with the surroundings. The thermal exergy is then calculated as,

(2-19) $\quad B_t = E_I - E_{I,0} - T(S - S_0) - p_0(V_0 - V).$

The difference between Eqs. (2-18) and (2-19) is that in the latter the final state of the system is defined as a state of equilibrium with the environment and the term $p_0(V_0 - V)$ is the work which the system performs against the environmental pressure. This work is of course lost, since the environment is treated as a source of useless energy. Using the definition of enthalpy, the thermal exergy can also be defined as,

(2-20) $\quad B_t = I - I_0 - T_0(S - S_0).$

In analogy to the thermal exergy, B_t, one can define the total exergy, B, but then the internal energy of the system, E_I, has to be replaced with the total energy, E_T, including the kinetic and the potential energy of the system.

EXAMPLE 2-2. Calculate exergy of water in an open system, if the water pressure is $p = 15$ bar and temperature $t = 200$ °C. Vapour parameters in the environment are $p_0 = 0.098$ bar and $t_0 = 20$ °C. SOLUTION: Exergy of a substance in an open system is $b = i - i_0 - T_0(s - s_0)$. From water property tables, one can find water enthalpy $i = 852.4$ kJ/kg, water entropy $s = 2.331$ kJ/kg.K, vapour enthalpy $i_0 = 2537.6$ kJ/kg and vapour entropy $s_0 = 9.063$ kJ/kg.K. Water exergy is thus equal to: b = 852.4 – 2537.6 – 293(2.331 – 9.063) = 314.8 kJ/kg.

2.2 Thermodynamic Processes

2.2.1   Ideal Gas

In many thermodynamic processes the system under consideration contains gas as a working fluid, for instance air or superheated vapour. To simplify an analysis of such a system, one is using a notion of the **ideal gas**, which is defined as a substance that satisfies the following conditions:

1. the **Clapeyron's equation of state**

2. the **Avogadro's law**

3. it has a constant specific heat.

To uniquely define the state of any system it is enough to know values of certain thermodynamic parameters. As indicate observations, the system state can be in most cases described with three thermodynamic parameters. In particular, a system containing gas can be described by known pressure, temperature and volume. In many cases one can establish relationship between these parameters as follows,

(2-21) $\quad f(p, T, v) = 0,$

which means that the number of independent thermodynamic parameters is reduced from three to two. A **state equation for ideal gas** has been formulated by Clapeyron as follows,

(2-22) $pv = RT$.

Here R is the **specific gas constant**. For gases R is a physical constant which is given by a ratio of the **universal gas constant** B and the molar mass M,

(2-23) $R = \dfrac{B}{M}$,

where the universal gas constant is equal to,

(2-24) $B = 8.314472$ J·K^{-1}·mol^{-1} .

Molar mass is the mass of one mole of a chemical element or a chemical compound. The molar mass of a substance may be calculated from the standard atomic weights listed for elements in the standard periodic table. The unit of molar mass in physics is kg/mol (this is different from chemistry, where unit g/mol is still used). To be consistent with the SI system used throughout this book, the molar mass will be defined in kg/mol.

TABLE 2.1. Molar mass and the specific gas constant of selected gases.

Gas	Molar mass 10^{-3} kg/mol	Gas Constant J/(kg.K)
He	4.003	2077
Air	29	287
O_2	32	258
N_2	28.016	297
H_2	2.016	4124
H_2O	18	462
CO_2	44	189

The Avogadro's law states that in equal volumes there is the same amount of molecules of ideal gases, if pressures and temperatures of gases are the same. In particular, under standard conditions (temperature and pressure equal to 273.15 K and 101325 Pa, respectively), the gas volume is equal to $V_m = 22.4138 \; 10^{-3}$ m^3.mol^{-1}. This is called the **standard molar volume** of an ideal gas. The number of molecules (or

atoms for monatomic gases) in that volume is given by the **Avogadro number** and is equal to $N_0 = 6.0220 \ 10^{23}$ mol^{-1}. The mass of the substance is equivalent to one mole.
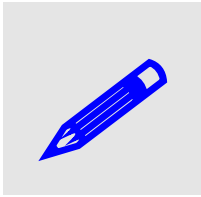
EXAMPLE 2-3. Calculate the universal gas constant knowing the standard molar volume of the ideal gas. SOLUTION: The Clapeyron equation for a standard molar volume is as follows: $p \cdot V_m = M \cdot R \cdot T = B \cdot T$. This gives the expression for the standard gas constant as follows: $B = p \cdot V_m / T = 101325 \cdot 0.022414 / 273.15 = 8.3144$ J/(K·mol).

The Avogadro law is depicted in FIGURE 2-6.
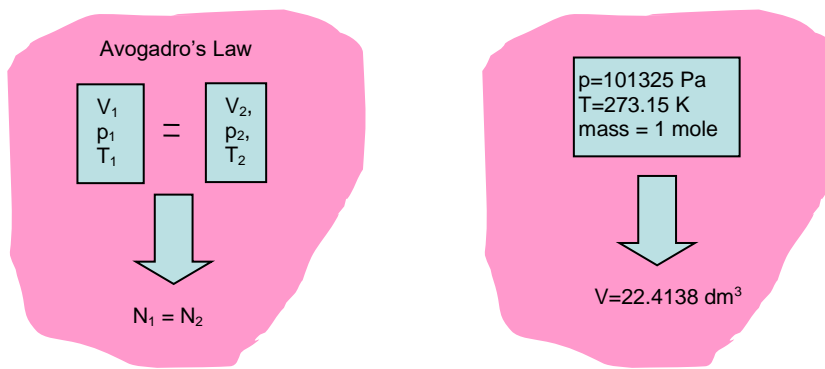
FIGURE 2-6. Principles of the Avogadro's law.

EXAMPLE 2-4. Calculate the gas constant for helium. SOLUTION: The molecular mass of helium is $M = 4.003$ g/mol $= 4.003 \cdot 10^{-3}$ kg/mol. Thus, using (2-23) and ((2-24) yields $R = 8.314472 / 0.004003 = 2077.06$ J·kg^{-1}·K^{-1} .

The specific heat at constant volume is defined as,

$$(2\text{-}25) \qquad c_v = \frac{\Delta Q_v}{\Delta T},$$

where ΔQ_v is a small amount of heat supplied to the gas under constant volume condition, and ΔT is the resulting increase of temperature. Similarly the specific heat at constant pressure is defined as,

$$(2\text{-}26) \qquad c_p = \frac{\Delta Q_p}{\Delta T},$$

where ΔQ_p is a small amount of heat supplied to the gas under constant pressure condition. The specific heat at constant pressure is always larger than the specific heat at constant volume, and their ratio plays an important role in gas thermodynamics,

(2-27) $\quad \dfrac{c_p}{c_v} = \kappa$.

Based on the equation of state and definitions of the internal energy and enthalpy, it can be shown that for an ideal gas the following is valid:

(2-28) $\quad R = c_p - c_v$.

Specific heat of any substance depends on the number of degrees of freedom of its molecules. With monatomic gases (like helium) heat energy comprises only translational motions along x, y and z-axis in the three dimensional space. It means that molecules in such gases (single atoms) have three degrees of freedom. Diatomic molecules have additional two degrees of freedom (rotations around axes perpendicular to the molecule axis). To this category belong many gases such as nitrogen, oxygen and even air, which is a mixture of gases that are predominantly diatomic. For molecules with three atoms or more (valid for gases such as water vapour, carbon dioxide and Freon) the number of degrees of freedom is six: three translations and three rotations. It can be shown that the **heat capacity ratio** (or **adiabatic index**) depends on the number of degrees of freedom as follows,

(2-29) $\quad \kappa = 1 + \dfrac{2}{n_f}$.

Here n_f is the number of degrees of freedom for a gas molecule. Thus, for monatomic gas (e.g. helium) the heat capacity ratio is $1 + 2/3 \approx 1.67$, whereas for water vapour it is equal to $1 + 2/6 \approx 1.33$.

For real gases c_p and c_v are not constant. If in a given temperature interval an averaged value of the specific heat is needed, then the average value can be found as,

(2-30) $\quad \overline{c}_x = \dfrac{\displaystyle\int_{T_1}^{T_2} c_x dT}{T_2 - T_1}, \quad x = p, v$.

In the same manner the adiabatic index for real gases is not constant and varies with the temperature.

TABLE 2.2. Heat capacity ratio (adiabatic index) for dry air as a function of temperature

Temp, ºC	0	20	100	200	400	1000	2000
κ	1.403	1.40	1.401	1.398	1.393	1.365	1.088

EXAMPLE 2-5. Calculate the volume occupied by 5 kg of nitrogen with temperature 127 °C and with pressure 10 bars. Calculate the specific volume and the density of nitrogen at these conditions. SOLUTION: The specific volume of nitrogen can be found from Eq. (2-22) as: $v = RT/p$, where R is the nitrogen gas constant: $R = B/M = 8.3147/28 = 296.7$ J/kg.K. Thus $v = 296.7 \cdot 400/10^6 = 0.119$ m³/kg. The total volume is found as $V = v \cdot m = 0.119 \cdot 5 = 0.594$ m³. The density is equal to: $\varrho = 1/v = 1/0.119 = 8.4$ kg/m³.

2.2.2   van der Waals Equation

The ideal gas model assumes that gas particles do not occupy any volume: they have a diameter equal to zero. This assumption is removed in the van der Waals model of gas, where particles are considered as rigid particles with a finite diameter d. The particles are subject to an attraction force. A finite size of particles means that repulsive forces between particles are considered as well. In addition, since particles have a finite size, they take some part of the system volume. The 'available' volume is thus $V' = V\text{-}b$, where b is a parameter taking into account the volume of particles, defined by van der Waals as 4 times volumes of all particles contained in one mole, that is $b = 4 \times N_0 v_p$, where v_p is the volume of a single particle. Similarly the real gas pressure must be modified as compared with the ideal gas due to the attraction forces. The pressure correction $p*$ is inversely proportional to the square of the volume of one mole of the gas, V_m: $p^* = a/V_m^2$, where a is the van der Waals coefficient. Thus, for one mole, the van der Waals equation is,

$$(2\text{-}31) \quad \left(p + \frac{a}{V_m^2} \right)\left(V_m - b \right) = \frac{B}{M} T \, .$$

The parameters a and b can be obtained as,

$$(2\text{-}32) \quad a = \frac{27 R^2 T_c^2}{64 p_c}, \quad b = \frac{R T_c}{8 p_c},$$

where T_c and p_c are the critical temperature and pressure, respectively. Equations (2-31) and (2-32) can be used to eliminate parameters a, b and B from the van der Waals equation and to replace them with the critical parameters p_c, T_c and V_c. After some transformations, the following reduced form of the van der Waals equation is obtained,

$$(2\text{-}33) \quad \left(p_R + \frac{3}{v_R^2} \right)\left(v_R - \frac{1}{3} \right) = \frac{8}{3} T_R \, .$$

Here $p_R = p/p_c$, $v_R = v/v_c$ and $T_R = T/T_c$. Equation (2-33) suggests that – when measured in parameters related to critical values (e.g. reduced parameters) – all fluids obey the same equation of state. This statement is known as the **principle of the corresponding states**. Unfortunately this principle can be applied with good accuracy only to simple substances, such as argon or methane, which have relatively symmetrical molecules. For substances with more complex molecules, the discrepancy between the theory and experimental data are significant.

2.2.3   Gas Mixtures

In many situations in nuclear reactor applications one is dealing with a mixture of gases rather than with a single gas. Such a mixture can also be treated as a mixture of ideal gases and several general conclusions can be drawn. A fundamental role in the theory of the ideal gas mixture plays the **Dalton's law**, which states that the total pressure of a mixture is equal to a sum of partial pressures of mixture components. This can be expressed as follows,

$$(2\text{-}34) \qquad p = \sum_i p_i \, ,$$

where p_i is the partial pressure of component i. The composition of a mixture can be defined in different ways. One way is by specifying the mass fraction of each component,

$$(2\text{-}35) \qquad g_i = \frac{m_i}{m} \, .$$

Here m_i is the mass of the component i in the mixture and m is the total mass of the mixture. An alternative way is to specify the volume fraction of each component,

$$(2\text{-}36) \qquad r_i = \frac{V_i}{V} \, ,$$

where V_i is the volume of the component i and V is the total volume of the mixture. According to the Dalton's law, for each mixture component the following relation is valid,

$$(2\text{-}37) \qquad p_i V = m_i R_i T$$

A summation of Eq. (2-37) for all components yields,

$$(2\text{-}38) \qquad V \sum_i p_i = T \sum_i m_i R_i \Rightarrow pV = m R_m T \, ,$$

where R_m is the mixture gas constant defined as,

$$(2\text{-}39) \qquad R_m = \frac{\sum_i m_i R_i}{m} = \sum_i g_i R_i \, .$$

The mixture density is obtained as,

$$(2\text{-}40) \qquad \rho_m = \frac{m}{V} = \frac{\sum_i \rho_i V_i}{V} = \sum_i r_i \rho_i$$

The relationship between the volume and mass fractions in a mixture is as follows,

$$(2\text{-}41) \quad r_i = \frac{V_i}{V} = \frac{m_i/\rho_i}{\sum_i m_i/\rho_i} = \frac{g_i/M_i}{\sum_i g_i/M_i},$$

where M_i is the molar mass of the component i in the mixture.

2.2.4 Gas Processes

Some gas processes have special features which can be analysed in more detail. Of special interest are cases when one of the system variables has a constant value during the considered process.

Gas processes are usually represented in a graphical form using the p-V coordinates, as shown in FIGURE 2-7. The process is indicated with the curve C, starting at point $A=(p_1,V_1)$ and ending at point $B=(p_2,V_2)$.
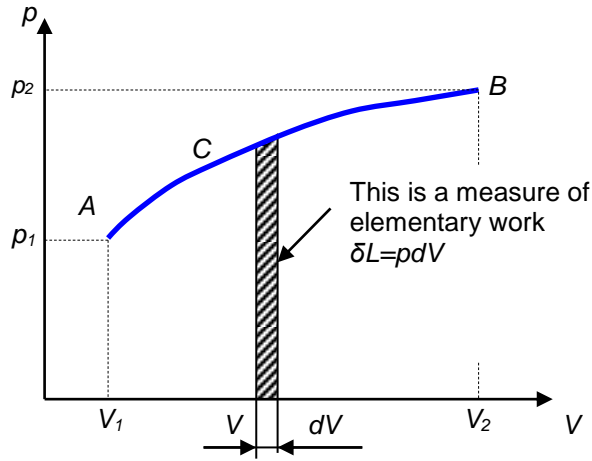
FIGURE 2-7. Typical representation of a gas process on the p-V plane.

The total work in the process from point A to B can be found as,

$$L = \int_{V_1}^{V_2} pdV .$$

Obviously, the work depends on the shape of the curve C.

An **isobaric process** is a thermodynamic process in which the pressure is constant. The state parameters in the isobaric process are changing according to the following equation,

$$(2\text{-}42) \quad \frac{v_1}{v_2} = \frac{T_1}{T_2}$$

According to the first principle of thermodynamics the heat associated with an isobaric process is as follows,

$$(2\text{-}43) \quad q_{1,2} = i_2 - i_1 = c_p\left(T_2 - T_1\right).$$

The isobaric process is schematically shown in FIGURE 2-8 using the p-V coordinates.
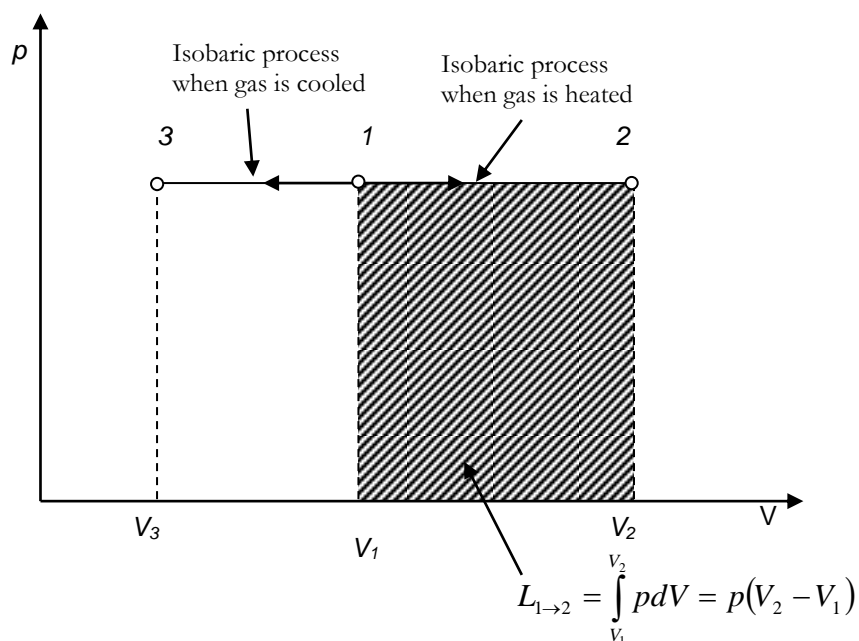
FIGURE 2-8. Isobaric process on p-V plane.

An **isochoric process** is a thermodynamic process in which the volume is constant. The state parameters in the isochoric process are changing according to the following equation,

(2-44) $\dfrac{p_1}{p_2} = \dfrac{T_1}{T_2}$.

According to the first principle of thermodynamics the heat of an isochoric process is as follows,

(2-45) $q_{1,2} = e_{I,2} - e_{I,1} = c_v \left(T_2 - T_1 \right)$.

The isochoric process is schematically shown in FIGURE 2-9 using the p-V coordinates.

An **isothermal process** is a thermodynamic process in which the temperature is constant. The state parameters in the isothermal process are changing according to the following equation,

(2-46) $p_1 v_1 = p_2 v_2 = RT$.

According to the first principle of thermodynamics the heat of an isothermal process is as follows,

(2-47) $q_{1,2} = RT \ln \dfrac{p_1}{p_2}$.
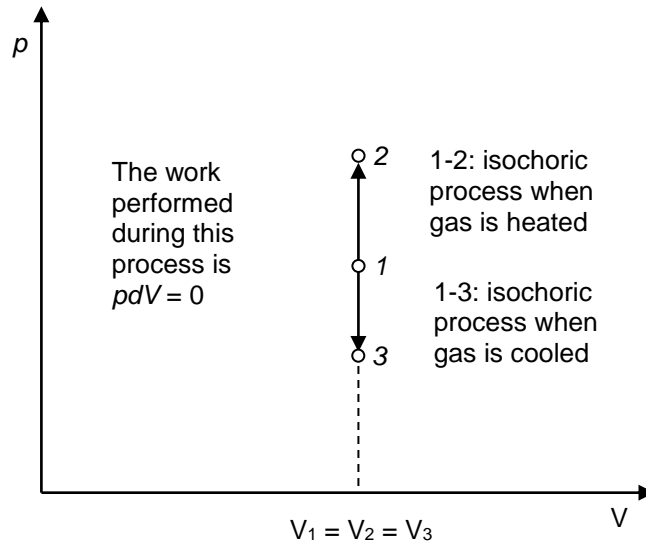
FIGURE 2-9. Isochoric process on p-V plane.

The isothermal process is schematically shown in FIGURE 2-10 using the p-V coordinates.
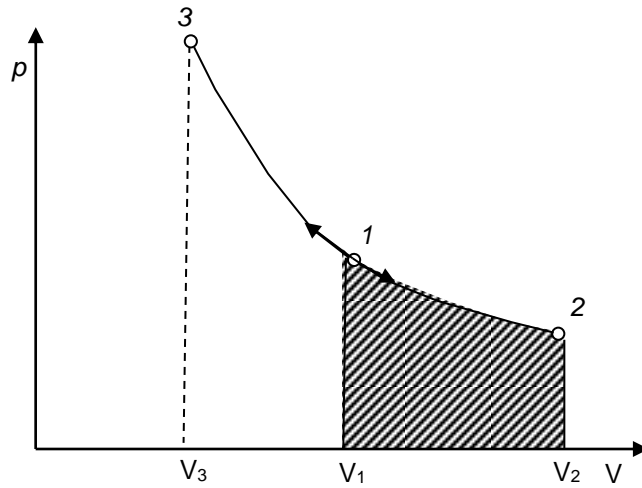
FIGURE 2-10. Isothermal process on p-V plane.

In the isothermal process the internal energy of gas does not change and the whole heat is utilized to perform work. Thus,

(2-48) $Q_{1\rightarrow 2} = L_{1\rightarrow 2} = \displaystyle\int_{V_1}^{V_2} p\,dV = mRT \int_{V_1}^{V_2} \dfrac{dV}{V} = mRT \ln \dfrac{V_2}{V_1}$.

An **adiabatic process** is a thermodynamic process in which no heat is transferred to or from the working fluid. When the process is reversible, the entropy change is also zero, and the process is referred to as an **isentropic process**. The state parameters in the adiabatic process are changing according to the following equation,

$$(2\text{-}49) \quad p_1 v_1^\kappa = p_2 v_2^\kappa .$$

The adiabatic process is schematically shown in FIGURE 2-11 using the *p-V* coordinates.
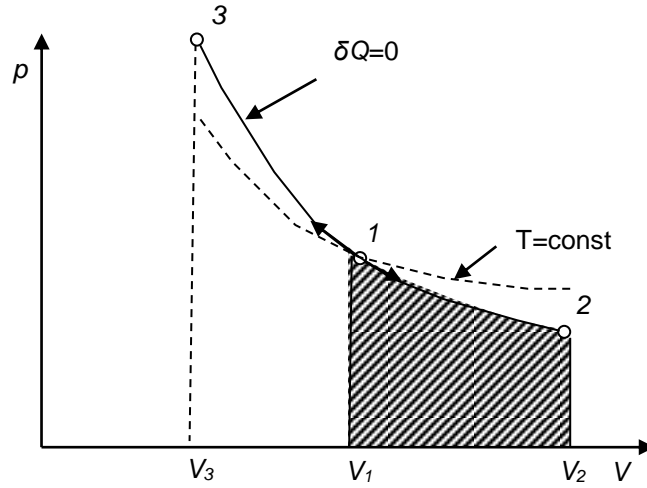
FIGURE 2-11. Adiabatic process on *p-V* plane.

The work in the adiabatic process (shown as the shaded area in FIGURE 2-11) is as follows,

$$(2\text{-}50) \quad L_{1\to 2} = \frac{p_1 V_1}{\kappa - 1}\left[1 - \left(\frac{V_1}{V_2}\right)^{\kappa - 1}\right] = \frac{p_1 V_1}{\kappa - 1}\left(1 - \frac{T_2}{T_1}\right) .$$

A cyclic process is a thermodynamic process which begins from and finishes at the same thermostatic state. It is a closed loop on the *p-V* plane and the area enclosed by the loop is the work resulting from the process,

$$(2\text{-}51) \quad L = \oint p dV .$$

There are several such cycles discussed in thermodynamics. Cycles that are relevant to the nuclear engineering are the Carnot cycle (as a theoretical reference), the Rankine cycle and the Brayton cycle. The characteristics of the cycles are summarized in TABLE 2.3 and they are described in a more detail in the following sections.

TABLE 2.3. Selected thermodynamic closed processes.

Cycle	Compression	Heat addition	Expansion	Heat Rejection
Carnot	adiabatic	isothermal	adiabatic	isothermal
Rankine	adiabatic	isobaric	adiabatic	isobaric
Brayton	adiabatic	isobaric	adiabatic	isobaric

2.2.5   Carnot Cycle

An important role in thermodynamics plays the **Carnot cycle**, which is schematically shown in FIGURE 2-12. In this cycle the heat Q is supplied to the system at a constant temperature T and heat Q_0 is removed from the system at constant temperature T_0.
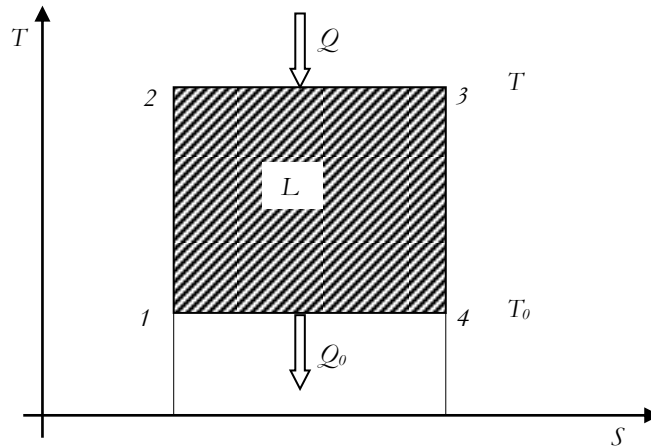
FIGURE 2-12. Carnot cycle.

The efficiency of the Carnot cycle is as flows,

$$(2\text{-}52) \quad \eta = \frac{Q - Q_0}{Q} = 1 - \frac{T_0(S_4 - S_1)}{T(S_3 - S_2)} = 1 - \frac{T_0}{T}.$$

As can be seen the efficiency of the Carnot cycle depends only on the temperature ratio of both the upper and the lower heat sources. Also, it increases with increasing temperature of the upper source that supplies heat to the system.
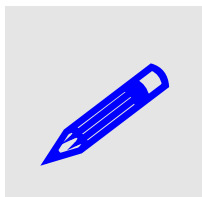
EXAMPLE 2-6. Calculate the efficiency of the reversible Carnot cycle if heat is supplied at temperature t = 700 °C and retrieved at temperature t = 20 °C.
SOLUTION: the efficiency of the cycle is found from Eq. (2-52) as follows,
$\eta = 1 - T_0/T = 1 - (20 + 273.15)/(700 + 273.15) = 0.698$.

2.2.6 Rankine Cycle

The **Rankine cycle** describes the operation of steam heat engines that are most widespread in the power generation plants. This cycle takes advantage of phase change of the working fluid to add and reject heat in an almost isothermal process. The schematic of the Rankine cycle is shown in FIGURE 2-13 using the *T-s* plane. Process 1-2*s* represents pumping of the working fluid from low to high pressure. Point 2*s* represents the cases when the pumping is performed without losses (isentropic process), whereas point 2 indicates conditions when losses in the pumping process are taken into account. Process 2-3-4 represents the heating of the working fluid: first the fluid is brought to the saturation at point 3 and then it is isothermally heated (evaporated) from point 3 to 4. Process 4-5 represents the vapour expansion in the turbine. Point 5*s* indicates an ideal case without losses (isentropic expansion), whereas point 5 indicates the conditions of the working fluid that leaves the turbine when the turbine losses are accounted for. Finally, the process 5-1 represents the heat rejection in the condenser.
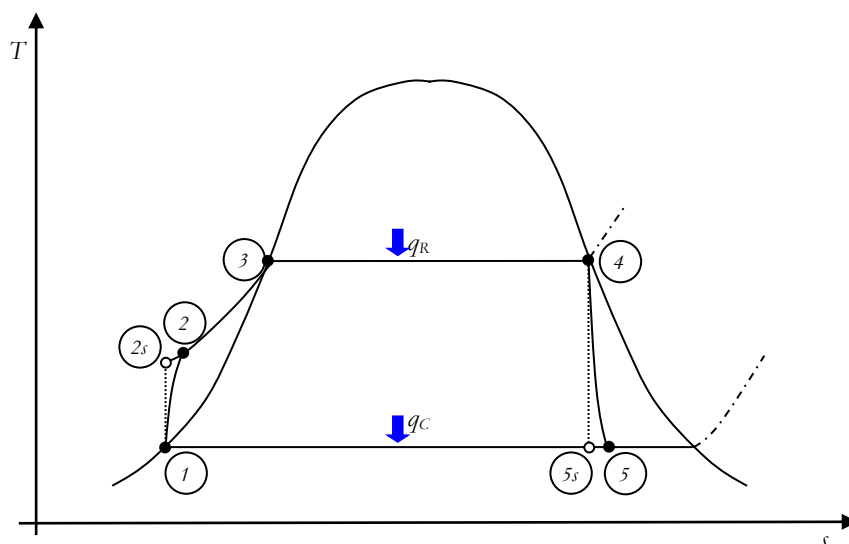
FIGURE 2-13. Rankine cycle.

If the mass flow rate of the working fluid in the cycle is *W*, then the following energy balances are valid:

Process 1-2: pumping power $\qquad N_{pump} = W(i_1 - i_2)$,

Process 2-4: heating $\qquad q_R = W(i_4 - i_2)$,

Process 4-5: turbine power $\qquad N_{turbine} = W(i_4 - i_5)$,

Process 4-1: heat rejection to condenser $\quad q_C = W(i_5 - i_1)$.

The efficiency of the cycle is obtained from Eq. (2-17) as,

$$\eta = \frac{N_{turbine} - \left| N_{pump} \right|}{q_R} = \frac{(i_4 - i_5) + (i_1 - i_2)}{(i_4 - i_2)}.$$

The losses in a turbine are determined by the internal efficiency which is defined as,

$$\eta_i = \frac{i_4 - i_5}{i_4 - i_{5s}}.$$

A more detailed analysis of the Rankine cycle is given in Chapter 5 in the section devoted to the turbine set systems.

2.2.7   Brayton Cycle

A schematic of the **Brayton cycle** (when all losses are neglected) is shown in FIGURE 2-14. Process 1-2 corresponds (neglecting the losses) to a compression of the working gas in a compressor. In process 2-3 the working gas is heated in a nuclear reactor core and in process 3-4 the gas is expanded and performs work in a turbine. After isobaric cooling in process 4-1, the gas flows back to the compressor.
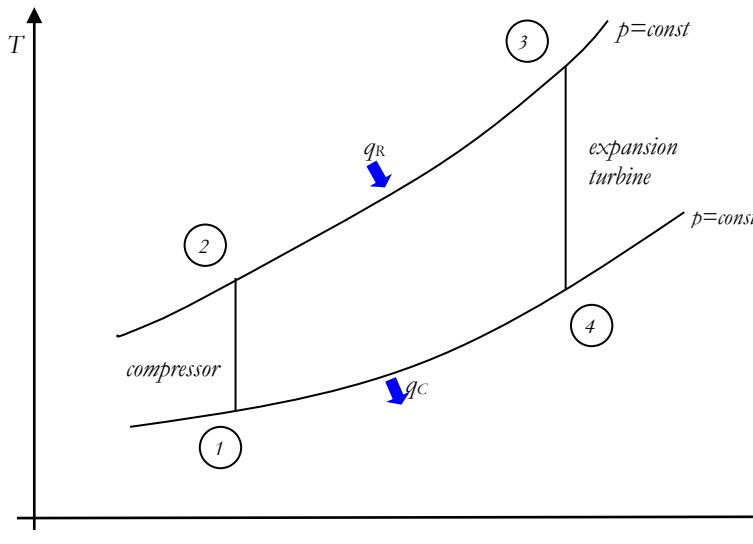
FIGURE 2-14. Brayton cycle.

The energy balances in all processes are as follows:

Process 1-2: compression power $N_{compress} = W(i_1 - i_2)$,

Process 2-3: heating $\qquad\qquad q_R = W(i_3 - i_2)$,

Process 3-4: turbine power $\qquad N_{turbine} = W\left(i_3 - i_4\right)$,

Process 4-1: heat rejection to condenser $q_C = W(i_4 - i_1)$.

The efficiency of the cycle is obtained from Eq. (2-17) as,

$$\eta = \frac{N_{turbine} - \left| N_{compress} \right|}{q_R} = \frac{\left(i_3 - i_4\right) + \left(i_1 - i_2\right)}{\left(i_3 - i_2\right)}.$$

2.2.8 Phase Change

Phase change is a process in which a substance undergoes transition from one phase to another. The best known examples of phase change are evaporation and condensation processes, or melting of ice. The phase-change processes are illustrated in FIGURE 2-15. A typical phase diagram on the T-p plane is shown in FIGURE 2-16.
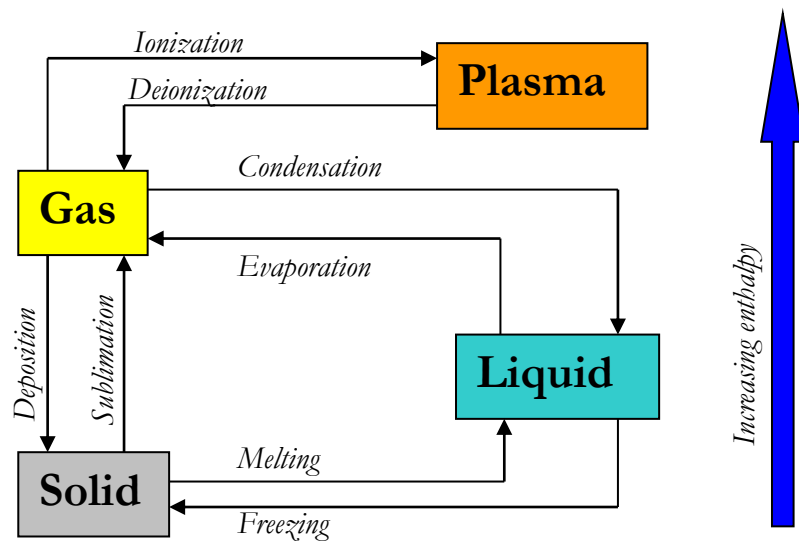
FIGURE 2-15. Phase-change processes.
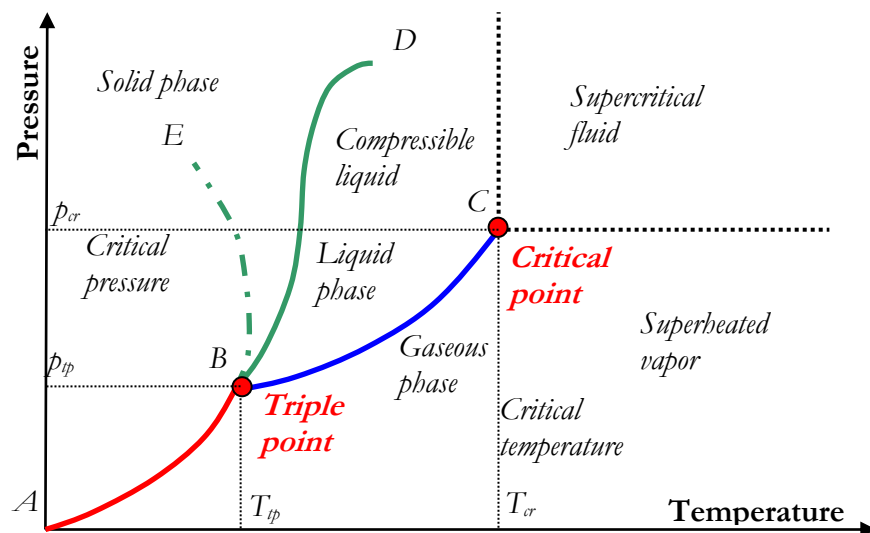
FIGURE 2-16. Phase diagram. Line B-E shows water anomalous behaviour.

The curves indicate various phase-change processes between solid and gas phase (curve A-B), the solid and liquid phase (curves B-D and B-E) and the liquid and gas phase (curve B-C). The dotted line shows the anomalous behaviour of water, which solid phase – ice – is less dense than the liquid phase and floats in it. The two

characteristic points shown in the plot are the **triple point** – where three phases coexists (for water it occurs exactly at $T = 273.16$ K and $p = 611.73$ Pa), and the **critical point**, where the differences between the liquid and the gas phase disappear and they become identical (for water it occurs exactly at $T = 647.096$ K and $p = 22.064$ MPa).

R E F E R E N C E S

[2-1]   Callen, H. B., *Thermodynamics and an Introduction to Thermostatistics*, 2nd Edition, John Wiley & Sons Inc., New York, 1985.

E X E R C I S E S

EXERCISE 2-1. A closed, thermally insulated tank is filled with gas that is mixed with a mixer powered from outside. Due to mixing during a certain period of time, the temperature of the gas increased from 20 °C to 30 °C. The increase of the internal energy is given as $\Delta E_i / \Delta T = 1$ kJ/K. Calculate the mixing work provided to the system.

EXERCISE 2-2. A steel rod with mass 5 kg has been submerged for a long time in 20 l of water with temperature 20 °C. The rod is next taken out of the water and heated in an oven up to 1100 °C. Subsequently the rod is again submerged in the water to be cooled down. Assuming that the water and the rod are exchanging temperature in perfect isolation from the surroundings, calculate their temperature at equilibrium. Heat capacities of steel and water are: $c_s = 0.46$ kJ.kg^{-1}.K^{-1} and $c_w = 4.19$ kJ.kg^{-1}.K^{-1}.

EXERCISE 2-3. The output power of a steam turbine is equal to 6 MW and it uses water steam with inlet mass flow rate 10 kg/s, inlet enthalpy 3260 kJ/kg and inlet velocity 90 m/s. The outlet steam parameters are as follows: enthalpy 2510 kJ/kg and velocity 230 m/s. Calculate the heat losses from the turbine to the environment.

EXERCISE 2-4. Calculate the volume of one kmol of ideal gas under absolute pressure equal to 980700 Pa and temperature 20 °C.

EXERCISE 2-5. Calculate mass of one kmol of ideal gas under absolute pressure equal to 980700 Pa and temperature 20 °C, which has density equal to 1.38 kg/m^3.

EXERCISE 2-6. A certain amount of oxygen is kept in a vessel with volume 20 m^3 under pressure 2 bar and temperature 20 °C. What will be the volume of the gas under normal conditions (pressure 101325 Pa and temperature 0 °C)?

EXERCISE 2-7. 5 kmols of nitrogen with initial parameters: pressure equal to 1 bar and temperature 0 °C reduced the volume after isothermal compression five times. What was the pressure of the gas after compression? Calculate the amount of released heat and the change of the internal energy, as well as the compression work.

EXERCISE 2-8. Calculate the efficiency of the Rankine cycle in which water is evaporated in a nuclear reactor at pressure $p_r = 70$ bar and the saturated steam is directed to a turbine where it is expanded to absolute pressure in condenser $p_c = 0.05$ bar. Assume that the internal efficiency of the turbine is equal to 0.98 and that there are no losses while compressing the condensate in the pump from p_c to p_r.

3. Fluid Mechanics

T he objective of fluid mechanics is to describe fluid motion under action of forces. It employs the fundamental principles, such as mass, momentum and energy conservation laws to fluids, that is, to both liquids and gases. A typical application of fluid mechanics is to evaluate forces acting on a body moving in surrounding fluid. Another example is related to evaluation of the mass and energy transport due to fluid motion. Initially fluid mechanics was dealing with investigation of water flow in pipes and that is why it was called *hydraulics* (from Greek: *hydros* – water and *aulo's* – pipe). Other names have been also used, such as *hydromechanics* or *hydrodynamics*, whereas the name *aerodynamics* is reserved for flows of compressible gases. Today *hydrodynamics* and *hydromechanics* are used exchangeably. In the international literature the two names are synonymous and are used in connection to motion of all kind of fluids, not only water.

Fluid mechanics is dealing with investigations of motions of fluids by applying the fundamental conservation principles. Typically the conservation laws are expressed in terms of partial differential equations. The objective of this chapter is to present the various formulations of governing equations and the methods of their solutions.

3.1 Mathematical Tools

The basic mathematical tools, which are used in fluid mechanics, are introduced in this section.

3.1.1   Coordinate System

Coordinate systems are necessary to uniquely describe the fluid motion in space. The most frequently used is the right-handed **Cartesian coordinate system**, shown in FIGURE 3-1.

In general, a coordinate system in the three-dimensional space is defined by choosing three linearly independent vectors. For the Cartesian coordinate system, the vectors $B=\{\mathbf{e}_x,\ \mathbf{e}_y,\ \mathbf{e}_z\}$ are shown in FIGURE 3-1. The set B is the **basis of the coordinate system**. The basis is orthonormal if the vectors have unit length and they are normal to each other. Sometimes the basis vectors will be represented as $B=\{\mathbf{e}_1,\ \mathbf{e}_2,\ \mathbf{e}_3\}$, where index 1 will be used for *x*-direction, index 2 for *y*-direction and 3 for *z*-direction. Using this notation, the orthonormal property of the basis vectors can be expressed as,

$$(3\text{-}1) \qquad \mathbf{e}_i \cdot \mathbf{e}_j = \delta_{ij} \equiv \begin{cases} 1 & i = j \\ 0 & i \neq j \end{cases},$$

where δ_{ij} is known as the **Kroneker delta**.
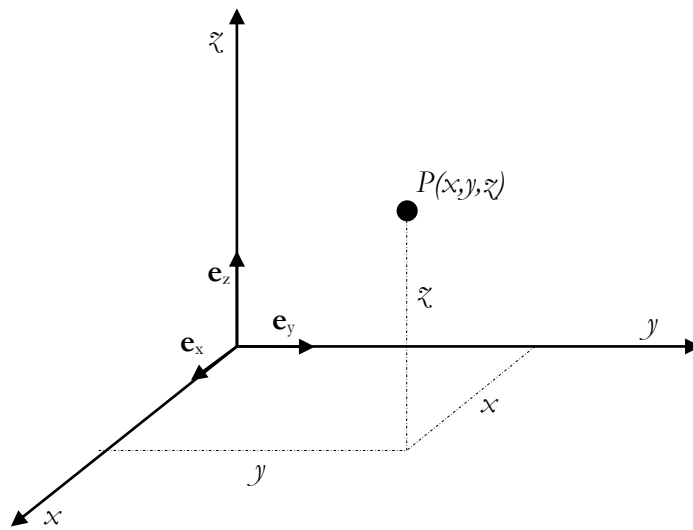
FIGURE 3-1. Cartesian system of coordinates.

Two additional coordinate systems that are frequently used in fluid mechanics are the cylindrical polar and the spherical polar coordinates, shown in FIGURE 3-2 and FIGURE 3-3, respectively.
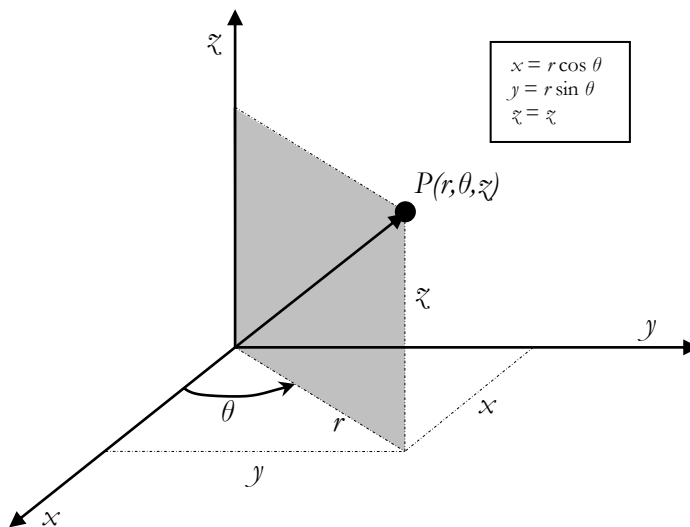
FIGURE 3-2. Cylindrical polar coordinate system.

$$x = r \sin \theta \cos \varphi$$
$$y = r \sin \theta \sin \varphi$$
$$z = r \cos \theta$$
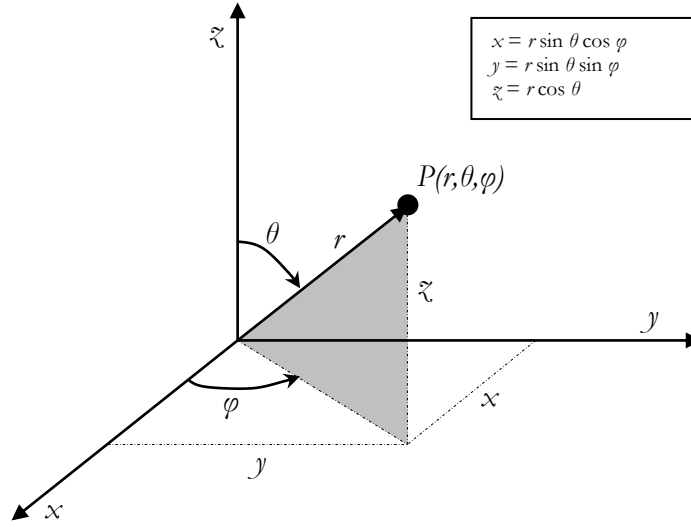
FIGURE 3-3. Spherical polar coordinate system.

3.1.2   Scalars, Vectors and Tensors

Scalar quantities can be uniquely described with a single number at any point in the three dimensional space. Typical scalar quantities in fluid mechanics are the fluid density and the temperature.

Vector quantities can be uniquely determined in terms of the basis vectors in the three-dimensional space. Let $B = \{\mathbf{e}_1, \mathbf{e}_2, \mathbf{e}_3\}$ be an orthonormal basis of the space. Then any vector $\mathbf{v}$ in the space can be expressed in terms of its components as,

$$(3\text{-}2) \qquad \mathbf{v} = v_1 \mathbf{e}_1 + v_2 \mathbf{e}_2 + v_3 \mathbf{e}_3 = \sum_{i=1}^{3} v_i \mathbf{e}_i .$$

Using the matrix notation, the vector can be graphically represented as,

$$(3\text{-}3) \qquad \mathbf{v} = \begin{bmatrix} v_1 & v_2 & v_3 \end{bmatrix}.$$

The **scalar** (or dot) product of two vectors $\mathbf{v}$ and $\mathbf{u}$ is defined as,

$$(3\text{-}4) \qquad \mathbf{v} \cdot \mathbf{u} = \mathbf{u} \cdot \mathbf{v} = u_1 v_1 + u_2 v_2 + u_3 v_3 = \sum_{i=1}^{3} u_i v_i .$$

Using the matrix notation, the scalar product is defined as,

$$(3\text{-}5) \qquad \mathbf{v} \cdot \mathbf{u} = \mathbf{u} \cdot \mathbf{v} = \begin{bmatrix} u_1 & u_2 & u_3 \end{bmatrix} \begin{bmatrix} v_1 \\ v_2 \\ v_3 \end{bmatrix} = u_1 v_1 + u_2 v_2 + u_3 v_3 .$$

The **cross product of two vectors** $\mathbf{v}$ and $\mathbf{u}$ is defined as,

$$(3\text{-}6) \qquad \mathbf{v} \times \mathbf{u} = \begin{vmatrix} \mathbf{e}_1 & \mathbf{e}_2 & \mathbf{e}_3 \\ v_1 & v_2 & v_3 \\ u_1 & u_2 & u_3 \end{vmatrix} = \begin{vmatrix} v_2 & v_3 \\ u_2 & u_3 \end{vmatrix} \mathbf{e}_1 - \begin{vmatrix} v_1 & v_3 \\ u_1 & u_3 \end{vmatrix} \mathbf{e}_2 + \begin{vmatrix} v_1 & v_2 \\ u_1 & u_2 \end{vmatrix} \mathbf{e}_3 =$$

$$(v_2 u_3 - u_2 v_3)\mathbf{e}_1 - (v_1 u_3 - u_1 v_3)\mathbf{e}_2 + (v_1 u_2 - u_1 v_2)\mathbf{e}_3$$

In fluid mechanics the flow velocity is described with vectors. Employing the Cartesian coordinate system in three-dimensional space, the velocity vector $\mathbf{v}$ is given as,

$$(3\text{-}7) \qquad \mathbf{v} \equiv \begin{bmatrix} u & v & w \end{bmatrix} \equiv \begin{bmatrix} v_1 & v_2 & v_3 \end{bmatrix} = \sum_{i=1}^{3} v_i \mathbf{e}_i .$$

The components of the velocity vector $\mathbf{v}$ in directions (x, y, z) are (u, v, w) or (v_1, v_2, v_3).

A **tensor of second order** can be obtained by a **dyadic product** of two vectors $\mathbf{u}$ and $\mathbf{v}$ as follows,

$$(3\text{-}8) \qquad \mathbf{uv} = \begin{bmatrix} u_1 \\ u_2 \\ u_3 \end{bmatrix} \begin{bmatrix} v_1 & v_2 & v_3 \end{bmatrix} = \begin{bmatrix} u_1 v_1 & u_1 v_2 & u_1 v_3 \\ u_2 v_1 & u_2 v_2 & u_2 v_3 \\ u_3 v_1 & u_3 v_2 & u_3 v_3 \end{bmatrix} .$$

In particular, nine different dyadic products of base unit vectors can be found. For example,

$$(3\text{-}9) \qquad \mathbf{e}_1 \mathbf{e}_3 = \begin{bmatrix} 1 \\ 0 \\ 0 \end{bmatrix} \begin{bmatrix} 0 & 0 & 1 \end{bmatrix} = \begin{bmatrix} 0 & 0 & 1 \\ 0 & 0 & 0 \\ 0 & 0 & 0 \end{bmatrix} .$$

The nine possible unit dyads form the basis of the space of second-order tensors: $\{\mathbf{e}_1\mathbf{e}_1, \mathbf{e}_1\mathbf{e}_2, \mathbf{e}_1\mathbf{e}_3, \mathbf{e}_2\mathbf{e}_1, \mathbf{e}_2\mathbf{e}_2, \mathbf{e}_2\mathbf{e}_3, \mathbf{e}_3\mathbf{e}_1, \mathbf{e}_3\mathbf{e}_2, \mathbf{e}_3\mathbf{e}_3\}$.

A second-order tensor can be thus written as a linear combination of the base unit dyads,

$$(3\text{-}10) \qquad \mathbf{\tau} = \sum_{i=1}^{3} \sum_{j=1}^{3} \tau_{ij} \mathbf{e}_i \mathbf{e}_j = \begin{bmatrix} \tau_{11} & \tau_{12} & \tau_{13} \\ \tau_{21} & \tau_{22} & \tau_{23} \\ \tau_{31} & \tau_{32} & \tau_{33} \end{bmatrix} .$$

A sum of two tensors is a new tensor given as,

$$(3\text{-}11) \qquad \mathbf{\tau} + \mathbf{\sigma} = \sum_{i=1}^{3} \sum_{j=1}^{3} (\tau_{ij} + \sigma_{ij}) \mathbf{e}_i \mathbf{e}_j = \begin{bmatrix} \tau_{11} + \sigma_{11} & \tau_{12} + \sigma_{12} & \tau_{13} + \sigma_{13} \\ \tau_{21} + \sigma_{21} & \tau_{22} + \sigma_{22} & \tau_{23} + \sigma_{23} \\ \tau_{31} + \sigma_{31} & \tau_{32} + \sigma_{32} & \tau_{33} + \sigma_{33} \end{bmatrix} .$$

The **single-dot product** (or tensor product) of two tensors is a new tensor given as,

$$(3\text{-}12) \quad \boldsymbol{\sigma} \cdot \boldsymbol{\tau} = \sum_{i=1}^{3} \sum_{l=1}^{3} \left(\sum_{j=1}^{3} \sigma_{ij}\tau_{jl} \right) \mathbf{e}_i \mathbf{e}_1 \ .$$

The **double-dot product** (or scalar product or inner product) of two tensors is a scalar given as,

$$(3\text{-}13) \quad \boldsymbol{\sigma} : \boldsymbol{\tau} = \sum_{i=1}^{3} \sum_{j=1}^{3} \sigma_{ij}\tau_{ji} = \sigma_{11}\tau_{11} + \sigma_{12}\tau_{21} + \sigma_{13}\tau_{31} + \sigma_{21}\tau_{12} + \sigma_{22}\tau_{22} + \sigma_{23}\tau_{32} +$$
$$\sigma_{31}\tau_{13} + \sigma_{32}\tau_{23} + \sigma_{33}\tau_{33}$$

A very useful operation in fluid mechanics is a dot product of a tensor and a vector. This product is defined as,

$$(3\text{-}14) \quad \mathbf{n} \cdot \boldsymbol{\tau} = \sum_{i=1}^{3} \left(\sum_{j=1}^{3} \tau_{ji} n_j \right) \mathbf{e}_i \ .$$

Expression given by Eq. (3-14) can be interpreted as an action of shear stress tensor $\boldsymbol{\tau}$ on a unit surface with normal vector $\mathbf{n}$. As a result of this action a unit force $\mathbf{f}$ will be created, which differs from $\mathbf{n}$ both in direction and size, as illustrated in FIGURE 3-4.
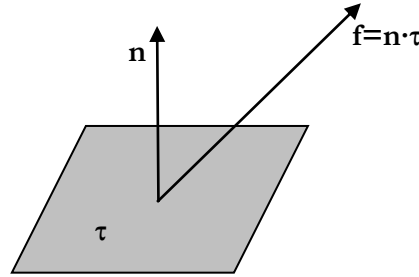
FIGURE 3-4. Action of tensor $\boldsymbol{\tau}$ on surface with normal vector $\mathbf{n}$.

The normal and the tangential components of the force $\mathbf{f}$ can be obtained as,

$$(3\text{-}15) \quad \mathbf{f}_n = (\mathbf{n} \cdot \mathbf{f})\mathbf{n} = \mathbf{n} \cdot (\mathbf{n} \cdot \boldsymbol{\tau})\mathbf{n} = (\mathbf{n}\mathbf{n} : \boldsymbol{\tau})\mathbf{n} \ ,$$

$$(3\text{-}16) \quad \mathbf{f}_t = \mathbf{f} - \mathbf{f}_n = \mathbf{n} \cdot \boldsymbol{\tau} - (\mathbf{n}\mathbf{n} : \boldsymbol{\tau})\mathbf{n} \ .$$

3.1.3   Differential Operators

The **nabla operator** is a vector defined as,

$$(3\text{-}17) \quad \nabla \equiv \begin{bmatrix} \dfrac{\partial}{\partial x} & \dfrac{\partial}{\partial y} & \dfrac{\partial}{\partial z} \end{bmatrix} \equiv \mathbf{e}_x \frac{\partial}{\partial x} + \mathbf{e}_y \frac{\partial}{\partial y} + \mathbf{e}_z \frac{\partial}{\partial z} \equiv \sum_{i=1}^{3} \mathbf{e}_i \frac{\partial}{\partial x_i} \ .$$

This vector operator can act on scalar, vector and tensor fields.

The gradient of a differentiable scalar field f is a vector field as follows,

$$(3\text{-}18) \quad \nabla f \equiv \mathrm{grad} f \equiv \left[\frac{\partial f}{\partial x} \quad \frac{\partial f}{\partial y} \quad \frac{\partial f}{\partial z} \right] \equiv \mathbf{e}_x \frac{\partial f}{\partial x} + \mathbf{e}_y \frac{\partial f}{\partial y} + \mathbf{e}_z \frac{\partial f}{\partial z} \equiv \sum_{i=1}^{3} \mathbf{e}_i \frac{\partial f}{\partial x_i} .$$

The divergence of a differentiable vector field **v** is a scalar field as follows,

$$(3\text{-}19) \quad \nabla \cdot \mathbf{v} \equiv \mathrm{div} \mathbf{v} \equiv \left[\frac{\partial}{\partial x} \quad \frac{\partial}{\partial y} \quad \frac{\partial}{\partial z} \right] \begin{bmatrix} u \\ v \\ w \end{bmatrix} \equiv \frac{\partial u}{\partial x} + \frac{\partial v}{\partial y} + \frac{\partial w}{\partial z} \equiv \sum_{i=1}^{3} \frac{\partial v_i}{\partial x_i} .$$

3.1.4 Substantial Time Derivative

Two different formulation of fluid flow are frequently used. These are the Eulerian and the Lagrangian formulation. In the Eulerian formulation, fluid flow is described from a point of view of a stationary observer, whereas in the Lagrangian formulation, the observer is moving with the fluid particles.

In the Eulerian formulation, once calculating the time derivative of a given flowing properties (e.g. a concentration of a substance or the temperature of the fluid), it is necessary to take into account the convective motion of the particles. Thus, the **substantial derivative** of a scalar quantity c is introduced,

$$(3\text{-}20) \quad \frac{Dc}{Dt} \equiv \frac{\partial c}{\partial t} + \mathbf{v} \cdot \nabla c .$$

Here the first term on the right-hand side represents the local time derivative (or partial derivative) of the scalar quantity c. It can be interpreted as a time rate of change of the scalar quantity once observing it from a fixed point. The second term results from the fluid motion.

For any scalar function $f(x,y,z,t)$ the following is valid:

$$\frac{D(\rho f)}{Dt} = \frac{\partial(\rho f)}{\partial t} + \mathbf{v} \cdot \nabla(\rho f) = \rho \frac{\partial f}{\partial t} + f \frac{\partial \rho}{\partial t} + \rho \left(u \frac{\partial f}{\partial x} + v \frac{\partial f}{\partial y} + w \frac{\partial f}{\partial z} \right) +$$

$$f \left(u \frac{\partial \rho}{\partial x} + v \frac{\partial \rho}{\partial y} + w \frac{\partial \rho}{\partial z} \right) = \rho \left(\frac{\partial f}{\partial t} + u \frac{\partial f}{\partial x} + v \frac{\partial f}{\partial y} + w \frac{\partial f}{\partial z} \right) +$$

$$f \left(\frac{\partial \rho}{\partial t} + u \frac{\partial \rho}{\partial x} + v \frac{\partial \rho}{\partial y} + w \frac{\partial \rho}{\partial z} \right) = \rho \frac{Df}{Dt} + f \frac{D\rho}{Dt}$$

.

The above expression is also valid for any vector function $\mathbf{f}(x,y,z,t)$.

If ρ is density, the second term on the right-hand-side can be further combined with the mass conservation equation.

3.1.5 Integral Theorems

In derivation of the conservation equations two integral theorems are frequently employed. The first one, the so called divergence theorem, allows replacing an integral over a volume with an integral over a surface that surrounds the volume. The second

one, referred to as the Leibniz's rule (or formula), allows to exchange the order of time differentiation and integration over a time-dependent domain.

The **divergence theorem** states that for an arbitrary closed region V with surface S and function $\varphi(x,y,z)$ with continuous first partial derivatives, the following is valid,

$$(3\text{-}21) \qquad \iiint\limits_{V} \nabla \varphi \, dV = \iint\limits_{S} \mathbf{n} \varphi \, dS \,.$$

Here $\mathbf{n}$ is a unit normal vector pointing outward from the surface S. Equation (3-21) is valid for φ which can be either a scalar, a vector or a tensor field.

The **Leibniz's formula** allows for calculation of the time derivative of the definite integral, where integration limits are function of time:

$$(3\text{-}22) \qquad \frac{d}{dt}\int\limits_{a(t)}^{b(t)} f(x,t)\,dx = \int\limits_{a(t)}^{b(t)} \frac{\partial f(x,t)}{\partial t}\,dx + f(b(t),t)\frac{db}{dt} - f(a(t),t)\frac{da}{dt}\,.$$

When integration of function $f(x,y,z,t)$ is performed on a surface $A(z,t)$ which is a function of distance z and time t, and which has a perimeter $P(z,t)$, the Leibniz's formula is as follows,

$$(3\text{-}23) \qquad \frac{\partial}{\partial t}\iint\limits_{A(z,t)} f(x,y;z,t)\,dA = \iint\limits_{A(z,t)} \frac{\partial f(x,y;z,t)}{\partial t}\,dA + \int\limits_{P(z,t)} f(x,y;z,t)\mathbf{v}\cdot\mathbf{n}\frac{dP}{\mathbf{n}\cdot\mathbf{n}_A}\,,$$

where $\mathbf{v}$ is a velocity vector and $\mathbf{n}$ and $\mathbf{n}_A$ are normal vectors explained in the figure below.
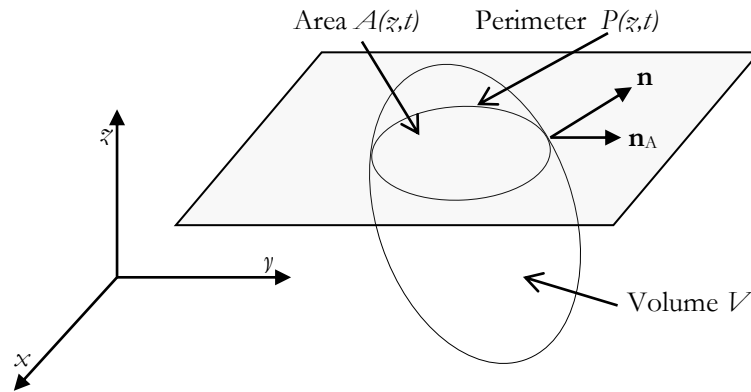
FIGURE 3-5. Area A and Perimeter P used in the Leibniz formula; $\mathbf{n}$ – a unit outward vector normal to surface surrounding volume V, $\mathbf{n}_A$ – a unit outward vector normal to P on the plain containing A.

In three-dimensional space, the formula (known also as the **Reynolds' transport theorem**) is as follows,

$$(3\text{-}24) \qquad \frac{d}{dt}\iiint\limits_{V(t)} f(\mathbf{r},t)\,dV = \iiint\limits_{V(t)} \frac{\partial f(\mathbf{r},t)}{\partial t}\,dV + \iint\limits_{S(t)} \mathbf{n}\cdot[f(\mathbf{r},t)\mathbf{v}]\,dS\,.$$

Here $\mathbf{v}$ is the velocity vector of surface S and $\mathbf{n}$ is an outward normal unit vector to surface S. The theorem is valid for scalar, vectorial and tensorial fields.
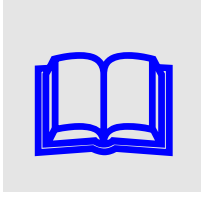
MORE READING: There are many excellent books dealing with mathematical tools in fluid mechanics. One strongly recommended here is a classical book by Rutherford Aris (*Vectors, Tensors, and the Basic Equations of Fluid Mechanics*, Dover Publications Inc. New York, ISBN 0-486-66110-5). This book not only introduces various topics in mathematical fluid mechanics, but also provides numerous examples and exercises to better elucidate this difficult domain.

3.2 Field Equations for Single-Phase Flows

Real fluids are collections of molecules that move around in respect to each other. Once trying to describe the motion of fluid, it is thus important to adopt a model that will approximate the fluid structure. In principle two such models are used in the theoretical fluid mechanics: the continuum model and the discrete model. Historically the continuum model was the first one which was adopted and still this model plays the major role in all kinds of engineering applications. In the following sections only the continuum model of fluids will be used. Since fluid mechanics is based on three fundamental principles, namely on the laws of conservation of mass, momentum and energy, they are treated in more detail below.

3.2.1 Mass Conservation

The mass conservation principle results from the fact that – in a framework of classical mechanics - mass cannot be created or destroyed. Thus, for a given material system (that is a system which boundaries are not crossed by mass) the following is valid,

(3-25) $\qquad \dfrac{Dm}{Dt} = 0$,

where m is the mass of the system. For a system with volume V the mass can be expressed in terms of the density ρ as,

$$m = \iiint\limits_V \rho dV \ .$$

Thus, the mass conservation equation reads,

(3-26) $\qquad \dfrac{D}{Dt} \iiint\limits_V \rho dV = 0$.

In view of the Reynolds' transport theorem, the mass conservation principle related to volume V and its surface S can be expressed by the following equation,

(3-27) $\qquad \iiint\limits_V \dfrac{\partial \rho}{\partial t} dV + \iint\limits_S \rho \mathbf{v} \cdot \mathbf{n} dS = 0$.

Here ρ is the fluid density, $\mathbf{v}$ is the fluid velocity vector and $\mathbf{n}$ is a vector normal to the surface S. The mass conservation equation can be transformed using the divergence

theorem, which describes the relation between the surface and the volume integrals as follows,

(3-28) $$\iint_S \rho\mathbf{v}\cdot\mathbf{n}dS = \iiint_V \nabla\cdot(\rho\mathbf{v})dV$$

Combining Eqs. (3-27) and (3-28) yields,

(3-29) $$\iiint_V \frac{\partial\rho}{\partial t}dV + \iiint_V \nabla\cdot(\rho\mathbf{v})dV = \iiint_V \left[\frac{\partial\rho}{\partial t}+\nabla\cdot(\rho\mathbf{v})\right]dV = 0\,.$$

Since the integration volume V is arbitrary, the expression under the integral must be equal to zero, and the **mass conservation equation** (also called the continuity equation) can be expressed as the following differential equation,

(3-30) $$\frac{\partial\rho}{\partial t}+\nabla\cdot(\rho\mathbf{v})=0\,.$$

This equation can be expressed in terms of the substantial derivative as follows. Since,

$$\frac{D\rho}{Dt}\equiv\frac{\partial\rho}{\partial t}+\mathbf{v}\cdot\nabla\rho\,,$$

then

$$\frac{\partial\rho}{\partial t}=\frac{D\rho}{Dt}-\mathbf{v}\cdot\nabla\rho\,,$$

and

$$\nabla\cdot(\rho\mathbf{v})=\rho\nabla\cdot\mathbf{v}+\mathbf{v}\cdot\nabla\rho\,.$$

Thus, the mass-conservation equation becomes,

(3-31) $$\frac{D\rho}{Dt}+\rho\nabla\cdot\mathbf{v}=0\,.$$

Note that Eqs. (3-30) and (3-31) are completely equivalent and no assumptions are made.

3.2.2   Momentum Conservation

The linear momentum conservation principle for fluids results from the Newton's second law applied to a control volume. Newton's second law for a material system moving relative to an inertial coordinate system is as follows,

(3-32) $$\mathbf{F}=\frac{D\mathbf{p}}{Dt}\,,$$

where $\mathbf{p}$ is the linear momentum of the system and $\mathbf{F}$ is the force acting on the system. The linear momentum of a differential fluid element with mass dm and velocity $\mathbf{v}$ is as follows,

$$(3\text{-}33) \quad d\mathbf{p} = dm\mathbf{v}.$$

The total momentum of a system with volume V is,

$$(3\text{-}34) \quad \mathbf{p} = \int_m \mathbf{v}\,dm = \iiint_V \mathbf{v}\rho\,dV.$$

The time derivative of the volume integral in Eq. (3-34) can be expanded using the Leibniz's and the divergence theorems as follows,

$$(3\text{-}35) \quad \frac{D}{Dt}\iiint_V \mathbf{v}\rho\,dV = \iiint_V \frac{\partial(\mathbf{v}\rho)}{\partial t}\,dV + \iint_S \mathbf{v}\rho\mathbf{v}\cdot\mathbf{n}\,dS =$$
$$\iiint_V \frac{\partial(\mathbf{v}\rho)}{\partial t}\,dV + \iiint_V \nabla\cdot\rho\mathbf{v}\mathbf{v}\,dV$$

The total force $\mathbf{F}$ acting on the system can be conveniently partitioned into the surface force $\mathbf{F}_S$, resulting from normal and tangential stresses applied on the surface S:

$$(3\text{-}36) \quad \mathbf{F}_S = -\iint_S p\mathbf{n}\,dS + \iint_S \mathbf{n}\cdot\boldsymbol{\tau}\,dS = -\iiint_V \nabla p\,dV + \iiint_V \nabla\cdot\boldsymbol{\tau}\,dV$$

and the body force $\mathbf{F}_B$, which – assuming that only the gravity force is involved – is as follows,

$$(3\text{-}37) \quad \mathbf{F}_B = \iiint_V \mathbf{g}\rho\,dV.$$

Substituting Eqs. (3-34) through (3-37) into Eq. (3-32) yields,

$$-\iiint_V \nabla p\,dV + \iiint_V \nabla\cdot\boldsymbol{\tau}\,dV + \iiint_V \rho\mathbf{g}\,dV = \iiint_V \frac{\partial(\mathbf{v}\rho)}{\partial t}\,dV + \iiint_V \nabla\cdot\rho\mathbf{v}\mathbf{v}\,dV,$$

which, for an arbitrary volume V is equivalent to the following partial differential equation,

$$(3\text{-}38) \quad \frac{\partial\rho\mathbf{v}}{\partial t} + \nabla\cdot\rho\mathbf{v}\mathbf{v} = -\nabla p + \nabla\cdot\boldsymbol{\tau} + \rho\mathbf{g}.$$

Equation (3-38) is a partial differential equation that describes the momentum conservation for fluid at any point in the flow domain. Solution of this equation provides the spatial distribution of pressure and velocities. The equation can be expressed in terms of the substantial derivative as follows. Since,

$$\frac{D(\rho\mathbf{v})}{Dt} \equiv \frac{\partial(\rho\mathbf{v})}{\partial t} + \mathbf{v}\cdot\nabla(\rho\mathbf{v}),$$

then

$$\frac{\partial(\rho\mathbf{v})}{\partial t} = \frac{D(\rho\mathbf{v})}{Dt} - \mathbf{v}\cdot\nabla(\rho\mathbf{v}).$$

But,

$$\frac{D(\rho\mathbf{v})}{Dt} = \rho\frac{D\mathbf{v}}{Dt} + \mathbf{v}\frac{D\rho}{Dt} = \rho\frac{D\mathbf{v}}{Dt} + \mathbf{v}(-\rho\nabla\cdot\mathbf{v}),$$

where the last term on the right-hand-side results from Eq. (3-31). Thus,

$$\frac{\partial(\rho\mathbf{v})}{\partial t} = \rho\frac{D\mathbf{v}}{Dt} - \mathbf{v}\rho\nabla\cdot\mathbf{v} - \mathbf{v}\cdot\nabla(\rho\mathbf{v}) = \rho\frac{D\mathbf{v}}{Dt} - \rho\nabla\cdot\mathbf{v}\mathbf{v}.$$

Finally, the momentum conservation equation becomes,

(3-39) $$\rho\frac{D\mathbf{v}}{Dt} = -\nabla p + \nabla\cdot\boldsymbol{\tau} + \rho\mathbf{g}.$$

Thus, the following equivalent forms of the momentum conservation equation can be written,

control volume formulations, resulting from Eqs. (3-32) through (3-37):

(3-40) $$\mathbf{F} = \mathbf{F}_S + \mathbf{F}_B = \frac{\partial}{\partial t}\iiint_V \mathbf{v}\rho dV + \iint_S \mathbf{v}\rho\mathbf{v}\cdot\mathbf{n}dS,$$

or

(3-41) $$-\iint_S p\mathbf{n}dS + \iint_S \mathbf{n}\cdot\boldsymbol{\tau}dS + \iiint_V \mathbf{g}\rho dV = \frac{\partial}{\partial t}\iiint_V \mathbf{v}\rho dV + \iint_S \mathbf{v}\rho\mathbf{v}\cdot\mathbf{n}dS.$$

Differential equation formulations,

$$\frac{\partial\rho\mathbf{v}}{\partial t} + \nabla\cdot\rho\mathbf{v}\mathbf{v} = -\nabla p + \nabla\cdot\boldsymbol{\tau} + \rho\mathbf{g},$$

or, in terms of the total derivative,

$$\rho\frac{D\mathbf{v}}{Dt} = -\nabla p + \nabla\cdot\boldsymbol{\tau} + \rho\mathbf{g}.$$

Depending on the type of an application, the most convenient formulation can be chosen.

3.2.3 Energy Conservation

The fluid energy conservation equation is obtained from the first law of thermodynamics applied to a fluid control volume:

$$(3\text{-}42) \qquad \frac{dE_T}{dt} = q - N .$$

Here E_T is the total energy of the fluid, including the internal and the kinetic energy, q is the heat added to the control volume per unit time from surroundings and N is the work done per unit time by fluid in the control volume on surroundings. The potential energy will be absorbed as the work done by the system against gravity.

The total energy of the fluid in a control volume with surface S and volume V is as follows,

$$E_T = \iiint_V \rho e_T dV = \iiint_V \rho \left(e_I + \frac{1}{2}v^2 \right) dV .$$

The time derivative of the total energy can be expanded using the Reynolds' transport theorem and the divergence formula as follows,

$$\frac{d}{dt}\iiint_V \left(e_I + \frac{1}{2}v^2 \right)\rho dV = \iiint_V \frac{\partial\left[\left(e_I + \frac{1}{2}v^2 \right)\rho\right]}{\partial t} dV + \iint_S \rho \left(e_I + \frac{1}{2}v^2 \right)\mathbf{v}\cdot\mathbf{n}dS =$$

$$\iiint_V \frac{\partial\left[\left(e_I + \frac{1}{2}v^2 \right)\rho\right]}{\partial t} dV + \iiint_V \nabla\cdot\mathbf{v}\rho\left(e_I + \frac{1}{2}v^2 \right) dV$$

The rate of heat added to the system can be calculated as a sum of the heat added by conduction through the control volume surface,

$$q_S = -\iint_S \mathbf{q}''\cdot\mathbf{n}dS = -\iiint_V \nabla\cdot\mathbf{q}''dV .$$

Here $\mathbf{q}''$ is the heat flux vector at surface S. The heat added due to volumetric heat sources q''' is as follows,

$$q_B = \iiint_V q'''dV .$$

In the same way, the total rate of work can be partitioned into the work performed by the surface forces (pressure and shear),

$$N_S = \iint_S p\mathbf{v}\cdot\mathbf{n}dS - \iint_S (\boldsymbol{\tau}\cdot\mathbf{v})\cdot\mathbf{n}dS = \iiint_V \nabla\cdot p\mathbf{v}dV - \iiint_V \nabla\cdot(\boldsymbol{\tau}\cdot\mathbf{v})dV ,$$

and the work performed by the bulk forces (here only gravity is considered),

$$N_B = \iiint\limits_V \mathbf{g} \cdot \mathbf{v} \rho dV \ .$$

Thus, the energy conservation equation can be written in a form of a partial differential equation as follows,

$$(3\text{-}43) \quad \frac{\partial\left[\left(e_I + \dfrac{1}{2}v^2\right)\rho\right]}{\partial t} + \nabla \cdot \mathbf{v}\rho\left(e_I + \frac{1}{2}v^2\right) = -\nabla \cdot \mathbf{q}'' + \mathbf{g} \cdot \mathbf{v}\rho -$$
$$\nabla \cdot \mathbf{v}p + \nabla \cdot (\boldsymbol{\tau} \cdot \mathbf{v}) + q'''$$

This equation can be formulated in terms of various primitive variables, depending on the type of application. In case of heat conduction in solids, the equation is expressed in terms of temperature. For fluids, either enthalpy or temperature formulation can be chosen.

To derive various formulations, it is useful to subtract the kinetic energy from Eq. (3-43) and to obtain the equation of change for the internal energy only. First, the equation of change for the kinetic energy can be obtained by the dot product of the velocity vector $\mathbf{v}$ with the equation of motion, Eq. (3-38). After doing so and making some rearrangements, the **equation of change for kinetic energy** is as follows[3-1],

$$(3\text{-}44) \quad \frac{\partial\left(\frac{1}{2}\rho v^2\right)}{\partial t} = -\nabla \cdot \left(\frac{1}{2}\rho v^2 \mathbf{v}\right) - \nabla \cdot (p\mathbf{v}) - p(-\nabla \cdot \mathbf{v}) +$$
$$\nabla \cdot (\boldsymbol{\tau} \cdot \mathbf{v}) - (-\boldsymbol{\tau} : \nabla\mathbf{v}) + \rho\mathbf{v} \cdot \mathbf{g}$$

By subtracting the kinetic energy of fluid given by Eq. (3-44), from the energy conservation equation given by Eq. (3-43), the **equation of change for internal energy** is obtained as follows,

$$(3\text{-}45) \quad \frac{\partial(e_I\rho)}{\partial t} + \nabla \cdot \rho e_I \mathbf{v} = -\nabla \cdot \mathbf{q}'' - p\nabla \cdot \mathbf{v} + \boldsymbol{\tau} : \nabla\mathbf{v} + q''' \ .$$

Using the substantial derivative, the equation becomes,

$$(3\text{-}46) \quad \rho\frac{De_I}{Dt} = -\nabla \cdot \mathbf{q}'' - p\nabla \cdot \mathbf{v} + \boldsymbol{\tau} : \nabla\mathbf{v} + q''' \ .$$

This equation can be expressed in terms of fluid enthalpy or fluid temperature by using the following relationships, known from the thermodynamics:

$$e_I = i - \frac{p}{\rho} \ .$$

Thus,

$$\frac{De_I}{Dt} = \frac{Di}{Dt} - \frac{D}{Dt}\left(\frac{p}{\rho}\right) = \frac{Di}{Dt} - \frac{1}{\rho}\frac{Dp}{Dt} + \frac{p}{\rho^2}\frac{D\rho}{Dt} = \frac{Di}{Dt} - \frac{1}{\rho}\frac{Dp}{Dt} - \frac{p}{\rho}\nabla\cdot\mathbf{v}.$$

The equation of change for the fluid enthalpy now becomes,

(3-47) $\quad \rho\dfrac{Di}{Dt} = -\nabla\cdot\mathbf{q}'' + \boldsymbol{\tau}:\nabla\mathbf{v} + \dfrac{Dp}{Dt} + q'''.$

Since the enthalpy is a function of the local temperature and pressure, the following is valid,

$$\frac{Di}{Dt} = \left(\frac{Di}{DT}\right)_p\frac{DT}{Dt} + \left(\frac{Di}{Dp}\right)_T\frac{Dp}{Dt} = c_p\frac{DT}{Dt} + \left[\upsilon - T\left(\frac{\partial\upsilon}{\partial T}\right)_p\right]\frac{Dp}{Dt} =$$
$$c_p\frac{DT}{Dt} + \left[\frac{1}{\rho} - T\left(\frac{\partial(1/\rho)}{\partial T}\right)_p\right]\frac{Dp}{Dt} = c_p\frac{DT}{Dt} + \frac{1}{\rho}\left[1 + \left(\frac{\partial\ln\rho}{\partial\ln T}\right)_p\right]\frac{Dp}{Dt}$$,

and the energy equation can be expressed in terms of the fluid temperature as,

(3-48) $\quad \rho c_p\dfrac{DT}{Dt} = -\nabla\cdot\mathbf{q}'' + \boldsymbol{\tau}:\nabla\mathbf{v} - \left(\dfrac{\partial\ln\rho}{\partial\ln T}\right)_p\dfrac{Dp}{Dt} + q'''.$

The equation can be further transformed by noting that,

(3-49) $\quad -\left(\dfrac{\partial\ln\rho}{\partial\ln T}\right)_p = -\left(\dfrac{1/\rho\,\partial\rho}{1/T\,\partial T}\right)_p = -\dfrac{T}{\rho}\left(\dfrac{\partial\rho}{\partial T}\right)_p = T\beta,$

where β is the thermal expansion coefficient. Thus, the energy equation becomes,

(3-50) $\quad \rho c_p\dfrac{DT}{Dt} = -\nabla\cdot\mathbf{q}'' + \boldsymbol{\tau}:\nabla\mathbf{v} + T\beta\dfrac{Dp}{Dt} + q'''.$

The energy equation given by Eq. (3-50) is exact, since no terms have been neglected. However, depending on application, some terms in the equation are significantly smaller than the other and can be neglected. For example, when applying the energy equation to coolants in nuclear reactor cores, the energy source term is dominant and the viscous dissipation term $\boldsymbol{\tau}:\nabla\mathbf{v}$ along with the pressure work term $T\beta\dfrac{Dp}{Dt}$ has practically no influence on the coolant temperature distribution. Neglecting these terms, the energy conservation equation becomes,

(3-51) $\quad \rho c_p\dfrac{DT}{Dt} = -\nabla\cdot\mathbf{q}'' + q'''.$

3.2.4 Generic Conservation Equation

The derived conservation equations for mass, momentum and energy exhibit some similarities in terms of various terms that are included and in the form of the

equations. This allows introducing a generic conservation equation, both in the differential and in the integral form, as presented in TABLE 3.1.

TABLE 3.1. Definition of symbols used in the generic conservation equation.

Equation	$\dfrac{\partial(\rho\psi)}{\partial t} + \nabla\cdot(\rho\mathbf{v}\,\psi) = -\nabla\cdot\mathbf{J} + \rho\phi$ $\iiint\limits_V \dfrac{\partial(\rho\psi)}{\partial t}\,dV + \iint\limits_S (\rho\mathbf{v}\,\psi)dS = -\iint\limits_S \mathbf{J}dV + \iiint\limits_V \rho\phi dV$		
	ψ	$\mathbf{J}$	ϕ
Mass	1	0	0
Momentum	$\mathbf{v}$	$p\mathbf{I} - \boldsymbol{\tau}$	$\mathbf{g}$
Energy	$e_I + \dfrac{1}{2}v^2$	$\mathbf{q}'' + (p\mathbf{I} - \boldsymbol{\tau})\cdot\mathbf{v}$	$\mathbf{g}\cdot\mathbf{v}$

3.2.5 Constitutive Equations

As can be seen the conservation equations do not constitute a closed system of equations and require additional relationships in order to be solved. This is simply due to the fact that the number of unknowns in the equations is larger than the number of equations. To close the system, the constitutive equations are used. Such equations describe the physical properties of the fluid or contain various hypotheses concerning the fluid behaviour.

The first constitutive equation stems from the **Newton's hypothesis** which assumes the proportionality between fluid stresses and deformations. Fluids that are well described by the Newton's hypothesis are termed as Newtonian fluids. The stress tensor for such fluids is expressed in terms of the deformation tensor as follows:

(3-52) $\boldsymbol{\tau} = \mu\!\left[\nabla\mathbf{v} + (\nabla\mathbf{v})^T\right] + \lambda(\nabla\cdot\mathbf{v})\mathbf{I}$.

Here $\boldsymbol{\tau}$ [N m^{-2}] is the shear stress tensor in the fluid, μ [Pa s] is the molecular dynamic viscosity of fluid, λ [Pa s] is the bulk viscosity and $\mathbf{v}$ [m s^{-1}] is the fluid velocity vector. The expression in the rectangular parentheses is the so-called **deformation rate tensor** (or, strictly speaking, a double of it):

$\mathbf{D} = \dfrac{1}{2}\!\left[\nabla\mathbf{v} + (\nabla\mathbf{v})^T\right]$, thus

Also, the **vorticity tensor** is defined as,

$\mathbf{W} = \dfrac{1}{2}\!\left[\nabla\mathbf{v} - (\nabla\mathbf{v})^T\right]$.

Here,

$$\nabla \mathbf{v} = \begin{bmatrix} \dfrac{\partial u}{\partial x} & \dfrac{\partial u}{\partial y} & \dfrac{\partial u}{\partial z} \\[2mm] \dfrac{\partial v}{\partial x} & \dfrac{\partial v}{\partial y} & \dfrac{\partial v}{\partial z} \\[2mm] \dfrac{\partial w}{\partial x} & \dfrac{\partial w}{\partial y} & \dfrac{\partial w}{\partial z} \end{bmatrix}; \qquad (\nabla \mathbf{v})^{T} = \begin{bmatrix} \dfrac{\partial u}{\partial x} & \dfrac{\partial v}{\partial x} & \dfrac{\partial w}{\partial x} \\[2mm] \dfrac{\partial u}{\partial y} & \dfrac{\partial v}{\partial y} & \dfrac{\partial w}{\partial y} \\[2mm] \dfrac{\partial u}{\partial z} & \dfrac{\partial v}{\partial z} & \dfrac{\partial w}{\partial z} \end{bmatrix}.$$

It can be seen that:

$$\nabla \mathbf{v} = \mathbf{D} + \mathbf{W}.$$

Thus, the shear stress tensor can be written as,

$$\boldsymbol{\tau} = 2\mathbf{D}\mu + \lambda(\nabla \cdot \mathbf{v})\mathbf{I}.$$

The constitutive equation that is used to close the energy equation is based on the **Fourier hypothesis**, which relates the heat flux to the temperature gradient as follows,

(3-53) $\mathbf{q}'' = -\lambda \nabla T$.

Here $\mathbf{q}''$ is the heat flux vector [W m^{-2}], T is the temperature [K] and λ is the thermal conductivity of fluid [W m^{-1} K^{-1}].

In addition, to constitutive equations belong property functions that express the physical properties of fluid (density, viscosity, thermal conductivity, specific heat) in terms of the solved primitive variables such as pressure and temperature.

3.2.6   Conservation Equations for Ideal Fluids

An ideal fluid is such a Newtonian fluid which has constant density and viscosity. In this case the conservation equations are as follows.

Mass:

(3-54) $\nabla \cdot (\rho \mathbf{v}) = 0$.

Momentum:

(3-55) $\dfrac{\partial \mathbf{v}}{\partial t} + \nabla \cdot \mathbf{v}\mathbf{v} = -\dfrac{1}{\rho}\nabla p + \nu \nabla^{2}\mathbf{v} + \mathbf{g}$.

Energy:

(3-56) $\dfrac{\partial i}{\partial t} + \nabla \cdot (i\mathbf{v}) = \dfrac{\lambda}{c_{p}\rho}\nabla^{2}i + \dfrac{1}{\rho}\dfrac{Dp}{Dt} + \nu \Phi_{v}$.

The last term in the energy equation describes the rate of irreversible conversion to internal energy, previously denoted as $\boldsymbol{\tau} : \nabla \mathbf{v}$. This term can cause significant temperature changes of fluid only when high velocity gradients occur.

3.2.7   Conservation Equations for Ideal Gas

For ideal gas the equation of state is as follows,

$$(3\text{-}57) \qquad \rho = \frac{p}{RT}.$$

Thus, the gas density is a function of both pressure and temperature. Assuming also that the gas viscosity and conductivity are constant, the conservation equations become as follows,

mass

$$(3\text{-}58) \qquad \frac{\partial \rho}{\partial t} + \nabla \cdot (\rho \mathbf{v}) = 0,$$

momentum

$$(3\text{-}59) \qquad \frac{\partial \rho \mathbf{v}}{\partial t} + \nabla \cdot \rho \mathbf{v} \mathbf{v} = -\nabla p + \mu \nabla^2 \mathbf{v} + \rho \mathbf{g},$$

energy

$$(3\text{-}60) \qquad \rho c_p \frac{DT}{Dt} = \lambda \nabla^2 T - p (\nabla \cdot \mathbf{v}).$$

The last term in the energy equation can be omitted in many cases but it causes significant temperature changes of gas flowing in expansions and compressions, such as in turbines and compressors.

3.2.8   Turbulence in Incompressible Flows

Viscous flows can be either laminar or turbulent, depending on the flow structure. In laminar flows liquid appears to flow in layers, which have stable and stationary character. On the contrary, in turbulent flows fluid particles move chaotically and flow is never stationary. Experiments performed in pipes indicate that the transition from laminar to turbulent flow occurs when the Reynolds number is larger than a certain critical value. For pipes, it has been established that laminar flow occurs when,

$$\text{Re} = \frac{\rho U D}{\mu} < 2300.$$

Above this value, the flow transits from laminar to turbulent.

Practically all fluid flows in industrial applications are turbulent in nature. In fuel assemblies of nuclear reactors the Reynolds number is usually higher than $2 \cdot 10^5$. In other components of the nuclear power plants the Reynolds number can even be higher and the flows are fully developed turbulent flows.

Turbulent flows are never stationary, since the local instantaneous parameters (velocity, pressure, and temperature) are fluctuating around mean values, as shown in FIGURE 3-6.
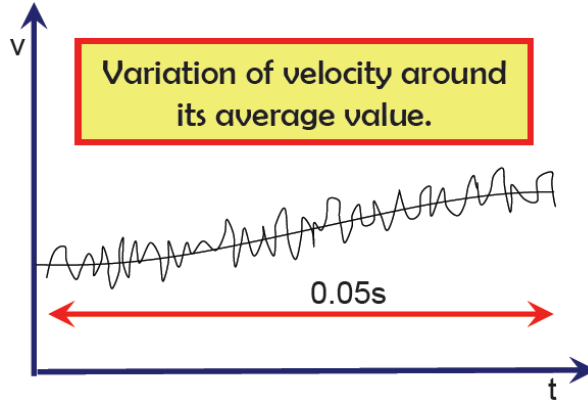
FIGURE 3-6. Velocity fluctuation in turbulent flow.

Any turbulent parameter can be represented as a sum of its average value and its fluctuating part as,

(3-61) $\quad \varphi(\mathbf{r},t) = \overline{\varphi}(\mathbf{r},t) + \varphi'(\mathbf{r},t),$

where the averaged value can be obtained as,

(3-62) $\quad \overline{\varphi}(\mathbf{r},t) = \dfrac{1}{\Delta t} \displaystyle\int_{t}^{t+\Delta t} \varphi(\mathbf{r},\tau) d\tau ,$

where Δt is a time interval that is larger than any significant fluctuation period of the parameter φ but is smaller than the time scale of the averaged parameter.

The **time averaging operator** has the following properties, which can be directly derived from the definition given by (3-62):

- average of a sum of two parameters is equal to the sum of the averages,

(3-63) $\quad \overline{\varphi(t) + \psi(t)} = \overline{\varphi}(t) + \overline{\psi}(t) ,$

- average of the fluctuating part is equal to zero,

(3-64)
$$\overline{\varphi'(t)} = \overline{\varphi(t) - \overline{\varphi}(t)} = \dfrac{1}{\Delta t} \int_{t}^{t+\Delta t} \left[\varphi(\tau) - \overline{\varphi}(\tau)\right] d\tau =$$
$$\dfrac{1}{\Delta t} \int_{t}^{t+\Delta t} \left[\varphi(\tau)\right] d\tau - \overline{\varphi}(t) \dfrac{1}{\Delta t} \int_{t}^{t+\Delta t} d\tau = \overline{\varphi}(t) - \overline{\varphi}(t) = 0$$

- average of the time derivative is equal to the time derivative of the average,

$$(3\text{-}65) \qquad \overline{\frac{\partial \varphi(t)}{\partial t}} = \frac{1}{\Delta t} \int\limits_{t}^{t+\Delta t} \frac{\partial \varphi(\tau)}{\partial \tau} d\tau \underset{\substack{Leibniz \\ rule}}{=} \frac{1}{\Delta t} \left(\varphi\big|_{t+\Delta t} - \varphi\big|_{t} \right) = \frac{\partial \overline{\varphi}(t)}{\partial t},$$

- average of the space derivative is equal to the space derivative of the average,

$$(3\text{-}66) \qquad \overline{\frac{\partial \varphi(t)}{\partial x}} = \frac{1}{\Delta t} \int\limits_{t}^{t+\Delta t} \frac{\partial \varphi(\tau)}{\partial x} d\tau = \frac{\partial}{\partial x} \frac{1}{\Delta t} \int\limits_{t}^{t+\Delta t} \varphi(\tau) d\tau = \frac{\partial \overline{\varphi}(t)}{\partial x}.$$

The time averaging can be applied to the instantaneous equations of motion, which yields the Reynolds Averaged Navier-Stokes (RANS) equations. The equations are expressed in terms of both the mean and fluctuating quantities. These fluctuating quantities have to be related to the mean quantities and to their gradients by proper closure relationships.

Consider incompressible turbulent flow with constant transport properties and with the following fluctuating variables,

$$(3\text{-}67) \qquad u = \overline{u} + u',\, v = \overline{v} + v',\, w = \overline{w} + w',\, p = \overline{p} + p',\, T = \overline{T} + T'.$$

Substituting expressions for velocities in Eq. (3-67) into the mass conservation equation yields,

$$(3\text{-}68) \qquad
\begin{aligned}
&\overline{\frac{\partial u}{\partial x} + \frac{\partial v}{\partial y} + \frac{\partial w}{\partial z}} = \frac{\partial \overline{u}}{\partial x} + \frac{\partial \overline{v}}{\partial y} + \frac{\partial \overline{w}}{\partial z} + \frac{\partial \overline{u'}}{\partial x} + \frac{\partial \overline{v'}}{\partial y} + \frac{\partial \overline{w'}}{\partial z} = \\
&\frac{\partial \overline{u}}{\partial x} + \frac{\partial \overline{v}}{\partial y} + \frac{\partial \overline{w}}{\partial z} = 0
\end{aligned},$$

and, as a consequence,

$$(3\text{-}69) \qquad \frac{\partial u'}{\partial x} + \frac{\partial v'}{\partial y} + \frac{\partial w'}{\partial z} = 0.$$

Thus the mean and the fluctuating velocity components each separately satisfy the mass conservation equation. In the Reynolds-Averaged Navier-Stokes (RANS) equations, only the equations for the mean values are considered.

The same procedure can be applied to the momentum equation, which yields,

$$(3\text{-}70) \qquad \rho \frac{D\overline{\mathbf{v}}}{Dt} = -\nabla \overline{p} + \nabla \cdot \boldsymbol{\tau}_e + \rho \mathbf{g},$$

where $\boldsymbol{\tau}_e$ is the **effective stress tensor** which consists of a laminar part and a turbulent part as follows,

$$(3\text{-}71) \qquad \boldsymbol{\tau}_e = \mu \left[\nabla \overline{\mathbf{v}} + \left(\nabla \overline{\mathbf{v}} \right)^T \right] + \boldsymbol{\tau}_t.$$

The apparent **turbulent stress tensor** is formally equal to,

$$(3\text{-}72) \quad \boldsymbol{\tau}_t = -\rho \begin{bmatrix} \overline{u'u'} & \overline{u'v'} & \overline{u'w'} \\ \overline{v'u'} & \overline{v'v'} & \overline{v'w'} \\ \overline{w'u'} & \overline{w'v'} & \overline{w'w'} \end{bmatrix}.$$

However, Eq. (3-72) introduces 6 new unknowns and thus is not very useful in practical applications. The traditional modelling assumption, which was first proposed by Boussinesq, is to model the turbulent tensor in analogy to the laminar one as,

$$(3\text{-}73) \quad \boldsymbol{\tau}_t = \mu_t \left[\nabla \overline{\mathbf{v}} + \left(\nabla \overline{\mathbf{v}} \right)^T \right],$$

where μ_t is the turbulent viscosity, for which several models exist. One popular model used recently for practical computations is the **k-ε model**, in which the turbulent viscosity is calculated as,

$$(3\text{-}74) \quad \mu_t = C_\mu \rho \frac{k^2}{\varepsilon},$$

where k and ε are the turbulent kinetic energy and the turbulent energy dissipation, respectively, which are computed from the following two differential equations,

$$(3\text{-}75) \quad \frac{\partial \rho k}{\partial t} + \nabla \cdot \left(\rho \overline{\mathbf{v}} k \right) - \nabla \cdot \left[\left(\mu + \frac{\mu_t}{\sigma_k} \right) \nabla k \right] = P + G - \rho \varepsilon,$$

$$(3\text{-}76) \quad \frac{\partial \rho \varepsilon}{\partial t} + \nabla \cdot \left(\rho \overline{\mathbf{v}} \varepsilon \right) - \nabla \cdot \left[\left(\mu + \frac{\mu_t}{\sigma_\varepsilon} \right) \nabla \varepsilon \right] = C_1 \frac{\varepsilon}{k} \left(P + C_3 \max(G,0) \right) - C_2 \rho \frac{\varepsilon^2}{k},$$

where P is the shear production term,

$$(3\text{-}77) \quad P = \mu_e \nabla \overline{\mathbf{v}} \cdot \left[\nabla \overline{\mathbf{v}} + \left(\nabla \overline{\mathbf{v}} \right)^T \right] - \frac{2}{3} \nabla \cdot \overline{\mathbf{v}} \left(\mu_e \nabla \cdot \overline{\mathbf{v}} + \rho k \right),$$

and G is the buoyant production term defined as,

$$(3\text{-}78) \quad G = \frac{\mu_e}{\rho \sigma_T} \mathbf{g} \cdot \nabla \rho \underset{\text{Boussinesq \quad approximation}}{\Longrightarrow} \frac{\mu_e}{\sigma_T} \beta \mathbf{g} \cdot \nabla T.$$

The turbulence model given by Eqs. (3-75) through (3-78) contains five constants, which more-or-less are treated as universal constants for channel flows and should not be changed by the user when there are no well supported reasons for doing that. The constants are as follows,

$$(3\text{-}79) \quad C_\mu = 0.09, \quad C_1 = 1.44, \quad C_2 = 1.92, \quad \sigma_k = 1.0, \quad \sigma_\varepsilon = 1.3.$$

Close to walls the turbulence model is not valid, and instead a so-called **logarithmic law-of-the-wall** is applied. In computations, first cell centre should be located at a certain distance from the wall, which corresponds approximately $y^+ \sim 25$, where y^+ is a dimensionless distance to the wall given as,

$$(3\text{-}80) \qquad y^+ = \frac{y u_\tau}{\nu}.$$

Here y is the distance from the wall in [m] and u_τ is the **friction velocity** defined in terms of the wall shear stress τ_w as,

$$(3\text{-}81) \qquad u_\tau = \sqrt{\frac{\tau_w}{\rho}}.$$

The **logarithmic velocity distribution** in the boundary layer is then given as,

$$(3\text{-}82) \qquad u^+ = \frac{1}{\kappa} \ln y^+ + B,$$

where κ and B are boundary layer constants and,

$$(3\text{-}83) \qquad u^+ = \frac{u}{u_\tau},$$

is a dimensionless velocity in the boundary layer.

3.3 Field Equations for Multi-Phase Flows

For single-phase flows the local conservation equations are valid at any point inside the considered flow field. Multi-phase flows contain several phases separated from each other with an interface. In principle, single-phase conservation equations are valid inside each of the phases; however, new type of conservation equations – so called jump conditions – have to be formulated for the interface.

The conservation equations for multi-phase flows can be formulated on various levels of approximations. The most general and rigorous approach is to use single-phase equations for each of the phases, treating the interface as a part of the solution. These types of equations are called the local instantaneous conservation equations. Another formulation is based on averaged conservation equations in which each phase is described with field equations valid in the whole domain of interest. This type of approach is called two-fluid, or more general, multi-fluid model of two-phase flows. In the following sections both the instantaneous and averaged equations are described in a more detail.

3.3.1 Local Instantaneous Conservation Equations

The starting point of any formulation of field equations for multi-phase flows are the single-phase conservation equations, derived in Sections 3.2.1, 3.2.2 and 3.2.3. The equations are as follow,

mass conservation of phase k:

(3-84) $\qquad \dfrac{\partial \rho_k}{\partial t} + \nabla \cdot \left(\rho_k \mathbf{v}_k \right) = 0 ,$

momentum conservation of phase k:

(3-85) $\qquad \dfrac{\partial \rho_k \mathbf{v}_k}{\partial t} + \nabla \cdot \rho_k \mathbf{v}_k \mathbf{v}_k = -\nabla p_k + \nabla \cdot \boldsymbol{\tau}_k + \rho_k \mathbf{g} ,$

energy conservation of phase k:

(3-86)
$$\dfrac{\partial \left[\left(e_{I,k} + \dfrac{1}{2} v_k^2 \right) \rho_k \right]}{\partial t} + \nabla \cdot \mathbf{v} \rho_k \left(e_{I,k} + \dfrac{1}{2} v_k^2 \right) = -\nabla \cdot \mathbf{q}_k'' + \mathbf{g} \cdot \mathbf{v}_k \rho_k -$$
$$\nabla \cdot \mathbf{v}_k p_k + \nabla \cdot \left(\boldsymbol{\tau}_k \cdot \mathbf{v}_k \right) + q_k'''$$

These equations can be solved provided proper initial and boundary conditions are formulated. Since the interface is one of the boundaries, special conditions – called jump conditions – have to be formulated. These conditions result from the conservation of mass, momentum and energy once crossing the interface, and are as follows:

mass jump condition:

(3-87) $\qquad \rho_1 \left(\mathbf{v}_1 - \mathbf{v}_i \right) \cdot \mathbf{n}_1 + \rho_2 \left(\mathbf{v}_2 - \mathbf{v}_i \right) \cdot \mathbf{n}_2 = 0 ,$

momentum jump condition:

(3-88) $\qquad \left[\rho_1 \left(\mathbf{v}_1 - \mathbf{v}_i \right) \mathbf{v}_1 + p_1 \mathbf{I} - \boldsymbol{\tau}_1 \right] \cdot \mathbf{n}_1 + \left[\rho_2 \left(\mathbf{v}_2 - \mathbf{v}_i \right) \mathbf{v}_2 + p_2 \mathbf{I} - \boldsymbol{\tau}_2 \right] \cdot \mathbf{n}_2 = -\left(t_\alpha^i a^{\alpha\beta} \rho \right)_{,\beta} ,$

energy jump condition:

(3-89)
$$\left[\rho_1 \left(\mathbf{v}_1 - \mathbf{v}_i \right) \left(e_{I,1} + \dfrac{1}{2} v_1^2 \right) + \left(p_1 \mathbf{I} - \boldsymbol{\tau}_1 \right) \cdot \mathbf{v}_1 + \mathbf{q}_1'' \right] \cdot \mathbf{n}_1 +$$
$$\left[\rho_2 \left(\mathbf{v}_2 - \mathbf{v}_i \right) \left(e_{I,2} + \dfrac{1}{2} v_2^2 \right) + \left(p_2 \mathbf{I} - \boldsymbol{\tau}_2 \right) \cdot \mathbf{v}_2 + \mathbf{q}_2'' \right] \cdot \mathbf{n}_2 = -\left(t_\alpha^i a^{\alpha\beta} \rho \cdot \mathbf{v}_i \right)_{,\beta} .$$

FIGURE 3-7 shows the various velocity and normal vectors at the interface used in the formulation of the jump conditions. According to a convention, the interface-normal vector for phase *k* points outwards from phase *k*.

The terms on the right-hand-sides of Eqs. (3-88) and (3-89) represent the momentum source and the work performed by the surface tension, respectively, where $t_\alpha^i = \partial x^i / \partial u^\alpha$ is the hybrid tensor between the space (*xⁱ*) and the surface (*uᵅ*)

coordinates, $a^{\alpha\beta}$ is the metric tensor of the interface and $(\ )_{,\beta}$ denotes the surface covariant derivative.
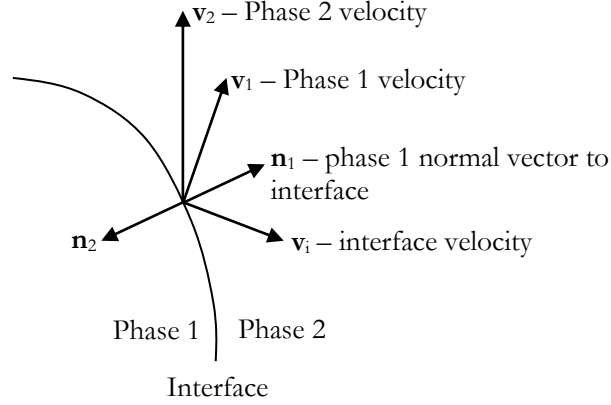

FIGURE 3-7. Interface with pertinent normal and velocity vectors.

3.3.2 Time-Averaged Conservation Equations

The local instantaneous equations presented in the previous section can be solved using numerical approaches developed for single-phase flows and extended with algorithms to track or capture the interface. Such solutions contain all details of the flow, including the transient evolution of the interface. In many practical applications, however, such detailed solutions cannot be obtained due to a tremendous computational effort that would be required. In such cases an approximation based on averaging of the conservation equations can be used.

There are various averaging procedures used in a formulation of the multi-fluid model of multi-phase flows. These procedures employ time, volume or ensemble averaging techniques. The latter technique is based on a statistical averaging of a sample of equivalent flow configurations and is commonly considered as the most rigorous averaging approach from the mathematical point of view. However, based on the Birkhoff's ergodic theorem it can be proved that all above mentioned averaging techniques are equivalent and lead to the same consistent set of averaged conservation equations. The differences rest in definitions of the averaged parameters.
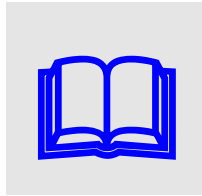
MORE READING: There is a broad literature dealing with the averaging techniques used in modelling of multiphase flows. The interesting reader is advised to consult any of books dealing with the fundamentals of multiphase flows, e.g. *Theory of Multicomponent Fluids* by D.A. Drew and S.L. Passman[3-3], *Thermo-Fluid Dynamics of Two-Phase Flow* by M. Ishii and T. Hibiki, or *Fundamentals of Multiphase Flow* by C.E. Brennen[3-2]. An excellent introduction to one-dimensional two-phase flows is given in *One-Dimensional Two-Phase Flow* by G.B. Wallis[3-5].

The instantaneous conservation equations given by Eqs. (3-84) through (3-86) can be written in a short form as,

$$(3\text{-}90) \qquad \frac{\partial(\rho_k \psi_k)}{\partial t} + \nabla \cdot \left(\rho_k \mathbf{v}_k \psi_k\right) = -\nabla \cdot \mathbf{J}_k + \rho_k \phi_k \ ,$$

where the parameters ψ_k, $\mathbf{J}_k$ and ϕ_k for each conservation equation are given in TABLE 3.2.

TABLE 3.2. Definition of symbols used in the generic conservation equation.

Equation	ψ_k	$\mathbf{J}_k$	ϕ_k
Mass	1	0	0
Linear momentum	$\mathbf{v}_k$	$p_k\mathbf{I} - \boldsymbol{\tau}_k$	$\mathbf{g}$
Total energy	$e_{I,k} + \dfrac{1}{2}v_k^2$	$\mathbf{q}_k'' + \left(p_k\mathbf{I} - \boldsymbol{\tau}_k\right)\cdot\mathbf{v}_k$	$\mathbf{g}\cdot\mathbf{v}_k$

Time-averaging of Eq. (3-90) is performed as follows,

$$(3\text{-}91)\quad \frac{1}{\Delta t}\int_{[\Delta t]}\frac{\partial(\rho_k\psi_k)}{\partial t}dt + \frac{1}{\Delta t}\int_{[\Delta t]}\nabla\cdot(\rho_k\mathbf{v}_k\psi_k)dt = \frac{1}{\Delta t}\int_{[\Delta t]}-\nabla\cdot\mathbf{J}_k dt + \frac{1}{\Delta t}\int_{[\Delta t]}\rho_k\phi_k dt,$$

where Δt is the averaging time interval. During this interval at any point P of the flow domain the existence of phase k can be described by the following phase indicator function, $X_k(P,t)$, shown in FIGURE 3-8:
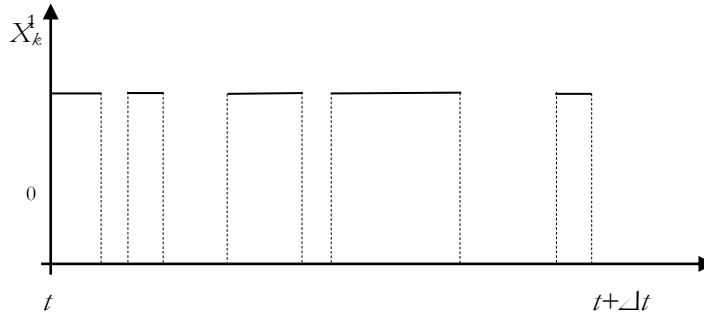
FIGURE 3-8. Phase indicator function over the averaging period.

$$(3\text{-}92)\quad X_k(P,t)=\begin{cases}1 & \text{if } P \text{ is occupied by phase } k \text{ at time } t \\ 0 & \text{if } P \text{ is not occupied by phase } k \text{ at time } t\end{cases}$$

Taking into account the Leibniz rule, the first term on the right-hand-side of Eq. (3-91) can be written as,

$$(3\text{-}93)\quad \frac{1}{\Delta t}\int_{[\Delta t]}\frac{\partial(\rho_k\psi_k)}{\partial t}dt = \frac{\partial}{\partial t}\left[\frac{1}{\Delta t}\int_{[\Delta t]}(\rho_k\psi_k)dt\right] - \frac{1}{\Delta t}\sum_{disc\in[\Delta t]}\frac{1}{|\mathbf{v}_i\cdot\mathbf{n}_k|}(\rho_k\psi_k)(\mathbf{v}_i\cdot\mathbf{n}_k).$$

The summation on the right-hand-side takes place over all time instances where the phase indicator function X_k suffers from a discontinuity.

Using the Gauss theorem, the second and third terms in Eq. (3-91) are as follows,

(3-94)
$$\frac{1}{\Delta t} \int_{[\Delta t]} \nabla \cdot \left(\rho_k \mathbf{v}_k \psi_k \right) dt = \nabla \cdot \left[\frac{1}{\Delta t} \int_{[\Delta t]} \left(\rho_k \mathbf{v}_k \psi_k \right) dt \right] +$$
$$\frac{1}{\Delta t} \sum_{disc \in [\Delta t]} \frac{1}{\left| \mathbf{v}_i \cdot \mathbf{n}_k \right|} \left(\rho_k \mathbf{v}_k \psi_k \right) \cdot \mathbf{n}_k$$

and

(3-95)
$$\frac{1}{\Delta t} \int_{[\Delta t]} \nabla \cdot \mathbf{J}_k \, dt = \nabla \cdot \left[\frac{1}{\Delta t} \int_{[\Delta t]} \mathbf{J}_k \, dt \right] + \frac{1}{\Delta t} \sum_{disc \in [\Delta t]} \frac{1}{\left| \mathbf{v}_i \cdot \mathbf{n}_k \right|} \mathbf{J}_k \cdot \mathbf{n}_k .$$

Substituting Eqs. (3-93) through (3-95) into (3-91) yields the following generic averaged conservation equation,

(3-96)
$$\frac{\partial \left(\overline{\rho_k \psi_k} \right)}{\partial t} + \nabla \cdot \left(\overline{\rho_k \mathbf{v}_k \psi_k} \right) + \nabla \cdot \overline{\mathbf{J}_k} - \overline{\rho_k \phi_k} =$$
$$- \frac{1}{\Delta t} \sum_{disc \in [\Delta t]} \frac{1}{\left| \mathbf{v}_i \cdot \mathbf{n}_k \right|} \left[\rho_k \psi_k \left(\mathbf{v}_k - \mathbf{v}_i \right) + \mathbf{J}_k \right] \cdot \mathbf{n}_k$$

where the overbar represents the averaging operator defined as,

(3-97)
$$\overline{\Phi} \equiv \frac{1}{\Delta t} \int_{[\Delta t]} \Phi \, dt .$$

The derived averaged conservation equation is expressed in terms of averaged products of unknown parameters. It is necessary to replace the averaged products by products of averaged parameters. This can be achieved with introduction of various definitions of weighted averages, as follows:

phasic weighted average,

(3-98)
$$\overline{\Phi}^X \equiv \frac{\dfrac{1}{\Delta t} \displaystyle\int_{[\Delta t]} \Phi X_k \, dt}{\dfrac{1}{\Delta t} \displaystyle\int_{[\Delta t]} X_k \, dt} ,$$

and **density-weighted average**,

(3-99) $\quad \overline{\Phi}^{X\rho} \equiv \dfrac{\dfrac{1}{\Delta t}\displaystyle\int_{[\Delta t]}\Phi\rho_k dt}{\dfrac{1}{\Delta t}\displaystyle\int_{[\Delta t]}\rho_k dt} = \dfrac{\overline{\Phi\rho_k}}{\overline{\rho_k}}.$

It should be noted that:

(3-100) $\quad \overline{X_k} \equiv \dfrac{1}{\Delta t}\displaystyle\int_{[\Delta t]} X_k dt = \dfrac{\Delta t_k}{\Delta t} = \alpha_k,$

where α_k is traditionally called the **volume fraction** of phase k, even though, based on Eq. (3-100) it could be called the *time fraction* of phase k. This quantity is a measure of the probability of existence of phase k at a given point P and time t.

Using Eq. (3-98), the **phasic weighted averaged density** is given as,

(3-101) $\quad \overline{\rho_k}^{X} \equiv \dfrac{\dfrac{1}{\Delta t}\displaystyle\int_{[\Delta t]}\rho_k X_k dt}{\dfrac{1}{\Delta t}\displaystyle\int_{[\Delta t]} X_k dt} = \dfrac{\overline{\rho_k}}{\alpha_k}.$

The first averaged product in Eq. (3-96) can be replaced with the product of averages as follows,

(3-102) $\quad \overline{\rho_k \psi_k} \equiv \dfrac{\overline{\rho_k \psi_k}}{\overline{\rho_k}}\dfrac{\overline{\rho_k}}{\alpha_k}\alpha_k = \overline{\psi_k}^{X\rho}\overline{\rho_k}^{X}\alpha_k.$

In a similar manner,

(3-103) $\quad \overline{\rho_k \phi_k} \equiv \dfrac{\overline{\rho_k \phi_k}}{\overline{\rho_k}}\dfrac{\overline{\rho_k}}{\alpha_k}\alpha_k = \overline{\phi_k}^{X\rho}\overline{\rho_k}^{X}\alpha_k.$

The second term in Eq. (3-96) contains averaging of a product of a conservative quantity and velocity, which in general can fluctuate around its average value as follows,

(3-104) $\quad \psi_k = \overline{\psi_k}^{X\rho} + \psi_k'', \qquad \mathbf{v}_k = \overline{\mathbf{v}_k}^{X\rho} + \mathbf{v}_k'',$

where ψ_k'' and $\mathbf{v}_k''$ are the fluctuating parts of the conserved quantity and the velocity vector, respectively. According to a convention, a single prime is used for fluctuation around time averaged values, whereas double prime is used for fluctuations around time averaged and density weighted values. Thus, the product in the second term becomes,

$$\overline{\rho_k \psi_k \mathbf{v}_k} = \overline{\rho_k \left(\overline{\psi_k}^{X\rho} + \psi_k''\right)\left(\overline{\mathbf{v}_k}^{X\rho} + \mathbf{v}_k''\right)} = \overline{\rho_k \overline{\psi_k}^{X\rho} \overline{\mathbf{v}_k}^{X\rho}} + \overline{\rho_k \overline{\psi_k}^{X\rho} \mathbf{v}_k''} +$$

$$(3\text{-}105)\quad \overline{\rho_k \psi_k'' \overline{\mathbf{v}_k}^{X\rho}} + \overline{\rho_k \psi_k'' \mathbf{v}_k''} = \overline{\rho_k \overline{\psi_k}^{X\rho} \overline{\mathbf{v}_k}^{X\rho}} + \overline{\psi_k}^{X\rho} \overline{\rho_k \mathbf{v}_k''} + \overline{\mathbf{v}_k}^{X\rho} \overline{\rho_k \psi_k''} \qquad .$$

$$+ \overline{\rho_k \psi_k'' \mathbf{v}_k''} = \alpha_k \overline{\rho_k}^{X} \overline{\psi_k}^{X\rho} \overline{\mathbf{v}_k}^{X\rho} + \overline{\rho_k \psi_k'' \mathbf{v}_k''}$$

Here the following identity, valid for any variable ξ_k, was used,

$$(3\text{-}106)\quad \overline{\overline{\xi_k}^{X\rho}} = \overline{\xi_k}^{X\rho} .$$

The above identity states that time averaging does not change the value of the average variable. As a consequence, the following is valid,

$$(3\text{-}107)\quad \overline{\rho_k \xi_k} = \overline{\rho_k \left(\overline{\xi_k}^{X\rho} + \xi_k''\right)} = \overline{\xi_k}^{X\rho} \overline{\rho_k}^{X} \alpha_k + \overline{\rho_k \xi_k''} .$$

Since also,

$$(3\text{-}108)\quad \overline{\rho_k \xi_k} = \frac{\overline{\rho_k \xi_k}}{\overline{\rho_k}} \frac{\overline{\rho_k}}{\alpha_k} \alpha_k = \overline{\xi_k}^{X\rho} \overline{\rho_k}^{X} \alpha_k ,$$

thus

$$(3\text{-}109)\quad \overline{\rho_k \xi_k''} = 0 .$$

The above result states that time average and density weighted double-prime fluctuation of any quantity is equal to zero. This is equivalent to the obvious condition that time average of the single-prime fluctuation of any quantity is equal to zero.

Thus, the conservation equation (3-96) becomes,

$$(3\text{-}110)\quad \begin{aligned} &\frac{\partial\left(\alpha_k \overline{\rho_k}^{X} \overline{\psi_k}^{X\rho}\right)}{\partial t} + \nabla \cdot \left(\alpha_k \overline{\rho_k}^{X} \overline{\psi_k}^{X\rho} \overline{\mathbf{v}_k}^{X\rho}\right) + \nabla \cdot \left(\overline{\rho_k \psi_k'' \mathbf{v}_k''}\right) + \nabla \cdot \left(\alpha_k \overline{\mathbf{J}_k}^{X}\right) \\ &- \alpha_k \overline{\rho_k}^{X} \overline{\phi_k}^{X\rho} = -\frac{1}{\Delta t} \sum_{disc\in[\Delta t]} \frac{1}{\left|\mathbf{v}_i \cdot \mathbf{n}_k\right|} \left[\rho_k \psi_k \left(\mathbf{v}_k - \mathbf{v}_i\right) + \mathbf{J}_k\right] \cdot \mathbf{n}_k \end{aligned} \quad .$$

This generic averaged conservation equation can be written for each conservation equation using the definitions from TABLE 3.2.

Self-interaction term

The third term on the left-hand-side of Eq. (3-110) is a self-interaction term for phase k. This term results from a fluctuating character of the velocity field as well as the transported quantity ψ_k. The name **self-interaction** refers to the fact that this term exists only because of the effect of the fluctuation of field k and is not caused by the interface. It is frequently termed as a turbulent flux of quantity ψ_k.

The self-interaction term of phase k can be expressed by the phasic averaging as follows,

(3-111) $\quad \overline{\rho_k \psi_k'' \mathbf{v}_k''} = \dfrac{\overline{\rho_k \psi_k'' \mathbf{v}_k''}}{\overline{\rho_k}} \dfrac{\overline{\rho_k}}{\alpha_k} \alpha_k \equiv \alpha_k \overline{\rho_k}^X \overline{\psi_k'' \mathbf{v}_k''}^{X\rho}.$

Introducing the turbulent flux of quantity ψ_k,

(3-112) $\quad \mathbf{J}_k^t \equiv \overline{\rho_k}^X \overline{\psi_k'' \mathbf{v}_k''}^{X\rho},$

the self-interaction term can be written as,

(3-113) $\quad \overline{\rho_k \psi_k'' \mathbf{v}_k''} = \alpha_k \mathbf{J}_k^t.$

Phase-interaction term

The expression on the right-hand-side of Eq. (3-110) represents the **phase-interaction term**. The name is motivated by the fact that this term describes all kind of interactions between phases. In particular, it describes the exchange of mass, momentum and energy between the phases. The term consists of two parts: the first part (designed below as Π_{ki}^C) results from convection of property ψ_k through the interface and the second part (designed below as Π_{ki}^M) is a molecular efflux of the quantity through the interface,

(3-114)
$$
\begin{aligned}
\Pi_{ki} &\equiv -\frac{1}{\Delta t} \sum_{disc \in [\Delta t]} \frac{1}{|\mathbf{v}_i \cdot \mathbf{n}_k|} \left[\rho_k \psi_k (\mathbf{v}_k - \mathbf{v}_i) + \mathbf{J}_k \right] \cdot \mathbf{n}_k = \\
&-\frac{1}{\Delta t} \sum_{disc \in [\Delta t]} \frac{\rho_k \psi_k (\mathbf{v}_k - \mathbf{v}_i) \cdot \mathbf{n}_k}{|\mathbf{v}_i \cdot \mathbf{n}_k|} - \frac{1}{\Delta t} \sum_{disc \in [\Delta t]} \frac{\mathbf{J}_k \cdot \mathbf{n}_k}{|\mathbf{v}_i \cdot \mathbf{n}_k|} \equiv \Pi_{ki}^C + \Pi_{ki}^M
\end{aligned}
$$

The convective part depends on the values of quantity ψ_k at the interface at all time instances when summation in Eq. (3-114) is performed. A plausible definition of the mean value of ψ_k at the interface is thus,

(3-115) $\quad \tilde{\psi}_{ki} \equiv \dfrac{-\dfrac{1}{\Delta t} \displaystyle\sum_{disc \in [\Delta t]} \dfrac{\rho_k \psi_k (\mathbf{v}_k - \mathbf{v}_i) \cdot \mathbf{n}_k}{|\mathbf{v}_i \cdot \mathbf{n}_k|}}{-\dfrac{1}{\Delta t} \displaystyle\sum_{disc \in [\Delta t]} \dfrac{\rho_k (\mathbf{v}_k - \mathbf{v}_i) \cdot \mathbf{n}_k}{|\mathbf{v}_i \cdot \mathbf{n}_k|}}.$

Since,

(3-116) $\quad \Gamma_{ki} \equiv -\dfrac{1}{\Delta t} \displaystyle\sum_{disc \in [\Delta t]} \dfrac{1}{|\mathbf{v}_i \cdot \mathbf{n}_k|} \left[\rho_k (\mathbf{v}_k - \mathbf{v}_i) \right] \cdot \mathbf{n}_k,$

is the interfacial mass transfer, the following is obtained,

(3-117) $\Pi_{ki}^{C} = \Gamma_{ki}\tilde{\psi}_{ki}$.

It should be noted that Γ_{ki} is a scalar quantity and is equal to the mass per unit volume and time that is gained by phase k from the interface. Since the mass is not created nor destroyed at the interface, the following condition is satisfied,

(3-118) $\displaystyle\sum_{k=1}^{N_p}\Gamma_{ki} = 0$.

The molecular phase-interaction term Π_{ki}^{M} results from the exchange of quantity ψ_k on the molecular level in absence of mass transfer, due to an action of efflux $\mathbf{J}_k$. It is plausible to postulate that this efflux can be expressed in terms of the interface-mean value, defined as,

(3-119) $\displaystyle\tilde{\mathbf{J}}_{ki} \equiv \frac{1}{N_{disc}}\sum_{disc\in[\Delta t]}\mathbf{J}_k$,

and a fluctuation part, such that

(3-120) $\mathbf{J}'_{ki} = \mathbf{J}_k - \tilde{\mathbf{J}}_{ki}$.

Averaging in Eq. (3-119) is consistent with the time averaging of the field variables, where N_{disc} is the number of discontinuities occurring during the averaging time period.

Thus, the molecular efflux through the interface is as follows,

(3-121)
$$\Pi_{ki}^{M} = -\frac{1}{\Delta t}\sum_{disc\in[\Delta t]}\frac{\left(\tilde{\mathbf{J}}_{ki} + \mathbf{J}'_{ki}\right)\cdot\mathbf{n}_k}{\left|\mathbf{v}_i\cdot\mathbf{n}_k\right|} = \left(-\frac{1}{\Delta t}\sum_{disc\in[\Delta t]}\frac{\mathbf{n}_k}{\left|\mathbf{v}_i\cdot\mathbf{n}_k\right|}\right)\cdot\tilde{\mathbf{J}}_{ki} +$$
$$-\frac{1}{\Delta t}\sum_{disc\in[\Delta t]}\frac{\mathbf{J}'_{ki}\cdot\mathbf{n}_k}{\left|\mathbf{v}_i\cdot\mathbf{n}_k\right|} = \nabla\alpha_k\cdot\tilde{\mathbf{J}}_{ki} + \Pi_{ki}^{Mf}$$
.

Here,

(3-122) $\displaystyle\Pi_{ki}^{Mf} \equiv -\frac{1}{\Delta t}\sum_{disc\in[\Delta t]}\frac{\mathbf{J}'_{ki}\cdot\mathbf{n}_k}{\left|\mathbf{v}_i\cdot\mathbf{n}_k\right|}$,

is the molecular efflux of quantity ψ_k through the interface due to fluctuations of $\mathbf{J}_k$ at the interface.

Generic conservation equation for phase k

Equation (3-114) can now be written as,

$$(3\text{-}123) \quad \frac{\partial\left(\alpha_k \overline{\rho_k}^X \overline{\psi_k}^{X\rho}\right)}{\partial t} + \nabla \cdot \left(\alpha_k \overline{\rho_k}^X \overline{\psi_k}^{X\rho} \overline{\mathbf{v}_k}^{X\rho}\right) + \nabla \cdot \left[\alpha_k \left(\overline{\mathbf{J}_k}^X + \mathbf{J}_k^t\right)\right]$$
$$- \alpha_k \overline{\rho_k}^X \overline{\phi_k}^{X\rho} = \Gamma_{ki}\tilde{\psi}_{ki} + \nabla\alpha_k \cdot \tilde{\mathbf{J}}_{ki} + \Pi_{ki}^{Mf}$$

The above generic equation can be formulated for the mass, the momentum and the energy conservation by substituting suitable expressions from TABLE 3.2.

Mass conservation equation

In case of the mass conservation equation, the quantities in Eq. (3-123) are given as,

$$\psi_k = 1, \mathbf{J}_k = \mathbf{0}, \phi_k = 0, \tilde{\psi}_{ki} = 1, \tilde{\mathbf{J}}_{ki} = \mathbf{0}, \mathbf{J}_k^t = \mathbf{0}, \Pi_{ki}^{Mf} = 0,$$

thus, the equation becomes,

$$(3\text{-}124) \quad \frac{\partial\left(\alpha_k \overline{\rho_k}^X\right)}{\partial t} + \nabla \cdot \left(\alpha_k \overline{\rho_k}^X \overline{\mathbf{v}_k}^{X\rho}\right) = \Gamma_{ki}.$$

Momentum conservation equation

For the momentum equation, the quantities in Eq. (3-123) are as follows,

$$\psi_k = \mathbf{v}_k, \mathbf{J}_k = p_k\mathbf{I} - \boldsymbol{\tau}_k, \phi_k = \mathbf{g},$$

$$\tilde{\psi}_{ki} \equiv \tilde{\mathbf{v}}_{ki},$$

$$\tilde{\mathbf{J}}_{ki} = \tilde{p}_{ki}\mathbf{I} - \tilde{\boldsymbol{\tau}}_{ki},$$

$$\mathbf{J}_k^t = \boldsymbol{\tau}_k^t = \overline{\rho_k}^X \overline{\mathbf{v}_k''\mathbf{v}_k''}^{X\rho},$$

$$\Pi_{ki}^{Mf} \equiv -\frac{1}{\Delta t} \sum_{disc\in[\Delta t]} \frac{\left(p_{ki}'\mathbf{I} - \boldsymbol{\tau}_{ki}'\right)\cdot\mathbf{n}_k}{\left|\mathbf{v}_i \cdot \mathbf{n}_k\right|} \equiv \mathbf{M}_{ki}.$$

Thus the momentum conservation equation is as follows,

$$(3\text{-}125) \quad \frac{\partial\left(\alpha_k \overline{\rho_k}^X \overline{\mathbf{v}_k}^{X\rho}\right)}{\partial t} + \nabla \cdot \left(\alpha_k \overline{\rho_k}^X \overline{\mathbf{v}_k}^{X\rho} \overline{\mathbf{v}_k}^{X\rho}\right) = -\nabla\left(\alpha_k \overline{p_k}^X\right) +$$
$$\nabla \cdot \left[\alpha_k \left(\overline{\boldsymbol{\tau}_k}^X + \boldsymbol{\tau}_k^t\right)\right] + \alpha_k \overline{\rho_k}^X \mathbf{g} + \Gamma_{ki}\tilde{\mathbf{v}}_{ki} + \tilde{p}_{ki}\nabla\alpha_k - \tilde{\boldsymbol{\tau}}_{ki}\cdot\nabla\alpha_k + \mathbf{M}_{ki}.$$

This equation can be transformed as follows,

$$(3\text{-}126) \quad \frac{\partial\left(\alpha_k \overline{\rho_k}^X \overline{\mathbf{v}_k}^{X\rho}\right)}{\partial t} + \nabla \cdot \left(\alpha_k \overline{\rho_k}^X \overline{\mathbf{v}_k}^{X\rho} \overline{\mathbf{v}_k}^{X\rho}\right) = -\alpha_k \nabla\overline{p_k}^X + \nabla \cdot \left[\alpha_k \left(\overline{\boldsymbol{\tau}_k}^X + \boldsymbol{\tau}_k^t\right)\right]$$
$$+ \alpha_k \overline{\rho_k}^X \mathbf{g} + \Gamma_{ki}\tilde{\mathbf{v}}_{ki} + \left(\tilde{p}_{ki} - \overline{p_k}^X\right)\nabla\alpha_k - \tilde{\boldsymbol{\tau}}_{ki}\cdot\nabla\alpha_k + \mathbf{M}_{ki}.$$

<u>Energy conservation equation</u>

For the energy conservation equation, the quantities in Eq. (3-123) are as follows,

$$\psi_k = e_{I,k} + \frac{1}{2}v_k^2, \mathbf{J}_k = \mathbf{q}_k'' + (p_k\mathbf{I} - \boldsymbol{\tau}_k)\cdot\mathbf{v}_k, \phi_k = \mathbf{g}\cdot\mathbf{v}_k,$$

$$\widetilde{\psi}_{ki} \equiv \widetilde{e}_{I,ki} + \frac{1}{2}\widetilde{v}_{ki}^2,$$

$$\widetilde{\mathbf{J}}_{ki} = \widetilde{\mathbf{q}}_k'' + \widetilde{\overline{(p_{ki}\mathbf{I} - \boldsymbol{\tau}_{ki})\cdot\mathbf{v}_{ki}}},$$

$$\mathbf{J}_k^t = \overline{\rho_k}^X\overline{e_{I,k}''\mathbf{v}_k''}^{X\rho} + \frac{1}{2}\overline{\rho_k}^X\overline{(v_k'')^2\mathbf{v}_k''}^{X\rho},$$

$$\Pi_{ki}^{Mf} \equiv -\frac{1}{\Delta t}\sum_{disc\in[\Delta t]}\frac{\left[(\mathbf{q}_{ki}'')' + (p_{ki}'\mathbf{I} - \boldsymbol{\tau}_{ki}')\cdot\mathbf{v}_{ki}'\right]\cdot\mathbf{n}_k}{|\mathbf{v}_i\cdot\mathbf{n}_k|} \equiv E_{ki}.$$

Thus the energy conservation equation takes the following form,

$$(3\text{-}127)\quad
\begin{aligned}
&\frac{\partial\left[\alpha_k\overline{\rho_k}^X\left(\overline{e_{I,k}}^{X\rho} + \frac{1}{2}\overline{v_k^2}^{X\rho}\right)\right]}{\partial t} + \nabla\cdot\left[\alpha_k\overline{\rho_k}^X\left(\overline{e_{I,k}}^{X\rho} + \frac{1}{2}\overline{v_k^2}^{X\rho}\right)\overline{\mathbf{v}_k}^{X\rho}\right] + \\
&\nabla\cdot\left[\alpha_k\left(\overline{\mathbf{q}_k''}^X + \overline{(p_k\mathbf{I} - \boldsymbol{\tau}_k)\cdot\mathbf{v}_k}^X + \overline{\rho_k}^X\overline{e_{I,k}''\mathbf{v}_k''}^{X\rho} + \frac{1}{2}\overline{\rho_k}^X\overline{(v_k'')^2\mathbf{v}_k''}^{X\rho}\right)\right] \\
&-\alpha_k\overline{\rho_k}^X\mathbf{g}\cdot\overline{\mathbf{v}_k}^{X\rho} = \Gamma_{ki}\left(\widetilde{e}_{I,ki} + \frac{1}{2}\widetilde{v}_{ki}^2\right) + \nabla\alpha_k\cdot\left[\widetilde{\mathbf{q}}_k'' + \widetilde{\overline{(p_{ki}\mathbf{I} - \boldsymbol{\tau}_{ki})\cdot\mathbf{v}_{ki}}}\right] + E_{ki}
\end{aligned}
\quad.$$

3.4 Single-Phase Flows in Channels

Fluid flows and heat transfer in channels are very important from the practical point of view. There are many examples of such flows, including coolant flow in nuclear fuel assemblies, coolant flow in the primary reactor circuits and steam flow from steam generators to turbines. Channel flows in industrial applications are almost always turbulent, transient and multi-dimensional in nature. However, for many purposes these flows can be considered as simplified, one-dimensional flows in which parameters of interests, such as pressure, temperature and velocity are area-averaged over the channel cross-section. Such one-dimensional models, both transient and steady-state, are very powerful tools to perform computations needed for many purposes, e.g. for system design and optimization or for safety analyses.

In this section, the general conservation principles are used to derive the governing equations for flows in closed channels. In principle, the governing equations could be derived from the general conservation equations by performing proper averaging of flow parameters across the channel cross-section. A more practical choice is however to employ a control volume that contains a small portion of the channel. Such control

volume is time independent (any translations of pipe walls are neglected) and application of conservation principles in the integral form is thus straightforward. The boundary of the control volume partly consists of channel walls and channel cross-sections. The channel walls are assumed to be impermeable, but heat flux through the walls is taken into account. The cross-section areas A and $A+\Delta A$ (see FIGURE 3-9) are normal to the channel (and to the control volume) axis. The positive direction in the control volume is indicated by a unit vector $\mathbf{e}_z$. This means that the normal vector to the cross-section area A directed away from the control volume is given as $\mathbf{n} = -\mathbf{e}_z$, whereas for area $A+\Delta A$ this vector is $\mathbf{n} = \mathbf{e}_z$.

The derivation of mass, momentum and energy balance equations for such control volume is performed in the following sections.

3.4.1   Mass Conservation Equation

The integral form of the mass conservation equation has been obtained in Section 3.2.1. Considering a channel control volume as shown in FIGURE 3-9, the mass conservation equation can be written as,

$$(3\text{-}128) \quad \int_{z}^{z+\Delta z}\left[\iint_{A(z')}\frac{\partial \rho}{\partial t}dA\right]dz' - \iint_{A(z)}\rho\mathbf{v}\cdot\mathbf{e}_z dA + \iint_{A(z+\Delta z)}\rho\mathbf{v}\cdot\mathbf{e}_z dA = 0.$$

The following **area-averaged variables** are introduced,

$$(3\text{-}129) \quad \langle\rho(z,t)\rangle \equiv \frac{1}{A(z)}\iint_{A(z)}\rho dA,$$

$$(3\text{-}130) \quad \langle U(z,t)\rangle_{\rho} \equiv \frac{\iint_{A(z)}\rho\mathbf{v}\cdot\mathbf{e}_z dA}{\iint_{A(z)}\rho dA} = \frac{\iint_{A(z)}\rho\mathbf{v}\cdot\mathbf{e}_z dA}{A(z)\langle\rho(z,t)\rangle}.$$

The mass conservation equation becomes,

$$(3\text{-}131) \quad \int_{z}^{z+\Delta z} A(z')\frac{\partial\langle\rho(z',t)\rangle}{\partial t}dz' - A\langle\rho\rangle\langle U\rangle_{\rho}\Big|_{(z,t)} + A\langle\rho\rangle\langle U\rangle_{\rho}\Big|_{(z+\Delta z,t)} = 0.$$

Dividing Eq. (3-131) with Δz and taking $\Delta z \to 0$ yields,

$$(3\text{-}132) \quad A(z)\frac{\partial\langle\rho(z,t)\rangle}{\partial t} + \frac{\partial\left[A(z)\langle\rho(z,t)\rangle\langle U(z,t)\rangle_{\rho}\right]}{\partial z} = 0.$$
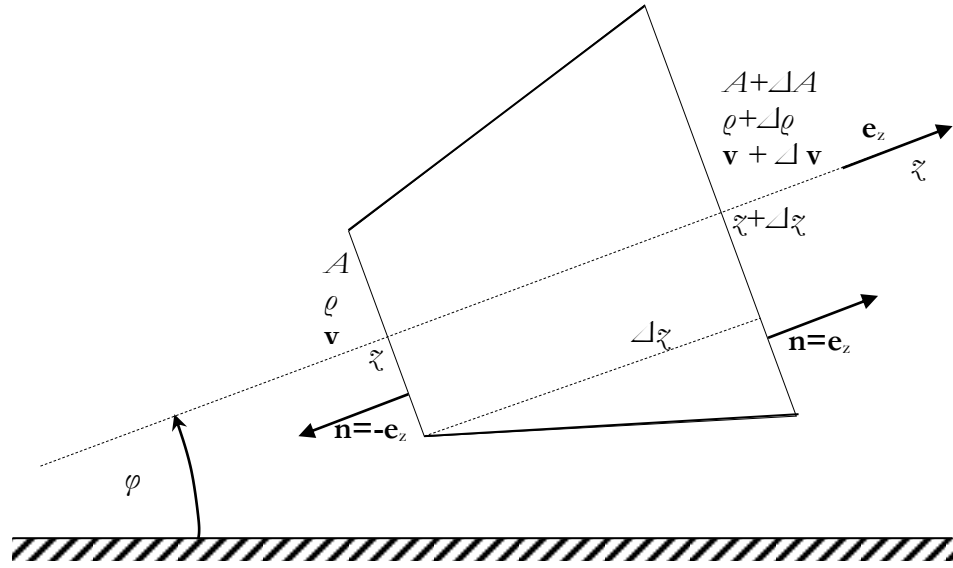
FIGURE 3-9. A control volume in a channel used for derivation of the mass conservation equation.

Equation (3-132) represents the mass conservation principle for transient flows in channels with arbitrary, location dependent, cross sections. It is expressed in terms of the area-averaged density and area-averaged velocity. It should be noted that in the definition of the area-averaged velocity the fluid density was used as a weighting function.

In some cases it is convenient to express the mass conservation equation in terms of the **mass flow rate**, W [kg s^{-1}], which is defined as follows,

$$(3\text{-}133) \quad W(z,t) \equiv \iint\limits_{A(z)} \rho \mathbf{v} \cdot \mathbf{e}_z dA = \langle \rho(z,t) \rangle \langle U(z,t) \rangle_\rho A(z),$$

or in terms of the **mass flux**, G [kg m^{-2} s^{-1}], defined as follows,

$$(3\text{-}134) \quad G(z,t) \equiv \frac{1}{A(z)} \iint\limits_{A(z)} \rho \mathbf{v} \cdot \mathbf{e}_z dA = \langle \rho(z,t) \rangle \langle U(z,t) \rangle_\rho = \frac{W(z,t)}{A(z)}.$$

The mass flow rate is a particularly useful flow variable in case of incompressible or steady-state flow. In both such cases the mass conservation equation becomes,

$$(3\text{-}135) \quad \frac{\partial W}{\partial z} = 0 \quad \Rightarrow \quad W = const.$$

In other worlds, for incompressible or steady-state flows in channels the mass flow rate does not depend on the axial location z in the channel.

3.4.2   Momentum Conservation Equation

The momentum conservation equation in arbitrary volume V was derived in Section 3.2.2 and is as follows,

$$(3\text{-}136) \quad \iiint_V \frac{\partial(\mathbf{v}\rho)}{\partial t} dV + \iint_S \mathbf{v}\rho\mathbf{v}\cdot\mathbf{n}dS = -\iint_S p\mathbf{n}dS + \iint_S \mathbf{n}\cdot\boldsymbol{\tau}dS + \iiint_V \mathbf{g}\rho dV.$$

This vectorial equation can be projected onto the axis of the channel by dot-multiplying it with the directional vector $\mathbf{e}_z$. Using the control volume as shown in FIGURE 3-10 and dividing both sides of the equation with the length Δz, the equation can be written as,

$$
\begin{aligned}
&\frac{1}{\Delta z} \int_z^{z+\Delta z}\left[\iint_{A(z')} \frac{\partial(\mathbf{e}_z\cdot\mathbf{v}\rho)}{\partial t} dA\right]dz' + \frac{1}{\Delta z}\iint_{A(z)}\mathbf{e}_z\cdot\mathbf{v}\rho\mathbf{v}\cdot(-\mathbf{e}_z)dA + \\
&\frac{1}{\Delta z}\iint_{A(z+\Delta z)}\mathbf{e}_z\cdot\mathbf{v}\rho\mathbf{v}\cdot\mathbf{e}_z dA = -\frac{1}{\Delta z}\iint_{A(z)}p\mathbf{e}_z\cdot(-\mathbf{e}_z)dA - \frac{1}{\Delta z}\iint_{A(z+\Delta z)}p\mathbf{e}_z\cdot\mathbf{e}_z dA - \\
&\frac{1}{\Delta z}\iint_{\Delta A_w}p\mathbf{e}_z\cdot\mathbf{n}_w dA_w + \frac{1}{\Delta z}\int_z^{z+\Delta z}\left[\int_{P_w(z')}\mathbf{e}_z\cdot(\mathbf{n}_w\cdot\boldsymbol{\tau}_w)dP_w\right]dz' + \\
&\frac{1}{\Delta z}\int_z^{z+\Delta z}\left[\iint_{A(z')}\mathbf{e}_z\cdot\mathbf{g}\rho dA\right]dz'
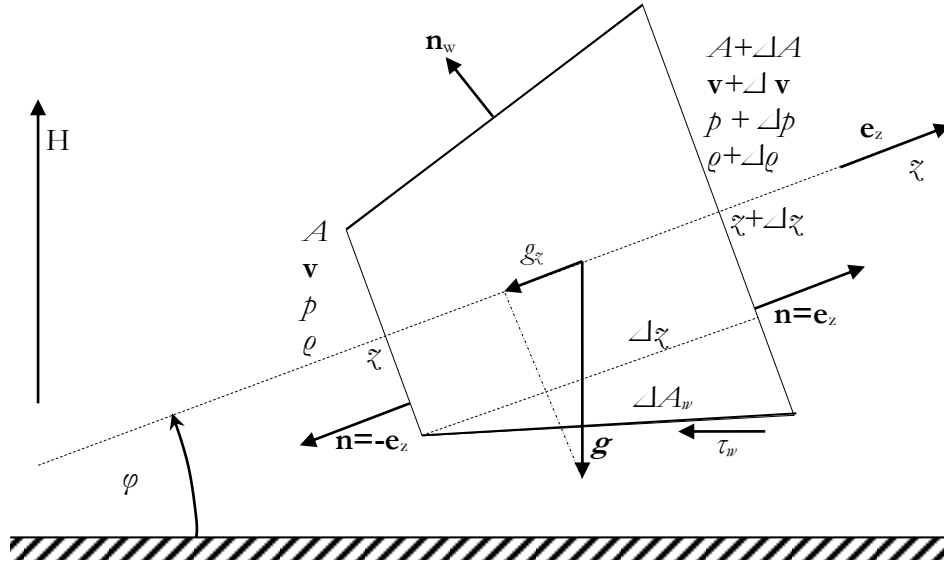\end{aligned}
$$

$(3\text{-}137)$

FIGURE 3-10. A control volume in a channel used for derivation of the momentum conservation equation.

Based on the definition given by Eq. (3-130), the first term on the left-hand side of Eq. (3-137), which represents a time change of the momentum in the control volume, can be written as,

(3-138)

$$\frac{1}{\Delta z}\int_{z}^{z+\Delta z}\left[\iint_{A(z')}\frac{\partial(\mathbf{e}_z\cdot\mathbf{v}\rho)}{\partial t}dA\right]dz' = \frac{1}{\Delta z}\int_{z}^{z+\Delta z}\left[\frac{\partial\left(\iint_{A(z')}\mathbf{e}_z\cdot\mathbf{v}\rho dA\right)}{\partial t}\right]dz' = $$

$$\frac{1}{\Delta z}\int_{z}^{z+\Delta z}\left\{\frac{\partial\big[\langle\rho(z',t)\rangle\langle U(z',t)\rangle_\rho A(z')\big]}{\partial t}\right\}dz' \xrightarrow[\Delta z\to 0]{} \frac{\partial\big[\langle\rho(z,t)\rangle\langle U(z,t)\rangle_\rho A(z)\big]}{\partial t}$$

Here the area-averaged density $\langle\rho(z,t)\rangle$ and the density-weighted area-averaged velocity $\langle U(z,t)\rangle_\rho$, defined in Eqs. (3-129) and (3-130), respectively, have been used.

The second and the third term on the left-hand side of Eq. (3-137) represent the inflow and outflow of momentum through channel cross-section at locations z and $z+\Delta z$ and can be written as,

$$\frac{1}{\Delta z}\left(\iint_{A(z+\Delta z)}\mathbf{e}_z\cdot\mathbf{v}\rho\mathbf{v}\cdot\mathbf{e}_z dA - \iint_{A(z)}\mathbf{e}_z\cdot\mathbf{v}\rho\mathbf{v}\cdot\mathbf{e}_z dA\right) = $$

(3-139) $$\frac{1}{\Delta z}\left[C_M\langle U\rangle\langle U\rangle_\rho\langle\rho\rangle A\Big|_{(z+\Delta z,t)} - C_M\langle U\rangle\langle U\rangle_\rho\langle\rho\rangle A\Big|_{(z,t)}\right].$$

$$\xrightarrow[\Delta z\to 0]{} \frac{\partial}{\partial z}\big[C_M(z,t)\langle U(z,t)\rangle\langle U(z,t)\rangle_\rho\langle\rho(z,t)\rangle A(z)\big]$$

Here, the following definition is introduced,

(3-140)

$$C_M(z,t)\equiv\frac{\dfrac{1}{A(z)}\displaystyle\iint_{A(z)}\mathbf{e}_z\cdot\mathbf{v}\rho\mathbf{v}\cdot\mathbf{e}_z dA}{\dfrac{1}{A(z)}\left(\displaystyle\iint_{A(z)}\mathbf{e}_z\cdot\mathbf{v}dA\right)\dfrac{1}{A(z)}\left(\displaystyle\iint_{A(z)}\rho\mathbf{v}\cdot\mathbf{e}_z dA\right)} = \frac{\dfrac{1}{A(z)}\displaystyle\iint_{A(z)}\mathbf{e}_z\cdot\mathbf{v}\rho\mathbf{v}\cdot\mathbf{e}_z dA}{\langle U(z,t)\rangle\langle U(z,t)\rangle_\rho\langle\rho\rangle},$$

where a new area-averaged velocity has been defined as,

(3-141) $$\langle U(z,t)\rangle\equiv\frac{1}{A(z)}\iint_{A(z)}\mathbf{v}\cdot\mathbf{e}_z dA.$$

This averaged velocity is in general different from the averaged velocity defined in Eq. (3-130). However, if the fluid density is uniformly distributed in the channel cross-section, the two velocities are equal to each other.

Parameter C_M is a space correlation coefficient for square velocity and results from the non-uniformity of velocity and density distributions in channel cross-sections. If the fluid density is constant, the numerical value of the factor depends on the shape of a

channel cross-section and on the velocity distribution. For laminar flows in circular pipes $C_M = 2$ and for turbulent flows, assuming $1/7$-th velocity profile, $C_M = 1.03$.

The first two terms on the right-hand-side of Eq. (3-137) represent the pressure force acting on fluid at channel cross-sections $A(z)$ and $A(z+\Delta z)$ and can be transformed as follows,

$$
(3\text{-}142) \quad
\begin{aligned}
&-\frac{1}{\Delta z}\iint_{A(z)} p\mathbf{e}_z \cdot (-\mathbf{e}_z)dA - \frac{1}{\Delta z}\iint_{A(z+\Delta z)} p\mathbf{e}_z \cdot \mathbf{e}_z dA = -\frac{1}{\Delta z}\left(\iint_{A(z+\Delta z)} pdA - \iint_{A(z)} pdA\right) = \\
&-\frac{1}{\Delta z}\left[A(z+\Delta z)\langle p(z+\Delta z,t)\rangle - A(z)\langle p(z,t)\rangle\right] \xrightarrow{\Delta z \to 0} -\frac{\partial}{\partial z}\left[A(z)\langle p(z,t)\rangle\right]
\end{aligned}
$$

Here the following definition of the cross-section averaged pressure has been introduced,

$$
(3\text{-}143) \quad \langle p(z,t)\rangle \equiv \frac{1}{A(z)}\iint_{A(z)} pdA .
$$

The third term on the right-hand-side of Eq. (3-137) results from the pressure action on the channel wall. This term can be expressed as,

$$
(3\text{-}144) \quad \frac{1}{\Delta z}\iint_{\Delta A_w} p\mathbf{e}_z \cdot \mathbf{n}_w dA_w = -\overline{p}(z,t)\frac{\Delta A}{\Delta z} \xrightarrow{\Delta z \to 0} -\overline{p}(z,t)\frac{dA(z)}{dz} ,
$$

where the following wall-area-averaged pressure has been introduced,

$$
(3\text{-}145) \quad \overline{p}(z,t) \equiv \frac{1}{\Delta A}\iint_{\Delta A_w} p\mathbf{e}_z \cdot \mathbf{n}_w dA_w = \frac{1}{\Delta A}\iint_{\Delta A} pdA .
$$

The friction force represented by the fourth term in Eq. (3-137) can be written as,

$$
(3\text{-}146) \quad
\begin{aligned}
&\frac{1}{\Delta z}\int_z^{z+\Delta z}\left[\int_{P_w(z')} \mathbf{e}_z \cdot (\mathbf{n}_w \cdot \boldsymbol{\tau}_w)dP_w\right]dz' = \\
&-\frac{1}{\Delta z}\int_z^{z+\Delta z} P_w(z')\widehat{\tau}_w(z',t)dz' \xrightarrow{\Delta z \to 0} -P_w(z)\widehat{\tau}_w(z,t)
\end{aligned}
$$

where the following perimeter-averaged wall shear stress has been introduced,

$$
(3\text{-}147) \quad \widehat{\tau}_w(z,t) \equiv \frac{1}{P_w(z)}\int_{P_w(z)} \mathbf{e}_z \cdot (\mathbf{n}_w \cdot \boldsymbol{\tau}_w)dP_w .
$$

Finally, the gravity term in Eq. (3-137) can be written as,

$$\frac{1}{\Delta z}\int_{z}^{z+\Delta z}\left[\iint_{A(z')}\mathbf{e}_z\cdot\mathbf{g}\rho dA\right]dz'=g_z\frac{1}{\Delta z}\int_{z}^{z+\Delta z}\left[\iint_{A(z')}\rho dA\right]dz'=$$

(3-148)

$$g_z\frac{1}{\Delta z}\int_{z}^{z+\Delta z}\left[A(z')\langle\rho(z',t)\rangle\right]dz'\xrightarrow[\Delta z]{}g_zA(z)\langle\rho(z,t)\rangle$$

Substituting the derived terms (3-138) through (3-148) into the momentum equation (3-137) yields,

(3-149)

$$A(z)\frac{\partial\left[\langle\rho(z,t)\rangle\langle U(z,t)\rangle_\rho\right]}{\partial t}+\frac{\partial}{\partial z}\left[C_M(z,t)\langle\rho(z,t)\rangle\langle U(z,t)\rangle_\rho\langle U(z,t)\rangle A(z)\right]=$$

$$-\frac{\partial}{\partial z}\left[A(z)\langle p(z,t)\rangle\right]+\overline{p}(z,t)\frac{dA(z)}{dz}-P_w(z)\widehat{\tau}_w(z,t)+g_zA(z)\langle\rho(z,t)\rangle$$

Assuming

$$\langle p(z,t)\rangle\cong\overline{p}(z,t),$$

and dividing both sides of Eq. (3-149) with channel cross-section area $A(z)$ yields,

(3-150) $$\frac{\partial\left(\langle\rho\rangle\langle U\rangle_\rho\right)}{\partial t}+\frac{1}{A}\frac{\partial}{\partial z}\left(C_M\langle\rho\rangle\langle U\rangle_\rho\langle U\rangle A\right)+\frac{\partial\langle p\rangle}{\partial z}+\frac{P_w\widehat{\tau}_w}{A}+\langle\rho\rangle g\sin\varphi=0,$$

where the functional dependency of variables on z and t have been dropped for clarity. The equation can be expressed in terms of the mass flow rate, W, as,

(3-151) $$\frac{1}{A}\frac{\partial W}{\partial t}+\frac{1}{A}\frac{\partial}{\partial z}\left(C_M\langle U\rangle W\right)+\frac{\partial\langle p\rangle}{\partial z}+\frac{P_w\widehat{\tau}_w}{A}+\langle\rho\rangle g\sin\varphi=0,$$

or, using the mass flux, G, as,

(3-152) $$\frac{\partial G}{\partial t}+\frac{1}{A}\frac{\partial}{\partial z}\left(C_M\langle U\rangle GA\right)+\frac{\partial\langle p\rangle}{\partial z}+\frac{P_w\widehat{\tau}_w}{A}+\langle\rho\rangle g\sin\varphi=0.$$

Equations (3-150) through (3-152) are exact one-dimensional momentum conservation equations, expressed in terms of various flow variables. Several special cases of the equations can be considered. In particular, when flow is steady-state, the mass conservation equation is given by Eq. (3-135) and the momentum conservation equation (3-151) becomes,

(3-153) $$\frac{W}{A}\frac{d}{dz}\left(C_M\langle U\rangle\right)+\frac{d\langle p\rangle}{dz}+\frac{P_w\widehat{\tau}_w}{A}+\langle\rho\rangle g\sin\varphi=0,$$

or, replacing W with $\langle\rho\rangle\langle U\rangle_\rho A$,

$$(3\text{-}154) \quad \langle U \rangle_\rho d\big(C_M \langle U \rangle\big) + \frac{d\langle p \rangle}{\langle \rho \rangle} + \frac{P_w \widehat{\tau}_w}{\langle \rho \rangle A} dz + g \sin \varphi dz = 0 \,.$$

Noting that $\sin \varphi dz = dH$ and assuming $C_M = const$ and $\langle U \rangle_\rho = C_U \langle U \rangle$, the momentum equation becomes,

$$(3\text{-}155) \quad C_M C_U d\!\left(\frac{\langle U \rangle^2}{2} \right) + \frac{d\langle p \rangle}{\langle \rho \rangle} + \frac{P_w \widehat{\tau}_w}{\langle \rho \rangle A} dz + g dH = 0 \,.$$

This equation can be integrated along channel axis from point $z = z_1$ to $z = z_2$ as follows,

$$(3\text{-}156) \quad C_M C_U \!\left(\frac{\langle U \rangle_2^2}{2} - \frac{\langle U \rangle_1^2}{2} \right) + \int_{z_1}^{z_2} \frac{d\langle p \rangle}{\langle \rho \rangle} + \int_{z_1}^{z_2} \frac{P_w \widehat{\tau}_w}{\langle \rho \rangle A} dz + g\big(H_2 - H_1\big) = 0 \,.$$

Assuming further that the fluid density is constant, thus $\langle \rho \rangle = \rho = const$, which means also that the space correlation velocity $C_U = 1$, yields,

$$(3\text{-}157) \quad C_M \rho \!\left(\frac{\langle U \rangle_2^2}{2} - \frac{\langle U \rangle_1^2}{2} \right) + \langle p \rangle_2 - \langle p \rangle_1 + \int_{z_1}^{z_2} \frac{P_w \widehat{\tau}_w}{A} dz + \rho g\big(H_2 - H_1\big) = 0$$

This equation is equivalent to the **Bernoulli equation**, which was first formulated for inviscid flows. It should be recalled that this equation is valid for steady-state flows of fluids with constant density, which was explicitly assumed in the derivation of the equation. It contains contributions resulting from kinetic and potential energy, pressure and also energy degradation due to friction (so-called irreversible pressure losses).

It is interesting to note that the terms in Eq.(3-157) have dimensions of energy per unit mass, even though the starting point for the derivation of the equation was the momentum balance. Indeed, the equation expresses the conservation of the mechanical energy along a channel including the energy degradation due to friction.

For practical applications (when the turbulent flow is prevailing) it is often assumed that $C_M = 1$. Dropping the averaging symbols, Eq. (3-157) can be written as,

$$(3\text{-}158) \quad \frac{\rho U_1^2}{2} + p_1 + \rho g H_1 = \frac{\rho U_2^2}{2} + p_2 + \rho g H_2 + \Delta p_f + \Delta p_{loc} \,.$$

Here Δp_f is a pressure loss due to friction and Δp_{loc} is a pressure loss due to local obstacles. The losses are positive if pressure decreases once moving from point *1* to *2*. To close the momentum equation it is necessary to provide expressions to calculate these irreversible pressure losses. This topic will be addressed in the following sections.

3.4.3 Energy Conservation Equation

The integral form of the energy conservation equation has been derived in Section 3.2.3 and is as follows,

$$
(3\text{-}159) \quad \iiint_V \frac{\partial \left[\left(i - \dfrac{p}{\rho} + \dfrac{1}{2} v^2 \right) \rho \right]}{\partial t} dV + \iint_S \rho \left(i - \frac{p}{\rho} + \frac{1}{2} v^2 \right) \mathbf{v} \cdot \mathbf{n} dS = - \iint_S \mathbf{q}'' \cdot \mathbf{n} dS +
$$

$$
\iiint_V q''' dV - \iint_S p(\mathbf{v} \cdot \mathbf{n}) dS + \iint_S (\boldsymbol{\tau} \cdot \mathbf{v}) \cdot \mathbf{n} dS + \iiint_V (\mathbf{g} \cdot \mathbf{v}) \rho dV
$$

where the specific enthalpy is used instead of the specific internal energy, since this form of the energy conservation equation is more useful in practical applications. Using the control volume shown in FIGURE 3-11, the first term on the left-hand-side of the equation can be integrated as follows,

$$
(3\text{-}160)
$$

$$
\frac{1}{\Delta z} \iiint_V \frac{\partial \left[\left(i - \dfrac{p}{\rho} + \dfrac{1}{2} v^2 \right) \rho \right]}{\partial t} dV =
$$

$$
\frac{1}{\Delta z} \int_z^{z+\Delta z} \left[\frac{\partial \left(\displaystyle\iint_{A(z')} \left(i\rho - p + \frac{1}{2} \rho v^2 \right) dA \right)}{\partial t} \right] dz' =
$$

$$
\frac{1}{\Delta z} \int_z^{z+\Delta z} \left[A \frac{\partial \left(\langle i \rangle_\rho \langle \rho \rangle \big|_{(z',t)} - \langle p(z',t) \rangle + \frac{1}{2} C_M \langle U \rangle \langle \rho \rangle \langle U \rangle_\rho \big|_{(z',t)} \right)}{\partial t} \right] dz'
$$

$$
\xrightarrow[\Delta z \to 0]{} A(z) \frac{\partial}{\partial t} \left(\langle i \rangle_\rho \langle \rho \rangle \big|_{(z,t)} - \langle p(z,t) \rangle + \frac{1}{2} C_M \langle U \rangle \langle U \rangle_\rho \langle \rho \rangle \big|_{(z,t)} \right)
$$

Here the following area-averaged and density-weighted specific enthalpy has been introduced,

$$
(3\text{-}161) \quad \langle i(z,t) \rangle_\rho \equiv \frac{\dfrac{1}{A(z)} \displaystyle\iint_{A(z)} i(z,t) \rho(z,t) dA}{\dfrac{1}{A(z)} \displaystyle\iint_{A(z)} \rho(z,t) dA} = \frac{\dfrac{1}{A(z)} \displaystyle\iint_{A(z)} i(z,t) \rho(z,t) dA}{\langle \rho(z,t) \rangle}
$$

The kinetic energy term in Eq. (3-160) has been approximated as follows,

$$
(3\text{-}162) \quad \frac{1}{2} \rho v^2 = \frac{1}{2} \rho v v \cong \frac{1}{2} \rho (\mathbf{e}_z \cdot \mathbf{v})(\mathbf{e}_z \cdot \mathbf{v})
$$

Strictly speaking the kinetic energy term contains a velocity magnitude in the three-dimensional space. Approximation (3-162) holds as long as the velocity projected on the channel axis is close to the magnitude of the total velocity. For most uni-directional flows this is the case.
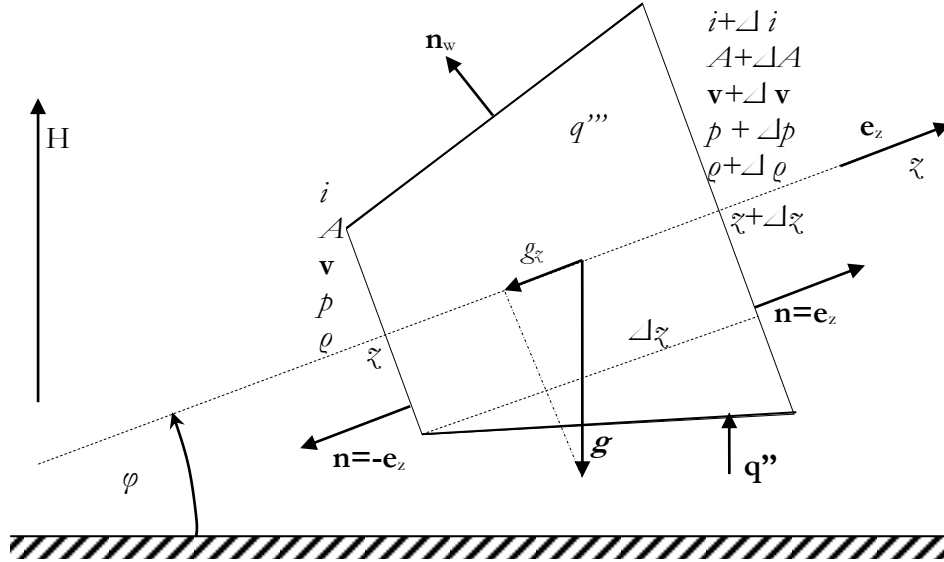

FIGURE 3-11. Channel control volume for energy conservation.

The second term on the left-hand-side of Eq. (3-159) represents the total energy convection through cross-sections $A(z)$ and $A(z+\Delta z)$. The term can be written as follows,

$$\frac{1}{\Delta z}\iint_S \rho\left(i - \frac{p}{\rho} + \frac{1}{2}v^2\right)\mathbf{v}\cdot\mathbf{n}dS =$$

$$-\frac{1}{\Delta z}\iint_{A(z)}\left(\rho i - p + \frac{1}{2}\rho v^2\right)\mathbf{v}\cdot\mathbf{e}_z dA + \frac{1}{\Delta z}\iint_{A(z+\Delta z)}\left(\rho i - p + \frac{1}{2}\rho v^2\right)\mathbf{v}\cdot\mathbf{e}_z dA =$$

$$\frac{\langle i\rangle_{\rho v}\langle\rho\rangle\langle U\rangle_\rho A\big|_{(z+\Delta z,t)} - \langle i\rangle_{\rho v}\langle\rho\rangle\langle U\rangle_\rho A\big|_{(z,t)}}{\Delta z} -$$

$$\frac{C_p\langle p\rangle\langle U\rangle A\big|_{(z+\Delta z,t)} - C_p\langle p\rangle\langle U\rangle A\big|_{(z,t)}}{\Delta z} +$$

$$\frac{C_{M2}\langle U\rangle^2\langle U\rangle_\rho\langle\rho\rangle A\big|_{(z+\Delta z,t)} - C_{M2}\langle U\rangle^2\langle U\rangle_\rho\langle\rho\rangle A\big|_{(z,t)}}{\Delta z}$$

$$\xrightarrow[\Delta z\to 0]{} \frac{\partial}{\partial z}\left\{\langle\rho\rangle\langle U(z,t)\rangle A(z,t)\left[\langle i(z,t)\rangle_{\rho v}\frac{\langle U(z,t)\rangle_\rho}{\langle U(z,t)\rangle} - \right.\right.$$

$$\text{(3-163)}\quad \left.\left. C_p(z,t)\frac{\langle p(z,t)\rangle}{\langle\rho\rangle} + \frac{1}{2}C_{M2}(z,t)\langle U(z,t)\rangle\langle U(z,t)\rangle_\rho\right]\right\}$$

.

Here the following averaged parameters have been introduced:

area-averaged, density and velocity weighted enthalpy,

$$(3\text{-}164) \quad \left\langle i(z,t)\right\rangle_{\rho v} \equiv \frac{\iint\limits_{A(z)} i(z,t)\rho(z,t)\mathbf{v}\cdot\mathbf{e}_z dA}{\iint\limits_{A(z)} \rho(z,t)\mathbf{v}\cdot\mathbf{e}_z dA} = \frac{\iint\limits_{A(z)} i(z,t)\rho(z,t)\mathbf{v}\cdot\mathbf{e}_z dA}{\left\langle\rho(z,t)\right\rangle\left\langle U(z,t)\right\rangle_\rho A(z)},$$

pressure-velocity correlation coefficient,

$$(3\text{-}165) \quad C_p(z,t) \equiv \frac{\dfrac{1}{A(z)}\iint\limits_{A(z)} p(z,t)\mathbf{v}\cdot\mathbf{e}_z dA}{\dfrac{1}{A(z)}\iint\limits_{A(z)} p(z,t)dA\cdot\dfrac{1}{A(z)}\iint\limits_{A(z)} \mathbf{v}\cdot\mathbf{e}_z dA} = \frac{\dfrac{1}{A(z)}\iint\limits_{A(z)} p(z,t)\mathbf{v}\cdot\mathbf{e}_z dA}{\left\langle p(z,t)\right\rangle U(z,t)},$$

space correlation coefficient for v^3,

$$(3\text{-}166) \quad C_{M2}(z,t) \equiv \frac{\iint\limits_{A(z)} \rho v_z^2(\mathbf{v}\cdot\mathbf{e}_z)dA}{\left\langle\rho\right\rangle\left\langle U(z,t)\right\rangle^2\left\langle U(z,t)\right\rangle_\rho A(z)}.$$

The first term on the right-hand side of Eq. (3-159) represents the heat sources due to heat flux applied to the channel walls and can be expressed as follows,

$$(3\text{-}167) \quad -\frac{1}{\Delta z}\iint\limits_S \mathbf{q}''\cdot\mathbf{n}dS = -\frac{1}{\Delta z}\iint\limits_{\Delta A_H} \mathbf{q}''\cdot\mathbf{n}dA_H = \frac{1}{\Delta z}\int\limits_z^{z+\Delta z}\int\limits_{P_H(z')} q''dP_H dz' =$$

$$\frac{1}{\Delta z}\int\limits_z^{z+\Delta z} P_H(z')\hat{q}''(z',t)dz' \xrightarrow[\Delta z\to 0]{} P_H(z)\hat{q}''(z,t),$$

where,

$$(3\text{-}168) \quad \hat{q}''(z,t) \equiv \frac{1}{P_H(z)}\int\limits_{P_H(z)} q''(z,t)dP_H,$$

is the perimeter-averaged heat flux.

The second term on the right-hand-side of Eq. (3-159) represents the volumetric heat sources in the channel and can be expressed as follows,

$$(3\text{-}169) \quad \frac{1}{\Delta z}\iiint\limits_V q'''dV = \frac{1}{\Delta z}\int\limits_z^{z+\Delta z}\iint\limits_{A(z')} q'''dAdz' =$$

$$\frac{1}{\Delta z}\int\limits_z^{z+\Delta z} A(z')\left\langle q'''(z',t)\right\rangle dz' \xrightarrow[\Delta z\to 0]{} A(z)\left\langle q'''(z,t)\right\rangle$$

here,

(3-170) $\quad \left\langle q'''(z,t) \right\rangle = \dfrac{1}{A(z)} \iint\limits_{A(z)} q''' dA$,

is the cross-section averaged volumetric heat source.

The third term on the right-hand side of Eq. (3-159) represents the work performed by pressure and is given as follows,

(3-171)

$$-\dfrac{1}{\Delta z} \iint\limits_{S} p(\mathbf{v} \cdot \mathbf{n}) dS = -\dfrac{1}{\Delta z} \left[-\iint\limits_{A(z)} p(\mathbf{v} \cdot \mathbf{e}_z) dA + \iint\limits_{A(z+\Delta z)} p(\mathbf{v} \cdot \mathbf{e}_z) dA + \right] =$$

$$-\dfrac{C_p A \langle p \rangle \langle U \rangle \big|_{(z+\Delta z,t)} - C_p A \langle p \rangle \langle U \rangle \big|_{(z,t)}}{\Delta z} \xrightarrow[\Delta z \to 0]{} -\dfrac{\partial \left[C_p A \langle p \rangle \langle U \rangle \right]}{\partial z}$$

Here the area-averaged pressure $\langle p \rangle$ and velocity $\langle U \rangle$ defined in Eqs. (3-143) and (3-141), respectively, are used.

The fourth term on the right-hand side of Eq. (3-159) represents the work performed by friction forces. This term can be expressed with the area-averaged parameters as follows,

(3-172)

$$\dfrac{1}{\Delta z} \iint\limits_{S} (\boldsymbol{\tau} \cdot \mathbf{v}) \cdot \mathbf{n} dS = -\dfrac{1}{\Delta z} \iint\limits_{A(z)} (\boldsymbol{\tau} \cdot v_z \mathbf{e}_z) \cdot \mathbf{e}_z dA + \dfrac{1}{\Delta z} \iint\limits_{A(z+\Delta z)} (\boldsymbol{\tau} \cdot v_z \mathbf{e}_z) \cdot \mathbf{e}_z dA +$$

$$\dfrac{1}{\Delta z} \iint\limits_{\Delta A_w} (\boldsymbol{\tau} \cdot \mathbf{v}) \cdot \mathbf{n}_w dA_w = -\dfrac{1}{\Delta z} \iint\limits_{A(z)} v_z \tau_{zz} dA + \dfrac{1}{\Delta z} \iint\limits_{A(z+\Delta z)} v_z \tau_{zz} dA$$

Here the following is valid,

(3-173) $\quad (\boldsymbol{\tau} \cdot v_z \mathbf{e}_z) \cdot \mathbf{e}_z = v_z \left(\begin{bmatrix} \tau_{xx} & \tau_{xy} & \tau_{xz} \\ \tau_{yx} & \tau_{yy} & \tau_{yz} \\ \tau_{zx} & \tau_{zy} & \tau_{zz} \end{bmatrix} \begin{bmatrix} 0 \\ 0 \\ 1 \end{bmatrix} \right) \cdot \begin{bmatrix} 0 & 0 & 1 \end{bmatrix} = v_z \begin{bmatrix} 0 & 0 & 1 \end{bmatrix} \begin{bmatrix} \tau_{xz} \\ \tau_{yz} \\ \tau_{zz} \end{bmatrix} = v_z \tau_{zz}$.

Integration of $(\boldsymbol{\tau} \cdot \mathbf{v}) \cdot \mathbf{n}_w$ on the wall surface gives 0 since the fluid velocity at stationary walls is 0. Thus,

(3-174)

$$\dfrac{1}{\Delta z} \iint\limits_{S} (\boldsymbol{\tau} \cdot \mathbf{v}) \cdot \mathbf{n} dS = \dfrac{A(z) \langle \tau_{zz} \rangle \langle U \rangle \big|_{(z+\Delta z,t)} - A(z) \langle \tau_{zz} \rangle \langle U \rangle \big|_{(z,t)}}{\Delta z}$$

$$\xrightarrow[\Delta z \to 0]{} \dfrac{\partial}{\partial z} \left[A(z) \langle \tau_{zz}(z,t) \rangle_v \langle U(z,t) \rangle \right]$$

where,

(3-175) $\displaystyle \left\langle \tau_{zz}(z,t) \right\rangle_v = \frac{\displaystyle \iint_{A(z)} (\mathbf{v} \cdot \mathbf{e}_z) \tau_{zz} dA}{\displaystyle \iint_{A(z)} (\mathbf{v} \cdot \mathbf{e}_z) dA} = \frac{\displaystyle \iint_{A(z)} v_z \tau_{zz} dA}{A(z) \langle U(z,t) \rangle},$

is the cross-section averaged and velocity weighted shear stress.

The fifth term on the right-hand side of Eq. (3-159) represents the work done by the gravity force. It can be transformed as follows,

$$\frac{1}{\Delta z} \iiint_V (\mathbf{g} \cdot \mathbf{v}) \rho dV = \frac{1}{\Delta z} \int_z^{z+\Delta z} \iint_{A(z')} (\mathbf{g} \cdot \mathbf{v}) \rho dA dz' \cong \frac{1}{\Delta z} \int_z^{z+\Delta z} \iint_{A(z')} (\mathbf{g} \cdot \mathbf{e}_z) v_z \rho dA dz' =$$

(3-176) $\displaystyle g_z \frac{1}{\Delta z} \int_z^{z+\Delta z} \iint_{A(z')} v_z \rho dA dz' = g_z \frac{1}{\Delta z} \int_z^{z+\Delta z} \rho(z',t) \langle U(z',t) \rangle_\rho A(z) dz'$

$\displaystyle \xrightarrow[\Delta z \to 0]{} g_z \langle \rho(z,t) \rangle \langle U(z,t) \rangle_\rho A(z)$

Thus the areas-averaged energy conservation equation is as follows,

(3-177)
$$\frac{\partial}{\partial t} \left\{ \left[\langle i(z,t) \rangle_\rho - \frac{\langle p(z,t) \rangle}{\langle \rho(z,t) \rangle} + \frac{1}{2} C_M(z,t) \langle U(z,t) \rangle \langle U(z,t) \rangle_\rho \right] \langle \rho(z,t) \rangle \right\} +$$

$$\frac{1}{A(z)} \frac{\partial}{\partial z} \left\{ \langle \rho \rangle \langle U(z,t) \rangle A(z,t) \left[\langle i(z,t) \rangle_{\rho v} \frac{\langle U(z,t) \rangle_\rho}{\langle U(z,t) \rangle} - C_p(z,t) \frac{\langle p(z,t) \rangle}{\langle \rho \rangle} + \right. \right.$$

$$\left. \left. \frac{1}{2} C_{M2}(z,t) \langle U(z,t) \rangle \langle U(z,t) \rangle_\rho \right] \right\} = \frac{\hat{q}''(z,t) P_H(z)}{A(z)} + \langle q'''(z,t) \rangle -$$

$$\frac{1}{A(z)} \frac{\partial}{\partial z} \left[C_p(z,t) \langle p(z,t) \rangle \langle U(z,t) \rangle A(z,t) \right] -$$

$$\frac{1}{A(z)} \frac{\partial}{\partial z} \left[A(z) \langle \tau_{zz}(z,t) \rangle_v \langle U(z,t) \rangle \right] + g_z \langle \rho(z,t) \rangle \langle U(z,t) \rangle_\rho$$

In practical applications it is often assumed that the following is valid,

(3-178)
$\langle i_\rho(z,t) \rangle \cong \langle i_{\rho v}(z,t) \rangle = i, \quad \langle U_\rho(z,t) \rangle \cong \langle U(z,t) \rangle = U,$

$C_M(z,t) \cong 1, \quad C_p(z,t) \cong 1, \quad C_{M2} \cong 1$

Using assumptions (3-178) and dropping the averaging notation, the energy conservation equation becomes,

(3-179)
$$\frac{\partial}{\partial t} \left[\left(i - \frac{p}{\rho} + \frac{1}{2} U^2 \right) \rho \right] + \frac{1}{A} \frac{\partial}{\partial z} \left[\rho U A \left(i - \frac{p}{\rho} + \frac{1}{2} U^2 \right) \right] = \frac{q'' P_H}{A} + q''' -$$

$$\frac{1}{A} \frac{\partial}{\partial z} (p U A) - \frac{1}{A} \frac{\partial}{\partial z} (A \tau_{zz} U) + g_z \rho U$$

This equation can also be written as,

$$(3\text{-}180) \quad \frac{\partial}{\partial t}\left[\left(i+\frac{1}{2}U^2\right)\rho\right] + \frac{1}{A}\frac{\partial}{\partial z}\left[\rho UA\left(i+\frac{1}{2}U^2\right)\right] = \frac{q''P_H}{A} + q''' -$$
$$\frac{1}{A}\frac{\partial}{\partial z}(A\tau_{zz}U) + g_z\rho U + \frac{\partial p}{\partial t}.$$

For steady-state flows the equation becomes,

$$(3\text{-}181) \quad \frac{1}{A}\frac{d}{dz}\left[\rho UA\left(i+\frac{1}{2}U^2\right)\right] = \frac{q''P_H}{A} + q''' - \frac{1}{A}\frac{d}{dz}(A\tau_{zz}U) + g_z\rho U.$$

Equation (3-181) can be further simplified for heated channels, when the kinetic and potential energy, as well the energy dissipation terms are negligible as compared to the specific enthalpy. In this case, the following energy equation can be used,

$$(3\text{-}182) \quad \frac{d}{dz}(\rho UAi) = q''P_H + q'''A.$$

On the contrary, in adiabatic channels Eq. (3-181) describes conservation of the mechanical energy. Since $i = e_I + p/\rho$ and the internal energy e_I is constant, the energy equation becomes,

$$(3\text{-}183) \quad \frac{d}{dz}\left[\left(\frac{p}{\rho} + \frac{1}{2}U^2\right)\right] + \frac{1}{A\rho U}\frac{d}{dz}(A\tau_{zz}U) + g\sin\varphi = 0.$$

Integration of the equation yields the Bernoulli equation as follows,

$$(3\text{-}184) \quad p_2 - p_1 + \frac{1}{2}\rho\left(U_2^2 - U_1^2\right) + \frac{\rho}{W}\left(A\tau_{zz}U\big|_{z_2} - A\tau_{zz}U\big|_{z_1}\right) + \rho g\left(H_2 - H_1\right) = 0.$$

Thus, as expected, the Bernoulli equation is a special case of the energy-conservation equation, when channel is adiabatic.

3.4.4 Wall Shear Stress in Laminar Flows

For laminar flows in a pipe, Eq. (3-52) becomes,

$$(3\text{-}185) \quad \tau = \mu\frac{dv_z}{dr}.$$

Assuming laminar, stationary, adiabatic flow of a Newtonian fluid in a vertical tube, the momentum conservation equation is as follows,

$$(3\text{-}186) \quad 0 = -\nabla p + \rho\mathbf{g} + \mu\nabla^2\mathbf{v}.$$

Assuming further that the pressure gradient is known, Eq. (3-186) can be solved for velocity as follows. In cylindrical coordinate system for present conditions the following is valid:

(3-187) $\quad \nabla^2 = \frac{1}{r}\frac{d}{dr}\left(r\frac{d}{dr}\right)$.

Also the velocity vector **v** reduces only to its axial component v_z (other components are equal to zero due to the flow symmetry and the fully developed flow conditions). Thus:

(3-188) $\quad \dfrac{\nabla p - \rho g}{\mu} \equiv \Pi = \frac{1}{r}\frac{d}{dr}\left(r\frac{dv_z}{dr}\right)$.

Equation (3-188) can be solved as,

(3-189)
$$\frac{d}{dr}\left(r\frac{dv_z}{dr}\right) = \Pi r \Rightarrow r\frac{dv_z}{dr} = \frac{\Pi r^2}{2} + C \Rightarrow \frac{dv_z}{dr} = \frac{\Pi r}{2} + \frac{C}{r} \Rightarrow$$
$$v_z = \frac{\Pi r^2}{4} + C\ln r + D$$

The constants C and D are found from boundary conditions: v_z is finite at r=0, therefore $C = 0$. For $r = R$ (at the pipe wall), the velocity is equal to zero, that is $v_z = 0$. Thus:

(3-190) $\quad D = -\dfrac{\Pi R^2}{4} \Rightarrow v_z = \dfrac{-\Pi R^2}{4}\left[1-\left(\frac{r}{R}\right)^2\right]$.

Equation (3-190) describes the so-called Poiseuille paraboloid, which represents the velocity distribution in a fully developed laminar flow in a tube. The average velocity in the tube is found as,

(3-191) $\quad U \equiv \dfrac{1}{\pi R^2}\int_0^R v_z(r)\cdot 2\pi r\,dr = \dfrac{-\Pi}{8}R^2$.

Combining Eqs. (3-190) and (3-191) yields,

(3-192) $\quad v_z = 2U\left[1-\left(\frac{r}{R}\right)^2\right]$.

The wall shear stress can be calculated as,

(3-193) $\quad \tau_w = -\tau(r)\big|_{r=R} \equiv -\mu\dfrac{dv_z}{dr}\bigg|_{r=R} = -\mu\dfrac{\Pi R}{2} = \dfrac{4\mu U}{R}$.

Even though the wall shear stress is proportional to the mean velocity (valid for laminar flows), it is customary to express wall shear stress in a non-dimensional manner by dividing it with the pipe dynamic pressure $\rho U^2/2$. There are two definitions of the friction factor commonly used in the friction loss calculations:

the **Darcy-Weisbach friction factor**,

$$(3\text{-}194) \quad \lambda \equiv \frac{4\tau_w}{\rho U^2/2},$$

the **Fanning friction factor**,

$$(3\text{-}195) \quad C_f \equiv \frac{\tau_w}{\rho U^2/2} = \frac{1}{4}\lambda.$$

Substituting Eqs. (3-194) and (3-195) into (3-193) yields the classic relations,

$$(3\text{-}196) \quad \lambda = \frac{64}{\mathrm{Re}} \quad C_f = \frac{16}{\mathrm{Re}},$$

where the **Reynolds number** appearing in Eq. (3-196) is defined as,

$$(3\text{-}197) \quad \mathrm{Re} = \frac{\rho UD}{\mu}.$$

Here $D = 2 \cdot R$ is the pipe diameter.

Laminar flow solutions shown above are in good agreement with experiments. Such flows undergo, however, transition to turbulent flows at approximately Re = 2300. For flows with Re = 10^4 or higher the flow is fully turbulent and Eqs. (3-196) are not valid. Relationships which are valid for turbulent flows are described in the next section.

3.4.5   Wall Shear Stress in Turbulent Flows

For turbulent flows in pipes, **Blasius** obtained experimental data and proposed the following correlation for the Fanning friction factor, valid for smooth tubes and for Re ≤ 10^5:

$$(3\text{-}198) \quad C_f = \frac{0.0791}{\mathrm{Re}^{0.25}}.$$

Commercial tubes have a roughness (somewhat different from sand-grain behaviour) and for such case **Colebrook** devised the following formula,

$$(3\text{-}199) \quad \frac{1}{\sqrt{\lambda}} = -2.0\log_{10}\left(\frac{k/D}{3.7} + \frac{2.51}{\mathrm{Re}\sqrt{\lambda}}\right).$$

Here k is the pipe roughness expressed in [m]. As can be seen, the Colebrook formula is implicit in its form, that is one has to iterate to find λ. This annoyance can be avoided by instead using an explicit formula given by **Haaland**,

(3-200) $\quad \dfrac{1}{\sqrt{\lambda}} = -1.8\log_{10}\left[\left(\dfrac{k/D}{3.7}\right)^{1.11} + \dfrac{6.9}{\text{Re}}\right].$

Both formulas are in a very good agreement with each other.

3.4.6 Local Pressure Losses

When local obstacles, flow area and/or flow direction changes occur, additional pressure losses appear. These losses are termed as **local (or minor) losses**.

Sudden expansion:

One of the common flow obstacles is a sudden cross-sectional area change. When flow has a direction from the smaller to the larger cross-sectional area, the obstacle is called a sudden enlargement. FIGURE 3-12 shows flow in a sudden enlargement and indicates positions of two cross-sections "1" and "2", between which a balance of mass, momentum and kinetic energy will be invoked.

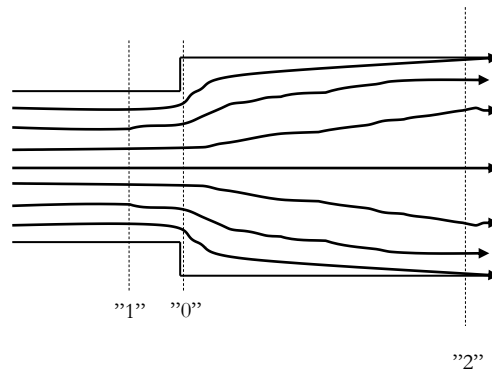FIGURE 3-12. Flow in a vicinity of a sudden expansion of a channel.

Mass balance:

(3-201) $\quad U_1 A_1 = U_2 A_2 .$

Momentum balance:

(3-202) $\quad F = \rho\left(U_1 A_1 U_1 - U_2 A_2 U_2\right) + p_1 A_1 - p_2 A_2 .$

Here F is the force exerted by walls on fluid and in general it consists of two parts: the first part, which will be neglected, comes from the friction between cross-sections "1" and "2". The second one is the pressure action on the enlargement surface $A_2 - A_1$ in cross-section "0". Using the fact that pressure in cross-section "0" is very close to the pressure in cross-section "1" and combining Eqs. (3-201) and (3-202) yields,

(3-203) $\quad -p_1\left(A_2 - A_1\right) = \rho U_2 A_2\left(U_1 - U_2\right) + p_1 A_1 - p_2 A_2 .$

Solving for the pressure difference gives,

$$(3\text{-}204) \quad p_2 - p_1 = \rho U_2 (U_1 - U_2) = \rho U_2^2 \left(\frac{A_2}{A_1} - 1 \right).$$

Since $A_2 > A_1$, the momentum balance predicts a rise in the pressure.

Mechanical energy balance:

Applying the Bernoulli equation yields:

$$(3\text{-}205) \quad \frac{1}{2} \rho U_1^2 + p_1 = \frac{1}{2} \rho U_2^2 + p_2 + \Delta p_I.$$

Here Δp_I is the irreversible pressure drop, or simply the local pressure loss due to a sudden enlargement. Combining Eqs. (3-204) and (3-205) yields,

$$(3\text{-}206) \quad -\Delta p_I = \frac{1}{2} \rho U_2^2 \left(\frac{A_2}{A_1} - 1 \right)^2.$$

It is customary to express the local pressure losses in the following general form:

$$(3\text{-}207) \qquad -\Delta p_{loss} = \xi_{loss} \frac{\rho U^2}{2} = \xi_{loss} \frac{G^2}{2\rho} = \xi_{loss} \frac{W^2}{2\rho A_{min}^2},$$

where ξ_{loss} is the local loss coefficient, U (or G) is the larger velocity (mass flux) of the two: the upstream and the downstream velocity (mass flux) in the obstacle vicinity and $A_{min} = \min(A_1, A_2)$ is the smaller cross section area. For sudden enlargement, the local pressure loss and the loss coefficient are as follows,

$$(3\text{-}208) \quad -\Delta p_I = \left(1 - \frac{A_1}{A_2} \right)^2 \cdot \frac{G_1^2}{2\rho}; \qquad \xi_{enl} = \left(1 - \frac{A_1}{A_2} \right)^2.$$

Sudden contraction:

When flow has a direction from larger to smaller cross-sectional area, the obstacle is called a sudden contraction. This type of obstacle is not a simple analogue to the sudden enlargement case due to the presence of a so-called *vena contracta* just downstream of the obstacle, as shown in FIGURE 3-13.

In a similar manner as for the sudden enlargement, the local pressure loss and the loss coefficient for the sudden contraction can be shown to be as follows:

$$(3\text{-}209) \quad -\Delta p_I = \left(\frac{A_2}{A_c} - 1 \right)^2 \cdot \frac{G_2^2}{2\rho}; \qquad \xi_{cont} = \left(\frac{A_2}{A_c} - 1 \right)^2$$

where A_c is the smallest flow cross-section area which occurs at a certain distance downstream of the area contraction, at the *vena contracta* location.
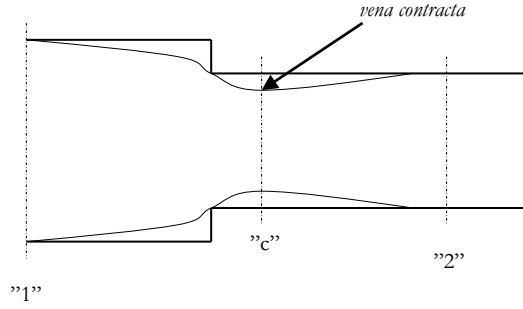

FIGURE 3-13. Flow in a vicinity of a sudden contraction of a channel.

The cross-section area A_c is not known exactly and depends on the area ration A_2/A_1. It is customary to give the contraction loss coefficient in a graphical or tabulated form in function of the area ratio A_2/A_1, see TABLE 3.3.

TABLE 3.3. Values of the local loss coefficient for a sudden contraction.

A_2/A_1	0	0.2	0.4	0.6	0.8	1.0
A_c/A_2	0.586	0.598	0.625	0.686	0.790	1.0
$(A_2/A_c - 1)^2$	0.5	0.45	0.36	0.21	0.07	0.0

Alternatively, the loss coefficient can be obtained from the following correlation,

$$(3\text{-}210) \quad \frac{A_c}{A_2} = 0.62 + 0.38\left(\frac{A_2}{A_1}\right)^3 .$$

For an arbitrary obstacle, such as channel bending, orifice or grid spacer in a fuel assembly, the local pressure loss is calculated from Eq. (3-207), where the local loss coefficient depends on the geometry details of the obstacle and is typically establish in an experimental manner.

The total pressure drop in a channel with length L, constant cross-section area and local obstacles can be calculated as described in the section below.

3.4.7   Total Pressure Drop
If the friction and local pressure losses are incorporated into the momentum equation, the total pressure drop is obtained as,

$$(3\text{-}211) \quad p_1 - p_2 = \left(\frac{4\tau_w}{D_h} + \rho g \sin\varphi\right)L + \Delta p_{loc} = \left(\frac{4L}{D_h}C_f + \xi\right)\frac{\rho U^2}{2} + \rho g L \sin\varphi ,$$

or, expressed in terms of mass flow rate, W,

$$(3\text{-}212) \quad p_1 - p_2 = \left(\frac{4L}{D_h} C_f + \xi \right) \frac{W^2}{2\rho A^2} + \rho g L \sin\varphi \,.$$

In a channel with a piecewise constant cross-section area and with local obstacles, the total pressure drop becomes,

$$(3\text{-}213) \quad p_1 - p_2 = \frac{W^2}{2\rho} \left[\underbrace{\sum_k \left(\frac{4L_k}{D_{h,k}} C_{f,k} \right) \frac{1}{A_k^2}}_{\text{friction loss}} + \underbrace{\sum_j \xi_j \frac{1}{A_{j,\min}^2}}_{\text{local loss}} + \underbrace{\frac{1}{A_2^2} - \frac{1}{A_1^2}}_{\text{reversible}} \right] + $$
$$\underbrace{\rho g \sum_k L_k \sin\varphi_k}_{\text{gravity}} \,.$$

Here index k is referring to the k-th piece of the channel with length L_k, hydraulic diameter $D_{h,k}$, cross-section area A_k, inclination angle φ_k and friction loss coefficient $C_{f,k}$. The local loss coefficients are given by ξ_j, where $A_{j,min}$ means the minimum cross-section area at the local loss location.

3.5 Multi-phase Flows in Channels

Multi-phase flows in channels are very common in many practical applications, such as boiling channels in nuclear reactor cores and pipelines in reactor cooling systems. These types of flows have predominantly uni-directional character and in a natural way lend themselves to a one-dimensional analysis, in which distributions of cross-section averaged parameters are calculated.

3.5.1   Area-Averaged Conservation Equations

Similarly as for the single-phase flows, the derivation of the area-averaged conservation equations for multi-phase flows is performed in a control volume that contains a differential length of a channel between two cross-sections with areas $A(z)$ and $A(z+\varDelta z)$, as shown in FIGURE 3-14. The major difference between derivations presented in Section 3.4 is that in case of multi-phase flows, the channel is filled with various phases and, in particular, each phase occupies only a portion of the total cross section area. In addition all terms describing the interfacial interactions must be considered.

Since phase k exists only at a certain fragment of the cross-section, integration over the whole cross-section area is equivalent to the integration over the portion of the area occupied by phase k. Clearly, the exact shape and size of the cross-section area occupied by phase k change with time, location and flow conditions. For bubbly flows the area corresponding to the gas phase may consists of several disconnected regions crossing through the bubbles. For high fractions of the gas phase a continuous gas region typically exists in the central part of the channel. Examples of various instantaneous phase distributions, corresponding to low and high content of phase k = 2, are shown in FIGURE 3-15.
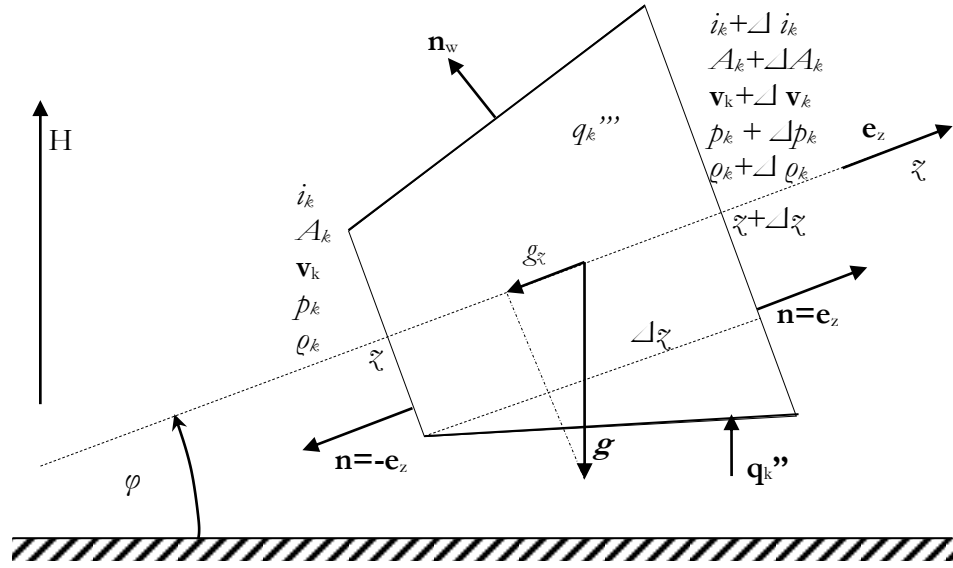
FIGURE 3-14. A control volume used for derivation of averaged conservation equations in multi-phase flow.
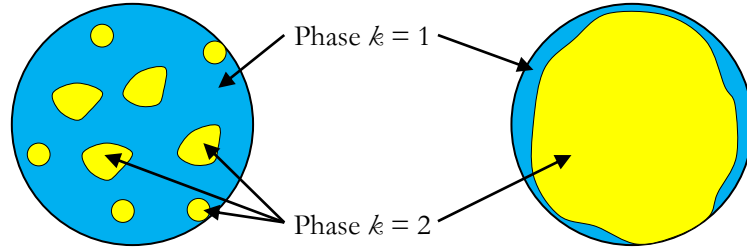

FIGURE 3-15. Examples of channel cross-sections occupied by various phases.

The following phase indicator function can be defined at each cross section at any location z along the channel:

$$(3\text{-}214) \quad X_k(P;z,t) \equiv \begin{cases} 1 & \text{if phase } k \text{ exists at point } P \text{ at time } t \\ 0 & \text{otherwise} \end{cases}.$$

Using this function, the instantaneous cross-section area at time t and location z occupied by phase k is thus given as,

$$(3\text{-}215) \quad A_k(z,t) = \iint\limits_{A(z)} X_k(P;z,t) dA.$$

Averaging of any parameter pertinent to phase k over channel cross-section is as follows,

$$(3\text{-}216) \quad \langle \xi_k(z,t) \rangle_X \equiv \frac{\iint\limits_{A(z)} X_k \xi_k dA_k}{\iint\limits_{A_k(z)} X_k dA_k} = \frac{1}{A_k(z,t)} \iint\limits_{A_k(z,t)} \xi_k dA_k,$$

where symbol $\langle\ \rangle_X$ indicates that averaging is performed only over this portion of cross section which is occupied by phase k. The notation is motivated by the fact that this is equivalent to calculation of a weighted average of parameter ξ_k using X_k as the weighting function. Averaging over the whole cross-section area is defined as,

$$(3\text{-}217) \quad \langle\xi_k(z,t)\rangle \equiv \frac{1}{A(z)}\iint\limits_{A(z)}\xi_k\,dA\,.$$

In particular, taking $\xi_k = X_k$ yields,

$$(3\text{-}218) \quad \langle\alpha_k(z,t)\rangle \equiv \frac{1}{A(z)}\iint\limits_{A(z)}X_k\,dA = \frac{A_k(z,t)}{A(z)}\,,$$

which is the instantaneous area fraction of phase k at location z and time t.

The generic conservation equation can be written in an integral form for any arbitrary volume V_k as follows,

$$(3\text{-}219) \quad \iiint\limits_{V_k}\frac{\partial\rho_k\psi_k}{\partial t}\,dV + \iint\limits_{S_k}(\rho_k\psi_k)\mathbf{v}_k\cdot\mathbf{n}\,dS + \iint\limits_{S_k}\mathbf{J}_k\cdot\mathbf{n}\,dS - \iiint\limits_{V_k}\rho_k\phi_k\,dV = 0\,,$$

where values of $\psi_k, \mathbf{J}_k, \phi_k$ for various conservation principles are given in TABLE 3.2. V_k in Eq. (3-219) is this part of control volume that is occupied by phase k, whereas S_k is the boundary of volume V_k. In case of multi-phase flows this boundary consists of three distinct parts: inflow and outflow boundaries, $A_k(z,t)$ and $A_k(z+\Delta z,t)$, respectively; the wall boundary ΔA_{kw}; and the interface boundary ΔA_{ki}. Thus for the control volume shown in FIGURE 3-14, the generic conservation equation can be written as,

$$
\begin{aligned}
(3\text{-}220)\quad & \int\limits_{z}^{z+\Delta z}\iint\limits_{A_k(z',t)}\frac{\partial\rho_k\psi_k}{\partial t}\,dA_k\,dz' - \iint\limits_{A_k(z,t)}\rho_k\psi_k v_{kz}\,dA_k + \iint\limits_{A_k(z+\Delta z,t)}\rho_k\psi_k v_{kz}\,dA_k \\
& + \iint\limits_{\Delta A_{ki}}(\rho_k\psi_k)\mathbf{v}_k\cdot\mathbf{n}_{ki}\,dA_{ki} - \iint\limits_{A_k(z,t)}\mathbf{J}_k\cdot\mathbf{e}_z\,dA_k + \iint\limits_{A_k(z+\Delta z,t)}\mathbf{J}_k\cdot\mathbf{e}_z\,dA_k \qquad . \\
& + \iint\limits_{\Delta A_{kw}}\mathbf{J}_k\cdot\mathbf{n}_{kw}\,dA_{kw} + \iint\limits_{\Delta A_{ki}}\mathbf{J}_k\cdot\mathbf{n}_{ki}\,dA_{ki} - \int\limits_{z}^{z+\Delta z}\iint\limits_{A_k(z',t)}\rho_k\phi_k\,dA_k\,dz' = 0
\end{aligned}
$$

The integration and time differentiation operators in the first integral can be exchanged by employing the Leibniz's rule as follows,

$$(3\text{-}221) \quad \iint\limits_{A_k(z,t)}\frac{\partial\rho_k\psi_k}{\partial t}\,dA_k = \frac{\partial}{\partial t}\iint\limits_{A_k(z,t)}\rho_k\psi_k\,dA_k - \int\limits_{P_{ki}(z,t)}\rho_k\psi_k\mathbf{v}_i\cdot\mathbf{n}_{ki}\frac{dP}{\mathbf{n}_{ki}\cdot\mathbf{n}_{kiA}}\,.$$

The following area-averaged quantities can be defined,

(3-222) $\quad \langle \rho_k \psi_k \rangle_X \equiv \dfrac{1}{A_k(z,t)} \iint\limits_{A_k(z,t)} \rho_k \psi_k dA_k$,

(3-223) $\quad \langle \rho_k \psi_k v_{kz} \rangle_X \equiv \dfrac{1}{A_k(z,t)} \iint\limits_{A_k(z,t)} \rho_k \psi_k v_{kz} dA_k$,

(3-224) $\quad \langle \mathbf{J}_k \cdot \mathbf{e}_z \rangle_X \equiv \dfrac{1}{A_k(z,t)} \iint\limits_{A_k(z,t)} \mathbf{J}_k \cdot \mathbf{e}_z dA_k$,

(3-225) $\quad \langle \rho_k \phi_k \rangle_X \equiv \dfrac{1}{A_k(z,t)} \iint\limits_{A_k(z,t)} \rho_k \phi_k dA_k$.

Using the definitions of the averaged values and dividing both sides of Eq. (3-220) with Δz yields,

(3-226)

$$
\frac{1}{\Delta z} \int\limits_{z}^{z+\Delta z} \frac{\partial \left[A_k(z',t) \langle \rho_k \psi_k \rangle \right]}{\partial t} dz' + \frac{A_k \langle \rho_k \psi_k v_{kz} \rangle_X \big|_{(z+\Delta z,t)} - A_k \langle \rho_k \psi_k v_{kz} \rangle_X \big|_{(z,t)}}{\Delta z}
$$

$$
\frac{A_k \langle \mathbf{J}_k \cdot \mathbf{e}_z \rangle_X \big|_{(z+\Delta z,t)} - A_k \langle \mathbf{J}_k \cdot \mathbf{e}_z \rangle_X \big|_{(z,t)}}{\Delta z} - \frac{1}{\Delta z} \int\limits_{z}^{z+\Delta z} A_k(z',t) \langle \rho_k \phi_k \rangle_X dz'
$$

$$
= -\frac{1}{\Delta z} \iint\limits_{\Delta A_{kw}} \mathbf{J}_k \cdot \mathbf{n}_{kw} dA_{kw} - \frac{1}{\Delta z} \iint\limits_{\Delta A_{ki}} (\rho_k \psi_k) \mathbf{v}_k \cdot \mathbf{n}_{ki} dA_{ki} - \frac{1}{\Delta z} \iint\limits_{\Delta A_{ki}} \mathbf{J}_k \cdot \mathbf{n}_{ki} dA_{ki}
$$

$$
+ \frac{1}{\Delta z} \int\limits_{z}^{z+\Delta z} \int\limits_{P_{ki}(z',t)} \rho_k \psi_k \mathbf{v}_i \cdot \mathbf{n}_{ki} \frac{dP}{\mathbf{n}_{ki} \cdot \mathbf{n}_{kiA}} dz'
$$

.

The terms on the right-hand-side represent the interaction of phase k with channel walls and with the interface. These terms can be written as follows,

(3-227) $\quad \dfrac{1}{\Delta z} \iint\limits_{\Delta A_{ki}} (\rho_k \psi_k) \mathbf{v}_k \cdot \mathbf{n}_{ki} dA_{ki} = \dfrac{1}{\Delta z} \int\limits_{z}^{z+\Delta z} \int\limits_{P_{ki}(z',t)} \rho_k \psi_k \mathbf{v}_k \cdot \mathbf{n}_{ki} \dfrac{dP}{\mathbf{n}_{ki} \cdot \mathbf{n}_{kiA}} dz'$,

(3-228) $\quad \dfrac{1}{\Delta z} \iint\limits_{\Delta A_{ki}} \mathbf{J}_k \cdot \mathbf{n}_{ki} dA_{ki} = \dfrac{1}{\Delta z} \int\limits_{z}^{z+\Delta z} \int\limits_{P_{ki}(z',t)} \mathbf{J}_k \cdot \mathbf{n}_{ki} \dfrac{dP}{\mathbf{n}_{ki} \cdot \mathbf{n}_{kiA}} dz'$,

(3-229) $\quad \dfrac{1}{\Delta z} \iint\limits_{\Delta A_{kw}} \mathbf{J}_k \cdot \mathbf{n}_{kw} dA_{kw} = \dfrac{1}{\Delta z} \int\limits_{z}^{z+\Delta z} \int\limits_{P_{kW}(z',t)} \mathbf{J}_k \cdot \mathbf{n}_{kw} \dfrac{dP}{\mathbf{n}_{kw} \cdot \mathbf{n}_{kwA}} dz'$.

Combining the equations and taking $\Delta z \to 0$ yields,

$$\frac{\partial\left[A_k(z,t)\langle\rho_k\psi_k\rangle\right]}{\partial t}+\frac{\partial\left[A_k\langle\rho_k\psi_k v_{kz}\rangle_X\right]}{\partial z}+\frac{\partial\left[A_k\langle\mathbf{J}_k\cdot\mathbf{e}_z\rangle_X\right]}{\partial z}-A_k(z,t)\langle\rho_k\phi_k\rangle_X$$

$$\text{(3-230)}$$

$$=-\int_{P_{kW}(z,t)}\mathbf{J}_k\cdot\mathbf{n}_{kw}\frac{dP}{\mathbf{n}_{kw}\cdot\mathbf{n}_{kwA}}dz-\int_{P_{ki}(z,t)}\left[\rho_k\psi_k(\mathbf{v}_k-\mathbf{v}_i)+\mathbf{J}_k\right]\cdot\mathbf{n}_{ki}\frac{dP}{\mathbf{n}_{ki}\cdot\mathbf{n}_{kiA}}dz$$

Dividing both sides of Eq. (3-230) with $A(z,t)$ and noting that $A_k(z,t)=\langle\alpha_k(z,t)\rangle A(z,t)$ yields,

$$\frac{\partial\left[\langle\alpha_k\rangle\langle\rho_k\psi_k\rangle_X\right]}{\partial t}+\frac{1}{A}\frac{\partial\left[A\langle\alpha_k\rangle\langle\rho_k\psi_k v_{kz}\rangle_X\right]}{\partial z}+\frac{1}{A}\frac{\partial\left[A\langle\alpha_k\rangle\langle\mathbf{J}_k\cdot\mathbf{e}_z\rangle_X\right]}{\partial z}-$$

$$\text{(3-231)}\quad\langle\alpha_k\rangle\langle\rho_k\phi_k\rangle_X=-\frac{1}{A}\int_{P_{kw}(z,t)}\mathbf{J}_k\cdot\mathbf{n}_{kw}\frac{dP_{kw}}{\mathbf{n}_{kw}\cdot\mathbf{n}_{kwA}}-$$

$$\frac{1}{A}\int_{P_{ki}(z,t)}\left[\rho_k\psi_k(\mathbf{v}_k-\mathbf{v}_i)+\mathbf{J}_k\right]\cdot\mathbf{n}_{ki}\frac{dP_{ki}}{\mathbf{n}_{ki}\cdot\mathbf{n}_{kiA}}$$

The conservation equations for mass, linear momentum and total energy can be obtained from this generic expression using the definitions of variables given in TABLE 3.2.

Mass conservation equation

For the mass conservation equation the variables in Eq. (3-231) are defined as follows,

$$\psi_k=1,\quad\mathbf{J}_k=0,\quad\phi_k=0,$$

thus, the conservation equation is as follows,

$$\text{(3-232)}\quad\frac{\partial\left[\langle\alpha_k\rangle\langle\rho_k\rangle_X\right]}{\partial t}+\frac{1}{A}\frac{\partial\left[A\langle\alpha_k\rangle\langle\rho_k v_{kz}\rangle_X\right]}{\partial z}=-\frac{1}{A}\int_{P_{ki}(z,t)}\rho_k(\mathbf{v}_k-\mathbf{v}_i)\cdot\mathbf{n}_{ki}\frac{dP_{ki}}{\mathbf{n}_{ki}\cdot\mathbf{n}_{kiA}}.$$

The term on the right-hand side represents the interfacial mass transfer. A perimeter-averaged mass transfer rate is defined as,

$$\text{(3-233)}\quad\widehat{\Gamma}_{ki}''\equiv\frac{1}{P_{ki}(z,t)}\int_{P_{ki}(z,t)}\rho_k(\mathbf{v}_k-\mathbf{v}_i)\cdot\mathbf{n}_{ki}\frac{dP_{ki}}{\mathbf{n}_{ki}\cdot\mathbf{n}_{kiA}}.$$

Equation (3-232) contains an averaged product of density and axial velocity. In general this term is not equal to a product of averaged density and averaged axial velocity. This annoyance can be removed by defining an averaged density-weighted velocity, as follows,

$$\text{(3-234)}\quad\langle U_k\rangle_{X\rho}\equiv\frac{\langle\rho_k v_{kz}\rangle_X}{\langle\rho_k\rangle_X}.$$

The mass conservation equation can now be written as,

(3-235) $$\boxed{\frac{\partial\left[\langle\alpha_k\rangle\langle\rho_k\rangle_X\right]}{\partial t}+\frac{1}{A}\frac{\partial\left[A\langle\alpha_k\rangle\langle\rho_k\rangle_X\langle U_k\rangle_{X\rho}\right]}{\partial z}=-a_{ki}\widehat{\Gamma}''_{ki}}\ .$$

Here a_{ki} is the **interfacial area density for channel flows** defined as,

(3-236) $$a_{ki}(z,t)\equiv\frac{P_{ki}(z,t)}{A(z)}\ .$$

Momentum conservation equation

In the momentum conservation equation the variables in Eq. (3-230) are defined as follows,

(3-237) $$\psi_k=\mathbf{v}_k,\ \mathbf{J}_k=p\mathbf{I}-\boldsymbol{\tau}_k,\ \phi_k=\mathbf{g},$$

thus, the averaged conservation equation is as follows,

(3-238)

$$\frac{\partial\left[\langle\alpha_k\rangle\langle\rho_k\mathbf{v}_k\rangle_X\right]}{\partial t}+\frac{1}{A}\frac{\partial\left[A\langle\alpha_k\rangle\langle\rho_k\mathbf{v}_k v_{kz}\rangle_X\right]}{\partial z}+\frac{1}{A}\frac{\partial\left[A\langle\alpha_k\rangle\langle(p_k\mathbf{I}-\boldsymbol{\tau}_k)\cdot\mathbf{e}_z\rangle_X\right]}{\partial z}$$

$$-\langle\alpha_k\rangle\langle\rho_k\mathbf{g}\rangle_X=-\frac{1}{A}\int\limits_{P_{kw}(z,t)}(p_k\mathbf{I}-\boldsymbol{\tau}_k)\cdot\mathbf{n}_{kw}\frac{dP_{kw}}{\mathbf{n}_{kw}\cdot\mathbf{n}_{kwA}}-$$

$$\frac{1}{A}\int\limits_{P_{ki}(z,t)}\left[\rho_k\mathbf{v}_k(\mathbf{v}_k-\mathbf{v}_i)+(p_k\mathbf{I}-\boldsymbol{\tau}_k)\right]\cdot\mathbf{n}_{ki}\frac{dP_{ki}}{\mathbf{n}_{ki}\cdot\mathbf{n}_{kiA}}$$

$\qquad\qquad\qquad\qquad\qquad\qquad\qquad\qquad\qquad\qquad\qquad\qquad$.

Multiplying both sides of the equation with the unit directional vector $\mathbf{e}_z$ of the channel, the following scalar momentum conservation equation is obtained,

$$\frac{\partial\left[\langle\alpha_k\rangle\langle\rho_k v_{kz}\rangle_X\right]}{\partial t}+\frac{1}{A}\frac{\partial\left[A\langle\alpha_k\rangle\langle\rho_k v_{kz}^2\rangle_X\right]}{\partial z}+\frac{1}{A}\frac{\partial\left[A\langle\alpha_k\rangle\mathbf{e}_z\cdot\langle(p_k\mathbf{I}-\boldsymbol{\tau}_k)\cdot\mathbf{e}_z\rangle_X\right]}{\partial z}$$

(3-239) $$-\langle\alpha_k\rangle\langle\rho_k\mathbf{e}_z\cdot\mathbf{g}\rangle_X=-\frac{1}{A}\int\limits_{P_{kw}(z,t)}\mathbf{e}_z\cdot\left[(p_k\mathbf{I}-\boldsymbol{\tau}_k)\cdot\mathbf{n}_{kw}\right]\frac{dP_{kw}}{\mathbf{n}_{kw}\cdot\mathbf{n}_{kwA}}-$$

$\qquad\qquad\qquad\qquad\qquad\qquad\qquad\qquad\qquad\qquad\qquad\qquad$.

$$\frac{1}{A}\int\limits_{P_{ki}(z,t)}\mathbf{e}_z\cdot\left\{\left[\rho_k\mathbf{v}_k(\mathbf{v}_k-\mathbf{v}_i)+(p_k\mathbf{I}-\boldsymbol{\tau}_k)\right]\cdot\mathbf{n}_{ki}\right\}\frac{dP_{ki}}{\mathbf{n}_{ki}\cdot\mathbf{n}_{kiA}}$$

The terms on the right-hand-side of the equation represent the phase interaction with channel walls and with the interface. The wall interaction term can be expressed in function of the perimeter-averaged pressure and shear stress defined as follows,

(3-240) $$\widehat{p}_{kw}(z,t)\equiv\frac{1}{P_{kw}(z,t)}\int\limits_{P_{kw}(z,t)}p_k\mathbf{e}_z\cdot\mathbf{n}_{kw}\frac{dP_{kw}}{\mathbf{n}_{kw}\cdot\mathbf{n}_{kwA}}\ ,$$

(3-241) $$\widehat{\tau}_{kw}(z,t)\equiv\frac{1}{P_{kw}(z,t)}\int\limits_{P_{kw}(z,t)}\mathbf{e}_z\cdot(\boldsymbol{\tau}_k\cdot\mathbf{n}_{kw})\frac{dP_{kw}}{\mathbf{n}_{kw}\cdot\mathbf{n}_{kwA}}\ .$$

Similar perimeter-averaged quantities can be defined for the interface,

perimeter-averaged velocity of phase k at the interface

$$
(3\text{-}242) \quad \widehat{U}_{ki}(z,t) \equiv \frac{\dfrac{1}{P_{ki}(z,t)} \displaystyle\int_{P_{ki}(z,t)} \mathbf{e}_z \cdot \left[\rho_k \mathbf{v}_k (\mathbf{v}_k - \mathbf{v}_i)\cdot \mathbf{n}_{ki}\right] \dfrac{dP_{ki}}{\mathbf{n}_{ki}\cdot\mathbf{n}_{kiA}}}{\dfrac{1}{P_{ki}(z,t)} \displaystyle\int_{P_{ki}(z,t)} \left[\rho_k (\mathbf{v}_k - \mathbf{v}_i)\cdot\mathbf{n}_{ki}\right] \dfrac{dP_{ki}}{\mathbf{n}_{ki}\cdot\mathbf{n}_{kiA}}} =
$$

$$
\frac{\dfrac{1}{P_{ki}(z,t)} \displaystyle\int_{P_{ki}(z,t)} \mathbf{e}_z \cdot \left[\rho_k \mathbf{v}_k (\mathbf{v}_k - \mathbf{v}_i)\cdot \mathbf{n}_{ki}\right] \dfrac{dP_{ki}}{\mathbf{n}_{ki}\cdot\mathbf{n}_{kiA}}}{\widehat{\Gamma}''_{ki}} .
$$

Here the perimeter-averaged interfacial mass transfer rate given by Eq. (3-233) was used;

perimeter-averaged pressure of phase k at the interface

$$
(3\text{-}243) \quad \widehat{p}_{ki}(z,t) \equiv \frac{1}{P_{ki}(z,t)} \int_{P_{ki}(z,t)} p_k \mathbf{e}_z \cdot \mathbf{n}_{ki} \frac{dP_{ki}}{\mathbf{n}_{ki}\cdot\mathbf{n}_{kiA}} ,
$$

perimeter-averaged shear stress of phase k at the interface

$$
(3\text{-}244) \quad \widehat{\tau}_{ki}(z,t) \equiv \frac{1}{P_{ki}(z,t)} \int_{P_{ki}(z,t)} \mathbf{e}_z \cdot \left(\boldsymbol{\tau}_k \cdot \mathbf{n}_{ki}\right) \frac{dP_{ki}}{\mathbf{n}_{ki}\cdot\mathbf{n}_{kiA}} .
$$

The first term on the left-hand-side of Eq. (3-230) can be represented by the averaged density and the averaged weighted velocity given by Eq. (3-234). The second term contains a square of the axial velocity and in general, the average of the square of a velocity is not equal to the square of the averaged velocity. Thus, the following space correlation coefficient for the square velocity of phase *k* is introduced,

$$
(3\text{-}245) \quad C_{\rho vk} \equiv \frac{\left\langle \rho_k v_{kz}^2 \right\rangle_X}{\left\langle \rho_k \right\rangle_X \left\langle v_{kz} \right\rangle_X^2} .
$$

Using Eqs. (3-240) through (3-245) in Eq. (3-239) yields the following area-averaged momentum conservation equation for phase *k*,

$$
\frac{\partial\left(\left\langle\alpha_k\right\rangle\left\langle\rho_k\right\rangle_X\left\langle U_k\right\rangle_{X\rho}\right)}{\partial t} + \frac{1}{A}\frac{\partial\left(A\left\langle\alpha_k\right\rangle\left\langle\rho_k\right\rangle_X C_{\rho vk}\left\langle U_k\right\rangle_{X\rho}^2\right)}{\partial z} +
$$

$$
(3\text{-}246) \quad \frac{1}{A}\frac{\partial\left(A\left\langle\alpha_k\right\rangle\left\langle p_k\right\rangle_X\right)}{\partial z} - \frac{1}{A}\frac{\partial\left(A\left\langle\alpha_k\right\rangle\left\langle\tau_{zz,k}\right\rangle_X\right)}{\partial z} - \left\langle\alpha_k\right\rangle\left\langle\rho_k\right\rangle_X g\sin\varphi = ,
$$

$$
- a_{kw}\left(\widehat{p}_{kw} - \widehat{\tau}_{kw}\right) - a_{ki}\left(\widehat{p}_{ki} - \widehat{\tau}_{ki}\right) - a_{ki}\widehat{\Gamma}''_{ki}\widehat{U}_{ki}
$$

where,

(3-247) $a_{kw}(z,t) \equiv \dfrac{P_{kw}(z,t)}{A(z)}$,

is the **wall area density for channel flows**.

Energy conservation equation

For the total energy conservation the variables in Eq. (3-231) are defined as follows,

$$\psi_k = e_{I,k} + \frac{1}{2}v_k^2 , \mathbf{J}_k = \mathbf{q}_k'' + (p_k \mathbf{I} - \boldsymbol{\tau}_k) \cdot \mathbf{v}_k , \phi_k = \mathbf{g} \cdot \mathbf{v}_k ,$$

thus, the area-averaged conservation equation of total energy for phase k is as follows,

(3-248)
$$
\frac{\partial \left[\langle \alpha_k \rangle \left\langle \rho_k \left(e_{I,k} + \frac{1}{2}v_k^2 \right) \right\rangle_X \right]}{\partial t} + \frac{1}{A} \frac{\partial \left[A \langle \alpha_k \rangle \left\langle \rho_k \left(e_{I,k} + \frac{1}{2}v_k^2 \right) v_{kz} \right\rangle_X \right]}{\partial z} +
$$
$$
\frac{1}{A} \frac{\partial \left[A \langle \alpha_k \rangle \langle (\mathbf{q}_k'' + (p_k \mathbf{I} - \boldsymbol{\tau}_k) \cdot \mathbf{v}_k) \cdot \mathbf{e}_z \rangle_X \right]}{\partial z} - \langle \alpha_k \rangle \langle \rho_k \mathbf{g} \cdot \mathbf{v}_k \rangle_X =
$$
$$
- \frac{1}{A} \int_{P_{kw}(z,t)} (\mathbf{q}_k'' + (p_k \mathbf{I} - \boldsymbol{\tau}_k) \cdot \mathbf{v}_k) \cdot \mathbf{n}_{kw} \frac{dP_{kw}}{\mathbf{n}_{kw} \cdot \mathbf{n}_{kwA}} -
$$
$$
\frac{1}{A} \int_{P_{ki}(z,t)} \left[\rho_k \left(e_{I,k} + \frac{1}{2}v_k^2 \right)(\mathbf{v}_k - \mathbf{v}_i) + (\mathbf{q}_k'' + (p_k \mathbf{I} - \boldsymbol{\tau}_k) \cdot \mathbf{v}_k) \right] \cdot \mathbf{n}_{ki} \frac{dP_{ki}}{\mathbf{n}_{ki} \cdot \mathbf{n}_{kiA}}
$$

The following averaged quantities are introduced,

area-averaged, density-weighted internal energy of phase k,

(3-249) $\langle e_{I,k} \rangle_{X\rho} \equiv \dfrac{\langle \rho_k e_{I,k} \rangle_X}{\langle \rho_k \rangle_X}$,

space correlation coefficient for cubic velocity of phase k,

(3-250) $C_{\rho v^3 k} \equiv \dfrac{\langle \rho_k v_{kz}^3 \rangle_X}{\langle \rho_k \rangle_X \langle U_k \rangle_{X\rho}^3}$,

space correlation coefficient for velocity and pressure of phase k,

(3-251) $C_{pvk} \equiv \dfrac{\langle p_k v_{kz} \rangle_X}{\langle p_k \rangle_X \langle U_k \rangle_{X\rho}}$,

space correlation coefficient for velocity and shear stress of phase k,

$$(3\text{-}252) \quad C_{\tau vk} \equiv \frac{\langle \tau_k v_{kz} \rangle_X}{\langle \tau_k \rangle_X \langle U_k \rangle_{X\rho}},$$

perimeter-averaged internal energy of phase k at the interface,

$$
(3\text{-}253) \quad
\widehat{e}_{I,ki} \equiv \frac{\dfrac{1}{P_{ki}(z,t)} \displaystyle\int_{P_{ki}(z,t)} \left[\rho_k e_{I,k}\left(\mathbf{v}_k - \mathbf{v}_i\right)\right] \cdot \mathbf{n}_{ki} \dfrac{dP_{ki}}{\mathbf{n}_{ki} \cdot \mathbf{n}_{kiA}}}{\dfrac{1}{P_{ki}(z,t)} \displaystyle\int_{P_{ki}(z,t)} \left[\rho_k\left(\mathbf{v}_k - \mathbf{v}_i\right)\right] \cdot \mathbf{n}_{ki} \dfrac{dP_{ki}}{\mathbf{n}_{ki} \cdot \mathbf{n}_{kiA}}} =
$$

$$
\frac{\dfrac{1}{P_{ki}(z,t)} \displaystyle\int_{P_{ki}(z,t)} \left[\rho_k\left(e_{I,k} + \dfrac{1}{2}v_k^2\right)\left(\mathbf{v}_k - \mathbf{v}_i\right)\right] \cdot \mathbf{n}_{ki} \dfrac{dP_{ki}}{\mathbf{n}_{ki} \cdot \mathbf{n}_{kiA}}}{\widehat{\Gamma}_{ki}''},
$$

perimeter-averaged heat flux from phase k to the interface,

$$(3\text{-}254) \quad \widehat{q}_{ki}''(z,t) \equiv \frac{1}{P_{ki}(z,t)} \int_{P_{ki}(z,t)} \widehat{\mathbf{q}}_k'' \cdot \mathbf{n}_{ki} \frac{dP_{ki}}{\mathbf{n}_{ki} \cdot \mathbf{n}_{kiA}},$$

perimeter-averaged, velocity weighted pressure of phase k at the interface

$$(3\text{-}255) \quad \widehat{p}_{ki}(z,t) \equiv \frac{\dfrac{1}{P_{ki}(z,t)} \displaystyle\int_{P_{ki}(z,t)} \left(p_k \mathbf{I} \cdot \mathbf{v}_k\right) \cdot \mathbf{n}_{ki} \dfrac{dP_{ki}}{\mathbf{n}_{ki} \cdot \mathbf{n}_{kiA}}}{\dfrac{1}{P_{ki}(z,t)} \displaystyle\int_{P_{ki}(z,t)} \mathbf{v}_k \cdot \mathbf{n}_{ki} \dfrac{dP_{ki}}{\mathbf{n}_{ki} \cdot \mathbf{n}_{kiA}}},$$

perimeter-averaged, velocity weighted shear stress of phase k at the interface

$$(3\text{-}256) \quad \widehat{\tau}_{ki}(z,t) \equiv \frac{\dfrac{1}{P_{ki}(z,t)} \displaystyle\int_{P_{ki}(z,t)} \left(\boldsymbol{\tau}_k \cdot \mathbf{v}_k\right) \cdot \mathbf{n}_{ki} \dfrac{dP_{ki}}{\mathbf{n}_{ki} \cdot \mathbf{n}_{kiA}}}{\dfrac{1}{P_{ki}(z,t)} \displaystyle\int_{P_{ki}(z,t)} \mathbf{v}_k \cdot \mathbf{n}_{ki} \dfrac{dP_{ki}}{\mathbf{n}_{ki} \cdot \mathbf{n}_{kiA}}}.$$

Substituting the above averaged quantities to Eq. (3-248) yields the following averaged energy conservation equation,

$$3\text{-}257 \quad \frac{\partial\left[\langle\alpha_k\rangle\langle\rho_k\rangle_X\left(\langle e_{I,k}\rangle_{X\rho}+\dfrac{C_{\rho vk}}{2}\langle U_k\rangle^2_{X\rho}\right)\right]}{\partial t}+$$

$$\frac{1}{A}\frac{\partial\left[A\langle\alpha_k\rangle\langle\rho_k\rangle_X\left(\langle e_{I,k}\rangle_{X\rho}+\dfrac{C_{\rho vk}}{2}\langle U_k\rangle^2_{X\rho}\right)\langle U_k\rangle_{X\rho}\right]}{\partial z}+$$

$$\frac{1}{A}\frac{\partial\left[A\langle\alpha_k\rangle\langle q''_k\rangle_X\right]}{\partial z}+\frac{1}{A}\frac{\partial\left[A\langle\alpha_k\rangle\langle p_k\rangle_X\right]}{\partial z}-\frac{1}{A}\frac{\partial\left[A\langle\alpha_k\rangle\langle\tau_{kzz}\rangle_X\right]}{\partial z}-$$

$$\langle\alpha_k\rangle\langle\rho_k\rangle_X\langle U_k\rangle_{X\rho}\,g\sin\varphi=-a_{kw}\hat{q}''_{kw}--a_{kw}\left(\hat{p}_{kw}-\hat{\tau}_{kw}\right)\hat{U}_{kw}-$$

$$a_{ki}\left[\hat{\Gamma}''_{ki}\left(\hat{e}_{I,k}+\frac{C_k}{2}\hat{U}^2_{ki}\right)+\hat{q}''_{ki}+\left(\hat{p}_{ki}-\hat{\tau}_{ki}\right)\hat{U}_{ki}\right]$$

The derived averaged mass, momentum and energy conservation equations require closure relationships for various cross-correlation coefficients and for the interface and wall interaction terms appearing on the right-hand-sides. In the following sections special cases of the equations will be considered.

3.5.2   Volume Fraction and Quality in Two-Phase Mixtures

There are two principal ways to describe the amount of each phase in two-phase flow mixtures. The first one is based on the volumetric concentration of each of the phases and is referred to as the phasic volume fraction. Traditionally in nuclear applications, the volume fraction of the vapour phase is also called the void fraction. The second way to express the amount of the vapour phase in the two-phase mixture is through the mass concentration of the vapour, where the ratio of the vapour mass to the total mixture mass is termed as the mixture quality. More detailed definitions of these quantities are given below.

Static quality of the two-phase mixture is defined as a ratio of the vapour mass to the total mixture mass,

$$(3\text{-}258)\quad \chi=\frac{M_v}{M_v+M_l}=\frac{M_v}{M}\,.$$

Here M_v is the vapour mass, M_l is the liquid mass and M is the total mixture mass. Note that v and l indices are used to indicate the vapour and liquid phases, meaning that the phases do not have to be at saturation conditions, thus the phases can in general be in thermodynamic non-equilibrium. The volume of the vapour in the mixture divided by the total volume of the mixture is termed as the **static void fraction**. In analogy to Eq. (3-258), the volume-averaged void fraction is computed as,

$$(3\text{-}259)\quad \beta=\frac{V_v}{V_v+V_l}=\frac{V_v}{V}\,.$$

The static quality can be expressed in terms of the volume-averaged static void fraction (and vice-versa) using the following relationships ($M_v=\rho_v V_v$ and $M_l=\rho_l V_l$),

$$(3\text{-}260) \quad \chi = \frac{\rho_v V_v}{\rho_v V_v + \rho_l V_l} = \frac{1}{1 + \dfrac{\rho_l V_l}{\rho_v V_v}} = \frac{1}{1 + \dfrac{\rho_l}{\rho_v}\left(\dfrac{1-\beta}{\beta}\right)},$$

and,

$$(3\text{-}261) \quad \beta = \frac{M_v/\rho_v}{M_v/\rho_v + M_l/\rho_l} = \frac{1}{1 + \dfrac{\rho_v M_l}{\rho_l M_v}} = \frac{1}{1 + \dfrac{\rho_v}{\rho_l}\left(\dfrac{1-\chi}{\chi}\right)}.$$

For flowing mixtures, these quantities can be computed in terms of the cross-sectional areas in the channel occupied by liquid, A_l, and vapour, A_v. The cross-section averaged void fraction is thus given as,

$$(3\text{-}262) \quad \alpha = \frac{A_v}{A_v + A_l}.$$

The mass flow rate is usually represented by symbol W and has unit [kg/s]. The individual mass flow rates of liquid and vapour are W_l and W_v, respectively, and their sum is equal to W. The mass flow rates of vapour and liquid can be expressed in terms of cross-section areas and average phase velocities, U_l and U_v, as follows,

$$(3\text{-}263) \quad W_l = \rho_l U_l A_l, \quad W_v = \rho_v U_v A_v.$$

In boiling channels it is convenient to use the fraction of the total mass flow which is composed of vapour and liquid. The **mass flow quality** , termed often **actual quality**, is defined as,

$$(3\text{-}264) \quad x_a = \frac{W_v}{W_v + W_l} = \frac{W_v}{W}.$$

In a similar manner as for the static quality, the flowing quality can be expressed in terms of the cross-section averaged void fraction as,

$$(3\text{-}265) \quad x_a = \frac{\rho_v U_v A_v}{\rho_v U_v A_v + \rho_l U_l A_l} = \frac{1}{1 + \dfrac{\rho_l U_l A_l}{\rho_v U_v A_v}} = \frac{1}{1 + \dfrac{\rho_l}{\rho_v}\cdot\dfrac{U_l}{U_v}\cdot\left(\dfrac{1-\alpha}{\alpha}\right)}.$$

The mass flow quality is termed as the actual quality, since it describes the actual amount of the vapour phase that is moving within the two-phase mixture. To avoid confusion in certain circumstances the flow (actual) quality will be designed with subscript a, that is x_a.

The **void fraction** for flowing two-phase mixture becomes,

$$\alpha = \frac{W_v/\left(\rho_v U_v\right)}{W_v/\left(\rho_v U_v\right) + W_l/\left(\rho_l U_l\right)} = \frac{1}{1 + \dfrac{W_l}{W_v} \cdot \dfrac{\rho_v}{\rho_l} \cdot \dfrac{U_v}{U_l}} =$$

(3-266)

$$\frac{1}{1 + \dfrac{\rho_v}{\rho_l} \cdot \dfrac{U_v}{U_l} \cdot \left(\dfrac{1 - x_a}{x_a}\right)} .$$

Even though Eq. (3-266) describes in a relatively simple form the dependence between the quality and the void fraction in a two-phase mixture flow, its applicability to practical calculations is limited. The difficulty stems from the fact that the phasic velocity ratio U_v/U_l (called the **slip ratio**) is not known. Additional models are thus required to be able to express the void fraction in terms of the quality. Two such models are described in the following sections.

3.5.3   Homogeneous Equilibrium Model

In this model the phases are assumed to be in an equilibrium – both in the dynamic and in the thermodynamic sense. The dynamic equilibrium assumption means that both phases are well mixed and move with the same velocity. The thermodynamic equilibrium assumption means that both phases co-exist in the saturation form; none of them is in the superheated or subcooled condition. Accordingly, the phase indices are changed from v to g and from l to f to reflect the saturation conditions for each of the phases.

The energy balance for a two-phase mixture can be written as,

(3-267) $$W \cdot i(z) + q'' \cdot P_H \cdot dz = W \cdot \left[i(z) + di\right],$$

which is analogous to the energy balance for the single-phase flow. The enthalpy distribution is thus obtained as,

(3-268) $$W \cdot i(z) + q'' \cdot P_H \cdot dz = W \cdot \left[i(z) + di\right] \Rightarrow \frac{di(z)}{dz} = \frac{q'' \cdot P_H}{W} .$$

For constant heat flux this yields,

(3-269) $$i(z) = i_i + \frac{q'' \cdot P_H}{W} z .$$

In addition to the flow quality defined in Eq. (3-264) a mixture **thermodynamic equilibrium quality** is introduced as follows,

(3-270) $$x_e \equiv \frac{i - i_f}{i_{fg}} .$$

Here i_f is the liquid phase saturation enthalpy, i is the mixture enthalpy and i_{fg} is the latent heat.

Combining Eqs. (3-269) and (3-270) yields,

(3-271) $\quad x_e(z) = x_{ei} + \dfrac{q'' \cdot P_h}{W \cdot i_{fg}} z$,

where

(3-272) $\quad x_{ei} \equiv \dfrac{i_i - i_f}{i_{fg}}$,

is the inlet thermodynamic equilibrium quality.

It should be noted that, unlike the flow quality, the thermodynamic quality can take negative values or can be larger than 1. In the former case the situation corresponds to a single phase subcooled liquid flow and in the latter case – superheated vapour flow. When the thermodynamic quality has a value between 0 and 1 and when assumptions valid for the homogeneous equilibrium model hold, the flow and the thermodynamic equilibrium quality are equivalent, that is $x_e = x$.

The void fraction has been expressed as a function of the local flow quality in Eq. (3-266). Since in the homogeneous equilibrium model the phasic velocities are equal, e.g.,

(3-273) $\quad U_g = U_f$.

The expression for the void fraction takes the following form,

(3-274) $\quad \alpha = \begin{cases} 0 & \text{for} \quad x_e \le 0 \\[2mm] \dfrac{1}{1 + \dfrac{\rho_g}{\rho_f} \cdot \left(\dfrac{1 - x_e}{x_e}\right)} & \text{for} \quad 0 < x_e < 1 \\[2mm] 1 & \text{for} \quad x_e \ge 1 \end{cases}$.

Combining Eqs. (3-274) and (3-271) gives the distribution of the void fraction as a function of the axial distance in a channel.

3.5.4 Drift Flux Model

Presence of the vapour phase has a significant influence on the local value of the mean coolant density. This, in turn, influences the local neutron flux and thus the local power of a nuclear reactor. Clearly, there is a feedback between the local power and the local void fraction in the reactor core. Due to that it is very important to be able to accurately estimate the local values of the void fraction.

Equations (3-261) and (3-266) give expressions for the void fraction in stationary and flowing mixture, respectively. In case of the stationary mixture Eq. (3-261) gives an exact expression for the void fraction. Knowing the densities of phases and the static quality, the corresponding void fraction can be computed.
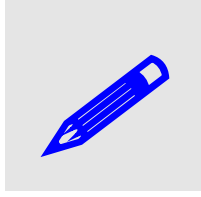
EXAMPLE 3-1. Comparison between the static quality and the void fraction. A tank contains a mixture of air and water, with $M_a = 1$ kg and $M_w = 999$ kg. Calculate the void fraction of the mixture assuming $\rho_a = 1$ kg/m³ and $\rho_w = 1000$ kg/m³.

SOLUTION: The static quality is found as $\chi = 1/(1+999) = 0.001$ and the static void fraction as $\beta = 1/(1 + (1 \cdot 0.999)/(1000 \cdot 0.001)) = 0.50025$. Thus, it would seem that the mass fraction of air is negligible (only 0.1%), whereas the air fills more than half of the vessel (50.025%). This example illustrates the importance of considering both the void fraction and the quality.

More interesting is the case with the flowing mixture, however, in such a case an accurate prediction of the void fraction is much more complex. Apparently Eq. (3-266) can be used for that purpose; however, one has to know the slip ratio, $S = U_g / U_f$. This parameter is not constant and depends in a complex manner on the flow quality x, the system pressure, the mass flux and the flow regime. Typically the slip ratio has been found from two-phase flow measurements.

In the simplest case it can be assumed that the phases move with the same velocity and thus the slip ratio is equal to 1. This assumption is the fundamental part of the Homogeneous Equilibrium Model presented in the previous section. According to this model, the void fraction can be found from Eq. (3-261) and is a function of the local quality and pressure only.

A direct and essential extension of the slip ratio and HEM approaches is the **Drift Flux Model** (DFM) proposed by Zuber and Findlay (1965). The model enables the slip between the phases as well as it takes into account the spatial pattern of the flow.

Given a two-phase mixture flowing in a channel, the following local quantities can be defined:

(3-275) $j_l \equiv (1-\alpha)u_l$,

(3-276) $j_v \equiv \alpha u_v$,

(3-277) $j = j_l + j_v$,

(3-278) $u_{vj} \equiv u_v - j = (1-\alpha)(u_v - u_l)$,

where α is the local void fraction, j_k is the **superficial velocity** and u_k is the local velocity of phase k ($k = v$ for the vapour phase and $k = l$ for the liquid phase). From Eq. (3-278) one gets,

(3-279) $\alpha u_{vj} = \alpha u_v - \alpha j = j_v - \alpha j$.

Equation (3-279) can be integrated over the channel cross-section to obtain,

(3-280) $\int_A \alpha u_{vj} dA = \int_A j_v dA - \int_A \alpha j dA$,

where A is the channel cross-section area. The following definitions can be introduced:

$$(3\text{-}281) \quad U_{vj} \equiv \frac{\int_A \alpha u_{vj} dA}{\int_A \alpha dA} = \frac{\int_A \alpha u_{vj} dA}{\langle \alpha \rangle A} \quad ,$$

$$(3\text{-}282) \quad \int_A \alpha j dA \equiv C_0 \int_A \alpha dA \cdot \int_A j dA = C_0 \cdot \langle \alpha \rangle \cdot J \cdot A \, ,$$

$$(3\text{-}283) \quad J_v = \frac{1}{A} \int_A j_v dA \, .$$

Combining Eqs. (3-280) through (3-283) yields,

$$(3\text{-}284) \quad \langle \alpha \rangle = \frac{J_v}{C_0 J + U_{vj}} \, .$$

Equation (3-284) is the celebrated **drift-flux void correlation**. It expresses the cross-section mean void fraction $\langle \alpha \rangle$ in terms of channel mean superficial velocity of gas, J_v, total superficial velocity, J, and two parameters, C_0 and U_{vj}. The first parameter is the so-called **drift-flux distribution parameter**. Its physical interpretation is clear from (3-282 and is simply a covariance coefficient for cross-section distributions of void fraction and total superficial velocity. The second coefficient is the so-called **drift velocity** and can be interpreted as cross-section averaged difference between gas velocity and superficial velocity, using local void fraction as a weighting function.

The drift-flux parameters are not constant and depend on flow conditions. For high pressure steam-water flows the parameters can be approximated with the following expressions,

$$(3\text{-}285) \quad C_0 = 1.13,$$

$$(3\text{-}286) \quad U_{vj} = 1.41 \left(\frac{\sigma g (\rho_l - \rho_v)}{\rho_l^2} \right)^{0.25} \, .$$

Here σ is the surface tension and g is the gravity acceleration.

TABLE 3.4 gives expressions for drift-flux parameters, which are valid in a wide range of flow conditions.

TABLE 3.4. Expressions for drift-flux parameters.

Flow pattern	Distribution parameter	Drift velocity
Bubbly $0 < \alpha \le 0.25$	$C_0 = \begin{cases} 1 - 0.5 p/p_c & D \ge 0.05 m \\ 1.2 & p/p_c < 0.5 \\ 1.4 - 0.4 p/p_c & p/p_c \ge 0.5 \end{cases} \quad D < 0.05 m$	$U_{vj} = 1.41 \left(\dfrac{\sigma g (\rho_l - \rho_v)}{\rho_l^2} \right)^{0.25}$
Slug/churn $0.25 < \alpha \le 0.75$	$C_0 = 1.15$	$U_{vj} = 0.35 \left(\dfrac{g D (\rho_l - \rho_v)}{\rho_l} \right)^{0.5}$

Annular $0.75 < \alpha \leq 0.95$	$C_0 = 1.05$	$U_{vj} = 23\left(\dfrac{\mu_l J_l}{\rho_v D}\right)^{0.5}\dfrac{(\rho_l - \rho_v)}{\rho_l}$
Mist $0.95 < \alpha < 1$	$C_0 = 1.0$	$U_{vj} = 1.53\left(\dfrac{\sigma g(\rho_l - \rho_v)}{\rho_v^2}\right)^{0.25}$

σ - surface tension, g – gravity acceleration, p – pressure, p_c – critical pressure, D – channel (hydraulic) diameter, J –superficial velocity, μ – viscosity, ϱ –density; subscripts: l – liquid, v - vapour.

The drift-flux void correlation given by Eq. (3-284) can be expressed in terms of the quality and the mass flux as follows,

(3-287)
$$\langle\alpha\rangle = \frac{J_v}{C_0 J + U_{vj}} = \frac{1}{C_0\dfrac{J_v + J_l}{J_v} + \dfrac{U_{vj}}{J_v}} =$$

$$\frac{1}{C_0\left(1 + \dfrac{\rho_v}{\rho_l}\dfrac{G_l}{G_v}\right) + \dfrac{\rho_v U_{vj}}{G_v}} = \frac{1}{C_0\left(1 + \dfrac{\rho_v}{\rho_l}\dfrac{1-x}{x}\right) + \dfrac{\rho_v U_{vj}}{Gx}}.$$

It can be noticed that using $C_0 = 1$ and $U_{vj} = 0$ gives the homogeneous void fraction correlation. Another observation is that for any $C_0 > 1$ and $U_{vj} > 0$, the void fraction predicted from Eq. (3-287) is lower than the void fraction predicted from the homogeneous model.

EXAMPLE 3-2. Find expression for the slip ratio S that will result in a void correlation which is equivalent to the drift-flux correlation given by Eq. (3-287). SOLUTION:

(3-288)
$$S = C_0 + (C_0 - 1)\frac{\rho_l x}{\rho_v(1-x)} + U_{vj}\frac{\rho_l}{G(1-x)}$$

The solution indicates that for the Homogeneous Equilibrium Model (when $C_0 = 1$ and $U_{vj} = 0$) the slip ratio, as could be expected, is equal to 1.

3.5.5 Pressure Drop in Multiphase Flows

The momentum conservation equation derived in Section 3.5.1 can be used to calculate the pressure drop for multiphase flows in channels. Dropping the averaging symbols and assuming unity cross-correlation coefficients, the equation can be written as follows,

(3-289)
$$\frac{\partial G_k}{\partial t} + \frac{1}{A}\frac{\partial}{\partial z}\left(\frac{A G_k^2}{\alpha_k \rho_k}\right) = -\frac{1}{A}\frac{\partial(A\alpha_k p_k)}{\partial z} + \frac{1}{A}\frac{\partial(A\alpha_k \tau_{zz,k})}{\partial z} +$$

$$\alpha_k \rho_k g \sin\varphi - a_{kw}(\hat{p}_{kw} - \hat{\tau}_{kw}) - a_{ki}(\hat{p}_{ki} - \hat{\tau}_{ki}) - a_{ki}\hat{\Gamma}''_{ki}\hat{U}_{ki}$$

This equation describes the motion of each of the phases. The equation can be solved only if all terms on the right-hand-side are determined.

One of the simplest models for prediction of pressure drops in multiphase flows can be obtained by considering only one momentum equation valid for the multi-phase

mixture. The mixture momentum equation can be obtained by adding balance equations for all phases as follows,

(3-290)
$$\frac{\partial}{\partial t}\sum_{k=1}^{N_p}G_k+\frac{1}{A}\frac{\partial}{\partial z}\left(A\sum_{k=1}^{N_p}\frac{G_k^2}{\alpha_k\rho_k}\right)=-\frac{1}{A}\frac{\partial}{\partial z}\left(A\sum_{k=1}^{N_p}\alpha_k p_k\right)+\frac{1}{A}\frac{\partial}{\partial z}\left(A\sum_{k=1}^{N_p}\alpha_k\tau_{zz,k}\right)+$$
$$g\sin\varphi\sum_{k=1}^{N_p}\alpha_k\rho_k-\sum_{k=1}^{N_p}a_{kw}\left(\hat{p}_{kw}-\hat{\tau}_{kw}\right)-\sum_{k=1}^{N_p}a_{ki}\left(\hat{p}_{ki}-\hat{\tau}_{ki}\right)-\sum_{k=1}^{N_p}a_{ki}\hat{\Gamma}_{ki}''\hat{U}_{ki}$$

After summation over all participating phases, the particular terms in the single-fluid momentum conservation equation are as follows,

(3-291)
$$\sum_{k=1}^{N_p}G_k=G\,,$$

(3-292)
$$\sum_{k=1}^{N_p}\frac{G_k^2}{\alpha_k\rho_k}=G^2\sum_{k=1}^{N_p}\frac{x_k^2}{\alpha_k\rho_k}=\frac{G^2}{\rho_M}\,,$$

(3-293)
$$\sum_{k=1}^{N_p}\alpha_k\rho_k=\rho_m\,,$$

(3-294)
$$\sum_{k=1}^{N_p}\alpha_k p_k=p\,,$$

(3-295)
$$\sum_{k=1}^{N_p}a_{kw}\left(\hat{p}_{kw}-\hat{\tau}_{kw}\right)\equiv\left(\frac{dp}{dz}\right)_w\,,$$

(3-296)
$$\sum_{k=1}^{N_p}\alpha_k\tau_{zz,k}\cong 0\,,$$

(3-297)
$$\sum_{k=1}^{N_p}a_{ki}\left(\hat{p}_{ki}-\hat{\tau}_{ki}\right)+\sum_{k=1}^{N_p}a_{ki}\hat{\Gamma}_{ki}''\hat{U}_{ki}\cong 0\,.$$

Assuming a steady-state flow, the momentum balance equation becomes,

(3-298)
$$-\frac{dp}{dz}=\left(\frac{dp}{dz}\right)_w+\rho_m g\sin\varphi+\frac{1}{A}\frac{d}{dz}\left(\frac{G^2 A}{\rho_M}\right).$$

Here two definitions for the mixture density have been introduced:

the **static mixture density**,

(3-299)
$$\rho_m=\sum_k\rho_k\alpha_k\,,$$

the **dynamic mixture density**,

$$(3\text{-}300) \quad \rho_M = \left(\sum_k \frac{x_k^2}{\rho_k \alpha_k} \right)^{-1}.$$

In case of two-phase flows, the two types of density definitions are as follows,

$$(3\text{-}301) \quad \rho_m = \rho_v \alpha + \rho_l (1-\alpha),$$

$$(3\text{-}302) \quad \rho_M = \frac{1}{\dfrac{x^2}{\rho_v \alpha} + \dfrac{(1-x)^2}{\rho_l (1-\alpha)}}.$$

In general the static and the dynamic density of two-phase mixture are not equal to each other. The difference between them depends on the phasic slip and the void fraction distribution in the channel cross-section.

When assuming the Homogeneous Equilibrium Model, it can be shown that the static and the dynamic mixture density are equal to each other and they are as follows,

$$(3\text{-}303) \quad \rho_m = \rho_M = \frac{\rho_l}{x \left(\dfrac{\rho_l}{\rho_v} - 1 \right) + 1}.$$

Equation (3-298) describes in a general form the pressure gradient change in a boiling channel of arbitrary shape. There are three distinct terms on the right-hand-side of Eq. (3-298). The first term is the friction pressure loss term, and represents the pressure gradient change due to the friction between two-phase mixture and the channel walls. The second term represents the pressure gradient due to the gravity. Finally, the third term is the acceleration term, since it represents the pressure gradient due to the mixture acceleration in the channel. All these terms will be described below in more detail.

3.5.6 Friction Pressure Loss

The **friction pressure loss** defined as,

$$(3\text{-}304) \quad \left(\frac{dp}{dz} \right)_w \equiv \sum_{k=1}^{N_p} a_{kw} \left(\widehat{p}_{kw} - \widehat{\tau}_{kw} \right) \cong \sum_{k=1}^{N_p} \frac{\tau_{w,k} P_{w,k}}{A}.$$

Using derivations shown in Sub-section 3.4.5, the friction force between phase k and wall can be expressed as,

$$(3\text{-}305) \quad \tau_{w,k} P_{w,k} = P_{w,k} \frac{C_{f,k}}{2} \rho_k U_k^2 = P_{w,k} \frac{C_{f,k}}{2\rho_k} G_k^2.$$

Here $P_{w,k}$ is the channel perimeter which is in a direct contact with phase k. Combining Eqs. (3-304) and (3-305) yields,

$$(3\text{-}306) \quad \left(\frac{dp}{dz}\right)_w = \frac{1}{A} \sum_k P_{w,k} \frac{C_{f,k}}{2\rho_k} G_k^2 .$$

For two-phase flows, the above expression is as follows,

$$(3\text{-}307) \quad \begin{aligned} \left(\frac{dp}{dz}\right)_{w,tp} &= \frac{1}{A}\left[P_{w,v} \frac{C_{f,v}}{2\rho_v} G_v^2 + P_{w,l} \frac{C_{f,l}}{2\rho_l} G_l^2 \right] = \\ &\frac{P_w}{A}\left[\frac{P_{w,v}}{P_w} \frac{C_{f,v}}{\rho_v} x^2 + \frac{P_{w,l}}{P_w} \frac{C_{f,l}}{\rho_l}(1-x)^2 \right] \frac{G^2}{2} \end{aligned} .$$

Equation (3-306) is not practical to predict the wall-friction pressure drop unless $P_{w,k}$ is known. In the majority of two-phase flow situations this is the case. Instead, the two-phase friction is expressed in terms of so-called **two-phase friction multipliers**, which are defined as,

$$(3\text{-}308) \quad \phi_l^2 = \frac{(dp/dz)_{w,tp}}{(dp/dz)_{w,l}} ,$$

$$(3\text{-}309) \quad \phi_{lo}^2 = \frac{(dp/dz)_{w,tp}}{(dp/dz)_{w,lo}} ,$$

$$(3\text{-}310) \quad \phi_v^2 = \frac{(dp/dz)_{w,tp}}{(dp/dz)_{w,v}} ,$$

where pressure drop with index w,l denotes the frictional pressure gradient that would result if the liquid flowed alone through the channel with a mass flow rate equal to G_l, w,lo denotes the frictional pressure gradient that would result if the liquid flowed alone through the channel with a mass flow rate equal to G and w,v denotes the frictional pressure gradient that would result if the vapour flowed alone through the channel with a mass flow rate equal to G_v.

Using Eq. (3-309), the two-phase pressure gradient due to friction can be found as,

$$(3\text{-}311) \quad \left(\frac{dp}{dz}\right)_{w,tp} = \phi_{lo}^2 \left(\frac{dp}{dz}\right)_{w,lo} ,$$

where the fictitious single-phase (liquid-only) pressure gradient is found from the standard expression,

$$(3\text{-}312) \quad \left(\frac{dp}{dz}\right)_{w,lo} = \frac{4C_{f,lo}}{D_h} \frac{G^2}{2\rho_l} .$$

Here $D_h = 4A/P_w$ is the hydraulic diameter of the channel and the friction coefficient $C_{f,lo}$ can be found from any of expressions valid for single phase flows, depending on

flow conditions. The two-phase friction multiplier ϕ_{lo}^2 has to be found from any expressions given below.

The two-phase flow can be treated as an equivalent of a single-phase flow. In such a case, the two-phase pressure gradient can be determined as,

$$(3\text{-}313) \quad \left(\frac{dp}{dz}\right)_{w,tp} = \frac{4C_{f,tp}}{D_h}\frac{G^2}{2\rho_{tp}}.$$

In this expression $C_{f,tp}$ is an effective Fanning friction factor for the two-phase flow and ρ_{tp} is an effective mixture density. Both these values are unknown; however, comparing the above expression with Eq. (3-307) suggests the following relationship,

$$(3\text{-}314) \quad \frac{C_{f,tp}}{\rho_{tp}} = \left[\frac{P_{w,v}}{P_w}\frac{C_{f,v}}{\rho_v}x^2 + \frac{P_{w,l}}{P_w}\frac{C_{f,l}}{\rho_l}(1-x)^2\right].$$

This equation is merely elucidating the physical meaning of the expression on the left-hand side, but it is not useful for practical calculations.

The friction pressure loss model introduced in this section is based on the following two assumptions:

- the effective two-phase friction factor $C_{f,tp}$ can be expressed in analogy to single-phase flows as a function of the mixture Reynolds number,

- the effective mixture density is equal to the static mixture density: $\rho_{tp} = \rho_m$.

Using these assumptions and combining Eqs. (3-311) through (3-313) yields,

$$(3\text{-}315) \quad \phi_{lo}^2 = \frac{C_{f,tp}}{C_{f,lo}}\frac{\rho_l}{\rho_m} = \frac{C_{f,tp}}{C_{f,lo}}\left[1+\left(\frac{\rho_l}{\rho_v}-1\right)x\right].$$

As mentioned above, the effective friction factor can be expressed as a function of the mixture Reynolds number. Using the Blasius formula as a prototype of such a function, the friction factors for liquid-only (*lo*) and for the two-phase mixture (*tp*) read as follows,

$$(3\text{-}316) \quad C_{f,lo} = \mathsf{A}\cdot\mathrm{Re}_{lo}^{-a} = \mathsf{A}\left(\frac{GD_h}{\mu_l}\right)^{-a} \quad C_{f,tp} = \mathsf{B}\cdot\mathrm{Re}_{tp}^{-b} = \mathsf{B}\left(\frac{GD_h}{\mu_m}\right)^{-b}.$$

Assuming next that coefficients in Eq. (3-316) for single-phase and two-phase flows are equal, that is $\mathsf{A} = \mathsf{B}$ and $a = b$, Eq. (3-315) becomes,

$$(3\text{-}317) \quad \phi_{lo}^2 = \left(\frac{\mu_m}{\mu_l}\right)^b\left[1+\left(\frac{\rho_l}{\rho_v}-1\right)x\right].$$

The **mixture viscosity** appearing in Eqs. (3-316) and (3-317) can be defined in different ways. It is customary to use some kind of weighted mean value, employing quality as the weighting factor. Three examples of the mixture viscosity are as follows,

(3-318)
$$\frac{1}{\mu_m} = \frac{x}{\mu_v} + \frac{1-x}{\mu_l},$$

(3-319)
$$\mu_m = x\mu_v + (1-x)\mu_l,$$

(3-320)
$$\frac{\mu_m}{\rho_m} = \frac{x\mu_v}{\rho_v} + \frac{(1-x)\mu_l}{\rho_l}.$$

Using Eq. (3-318) in (3-317), and taking $a = b = 0.25$ (valid for the Blasius correlation) yields,

(3-321)
$$\phi_{lo}^2 = \left[1 + \left(\frac{\mu_l}{\mu_v} - 1\right)x\right]^{-0.25}\left[1 + \left(\frac{\rho_l}{\rho_v} - 1\right)x\right].$$

Combining Eqs. (3-311), (3-312) and (3-321) yields the following expression for the friction pressure term:

(3-322)
$$\left(\frac{dp}{dz}\right)_{w,tp} = \left[1 + \left(\frac{\mu_l}{\mu_v} - 1\right)x\right]^{-0.25}\left[1 + \left(\frac{\rho_l}{\rho_v} - 1\right)x\right]C_{f,lo}\frac{4}{D_h}\frac{G^2}{2\rho_l} = \phi_{lo}^2 C_{f,lo}\frac{4}{D_h}\frac{G^2}{2\rho_l}.$$

The above equation is an example of many possible formulations, depending on the choice of the two-phase flow multiplier.

Two phase flow multipliers play an important role in prediction of the pressure drop in two-phase flows. As can be expected, there are plenty of correlations available in the open literature. In addition, manufactures of the nuclear fuel perform pressure drop tests using their own designs and develop fuel-specific two-phase flow multipliers. As an example, a model proposed by Lockhart and Martinelli will be described below.

Lockhart and Martinelli proposed a generalized correlation method for determining the two-phase multiplier ϕ_l^2 and ϕ_v^2 from which the frictional pressure gradient can be predicted for adiabatic gas-liquid flow in round tubes. The correlations are based on data from a series of measurements of adiabatic two-phase flow in horizontal tubes. The correlations are as follows,

(3-323)
$$\phi_l^2 = 1 + \frac{C}{X} + \frac{1}{X^2},$$

(3-324)
$$\phi_v^2 = 1 + CX + X^2.$$

Here X is the **Martinelli parameter**, defined as

$$(3\text{-}325) \quad X = \left[\frac{(dp/dz)_l}{(dp/dz)_v} \right]^{0.5} .$$

This parameter will have different forms depending on whether phases are laminar or turbulent. As an example assume that both phases are turbulent, then,

$$(3\text{-}326) \quad \left(\frac{dp}{dz} \right)_l = A \left(\frac{G_l D_h}{\mu_l} \right)^{-a} \frac{G_l^2}{2\rho_l}; \quad \left(\frac{dp}{dz} \right)_v = A \left(\frac{G_g D_h}{\mu_v} \right)^{-a} \frac{G_v^2}{2\rho_v},$$

and the X-parameter in Eq. (3-325) becomes,

$$(3\text{-}327) \quad X_{tt} = \left[\left(\frac{\mu_l}{\mu_v} \right)^{0.25} \left(\frac{1-x}{x} \right)^{1.75} \frac{\rho_v}{\rho_l} \right]^{0.5} .$$

The tt subscript indicates that both phases are turbulent. Other possible subscript combinations will be lt, tl and ll, meaning laminar liquid – turbulent vapour, turbulent liquid – laminar vapour and both phases laminar, respectively.

The recommended value of the constant C in Eqs. (3-323) and (3-324) differs, depending on the flow regime associated with the flow of the vapour and the liquid alone in the channel. There are four possible combinations in which each phase can be either laminar or turbulent. The values of C are shown in TABLE 3.5.

TABLE 3.5. C constant for correlations, given by Eqs. (3-323) and (3-324).

Liquid \ Gas ->	Laminar	Turbulent
Laminar	5	12
Turbulent	10	20

The two phase flow multiplier ϕ_{lo}^2 can be expressed in terms of ϕ_l^2 as follows,

$$(3\text{-}328) \quad \phi_{lo}^2 = \frac{(dp/dz)_{w,tp}}{(dp/dz)_{w,lo}} = (1-x)^{1.75} \phi_l^2 .$$

3.5.7 Gravity Pressure Gradient

The **gravity pressure gradient** is defined as,

$$(3\text{-}329) \quad -\left(\frac{dp}{dz} \right)_{grav} = \rho_m g \sin\varphi .$$

Here $\sin\varphi$ is equal to 1 for vertical channels and to 0 for horizontal channels. Since, in general, the mixture density ρ_m can change along a channel, the pressure gradient will change as well.

3.5.8   Acceleration Pressure Gradient

The **acceleration pressure gradient** can be evaluated as,

$$(3\text{-}330) \quad -\left(\frac{dp}{dz}\right)_{acc} = \frac{1}{A}\frac{d}{dz}\left(\frac{G^2 A}{\rho_M}\right).$$

For constant G and A, this expression reduces to:

$$(3\text{-}331) \quad -\left(\frac{dp}{dz}\right)_{acc} = G^2 \frac{d}{dz}\left(\frac{1}{\rho_M}\right).$$

Substituting the expression for the dynamic mixture density ρ_M into the above equation gives,

$$(3\text{-}332) \quad -\left(\frac{dp}{dz}\right)_{acc} = G^2 \frac{d}{dz}\left[\frac{x^2}{\alpha\rho_v} + \frac{(1-x)^2}{(1-\alpha)\rho_l}\right].$$

Using the HEM, the acceleration pressure gradient is obtained as follows,

$$(3\text{-}333) \quad -\left(\frac{dp}{dz}\right)_{acc} = G^2 \frac{d}{dz}\left[x\left(\frac{1}{\rho_g} - \frac{1}{\rho_f}\right) + \frac{1}{\rho_f}\right] = \left(\frac{1}{\rho_g} - \frac{1}{\rho_f}\right)G^2 \frac{dx}{dz}.$$

Equation (3-298) describes all pressure drop terms that appear in an arbitrary channel with two-phase flow in which there are no local pressure drops. If the channel contains local obstacles or sudden cross-section area changes, the corresponding pressure drops must be added to the previously described ones. This procedure is very much the same as that described in previous section for single-phase flows. However, some important differences, described below, have to be taken into account while applying the single-phase theory to two-phase flows.

3.5.9   Local Pressure Loss

The local pressure loss for single phase has been discussed in the previous section. The single-phase flow theory will be now extended to two-phase flow situations. Using sections "1" and "2" to represent locations before and after local obstacle, the momentum balance equation can be written,

$$(3\text{-}334) \quad \begin{aligned} F = {}&(1-\alpha_1)\rho_l U_{l1} A_{l1} U_{l1} + \alpha_1 \rho_v U_{v1} A_{v1} U_{v1} - \\ &[(1-\alpha_2)\rho_l U_{l2} A_{l2} U_{l2} + \alpha_2 \rho_v U_{v2} A_{v2} U_{v2}] + p_1 A_1 - p_2 A_2 \end{aligned}.$$

With similar arguments as for the single-phase flow case, the force F is taken equal to $p_1(A_2 - A_1)$, and using $s = A_1/A_2$, Eq. (3-334) yields,

$$(3\text{-}335) \quad p_2 - p_1 = \frac{G_1^2}{\rho_l} s\left\{\left[\frac{(1-x)^2}{1-\alpha_1} + \frac{\rho_l}{\rho_v}\frac{x^2}{\alpha_1}\right] - s\left[\frac{(1-x)^2}{1-\alpha_2} + \frac{\rho_l}{\rho_v}\frac{x^2}{\alpha_2}\right]\right\}.$$

The corresponding irreversible pressure drop, assuming incompressible two-phase flow with $\alpha_1 = \alpha_2 = \alpha$, becomes,

$$-\Delta p_I = \frac{G_1^2}{\rho_l}(1-s) \times$$

$$(3\text{-}336) \qquad \left\{ s\left[\frac{(1-x)^2}{1-\alpha} + \frac{\rho_l}{\rho_v}\frac{x^2}{\alpha} \right] - \frac{\dfrac{1+s}{2}\left[\dfrac{(1-x)^3}{(1-\alpha)^2\rho_l} + \dfrac{\rho_l}{\rho_v^2}\dfrac{x^3}{\alpha} \right]}{\dfrac{x}{\rho_v} + \dfrac{1-x}{\rho_l}} \right\}.$$

It has been assumed that there is no phase change between sections "1" and "2", that is $x_1 = x_2$. However, void fractions at the two sections are usually not equal to each other. It has been observed that the void fraction significantly increases downstream of the enlargement. This effect disappears at some distance, however. This distance is evaluated to be between $L/D = 10$ up to 70. Nevertheless, Eq. (3-336) can be simplified by assuming the homogeneous model and the resultant irreversible pressure drop will become as follows,

$$(3\text{-}337) \qquad -\Delta p_I = \left[1 + x\left(\frac{\rho_l}{\rho_v} - 1 \right) \right]\left(1 - \frac{A_1}{A_2} \right)^2 \frac{G_1^2}{2\rho_l}.$$

This equation can be compared with its equivalent for the single-phase flow through a sudden enlargement. As can be seen, a new term appears, which can be identified as a two-phase multiplier for the local pressure loss,

$$(3\text{-}338) \qquad \phi_{lo,d}^2 = \left[1 + x\left(\frac{\rho_l}{\rho_v} - 1 \right) \right].$$

The subscript *lo,d* is used to indicate that the multiplier given by Eq. (3-338) is valid for local losses, where the viscous effects can be neglected and only the *d*ensity ratio between the two phases plays any role.

The corresponding irreversible pressure drop for homogeneous two-phase flow through a sudden contraction becomes (see previous section for single-phase flow equivalent),

$$(3\text{-}339) \qquad -\Delta p_I = \left[1 + x\left(\frac{\rho_l}{\rho_v} - 1 \right) \right]\left(\frac{A_2}{A_c} - 1 \right)^2 \frac{G_2^2}{2\rho_l}.$$

Even here the two-phase multiplier given by Eq. (3-338) appears together with the local loss coefficient valid for single-phase flows.

In general, a local irreversible pressure drop for two-phase flows can be expressed as:

$$(3\text{-}340) \qquad \Delta p_{I,tp} = \phi_{lo,d}^2 \Delta p_{I,lo},$$

where *tp* stands for *two-phase* and *lo* for *liquid only*. As can be seen, the local pressure drop for two-phase flows can be obtained from a multiplication of the corresponding local pressure drop for single-phase flow and a proper two-phase multiplier. A similar principle is valid for the frictional pressure drop for single- and two-phase flows. It can be noted that the local two-phase multiplier given by Eq. (3-338) is not the same as the frictional two-phase multiplier, given by Eq. (3-321). The reason for this difference stems from the neglect of viscous losses in the case of the local pressure losses. Nevertheless, it should be mentioned that in many in practical calculations, the multiplier is assumed the same for both frictional and local pressure losses.

3.5.10 Total Pressure Drop

Equation (3-298) gives an expression for the pressure gradient change along a boiling channel. In practical calculation it is usually required to determine the over-all pressure drop in a channel of a given length and shape. The total pressure drop can be readily obtained from an integration of Eq. (3-298) along the channel length as follows,

$$(3\text{-}341) \quad -\int_0^L \frac{dp}{dz}dz \equiv -\big[p(L)-p(0)\big] \equiv -\Delta p =$$
$$\int_0^L \left(\frac{dp}{dz}\right)_{w,tp} dz + \int_0^L \rho_m g \sin\varphi\, dz + \int_0^L \frac{1}{A}\frac{d}{dz}\left(\frac{G^2 A}{\rho_M}\right)dz .$$

Assuming that the channel has a constant cross-section area and using expressions for the friction, gravity and acceleration terms, the following expression is obtained,

$$(3\text{-}342) \quad -\Delta p = C_{f,lo}\frac{2}{D_h}\frac{G^2}{\rho_l}\int_0^L \phi_{lo}^2 dz + g\sin\varphi\int_0^L \big[\alpha\rho_v + (1-\alpha)\rho_l\big]dz +$$
$$G^2\int_0^L \frac{d}{dz}\left[\frac{x^2}{\alpha\rho_v} + \frac{(1-x)^2}{(1-\alpha)\rho_l}\right]dz .$$

It is customary to introduce integral multipliers into the above equations which are defined as follows.

The integral **acceleration multiplier** is defined as,

$$(3\text{-}343) \quad r_2 \equiv \rho_l\int_0^L \frac{d}{dz}\left[\frac{x^2}{\alpha\rho_v} + \frac{(1-x)^2}{(1-\alpha)\rho_l}\right]dz =$$
$$\left[\frac{x^2\rho_l}{\alpha\rho_v} + \frac{(1-x)^2}{(1-\alpha)}\right]_{ex} - \left[\frac{x^2\rho_l}{\alpha\rho_v} + \frac{(1-x)^2}{(1-\alpha)}\right]_{in} .$$

Here subscripts *ex* and *in* mean that the expression in the rectangular parentheses is evaluated at the channel *ex*it (*z=L*) and at the channel *in*let (*z=0*), respectively. For heated channel with $x = \alpha = 0$ at the inlet and x_{ex} with α_{ex} at the outlet, the multiplier is as follows,

$$(3\text{-}344) \quad r_2 = \left[\frac{x^2\rho_l}{\alpha\rho_v} + \frac{(1-x)^2}{(1-\alpha)}\right]_{ex} - 1 .$$

For the HEM, the integral acceleration multiplier is as follows,

$$(3\text{-}345) \quad r_2 \equiv \rho_l \left(\frac{1}{\rho_v} - \frac{1}{\rho_l} \right) \int_0^L \frac{dx}{dz} dz = \left(\frac{\rho_l}{\rho_v} - 1 \right) \left(x_{ex} - x_{in} \right).$$

Equation (3-347) is valid only for non-negative inlet quality, that is when $x_{in} \geq 0$.

The integral **friction multiplier** is defined as,

$$(3\text{-}346) \quad r_3 = \frac{1}{L} \int_0^L \phi_{lo}^2 dz .$$

Assuming uniformly-heated channel and taking ϕ_{lo}^2 derived from the HEM, the friction multiplier is obtained as follows,

$$(3\text{-}347) \quad r_3 = \int_0^1 \frac{1 + x_{ex} \left(\dfrac{\rho_l}{\rho_v} - 1 \right) \zeta}{\left[1 + x_{ex} \left(\dfrac{\mu_l}{\mu_v} - 1 \right) \zeta \right]^{0.25}} d\zeta .$$

The integral **gravity multiplier** is calculated as,

$$(3\text{-}348) \quad r_4 = \frac{1}{L\rho_l} \int_0^L \left[\alpha\rho_v + (1-\alpha)\rho_l \right] dz = 1 - \frac{\rho_l - \rho_v}{\rho_l} \frac{1}{L} \int_0^L \alpha dz .$$

For uniformly heated channel and employing the HEM, the gravity multiplier is given as,

$$(3\text{-}349) \quad r_4 = 1 - x_{ex} \int_0^1 \frac{\zeta}{\rho_g / (\rho_f - \rho_g) + x_{ex}\zeta} d\zeta ,$$

or, after integration,

$$(3\text{-}350) \quad r_4 = \frac{\rho_g}{(\rho_f - \rho_g) x_{ex}} \ln \frac{\rho_g + (\rho_f - \rho_g) x_{ex}}{\rho_g} .$$

The total pressure drop in a channel with length L, hydraulic diameter D_h and constant mass flux G can be then found as,

$$(3\text{-}351) \quad -\Delta p = r_3 C_{f,lo} \frac{4L}{D_h} \frac{G^2}{2\rho_l} + r_4 L \rho_l g \sin\varphi + r_2 \frac{G^2}{\rho_l} .$$

If the channel contains a number of local losses ($i = 1, .., N$), the total pressure drop will be as follows,

$$(3\text{-}352) \quad -\Delta p = r_3 C_{f,lo} \frac{4L}{D} \frac{G^2}{2\rho_l} + r_4 L \rho_l g \sin\varphi + r_2 \frac{G^2}{\rho_l} + \left(\sum_{i=1}^{N} \phi_{lo,d,i}^2 \xi_i \right) \frac{G^2}{2\rho_l}.$$

Here ξ_i indicates the local loss coefficient of the i-th obstacle and $\phi_{lo,d,i}^2$ is the corresponding local two-phase flow multiplier. The multipliers have been plotted in function of exit quality and system pressure and are shown in figures below.

It should be noted that Eq. (3-352) and the two-phase flow multipliers shown in FIGURE 3-16 through FIGURE 3-18 are valid only for channels with saturated conditions at the inlet. If subcooled conditions prevail at the channel inlet, the channel should be divided into single-phase flow and two-phase flow parts and pressure drops should be calculated separately in each of the two parts.
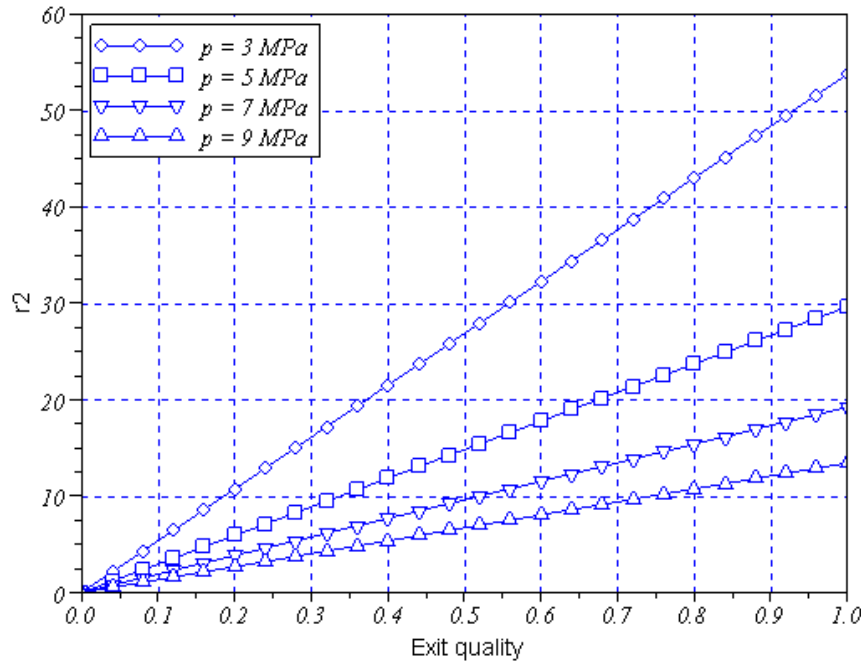
FIGURE 3-16. Acceleration multiplier as a function of the exit quality and the system pressure for a water-steam saturated mixture.
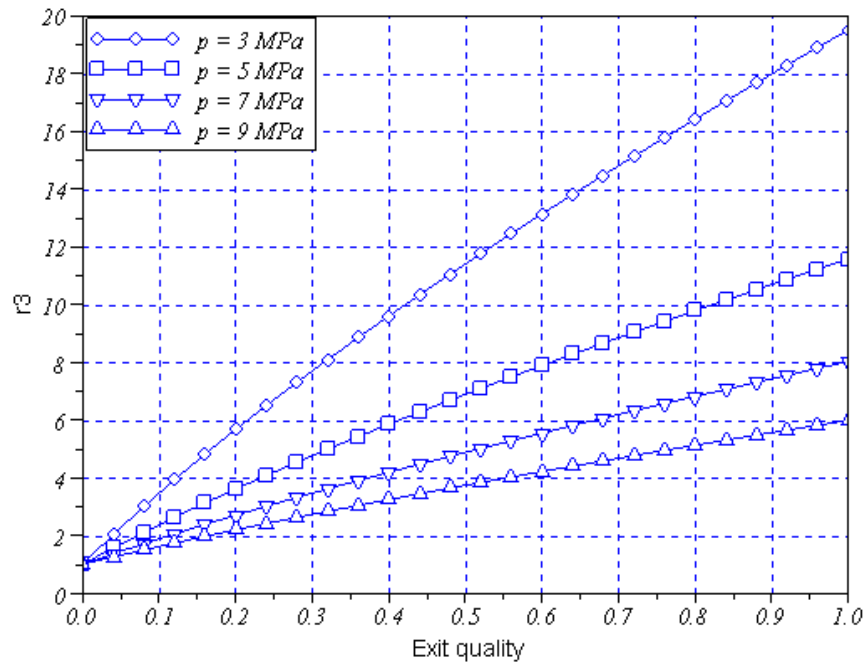
FIGURE 3-17. Friction multiplier as a function of the exit quality and the system pressure for a saturated water-steam mixture flow in a uniformly heated channel.
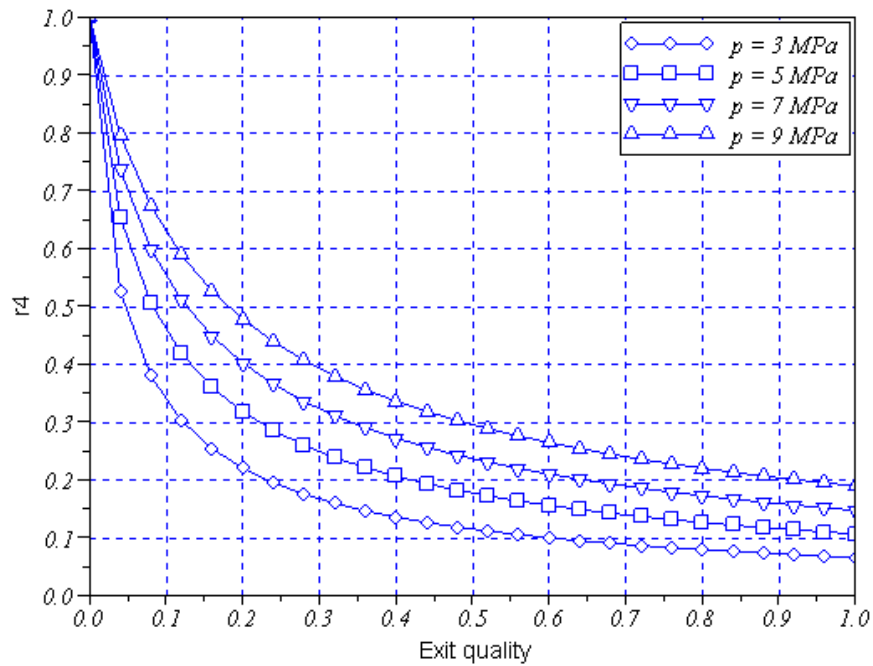
FIGURE 3-18. Gravity multiplier as a function of the exit quality and the system pressure for a water-steam mixture flow in a uniformly heated channel.

R E F E R E N C E S

[3-1]   Bird, R.B., W.E. Stewart and E.N. Lightfoot, *Transport Phenomena*, Wiley, New York, 2002.

[3-2]   Brennen, C.E., *Fundamentals of Multiphase Flow*, Cambridge,, 2005, ISBN 0-521-84804-0.

[3-3]   Drew, D.D. and Passman, S.L., *Theory of Multicomponent Fluids*, Springer, 1998, ISBN 0-387-98380-5.

[3-4]   Ishii, M. and Hibiki, T., Thermo-fluid Dynamics of Two-phase Flow, Springer, 2006, ISBN 0-387-28321-8.

[3-5]   Wallis, G.B., *One-Dimensional Two-Phase Flow*, McGraw-Hill, 1969.

[3-6]   White, F. M., *Viscous Fluid Flow*, McGraw-Hill Inc., 1991, ISBN 0-07-069712-4.

E X E R C I S E S

EXERCISE 3-1. Plot void fraction in function of flow quality (in a range from 0 to 1) assuming flow of water and vapour mixture at saturation conditions and at pressure p = 70 bar. Compare two cases: in one case both phases have the same averaged velocity; in the other case the vapour phase flows with mean velocity which is 20% higher than the mean liquid velocity.

EXERCISE 3-2. Compare void fraction predicted from the homogeneous model and the drift-flux model for steam-water flow. Assume $p = 70$ bar, $G = 1200$ kg m^{-2} s^{-1} and (3-285) with (3-286) for drift-flux parameters. Make a plot of void fraction as a function of quality. Plot slip ratio given by (3-288) in function of quality for the same conditions.

EXERCISE 3-3. Plot two-phase multiplier as a function of quality assuming two-phase flow of water-vapour mixture under 70 bar pressure.

EXERCISE 3-4. Derive expressions for integral multipliers r_2, r_3 and r_4 for channels with saturated liquid at the inlet and with uniform heat flux distribution along channel length. Hint: in integrals along channel length use substitution: $dz = const * dx$, which is valid for uniformly heated channels.

4. Heat Transfer

H eat is a form of energy in transit and is intimately coupled to the movement of atoms and molecules. There are three different means of heat transfer: conduction, convection and radiation. In solid bodies heat is conducted from regions of higher temperature to regions of lower temperature through dispersion of the thermal oscillations of atoms about their equilibrium states. The ability of the dispersion is expressed in terms of the thermal conductivity of the solid body. Convection takes place when heat is transported because of the motion of material. This type of heat transfer is typical for gases and liquids. Radiation heat transfer occurs when thermal motion of atoms causes emission of electromagnetic radiation. For relatively low temperatures the radiation in infra-red region prevails, whereas with temperatures above 900 K radiation takes place in the visible wave lengths.

The goal of heat transfer analyses which are typically performed in nuclear power plants is to calculate the amount of heat that is transferred in various systems under considerations. In particular, heat, which is generated in the nuclear fuel elements, has to be transferred to coolant and finally converted into kinetic energy in turbines. After reactor shut down, the decay heat which is still generated in the reactor core has to be removed in order to protect the core from potential damage resulting from overheating. All these processes involve various means of heat transfer combined together. An adequate heat transfer model has to take this fact into account, which, together with typical complexity of involved geometry, makes an overall heat transfer analysis in a nuclear system a very complex task.

The objective of this chapter is to present the basic aspects of heat transfer that take place in nuclear systems. The focus is on the prediction of the maximum temperature of materials in various heat transfer devices such as nuclear reactor cores, steam generators and heat exchangers.

4.1 Heat Conduction

Heat conduction refers to the transfer of heat by means of molecular interactions without any accompanying macroscopic displacement of matter. The flow of heat by conduction is governed by the **Fourier's law**:

(4-1) $$\mathbf{q}''(\mathbf{r}, t) = -\lambda \nabla T(\mathbf{r}, t),$$

where $\mathbf{q}''(\mathbf{r}, t)$ [W m^{-2}] is the heat flux vector expressing the rate at which heat flows across a unit area at location $\mathbf{r}$ and time t, $T(\mathbf{r},t)$ [K] is the local temperature and λ [W m^{-1} K^{-1}] is the thermal conductivity of the conducting material. The Fourier's law states

that the amount of heat per unit area and unit time that is conducted through matter is proportional to the gradient of temperature. The minus sign in Eq. (4-1) results from the fact that heat is conducted from locations with higher temperature to locations with lower temperature.

Consider stationary heat conduction through an infinite plate with thickness d, where plate surfaces are kept at two different but constant temperatures T_1 and T_2, as shown in FIGURE 4-1.
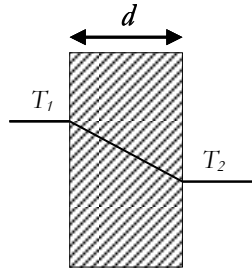
FIGURE 4-1. Heat conduction through an infinite flat plate.

The Fourier's law for a stationary one-dimensional case reads,

$$(4\text{-}2) \qquad q'' = -\lambda \frac{dT}{dx}.$$

Assuming further that the thermal conductivity is constant, Eq. (4-2) can be integrated across the plate thickness to give,

$$(4\text{-}3) \qquad \int_0^d q'' dx = -\lambda \int_{T_1}^{T_2} dT = \lambda(T_1 - T_2).$$

From the energy conservation principle it can be concluded that,

$$(4\text{-}4) \qquad q_1'' = q_2'' = q'' = const.$$

Combining Eqs. (4-4) and (4-3) yields,

$$(4\text{-}5) \qquad q'' = \frac{\lambda}{d}(T_1 - T_2).$$

The solution expressed by Eq. (4-5) states that for given thermal conductivity the heat flux increases with increasing temperature drop across the plate and decreases with increasing plate thickness. It should be noted that this simple solution has been obtained directly from the Fourier's law; however, the energy conservation principle has been employed through Eq. (4-4). The energy conservation principle can be combined with the Fourier's law leading to the heat conduction equation.

A general form of the energy conservation equation has been derived in the previous Chapter. The equation expressed in terms of temperature reads as follows,

$$\rho c_p \frac{DT}{Dt} = -\nabla \cdot \mathbf{q}'' + \boldsymbol{\tau} : \nabla \mathbf{v} - \left(\frac{\partial \ln \rho}{\partial \ln T}\right)_p \frac{Dp}{Dt} + q'''.$$

Assuming pure conduction heat transfer in a solid body and employing the Fourier's law, the equation becomes,

$$(4\text{-}6) \qquad \rho c_p \frac{\partial T}{\partial t} = \nabla \cdot \left(\lambda \nabla T\right) + q'''.$$

Here ρ [kg m^{-3}] is the density and c_p [J kg^{-1} K^{-1}] is the specific heat and q''' [W m^{-3}] is the heat source per unit volume. The properties of the conducting matter can in general be a function of the location, temperature and even time. Thus, Eq. (4-6) is a non-linear partial differential equation. Distribution of the temperature in any arbitrary volume can be found provided that the boundary and the initial conditions are known.

The initial conditions are typically specified by a given temperature distribution in the whole region of interest at given time $t = t_0$. Usually $t_0 = 0$ and the initial condition can be written as,

$$(4\text{-}7) \qquad T(\mathbf{r}, 0) = T_0(\mathbf{r}),$$

where $T_0(\mathbf{r})$ is a known function of spatial coordinates.

The boundary conditions can be specified in several different ways, depending on what kind of a parameter is known at the boundary. If the boundary temperature is known, a boundary condition of the first kind (or the Dirichlet boundary conditions) is specified:

$$(4\text{-}8) \qquad T(\mathbf{r}, t)\big|_{r=\mathbf{r}_B} = T_B(\mathbf{r}_B, t).$$

Here $\mathbf{r}_B$ is a coordinate on the boundaries where the temperature T_B is a known function of time and location. If the boundary heat flux is known, a boundary condition of the second kind (or the Neumann boundary conditions) is specified:

$$(4\text{-}9) \qquad q''(\mathbf{r}, t)\big|_{\mathbf{r}=\mathbf{r}_B} \equiv -\lambda \frac{\partial T(\mathbf{r}, t)}{\partial n}\bigg|_{\mathbf{r}=\mathbf{r}_B} = \phi(\mathbf{r}_B, t),$$

where $\phi(\mathbf{r}_B, t)$ is a given function describing the heat flux distribution at the boundary. If a convective heat transfer to fluid with a known bulk temperature T_f takes place, a boundary condition of the third kind (or the Newton boundary conditions) is specified:

$$(4\text{-}10) \qquad -\lambda \frac{\partial T(\mathbf{r}, t)}{\partial n}\bigg|_{\mathbf{r}=\mathbf{r}_B} = h\left[T(\mathbf{r}, t)\big|_{\mathbf{r}=\mathbf{r}_B} - T_f\right],$$

where h [W m^{-2} K^{-1}] is the convective heat transfer coefficient and T_f is the fluid bulk temperature (for flows in channels this temperature is equal to the mean velocity-

weighted temperature in the cross-section of the channel). If two solid bodies are in direct contact with each other, the boundary conditions of the fourth kind are specified:

(4-11) $T_1(\mathbf{r},t)\big|_{\mathbf{r}=\mathbf{r}_B} = T_2(\mathbf{r},t)\big|_{\mathbf{r}=\mathbf{r}_B}$ and $-\lambda_1 \dfrac{\partial T_1(\mathbf{r},t)}{\partial n}\bigg|_{\mathbf{r}=\mathbf{r}_B} = -\lambda_2 \dfrac{\partial T_2(\mathbf{r},t)}{\partial n}\bigg|_{\mathbf{r}=\mathbf{r}_B}$.

The heat conduction equation (4-6) together with the initial and boundary conditions given by Eqs. (4-7) through (4-11) describe a non-stationary temperature distribution in an arbitrary body with volumetric heat sources. Several special conditions can be considered depending on the material property, presence of heat sources and the geometry of the region under consideration.

Assuming that properties of the conducting material are constant, Eq. (4-6) can be re-written as,

(4-12) $\dfrac{\partial T}{\partial t} = \dfrac{\lambda}{\rho c_p}\nabla^2 T + \dfrac{q'''}{\rho c_p}$.

The new property group appearing in Eq. (4-12) is the thermal diffusivity coefficient,

(4-13) $a = \dfrac{\lambda}{\rho \cdot c_p}$.

If there are no volumetric heat sources, Eq. (4-12) becomes,

(4-14) $\dfrac{\partial T(\mathbf{r},t)}{\partial t} = a\nabla^2 T(\mathbf{r},t)$.

This form of equation is known in the literature as the Fourier equation of conduction. For steady-state conduction the equation simplifies to,

(4-15) $\nabla^2 T(\mathbf{r}) = -\dfrac{q'''(\mathbf{r})}{\lambda}$,

which is often referred to as the Poisson equation. Finally, the simplest form of the conduction equation, also known as the Laplace equation, is obtained for situations when there is no heat source in the conducting region,

(4-16) $\nabla^2 T(\mathbf{r}) = 0$.

In Eqs. (4-12) and (4-14) through (4-16) the Laplacian operator $\nabla^2 \equiv \nabla \cdot \nabla$ (sometimes denoted by Δ) has been used. The Laplacian operator in various systems of coordinates is as follows:

Cartesian system of coordinates (x,y,z):

(4-17) $\quad \nabla^2 \equiv \left(\dfrac{\partial^2}{\partial x^2} + \dfrac{\partial^2}{\partial y^2} + \dfrac{\partial^2}{\partial z^2} \right).$

Cylindrical polar system of coordinates (r,θ,z):

(4-18) $\quad \nabla^2 \equiv \left(\dfrac{\partial^2}{\partial r^2} + \dfrac{1}{r} \dfrac{\partial}{\partial r} + \dfrac{1}{r^2} \dfrac{\partial^2}{\partial \theta^2} + \dfrac{\partial^2}{\partial z^2} \right),$

Spherical polar system of coordinates (r,θ,φ):

(4-19) $\quad \nabla^2 \equiv \left(\dfrac{\partial^2}{\partial r^2} + \dfrac{2}{r} \dfrac{\partial}{\partial r} + \dfrac{1}{r^2 \sin^2 \theta} \dfrac{\partial^2}{\partial \varphi^2} + \dfrac{1}{r^2} \dfrac{\partial^2}{\partial \theta^2} + \dfrac{1}{r^2} \cot \theta \dfrac{\partial}{\partial \theta} \right).$

If the geometry under consideration and the boundary conditions are symmetrical, the spatial dimension of the problem can be reduced, which usually significantly simplifies the solution of the differential equation. In particular, temperature distribution in a finite cylinder with boundary and initial conditions which are independent on θ will be θ-independent as well, and the adequate Laplacian operator simplifies to its axisymmetric form as follows,

(4-20) $\quad \nabla^2 \equiv \left(\dfrac{\partial^2}{\partial r^2} + \dfrac{1}{r} \dfrac{\partial}{\partial r} + \dfrac{\partial^2}{\partial z^2} \right).$

In the same manner, heat conduction in a sphere which is radius-only dependent is described with the following Laplacian,

(4-21) $\quad \nabla^2 \equiv \left(\dfrac{d^2}{dr^2} + \dfrac{2}{r} \dfrac{d}{dr} \right).$
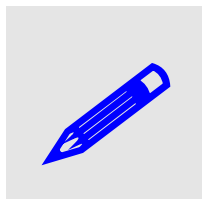
EXAMPLE 4-1. Calculate the temperature distribution in an infinite cylindrical wall cooled on the outer surface with a fluid at constant temperature equal to T_f and heated on the inner surface with a constant heat flux q'', as shown in FIGURE 4-2.
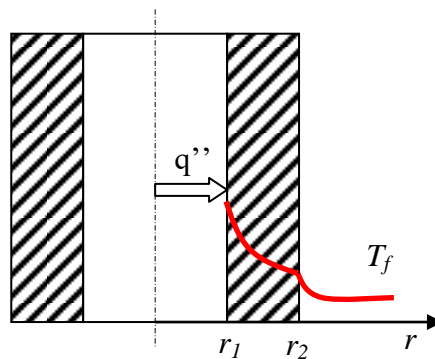
FIGURE 4-2. Steady-state heat conduction through an infinite cylindrical wall.

SOLUTION: The conduction equation is obtained from (4-16) and (4-20) as follows:

(4-22) $\quad \dfrac{d}{dr}\left(r\,\dfrac{dT}{dr} \right) = 0$,

and boundary conditions can be written as,

(4-23) $\quad -\lambda\,\dfrac{dT}{dr}\bigg|_{r=r_1} = q''\,, \; -\lambda\,\dfrac{dT}{dr}\bigg|_{r=r_2} = h\Big(T\big|_{r=r_2} - T_f\Big).$

Solving (4-22) yields,

(4-24) $\quad T = C\ln r + D$.

Substituting Eq. (4-24) into boundary conditions (4-23) yields the following system of two equations with two unknowns C and D:

(4-25)
$$
\left.
\begin{aligned}
-\lambda\,\frac{C}{r_1} &= q''\,, \Rightarrow C = -\frac{q''r_1}{\lambda} \\[2mm]
-\lambda\,\frac{C}{r_2} &= h\big(C\ln r_2 + D - T_f\big), \Rightarrow D = -\lambda\,\frac{C}{hr_2} - C\ln r_2 + T_f
\end{aligned}
\right\} \Rightarrow
$$

$$
\Rightarrow D = T_f + \frac{q''r_1}{\lambda}\left(\frac{\lambda}{hr_2} + \ln r_2 \right)
$$

The solution is thus,

(4-26) $\quad T(r) = -\dfrac{q''r_1}{\lambda}\ln r + \dfrac{q''r_1}{\lambda}\ln r_2 + \dfrac{q''r_1}{hr_2} + T_f = \dfrac{q''r_1}{\lambda}\ln\dfrac{r_2}{r} + \dfrac{q''r_1}{hr_2} + T_f$.

The temperatures on the inner and outer surfaces are obtained as:

$$
T(r_1) \equiv T_1 = \frac{q''r_1}{\lambda}\ln\frac{r_2}{r_1} + \frac{q''r_1}{hr_2} + T_f\,, \qquad T(r_2) \equiv T_2 = \frac{q''r_1}{hr_2} + T_f\,.
$$
Thus, the temperature difference T_1-T_2 is as follows:

$$
T_1 - T_2 = \frac{q''r_1}{\lambda}\ln\frac{r_2}{r_1}.
$$

EXAMPLE 4-2. Calculate the temperature distribution in a spherical wall, with constant temperatures T_i and T_o on the inner and outer surfaces of the wall, as shown in the figure below.
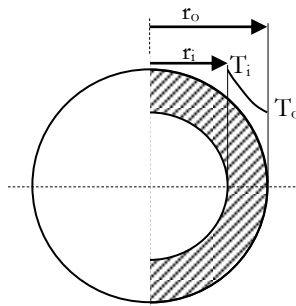
FIGURE 4-3. Heat conduction through a spherical wall.

Since temperatures on the inner and outer surfaces are constant, the solution should depend only on the

radial direction, r. Using (4-21), the heat conduction equation is as follows,

$$\frac{d^2T}{dr^2} + \frac{2}{r}\frac{dT}{dr} = 0,$$

with boundary conditions,

at $r = r_i$ $T = T_i$,
at $r = r_o$ $T = T_o$.

The solution of the conduction equation is given as,

$$T = \frac{C_1}{r} + C_2.$$

Using the boundary condition, the solution is found as,

$$\frac{T_i - T}{T_i - T_o} = \frac{\dfrac{1}{r_i} - \dfrac{1}{r}}{\dfrac{1}{r_i} - \dfrac{1}{r_o}}.$$

4.1.1 Steady-State Heat Conduction with Heat Sources

Various solutions of the Poisson conduction equation can be found for simple geometries such as a flat plate, a cylinder and a sphere.

Flat plate

The temperature distribution in a flat plate with uniformly distributed heat sources and uniform temperatures on both surfaces is described with the following equation,

(4-27) $\dfrac{d^2T}{dx^2} = -\dfrac{q'''}{\lambda}$,   with $T = T_1$ at $x = 0$ and $T = T_2$ at $x = d$.

The solution of the equation is as follows,

(4-28) $T = -\dfrac{q'''}{2\lambda}x^2 + C_1 x + C_2$.

Applying the boundary conditions yields,

(4-29) $T - T_1 = (T_2 - T_1)\dfrac{x}{d} + \dfrac{q'''d^2}{2\lambda}\left(\dfrac{x}{d} - \dfrac{x^2}{d^2}\right)$.

As can be seen, a parabolic temperature distribution has been obtained, with a maximum value at the plate centreline $x = d/2$,

(4-30) $T_{max} = \dfrac{(T_2 + T_1)}{2} + \dfrac{q'''d^2}{8\lambda}$.

Solution (4-29) is a superposition of two parts: the first part represented by the first term on the right-hand-side of Eq. (4-29) is a solution of the conduction equation (4-27) with $q''' = 0$, whereas the second corresponds to a solution of full equation with boundary conditions $T = T_l$ at $x = 0$ and $T = T_l$ at $x = d$.

Cylindrical infinite wall

The axisymmetric one-dimensional Poisson equation is as follows,

$$(4\text{-}31) \quad \frac{d^2 T}{dr^2} + \frac{1}{r}\frac{dT}{dr} = -\frac{q'''}{\lambda}.$$

If the inner and the outer wall surface temperatures are known, the boundary conditions can be written as,

at $r = r_i$ $T = T_i$ and at $r = r_o$ $T = T_o$

Double integration of Eq. (4-31) yields,

$$(4\text{-}32) \quad T = -\frac{q''' r^2}{4\lambda} + C_1 \ln r + C_2.$$

Employing the boundary condition, the solution becomes as follows,

$$(4\text{-}33) \quad T - T_i = -\frac{q'''\left(r^2 - r_i^2\right)}{4\lambda} + \left[\left(T_o - T_i\right) + \frac{q'''\left(r_o^2 - r_i^2\right)}{4\lambda} \right] \frac{\ln \dfrac{r}{r_i}}{\ln \dfrac{r_o}{r_i}}.$$

As can be seen, similarly as for the flat plate, the solution is a superposition of two parts: one with $q''' = 0$ and the other with boundary conditions corresponding to equal temperatures on the inner and outer wall surface. When $q''' = 0$, solution (4-33) simplifies to the solution obtained for a cylindrical infinite wall without heat sources,

$$(4\text{-}34) \quad T - T_i = \left(T_o - T_i\right) \frac{\ln \dfrac{r}{r_i}}{\ln \dfrac{r_o}{r_i}}.$$

Infinite cylinder

The difference between the infinite cylinder and the infinite cylindrical wall is that in the former case proper boundary conditions must be specified at the cylinder centreline at $r = 0$. It can be seen that the solution found for the cylindrical wall, Eq. (4-33), exhibits a singularity when $r_i \to 0$. Thus, the boundary conditions for the cylinder are as follows,

at $r = 0$ T is *finite* and at $r = r_o$ $T = T_o$

With these boundary conditions the constant C_1 in Eq. (4-32) must be equal to zero, and the solution is as follows,

$$(4-35) \quad T - T_o = \frac{q'''\left(r_o^2 - r^2\right)}{4\lambda}.$$

Thus a parabolic temperature distribution is obtained with a maxim temperature at the cylinder centreline equal to,

$$(4-36) \quad T_{max} = \frac{q'''r_o^2}{4\lambda} + T_o.$$

Sphere

One dimensional conduction equation with heat sources in spherical coordinates is as follows,

$$(4-37) \quad \frac{d^2T}{dr^2} + \frac{2}{r}\frac{dT}{dr} = -\frac{q'''}{\lambda},$$

and the temperature boundary conditions can be written as,

at $r = 0$ T is *finite* and at $r = r_o$ $T = T_o$.

Integration of Eq. (4-37) yields,

$$(4-38) \quad T = -\frac{q'''r^2}{6\lambda} + \frac{C_1}{r} + C_2.$$

The constants C_1 and C_2 can be found from the boundary conditions and the final solution is as follows,

$$(4-39) \quad T - T_o = \frac{q'''r_o^2}{6\lambda}\left[1 - \left(\frac{r}{r_o}\right)^2\right].$$

The temperature distribution follows thus a parabolic shape, in a similar manner as it was obtained for the flat plate and the cylinder. The maximum temperature is located at the sphere centre and is equal to,

$$(4-40) \quad T_{max} = \frac{q'''r_o^2}{6\lambda} + T_o.$$

4.1.2   Steady-State Heat Conduction in Fuel Elements

Fuel elements in nuclear reactors have a composite structure with several layers. Typical structure of a cylindrical fuel rod is shown in FIGURE 4-4. The central part of the fuel element is filled with cylindrical nuclear fuel pellets. The pellets are surrounded by two annular layers: a gas gap, which is filled with the gaseous fission products

during reactor operation, and a metallic cladding, which is preventing fission products to leak to coolant.
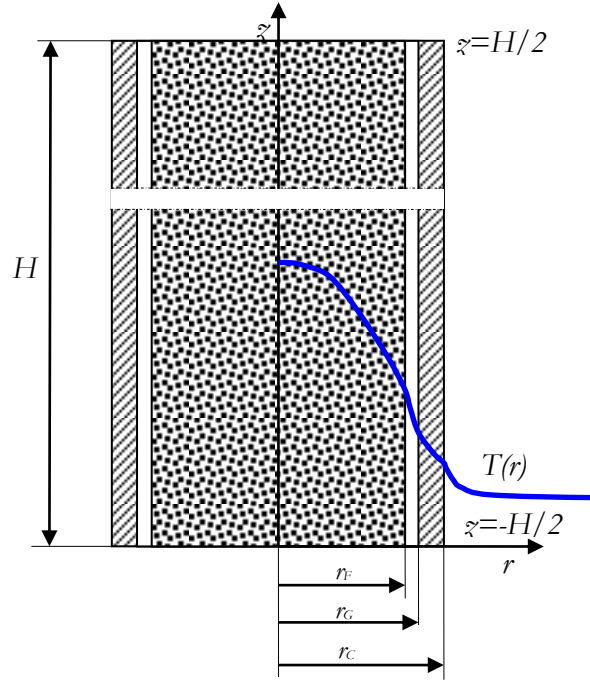
FIGURE 4-4. Structure of a cylindrical nuclear fuel rod.

The heat conduction equation has to be solved separately in each part of the fuel structure employing proper conditions at the boundaries. For the cylindrical nuclear fuel rod, the heat conduction equations and the boundary conditions are as follows,

heat conduction in fuel pellet

$$(4\text{-}41) \quad \frac{1}{r}\frac{\partial}{\partial r}\left(r\lambda_F\frac{\partial T_F}{\partial r}\right) + \frac{\partial}{\partial z}\left(\lambda_F\frac{\partial T_F}{\partial z}\right) = -q'''(r,z),$$

heat conduction in gas gap

$$(4\text{-}42) \quad \frac{1}{r}\frac{\partial}{\partial r}\left(r\lambda_G\frac{\partial T_G}{\partial r}\right) + \frac{\partial}{\partial z}\left(\lambda_G\frac{\partial T_G}{\partial z}\right) = 0,$$

heat conduction in clad

$$(4\text{-}43) \quad \frac{1}{r}\frac{\partial}{\partial r}\left(r\lambda_C\frac{\partial T_C}{\partial r}\right) + \frac{\partial}{\partial z}\left(\lambda_C\frac{\partial T_C}{\partial z}\right) = 0,$$

boundary condition at the centreline

$$(4\text{-}44) \quad T_F\big|_{r=0} = finite,$$

4-th kind boundary condition at fuel-gas interface

$$(4\text{-}45) \qquad T_F\big|_{r=r_F} = T_G\big|_{r=r_F}, \qquad \lambda_F \frac{\partial T_F}{\partial r}\bigg|_{r=r_F} = \lambda_G \frac{\partial T_G}{\partial r}\bigg|_{r=r_F}$$

4-th kind boundary condition at gas-cladding interface

$$(4\text{-}46) \qquad T_G\big|_{r=r_G} = T_C\big|_{r=r_G}, \qquad \lambda_G \frac{\partial T_G}{\partial r}\bigg|_{r=r_G} = \lambda_C \frac{\partial T_C}{\partial r}\bigg|_{r=r_G}$$

3-rd kind boundary condition at clad-fluid boundary

$$(4\text{-}47) \qquad -\lambda_C \frac{\partial T_C}{\partial r}\bigg|_{r=r_C} = h\Big(T_C\big|_{r=r_C} - T_f\Big).$$

Since the above conduction problem is two-dimensional, additional conditions are needed at $z = -H/2$ and $z = H/2$. Assuming that both ends of the fuel rod are thermally insulated, the conditions are as follows,

$$(4\text{-}48) \qquad \frac{\partial T_k}{\partial z}\bigg|_{z=-H/2} = \frac{\partial T_k}{\partial z}\bigg|_{z=H/2} = 0, \quad k = F, G, C.$$

The heat source in Eq. (4-41) results from fissions of the fuel material and in general is non-uniformly distributed in fuel pellets. Based on neutron distribution in reactor core and fuel material, the heat source distribution can be approximated as,

$$(4\text{-}49) \qquad q'''(r,z) = q_0''' I_0\!\left(\frac{r}{L_F}\right) \cos\!\left(\frac{\pi z}{\tilde{H}}\right),$$

where I_0 is the modified Bessel function of the first kind and zero-th order, q_0''' is the heat source at the origin ($r{=}0$, $z{=}0$), L_F is the neutron diffusion length in the fuel material and $\tilde{H} = H + 2d$ is the extrapolated length of the fuel rod. Here d is a so-called extrapolation length. Often a total power of a fuel rod, q_R, is known rather than the power density at the origin. Then, the heat source distribution can be found as,

$$(4\text{-}50) \qquad q'''(r,z) = \frac{q_R}{4\tilde{H} r_F L_F I_1\!\left(\dfrac{r_F}{L_F}\right) \sin\!\left(\dfrac{\pi H}{2\tilde{H}}\right)} I_0\!\left(\frac{r}{L_F}\right) \cos\!\left(\frac{\pi z}{\tilde{H}}\right),$$

where I_0 and I_1 are the modified Bessel functions of the first kind, of the zero and the first order, respectively.

The fluid bulk temperature T_f appearing in the boundary condition (4-47) is not constant and is changing along the fuel rods. This temperature can be obtained from an energy balance for the fluid surrounding the fuel rod.

The thermal conductivities of fuel, gas gap and cladding appearing in Eqs. (4-41) through (4-50) are in general depending on the temperature and also on the fuel

burnup. Due to that the equations cannot be solved analytically and a numerical approach should be used. However, for the purpose of a preliminary fuel rod design it is practical to use simplified analytical solutions rather than detailed numerical solutions. Analytical solutions, even though not very accurate, are very powerful tools in practical applications, since they provide relationships between various parameters in a transparent way enabling optimization of the fuel design process.

An analytical solution of Eqs. (4-41) through (4-50) can be obtained if the following assumptions are adopted:

1. Heat conduction in z-direction is small compared to the conduction in the r-direction and can be neglected.

2. Material properties are constant.

3. Heat source distribution is a function of z-coordinate only.

With these assumptions, the conduction equations become,

heat conduction in fuel pellet

$$(4\text{-}51) \quad \frac{1}{r}\frac{d}{dr}\left(r\frac{dT_F}{dr}\right) = -\frac{q'''(z)}{\lambda_F},$$

heat conduction in gas gap

$$(4\text{-}52) \quad \frac{1}{r}\frac{d}{dr}\left(r\frac{dT_G}{dr}\right) = 0,$$

heat conduction in clad

$$(4\text{-}53) \quad \frac{1}{r}\frac{d}{dr}\left(r\frac{dT_C}{dr}\right) = 0,$$

and the boundary conditions are given by Eqs. (4-44) through (4-47).

The volumetric heat sources q''' can be expressed in terms of two other parameters often used in a design and safety analyses of nuclear fuel elements: the **linear heat density**, q', and the **heat flux on the clad outer surface**, q'':

$$(4\text{-}54) \quad q''' = \frac{q'}{\pi r_F^2},$$

$$(4\text{-}55) \quad q''' = q''\frac{2r_C}{r_F^2}.$$

Expressing the heat sources in terms of the linear power, the general solutions of the conduction equation in the fuel, gas gap and clad regions are as follows,

(4-56) $\quad T_F = -\dfrac{q'}{4\pi\lambda_F}\left(\dfrac{r}{r_F}\right)^2 + C_{F1}\ln r + C_{F2}$,

(4-57) $\quad T_G = C_{G1}\ln r + C_{G2}$,

(4-58) $\quad T_C = C_{C1}\ln r + C_{C2}$.

Applying the boundary conditions yields:

at $r = 0$, T_F is finite, thus $C_{F1} = 0$,

at $\mathrm{r} = r_F$:

$$T_F(r_F) = T_G(r_F) \quad\Rightarrow\quad C_{F2} = \frac{q'}{4\pi\lambda_F} + C_{G1}\ln r_F + C_{G2},$$

$$\lambda_F\left.\frac{dT_F}{dr}\right|_{r=r_F} = \lambda_G\left.\frac{dT_G}{dr}\right|_{r=r_F} \quad\Rightarrow\quad C_{G1} = -\frac{q'}{2\pi\lambda_G},$$

at $r = r_G$:

$$T_G(r_G) = T_C(r_G) \quad\Rightarrow\quad C_{G2} = C_{C2} + (C_{C1} - C_{G1})\ln r_G,$$

$$\lambda_C\left.\frac{dT_C}{dr}\right|_{r=r_G} = \lambda_G\left.\frac{dT_G}{dr}\right|_{r=r_G} \quad\Rightarrow\quad C_{C1} = -\frac{q'}{2\pi\lambda_C},$$

at $r = r_C$:

$$-\lambda_C\left.\frac{dT_C}{dr}\right|_{r=r_C} = h\left(T_C\big|_{r=r_C} - T_f\right) \quad\Rightarrow\quad C_{C2} = T_f - C_{C1}\left(\frac{\lambda_C}{hr_C} + \ln r_C\right).$$

Using the constants in solutions (4-56) through (4-58) gives the following expressions for the temperature distributions in different layers,

clad

(4-59) $\quad T_C(r,z) = \dfrac{q'(z)}{2\pi\lambda_C}\ln\dfrac{r_C}{r} + \dfrac{q'(z)}{2\pi r_C h} + T_f(z)$

gas gap

(4-60) $\quad T_G(r,z) = \dfrac{q'(z)}{2\pi\lambda_G}\ln\dfrac{r_G}{r} + \dfrac{q'(z)}{2\pi\lambda_C}\ln\dfrac{r_C}{r_G} + \dfrac{q'(z)}{2\pi r_C h} + T_f(z)$,

fuel

$$(4\text{-}61) \qquad T_F\left(r,z\right) = \frac{q'(z)}{4\pi\lambda_F}\left[1-\left(\frac{r}{r_F}\right)^2\right] + \frac{q'(z)}{2\pi\lambda_G}\ln\frac{r_G}{r_F} + \frac{q'(z)}{2\pi\lambda_C}\ln\frac{r_C}{r_G} + \frac{q'(z)}{2\pi r_C h} + T_f\left(z\right).$$

4.1.3 Heat Conduction with Temperature-Dependent Conductivity

The assumption of a constant thermal conductivity in fuel pellets is not acceptable when accurate temperature predictions are required. This is particularly true for UO_2 fuel materials, in which the thermal conductivity is a strong function of temperature. Thus, assuming steady-state heat conduction in an infinite rod, the temperature distribution is described with the following differential equation,

$$(4\text{-}62) \qquad \frac{1}{r}\frac{d}{dr}\left(r\lambda_F(T)\frac{dT}{dr}\right) = -q'''(r).$$

This equation can be integrated from $r = 0$ to r as follows,

$$r'\lambda_F(T)\frac{dT}{dr}\bigg|_0^r = r\lambda_F(T)\frac{dT}{dr} = \int_0^r r'q'''(r')dr'\,.$$

The equation can be now written as,

$$\lambda_F(T)dT = -\left(\frac{1}{r}\int_0^r r'q'''(r')dr'\right)dr\,.$$

Second integration of the equation yields,

$$(4\text{-}63) \qquad \int_{T_{Fc}}^{T}\lambda_F(T')dT' = -\int_0^r\left[\frac{1}{r'}\int_0^{r'}r''q'''(r'')dr''\right]dr'\,.$$

Here T_{Fc} is the fuel temperature at the centreline. The integral on the left-hand side is called the **conductivity integral** and is often provided in a graphical form as $\int_0^T \lambda dT$ versus temperature T. It should be noted that $\int_{T_0}^{T}\lambda dT = \int_0^T \lambda dT - \int_0^{T_0}\lambda dT$, thus the graphs can be used to calculate the left-hand-side of Eq. (4-63). Alternatively, the thermal conductivity is give as an analytical function of the fuel temperature.

Assuming constant heat source on the right-hand-side of Eq. (4-63), the following relationship is obtained,

$$(4\text{-}64) \qquad \int_{T_{Fc}}^{T}\lambda_F(T')dT' = -\frac{q'''r^2}{4}\,.$$

Defining the **average fuel conductivity** as,

(4-65) $\left\langle \lambda_F \right\rangle \equiv \dfrac{1}{T - T_{Fc}} \displaystyle\int_{T_{Fc}}^{T} \lambda_F(T')dT'$,

Eq. (4-64) can be written as,

(4-66) $T - T_{Fc} = -\dfrac{q'''r^2}{4\left\langle \lambda_F \right\rangle}$.

Even though obtained expression is similar to the one valid for a constant thermal conductivity, it is implicit in temperature, since the right-hand-side of Eq. (4-66) is a function of temperature T. Thus once using the expressions iterations are needed.

4.2 Convective Heat Transfer

Convection is one of the most common modes of heat transfer. The characteristic feature of the convective heat transfer is that heat is transported through large-scale (as compared to fluid molecules) fluid motion. Depending on the fluid flow character, the convective heat transfer is further classified in several categories:

- natural convection, when fluid flow is driven by the buoyancy forces

- forced convection, when fluid flow is driven by external forces, e.g. due to a pump

- laminar convection, when fluid flow is laminar

- turbulent convection, when fluid flow is turbulent.

Both natural and forced convection can be either laminar or turbulent, depending on the nature of the flow.

Convective heat transfer from a solid surface to the incident fluid is often described by the **Newton's equation of cooling**,

(4-67) $q'' = h\left(T_w - T_f\right)$,

where q'' [W m^{-2}] is the heat flux at the wall surface, h [W m^{-2} K^{-1}] is the convective heat transfer coefficient, T_w [K] is the wall surface temperature and T_f [K] is the fluid bulk temperature. The convective heat transfer coefficient depends upon the fluid properties and flow conditions. Its determination is discussed in the following sections.

The value of the heat transfer coefficient can change on the heated surface. It is thus important to distinguish between the local value of the coefficient, valid on a small surface surrounding a given point, and the mean value, typically obtained from a proper averaging of the local values. Such averaging can be achieved as,

$h = \dfrac{1}{F} \displaystyle\int_{F} h_{loc}dF$,

where h_{loc} is the local heat transfer coefficient and F is the heat transfer surface.

If the mean heat transfer coefficient between given solid and fluid is known, then the amount of heat exchanged through surface F can be found as,

$$q = hF\Delta T \,.$$

Here ΔT is a proper mean temperature difference between solid surface and fluid.

Often it can be assumed that the heat transfer coefficient is a function of distance only, as is the case for flow along a plate or flow in pipes. For such cases the mean heat transfer coefficient can be found as,

$$h = \frac{1}{L}\int_0^L h_z dz \,,$$

and the exchanged heat is found as,

$$q = hF\left(T_w - T_f\right)_m \,,$$

where,

$$(4\text{-}68) \quad \left(T_w - T_f\right)_m = \frac{1}{L}\int_0^L \left(T_w - T_f\right) dz = \frac{\left(T_w - T_f\right)_i - \left(T_w - T_f\right)_o}{\ln\dfrac{\left(T_w - T_f\right)_i}{\left(T_w - T_f\right)_o}} \,,$$

is the logarithmic mean temperature difference. In the above expressions $\left(T_w - T_f\right)_i$ and $\left(T_w - T_f\right)_o$ are the inlet and outlet temperature differences between the solid surface and fluid. Occasionally the temperature difference is defined as mean arithmetic as follows,

$$(4\text{-}69) \quad \left(T_w - T_f\right)_{ar} = \frac{\left(T_w - T_f\right)_i + \left(T_w - T_f\right)_o}{2} \,,$$

and the total exchanged heat is found as,

$$q = h_{ar}F\left(T_w - T_f\right)_{ar} \,.$$

Clearly, to avoid errors, once giving the mean heat transfer coefficient for a specific heat exchange system, it should be clarified which mean temperature difference should be applied.

Equation (4-67) is applicable for all kinds of flows: laminar and turbulent; for both gases and liquids, and describes a heat transfer mechanism which is termed the convection. When the fluid motion is caused by pumps, fans, or in general by pressure gradients, the forced convection takes place. Otherwise when fluid motion is caused be density gradients in the fluid, the natural convection occurs. The simplicity of Eq.

(4-67) is deceiving, however. In fact, the heat transfer coefficient h is hiding the complexity of the solid-fluid heat transfer, and, as can be expected, a proper correlation must be used to obtain the coefficient which will be valid for specific flow conditions.

Performing an analysis of the convective heat transfer it is necessary to formulate the governing equations of mass, momentum and energy conservation together with proper boundary conditions for heat transfer between fluid and solid. The dimensional analysis of the governing equations and boundary conditions leads to a new dimensional number called the **Nusselt number**,

(4-70) $\quad \text{Nu} = \dfrac{h \cdot L}{\lambda}$,

where,

$\quad\quad L \quad\quad$ - a characteristic linear dimension [m],
$\quad\quad \lambda \quad\quad$ - the thermal conductivity of the fluid [W m^{-1} K^{-1}].

The dimensional analysis leads further to a general relationship to determine the Nusselt number. In the case of the forced convection the relationship is as follows,

(4-71) $\quad \text{Nu} = f\left(\text{Re}, \text{Pr}, \dots\right)$,

whereas for the natural (or free) convection the relationship becomes,

(4-72) $\quad \text{Nu} = f\left(\text{Gr}, \text{Pr}, \dots\right)$.

The other dimensionless numbers appearing in the relationships are the Reynolds number,

$\quad\quad \text{Re} = \dfrac{U \cdot L}{\nu}$,

the **Grashof number**,

(4-73) $\quad \text{Gr} = \dfrac{\beta g L^3}{\nu^2} \Delta T$,

and the **Prandtl number**,

(4-74) $\quad \text{Pr} = \dfrac{\nu}{a} = \dfrac{c_p \mu}{\lambda}$

where,

$\quad\quad \nu \quad\quad\quad\quad\quad$ - the kinematic viscosity [m^2 s^{-1}],
$\quad\quad \mu = \nu\rho \quad\quad\quad$ - the dynamic viscosity [Pa s],
$\quad\quad a = \lambda/\left(\rho c_p\right) \quad$ - the thermal diffusivity [m^2 s^{-1}],

$$\beta \qquad\qquad \text{- the volumetric expansion coefficient } [\text{K}^{-1}],$$

$$\Delta T = T - T_\infty \quad \text{- a characteristic temperature difference } [\text{K}].$$

As can be seen, for natural convection the Reynolds number is replaced with the Grashof number. Expressions (4-71) and (4-72) have different forms for various situations and can be derived either analytically or experimentally. Some special forms of the expressions are given in the following Sections.

4.2.1 Laminar Forced Convection

In laminar forced convection the heat transfer in fluid is resulting from both conduction and convection, and the temperature distribution can be obtained from a solution of the energy equation. In the cylindrical system of coordinates, assuming axisymmetric flow, the energy conservation equation for liquid becomes,

(4-75)
$$\frac{w}{a}\frac{\partial T}{\partial z} = \frac{1}{r}\frac{\partial}{\partial r}\left(r\frac{\partial T}{\partial r}\right) + \frac{\partial^2 T}{\partial z^2},$$

where the viscous dissipation term has been neglected. In addition, the term $\dfrac{\partial^2 T}{\partial z^2}$ describing the heat conduction in the axial direction of the pipe is only important when the flowing fluid is the liquid metal. For water, as it is assumed in the present case, the term can be dropped. Assuming further constant heat flux on the pipe wall surface and a constant heat transfer coefficient, the axial temperature derivative will be,

(4-76)
$$\frac{\partial T}{\partial z} = \frac{dT_w}{dz} = \frac{dT_m}{dz},$$

where T_w is the wall surface temperature and T_m is the mean liquid temperature in the pipe. Thus, the equation to be solved is as follows,

(4-77)
$$\frac{w}{a}\frac{dT_m}{dz} = \frac{1}{r}\frac{d}{dr}\left(r\frac{dT}{dr}\right)$$

or, using Eq. (3-192),

(4-78)
$$\frac{2U}{a}\left[1 - \left(\frac{r}{R}\right)^2\right]\frac{dT_m}{dz} = \frac{1}{r}\frac{d}{dr}\left(r\frac{dT}{dr}\right).$$

Double integration of the above equation yields,

(4-79)
$$T = T_w - \frac{2UR^2}{a}\left[\frac{3}{16} - \left(\frac{r}{2R}\right)^2 + \left(\frac{r}{2R}\right)^4\right]\frac{dT_m}{dz}.$$

The mean temperature in the pipe cross-section can be calculated as,

$$(4\text{-}80) \qquad T_m \equiv \frac{\int_A wTdA}{\int_A wdA} = \frac{2}{UR^2}\int_0^R wTrdr = T_w - \frac{11}{96}\frac{2UR^2}{a}\frac{dT_m}{dz}\,.$$

The heat flux can be expressed in terms of the Newton law of cooling as,

$$(4\text{-}81) \qquad q'' = h\big(T_w - T_m\big) = h\,\frac{11}{96}\frac{2UR^2}{a}\frac{dT_m}{dz}\,.$$

The same heat flux can be obtained from the temperature gradient of the fluid in the vicinity of the pipe wall as,

$$(4\text{-}82) \qquad -q'' = \lambda\left(\frac{dT}{dr}\right)_{r=R} = -\frac{\lambda UR}{2a}\frac{dT_m}{dz}\,.$$

Combining Eqs. (4-81) and (4-82) gives the heat transfer coefficient and the Nusselt number as follows,

$$(4\text{-}83) \qquad h = \frac{48}{11}\frac{\lambda}{2R} \Rightarrow \mathrm{Nu} = \frac{h\cdot 2R}{\lambda} = \frac{48}{11} \approx 4.364\,.$$

It should be recalled that the above value of the Nusselt number has been obtained for a laminar convective heat transfer in a pipe with uniform distribution of heat flux. Similar analysis can be performed for a case with a uniform distribution of the wall temperature, and the resultant Nusselt number is as follows,

$$(4\text{-}84) \qquad \mathrm{Nu} = 3.658\,.$$

In both above-mentioned cases the analytical solution could be obtained, and the resulting Nusselt number proved to be constant, independent of the Reynolds and the Prandtl numbers. For more complex situations empirical expressions are employed.

One of frequently used empirical correlations was given by Sieder and Tate[4-18] and is as follows,

$$(4\text{-}85) \qquad \mathrm{Nu}_{ar} = 1.86\left(\mathrm{Re}\,\mathrm{Pr}\,\frac{D_h}{L}\right)^{1/3}\left(\frac{\mu_f}{\mu_w}\right)^{0.14},$$

where,

μ_f - the dynamic viscosity calculated at mean arithmetic between inlet and outlet temperature,

μ_w - the dynamic viscosity calculated at the wall temperature,

L - the channel length,

D_h - the channel hydraulic diameter,

Nu_{ar} - the Nusselt number based on heat transfer coefficient defined for arithmetic mean temperature, $\mathrm{Nu}_{ar} = h_{ar} D_h / \lambda$.

All fluid physical parameters are calculated at the saturation liquid temperature T_f.

The product of the Reynolds and the Prandtl number often occurs in various expressions, and can be replaced by the Peclet number as follows,

$$\mathrm{Pe} = \mathrm{Re}\,\mathrm{Pr} = \frac{UD_h}{\nu}\frac{\nu}{a} = \frac{\rho c_p UD_h}{\lambda}.$$

Since in laminar flows the free convection (discussed in more detail in Section 4.2.3) can play a significant role, in some correlations this effect is accounted for by introduction of the Grashof number. Michiejev[4-16] proposed the following expression, valid for various channels with $L/D_h > 50$,

$$(4\text{-}86) \qquad \mathrm{Nu} = 0.15\,\mathrm{Re}^{0.33}\,\mathrm{Pr}_f^{0.43}\,\mathrm{Gr}^{0.1}\left(\frac{\mathrm{Pr}_f}{\mathrm{Pr}_w}\right)^{0.25},$$

where the Grashof number is defined as follows,

$$Gr = \frac{g\beta D_h^3 \Delta T}{\nu^2}.$$

The reference temperature, used to determine the fluid properties, is the arithmetic mean of the channel inlet and outlet temperature, and the reference linear dimension is the hydraulic diameter of the channel, D_h. Pr_f and Pr_w are Prandtl numbers calculated at mean fluid temperature and wall temperature, respectively.

4.2.2 Turbulent Forced Convection

In essentially all cases of practical importance for heat transfer analysis in nuclear reactors, the coolant is under turbulent flow conditions. Satisfactory predictions of heat transfer coefficients in long, straight channels of uniform cross section can be made on the assumption that the only variables involved are the mean velocity of the fluid, the diameter (or equivalent diameter) of the channel, the density, heat capacity, viscosity, and thermal conductivity of the fluid. Using the dimensional analysis of the governing equations it can be shown that the heat transfer processes for turbulent flow conditions can be expressed in terms of an expression that mainly contains three dimensionless numbers: the Reynolds number (Re), the Nusselt number (Nu) and the Prandtl number (Pr), and the general form of the expression is as follows,

$$(4\text{-}87) \qquad \mathrm{Nu} = f\left(\mathrm{Re}, \mathrm{Pr}, \ldots\right).$$

Expressions of this kind are derived from experiments and are usually valid in channels at a certain distance from inlet, where both the thermal and hydrodynamic boundary layer are developed. For fluids with Prandtl number around 1, the inlet developing length in channels is equivalent to $50 \div 60$ hydraulic diameters.

The temperature and the velocity profile in turbulent flows are more flat as compared with laminar flows. This fact influences the choice of the reference temperature that is used to calculate the fluid properties. Often as the reference temperature it is taken the arithmetic mean between the fluid and the wall temperature,

$$T_{ref} = \frac{T_f + T_w}{2}.$$

Occasionally the reference temperature is defined as,

$$T_{ref} = T_f + 0.4\left(T_w - T_f\right),$$

or,

$$T_{ref} = T_f + 0.6\left(T_w - T_f\right).$$

Dittus-Boelter[4-10] proposed the following correlation for forced-convective heat transfer in long straight pipes:

(4-88) $\mathrm{Nu} = 0.023\,\mathrm{Re}^{0.8}\,\mathrm{Pr}^{\,n}$,

valid for $L/D_h > 60$, Re > 10000 and 0.7 < Pr < 100. The exponential n is equal to 0.4 for heating and 0.3 for cooling. The fluid properties should be calculated with the mean fluid temperature.

Colburn[4-8] introduced the Stanton number to replace the Nusselt number as follows,

(4-89) $\mathrm{St} = \dfrac{\mathrm{Nu}}{\mathrm{Re}\,\mathrm{Pr}} = \dfrac{hD_h\mu\lambda}{h\rho U D_h \mu c_p} = \dfrac{h}{\rho U c_p}$,

and the correlation is given as,

(4-90) $\mathrm{St} = 0.023\,\mathrm{Re}^{-0.2}\,\mathrm{Pr}^{-2/3}$,

or using the Nusselt number,

(4-91) $\mathrm{Nu} = 0.023\,\mathrm{Re}^{0.8}\,\mathrm{Pr}^{1/3}$.

The correlation is valid for $L/D_h > 60$, Re > 10000 and 0.7 < Pr < 160. The reference temperature is defined as the mean arithmetic from the wall and the average fluid temperature. Specific heat c_p should be calculated at the average fluid temperature.

4.2.3   Natural Convection

Natural (or free) convection occurs when fluid flow is driven by buoyancy forces, usually due to gravity. In the vicinity of the body that exchanges heat with fluid there are temperature gradients that cause density changes in the fluid. The density changes are causing the buoyancy force, which result in local fluid motion. To capture this effect, the buoyancy force must be introduced into the momentum equation for fluid. This force per unit volume is equal to,

$$g(\rho_\infty - \rho),$$

where:

ρ_∞ - fluid density far from the heated wall, where temperature T_∞ prevails

ρ - fluid density in the boundary layer close to the heated wall,

g   - acceleration of gravity.

The expression for the buoyancy force may be transformed through introduction of the coefficient of the thermal expansion for fluid,

(4-92) $\beta = \dfrac{1}{\upsilon_0} \left(\dfrac{\partial \upsilon}{\partial T} \right)_p ,$

where $\upsilon = 1/\rho$ is the specific volume of fluid and the differentiation in Eq. (4-92) is performed at constant pressure.

Since

$$\upsilon \cong \upsilon_\infty + \left(\frac{\partial \upsilon}{\partial T} \right)_p (T - T_\infty) = \upsilon_\infty [1 + \beta(T - T_\infty)],$$

then

(4-93) $g(\rho_\infty - \rho) = g\rho \left(\dfrac{\rho_\infty}{\rho} - 1 \right) = g\rho\beta(T - T_\infty) = g\rho\beta\Delta T .$

The mathematical description of the natural convection is based, as can be expected, on formulation of the conservation equations for mass, momentum and energy. Introducing a few practical approximations,

- constant density in the continuity equation,

- neglect of the pressure gradient in the momentum equation,

- neglect of energy dissipation function,

- constant viscosity,

the conservation equations are as follows,

$$\nabla \cdot \mathbf{v} = 0 ,$$

$$\nabla \cdot (\mathbf{vv}) = \nu\nabla^2 \mathbf{v} + \mathbf{g}\beta\Delta T ,$$

$$\mathbf{v}\nabla T = a\nabla^2 T .$$

Performing a dimensional analysis of equations, it can be shown that the general expression describing the free convection heat transfer is as follows,

$$\mathrm{Nu} = f(\mathrm{Gr}, \mathrm{Pr}, \ldots),$$

where,

$$\mathrm{Nu} = \frac{h \cdot D_h}{\lambda} \qquad \text{- Nusselt number,}$$

$$\mathrm{Gr} = \frac{\beta g L^3}{\nu^2} \Delta T \qquad \text{- Grashof number,}$$

$$\mathrm{Pr} = \frac{\nu}{a} = \frac{c_p \mu}{\lambda} \qquad \text{- Prandtl number.}$$

Various empirical expressions are provided for prediction of the Nusselt number, derived specifically for laminar or turbulent flows in different geometry configurations. Some examples are given below.

Laminar free convection

$$(4\text{-}94) \qquad \mathrm{Nu} = \begin{cases} const & \text{for} & \mathrm{Gr\,Pr} < 10^{-3} \\ 1.18(\mathrm{Gr\,Pr})^{1/8} & \text{for} & 10^{-3} < \mathrm{Gr\,Pr} < 5 \cdot 10^2 \\ 0.54(\mathrm{Gr\,Pr})^{1/4} & \text{for} & 5 \cdot 10^2 < \mathrm{Gr\,Pr} < 2 \cdot 10^7 \end{cases}.$$

The constant in Eq. (4-94) is equal to 0.5 for an infinite cylinder and 2 for a sphere.

Turbulent free convection (Michiejev[4-16])

$$(4\text{-}95) \qquad \mathrm{Nu} = 0.135(\mathrm{Gr\,Pr})^{1/3},$$

valid when,

$$2 \cdot 10^7 < \mathrm{Gr\,Pr} < 10^{13}$$

with the reference temperature defined as,

$$T_{ref} = \frac{T_w + T_\infty}{2}.$$
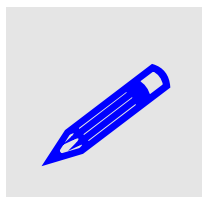
EXAMPLE 4-3. Calculate the convective heat transfer coefficient on a pipe wall with diameter $d = 400$ mm, which has the external temperature $T_w = 80°C$ and is surrounded by air with temperature $T_\infty = 20$ °C. SOLUTION: The mean temperature of the boundary layer is found as,

$$T_m = \frac{T_w + T_\infty}{2} = \frac{80 + 20}{2} = 50°C.$$

At this temperature, the air properties are as follows: viscosity $\nu = 17.95 \cdot 10^{-6}$ m²/s, thermal conductivity $\lambda = 0.0283$ W/m.K, Prandtl number Pr = 0.722, and the volumetric expansion coefficient $\beta = 1/(273+50) = 3.1 \cdot 10^{-3}$ 1/K.

The product GrPr is found as,

$$\mathrm{Gr\,Pr} = \frac{9.81 \cdot 3.1 \cdot 10^{-3}(80 - 20) \cdot 0.4^3 \cdot 0.722}{\left(17.95 \cdot 10^{-6}\right)^2} \approx 2.62 \cdot 10^8 \cdot$$

This value indicate that Eq. (4-95) should be used,

$$\mathrm{Nu} = 0.135(\mathrm{Gr\,Pr})^{1/3} = 0.135\left(2.62 \cdot 10^8\right)^{1/3} \approx 86.5$$

The heat transfer coefficient is found as,

$$h = \mathrm{Nu}\,\frac{\lambda}{d} = 86.5\,\frac{0.0283}{0.4} \approx 6.1 \ \mathrm{W/m^2.K.}$$

4.3 Radiative Heat Transfer

In radiative heat transfer, heat is transferred between bodies by electromagnetic radiation. Thermal radiation is generated when heat from the movements of charged particles within atoms is converted to electromagnetic radiation.

Thermal radiation possesses the following properties,

- thermal radiation, even at a single temperature, occurs at a wide range of frequencies. The frequency spectrum is given by the **Planck's law of radiation**:

$$u(\nu, T) = \frac{2h\nu^3}{c^2} \cdot \frac{1}{e^{\frac{h\nu}{k_B T}} - 1}.$$

- The main frequency of the emitted radiation increases with increasing temperature, following the **Wien's law**:

$$\lambda_{\max} = \frac{b}{T}.$$

- The total energy radiated rises with the fourth power of the absolute temperature of the body, according to the **Stefan-Boltzmann law**:

$$q = \sigma A T^4.$$

  For non-black bodies one has to consider emissivity correction factor, which in general depends on the body material and also on the radiation frequency:

$$q = e\sigma A T^4.$$

Constants appearing in the radiation formula are given in the table below.

TABLE 4.1. Constants used in the radiation formula.

Symbol	Name	Value
h	Planck's constant	$6.6260693 \cdot 10^{-34}$ J·s
b	Wien's displacement constant	$2.8977685 \cdot 10^{-3}$ m·K
k_B	Boltzmann constant	$1.3806505 \cdot 10^{-23}$ J·K^{-1}
σ	Stefan-Boltzmann constant	$5.670400 \cdot 10^{-8}$ W·m^{-2}·K^{-4}
c	Speed of light	299792458 m·s^{-1}

4.3.1 Heat Transfer between Two Parallel Surfaces

Radiative heat transfer is complicated since each surface emits not only own radiation, but also radiation reflected from other bodies. A case of two parallel infinite surfaces exchanging heat through radiation is shown in FIGURE 4-5, where it is shown how radiation emitted from surface 1 is consecutively reflected, absorbed and resubmitted by both surfaces. Similar picture may be created for a radiation beam radiated from surface 2. Combination of the two cases gives the net heat exchange by radiation between the two surfaces.
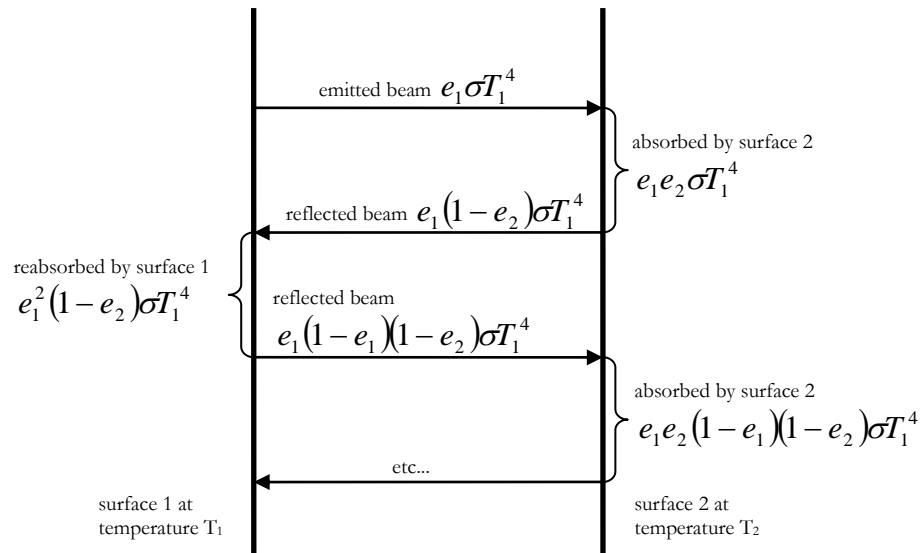
FIGURE 4-5. Radiative heat transfer between two parallel surfaces.

Considering a portion of surfaces with area A, the net heat transferred from surface *1* to *2* is,

$$q_{1 \to 2} = A\sigma e_1 e_2 T_1^4 + A\sigma e_1 e_2 (1-e_1)(1-e_2)T_1^4 + A\sigma e_1 e_2 (1-e_1)^2 (1-e_2)^2 T_1^4 + ...$$

The corresponding heat transferred from surface *2* to *1* is,

$$q_{2\to1} = A\sigma e_1 e_2 T_2^4 + A\sigma e_1 e_2 (1-e_1)(1-e_2)T_2^4 + A\sigma e_1 e_2 (1-e_1)^2 (1-e_2)^2 T_2^4 + ...$$

Thus, the net heat exchange is as follows,

$$q_{12} = q_{1\to2} - q_{2\to1} = A\sigma e_1 e_2 \left(T_1^4 - T_2^4\right)\sum_{i=0}^{\infty}(1-e_1)^i (1-e_2)^i .$$

Performing summation yields,

$$(4\text{-}96)\qquad q_{12} = \frac{A\sigma\left(T_1^4 - T_2^4\right)}{\dfrac{1}{e_1} + \dfrac{1}{e_2} - 1}.$$

4.3.2 Heat Transfer in Closed Volumes

Radiative heat transfer between two surfaces in a closed system can be encountered in many practical situations, such as heat transfer between fuel rods surrounded by box walls in BWR fuel assemblies. A schematic of heat transfer in a closed system is shown in FIGURE 4-6.
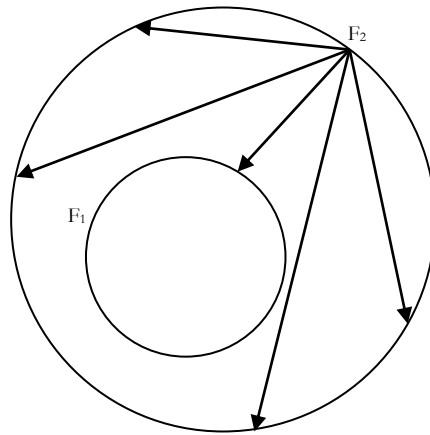
FIGURE 4-6. Radiative heat transfer in a closed system.

In the case when a smaller body is inside a bigger one (as indicated in the figure), only a fraction of the radiation from the bigger body reaches the smaller body surface. In such a case Eq. (4-96) is not valid and must be modified. If φ is a fraction of energy radiated by the bigger body and absorbed by the smaller one, then $1-\varphi$ is returned to the same surface. For shapes as shown in the figure, this fraction is equal to,

$$\varphi = \frac{F_1}{F_2},$$

and this is even a good approximation for other shapes, provided that one surface is totally surrounded by the other one. Performing reasoning similar to parallel surfaces, it can be shown that heat transferred from surface 1 to 2 is as follows,

(4-97) $q_{12} = \dfrac{F_1 \sigma\left(T_1^4 - T_2^4\right)}{\dfrac{1}{e_1} + \varphi\left(\dfrac{1}{e_2} - 1\right)}$.
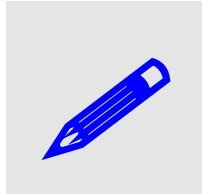
EXAMPLE 4-4. Calculate heat transferred between single rod with outer diameter 10mm placed in a closed rectangular box with side length 140 mm. Assume that both the rod and the box are made of steel with emissivity equal to 0.736 and have length 3.6 m. Rod temperature is 1000 K and the box temperature is 600 K.
SOLUTION: The viewing factor is found as

$\varphi = \pi d / (4w) = 10 \cdot 3.1416 / (4 \cdot 140) \approx 0.056$. Equation (4-97) yields,

$q_{12} = \dfrac{F_1 \sigma\left(T_1^4 - T_2^4\right)}{\dfrac{1}{e_1} + \varphi\left(\dfrac{1}{e_2} - 1\right)} = \dfrac{\pi \cdot 0.01 \cdot 3.6 \cdot 5.67 \cdot 10^{-8}\left(1000^4 - 600^4\right)}{\dfrac{1}{0.736} + 0.056\left(\dfrac{1}{0.736} - 1\right)} \approx 4048 \text{ W}$

Thus the heat transferred from the hot rod inside the box to the box walls is equal to 4.048 kW/m².

4.3.3   Radiation of Gases and Vapours

Gases with symmetric molecules (O_2, N_2, H_2, etc.) are practically transparent to radiation and are classified as "radiatively nonparticipating" media. However, gases and vapours with non-symmetric molecules (CO_2, H_2O, CO, etc.) may emit, scatter and absorb significant amounts of energy and are classified as "radiatively participating" media.

As shown by experiments, the Stefan-Boltzmann law does not apply to gases, and for water vapour the following expression has been obtained,

$$E_{H_2O} = 4.07 \cdot 10^{-6}\, p^{0.8} L^{0.6} T^3 ,$$

where p – vapour's pressure [Pa], L – mean thickness of vapour layer [m], T – absolute vapour temperature [K] and E_{H_2O} - radiated energy [W·m⁻²].

4.4 Pool Boiling Heat Transfer

Boiling heat transfer occurs when the heated fluid undergoes phase change from liquid to vapour. This is a very complex process due to physical and chemical surface phenomena that occur both at the solid-fluid and liquid-vapour interfaces.

One of the characteristic features of the boiling heat transfer is its high heat transfer coefficient. This fact makes the boiling heat transfer an interesting topic since it enables transfers of large heat fluxes, which are required in many practical applications.

Depending on the applied heating, boiling can be:

a) homogeneous, when heat is supplied in the whole liquid volume, and vapour is generated in any point in the volume

b) heterogeneous, when heat is supplied through a solid wall and vapour is generated on the solid surface.

Another classification reflects the fluid behaviour during boiling. Based on that boiling can be:

a) pool boiling, when fluid is at rest. This case corresponds to the free-convection heat transfer considered for single-phase flows.

b) flow (or forced-convective) boiling, when fluid is in motion due to external agitation, created with pumps. This type of boiling corresponds to the forced convection heat transfer considered for single-phase flows.

Boiling heat transfer is often presented graphically on a $\lg q'' - \lg \Delta T_{sup}$ plane, where q'' is the heat flux and $\Delta T_{sup} = T_w - T_s$ is the wall superheat. An example of the **boiling curve** *ABCDEFGHI* with pertinent heat transfer modes are shown in FIGURE 4-7. Points *F* and *G* represent important transition points which in literature got various names. For point *F* such names as boiling crisis of the first and second kind, Critical Heat Flux (CHF) or burnout are used (however, in this book only CHF is used, as the most proper one). Point *G* is often referred to as the point of the minimum film boiling. Since these transition points play very important role in thermal-hydraulic analyses of nuclear power plants, they will be discussed in more detail in the following sections.
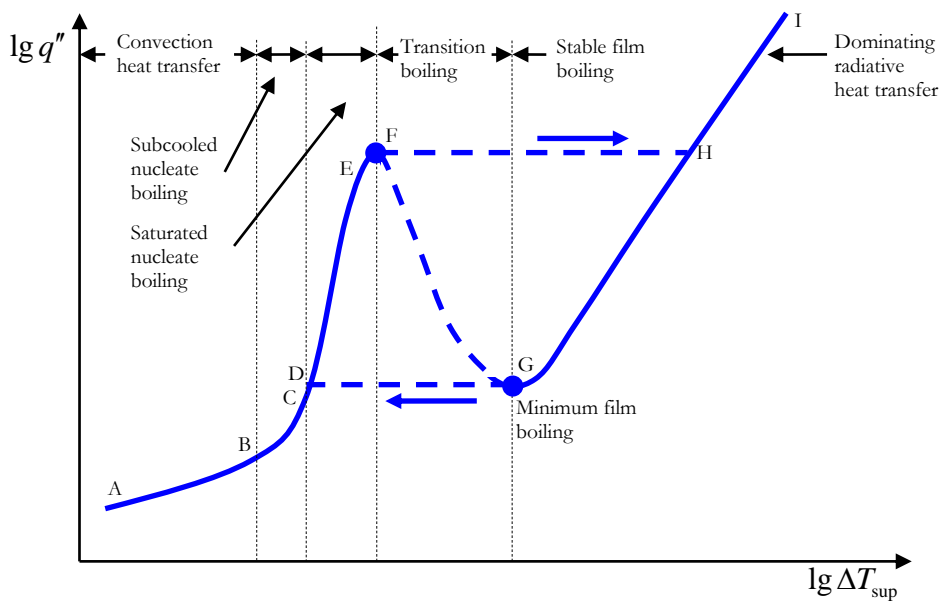
FIGURE 4-7. Boiling curve and pertinent heat transfer modes.

The straight line *AB* corresponds to the convective heat transfer. Heat transfer intensity significantly increases when nucleate boiling starts at point B. In subcooled nucleate boiling region, *BC*, small bubbles are created on the heated surface, as shown in FIGURE 4-8, picture to the left. In that boiling regime, the bubbles after detachment collapse due to condensation. Picture to the right shows the saturated nucleate boiling, when bubbles detach from the heated surface and move to the surface. This type of boiling is represented by curve *CE*. At point *E* the intensity of boiling is so high that a vapour layer starts to cover the heated surface and liquid cannot penetrate it and provide a proper cooling. Point *E* is sometimes referred to as the point of the departure from the stable nucleate boiling or shortly the point of the nucleate boiling crisis. Further increase of the wall temperature or the heat flux leads to the maximum (point *F*) which is called CHF.
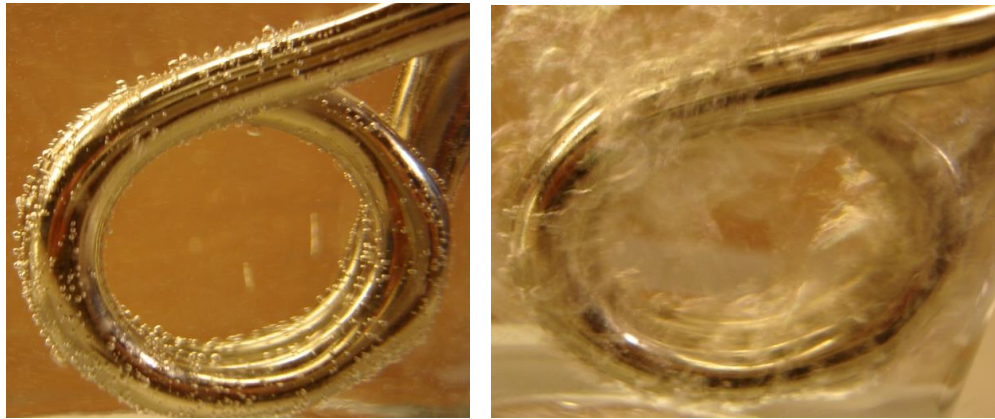
FIGURE 4-8. Subcooled nucleate boiling (left) and saturated nucleate boiling (right).

After reaching the CHF point, the boiling curve will proceed to either point *G* or *H*, depending whether the heat flux or the wall temperature is the controlled parameter. When heat flux is the controlled parameter (which is the case in nuclear reactors), the wall temperature jump will be experienced and the line *FH* will be followed. Sometimes the heater will be destroyed due to the violent temperature increase and because of that the process is called "burnout". When the heater temperature is the controlled parameter, the heat flux will decrease as indicated by curve *FG*. Heat transfer in this region is called the transition boiling, and both the nucleate and the film boiling co-exist. After crossing point *G* the stable film boiling is established.

In summary, for heat-flux controlled boiling with increasing heat flux the curve *ABCDEFHI* will be followed, whereas with the wall-temperature controlled boiling with increasing temperature the curve *ABCDEFGHI* will be followed. In the reversed process, when heat flux is decreased from point *I*, the curve *IHGDCBA* will be followed and for the wall-temperature controlled case the curve *IHGFEDCBA* will be followed.

The boiling curve shown in FIGURE 4-7 is valid for both the pool boiling (liquid is stationary) and the flow boiling (liquid is forced to move). The difference between these two cases will be seen by comparing the curve shapes and the location of the particular characteristic points.

4.4.1 Heat Transfer coefficient in Pool Boiling

From experimental data it is evident that the heat transfer coefficient for pool boiling is proportional to the heat flux as,

$$h = C(q'')^n,$$

where *C* is a constant which depends on the system pressure and the type of fluid. The exponential *n* has a value of 0.67÷0.7, depending to a certain extend on the surface roughness.

Forster and Zuber[4-11] proposed a semi-empirical expression for heat transfer coefficient valid for water,

(4-98) $h = 0.56(q'')^{0.7} p^{0.15},$

where h is the heat transfer coefficient [W·m^{-2}·K^{-1}], q'' is the heat flux [W·m^{-2}] and p is the pressure [Pa]. The correlation is valid for pressure in the range 0.2÷100 10^5 Pa.

Most of the theoretical expressions derived for the heat transfer coefficient in nucleate boiling use the following relationship as the starting point,

$$(4\text{-}99) \qquad \mathrm{Nu}_b = a\,\mathrm{Re}_b^{m_1}\,\mathrm{Pr}_f^{m_2},$$

where a – a constant coefficient, m_1 and m_2 – constant exponents, Nu_b – boiling Nusselt number, Re_b – boiling Reynolds number and $\mathrm{Pr}_f = c_p\mu/\lambda$ – Prandtl number for saturated liquid. The non-dimensional numbers Nu_b and Re_b are expressed in different ways by different authors.

Rohsenow used the following expression for the Reynolds number,

$$(4\text{-}100) \qquad \mathrm{Re}_b = \frac{q''}{i_{fg}\mu_f}\left[\frac{\sigma}{g(\rho_f - \rho_g)}\right]^{0.5}.$$

and the Nusselt number,

$$(4\text{-}101) \qquad \mathrm{Nu}_b = \frac{q''}{\Delta T_{\sup}\lambda_f}\left[\frac{\sigma}{g(\rho_f - \rho_g)}\right]^{0.5}.$$

The constant a in Eq. (4-99) depends on the properties of the heater and the fluid. For water on mechanically polished stainless steel the coefficient is $a = 1/0.0132 = 75.8$. The constant exponents m_1 and m_2 for water are 2/3 and -0.7, respectively.

4.4.2 Critical Heat Flux in Pool Boiling

Another limitation to the correlation given by Eq. (4-98) is set by the occurrence of the critical heat flux. The value of pool boiling CHF may be evaluated from a proper correlation valid for given conditions. Zuber[4-20] derived an expression for CHF by analysing the stability of a flux of vapour bubbles generated at the heated surface. The correlation is as follows,

$$(4\text{-}102) \qquad q''_{cr} = \frac{\pi}{24}i_{fg}\rho_g\left[\frac{\sigma g(\rho_f - \rho_g)}{\rho_g^2}\right]^{1/4}\left[\frac{\rho_f}{\rho_f + \rho_g}\right]^{1/2},$$

where $i_{fg} = i_g - i_f$ is the latent heat [J·kg^{-1}], σ is the surface tension [N·m^{-1}], ρ_g is the vapour density [kg·m^{-3}], ρ_f is the liquid density [kg·m^{-3}] and q''_{cr} is the critical heat flux [W·m^{-2}].
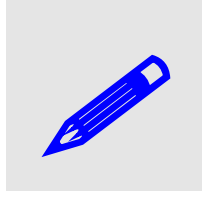
EXAMPLE 4-5. Calculate the heat transfer coefficient and the wall superheat for boiling water at pressure $p = 7$ MPa, and heat flux $q'' = 0.2$ MW·m⁻². Check if the heat flux is lower than the critical heat flux at that pressure. SOLUTION: Using the Foster-Zuber correlation, the heat transfer coefficient is found as,

$h = 0.56 \cdot (200000)^{0.7} \cdot (7000000)^{0.15} \approx 30.6 \, \text{kW} \cdot \text{m}^{-2} \cdot \text{K}^{-1}$. The wall superheat is

found as $\Delta T_{sup} = T_w - T_s = \dfrac{q''}{h} = \dfrac{200000}{30600} \approx 6.5 \, \text{K}$. The critical heat flux is found

from the Zuber correlation as

$q''_{cr} = \dfrac{\pi}{24} 1505132 \cdot 36.5 \left[\dfrac{0.017 \cdot 9.81(740 - 36.5)}{36.5^2} \right]^{1/4} \left[\dfrac{740}{740 + 36.5} \right]^{1/2} \approx 3.82 \, MW \cdot m^{-2}$. As can be seen, the

given heat flux is much smaller than the critical one.

4.4.3   Minimum Film Boiling

The minimum film boiling condition corresponds to point G in FIGURE 4-7. Sometimes this condition is referred to as the Leidenfrost point. The minimum film boiling heat flux depends on the considered geometry.

For a flat infinite horizontal surface, Berenson[4-1] proposed,

$$(4\text{-}103) \quad q''_{MFB,flat} = 0.09 \rho_g i_{fg} \left[\frac{g \sigma (\rho_f - \rho_g)}{(\rho_f + \rho_g)^2} \right]^{0.25} .$$

For horizontal cylinders with radius R, Lienhard and Wong[4-15] proposed,

$$(4\text{-}104) \quad q''_{MFB,cyl} = 0.515 \left\{ \frac{18}{\left(\dfrac{R}{L_b} \right)^2 \left[2 \left(\dfrac{R}{L_b} \right)^2 + 1 \right]} \right\}^{0.25} q''_{MFB,flat} ,$$

where L_b (the so-called capillary length scale) is given as,

$$(4\text{-}105) \quad L_b = \sqrt{\frac{\sigma}{g(\rho_f - \rho_g)}} ,$$

and $q''_{MFB,flat}$ is calculated from Eq. (4-103).

4.4.4   Transition Boiling

The transition boiling heat transfer will occur when the heater wall temperature is controlled, rather than heat flux. For such conditions and a vertical wall, Dhir and Liaw[4-9] modelled transition boiling and proposed that heat flux during this type of boiling is obtained by superposition of the volume-fraction-weighted contributions to the total heat transfer associated with the dry and wet areas on the surface,

$$(4\text{-}106) \quad q'' = h(T_w - T_s) = \bar{h}_f (1 - \alpha_w)(T_w - T_s) + \bar{h}_g \alpha_w (T_w - T_s),$$

where a_w is the void fraction at the wall.

The heat transfer coefficient in the dry region – developed by Bui and Dhir for film boiling on vertical walls – is as follows[4-6],

(4-107) $$\overline{h}_g = 0.47 \left\{ \left[\frac{\lambda_g^3 g \rho_g (\rho_f - \rho_g) i_{fg}}{\mu_g (T_w - T_s)} \right] \left[\frac{g(\rho_f - \rho_g)}{\sigma} \right]^{0.5} \right\}^{0.25} .$$

Heat transfer coefficient in the wet region is given as,

$$\overline{h}_f = \frac{2}{L^2 (1 - \alpha_w)} \int_0^{\pi/4} C \lambda_f (L \sec \psi + D_w) d\psi$$

where

$$C = \sum_{n=1}^{\infty} \frac{2 \sin^2(\xi_n b)}{\xi_n b + \sin(\xi_n b) \cos(\xi_n b)}$$

$$b = \frac{L \sec \psi - D_w}{2}$$

ξ_n is given by solution of $\xi_n b \tanh(\xi_n b) = 0$.

Here L and D_w are the distance between vapour stems and diameter of vapour stems, respectively. Geometrical considerations give also,

$$\alpha_w = \frac{\pi D_w^2}{4L^2} .$$

NOTE CORNER: Transition Boiling is often mixed up with another term: Boiling Transition. Caution should be, however, exercised: Transition Boiling is a kind of boiling described in this section and indicated in FIGURE 4-7 with curve *FG*. The term Boiling Transition which can be found in the international literature is synonymous with Boiling Crisis, or Critical Heat Flux, as used in this book. Even though no name is perfect, it is preferred here to avoid the term Boiling Transition just not to be confused with the Transition Boiling.

4.5 Convective Boiling in Heated Channels

Convective boiling in heated channels occurs in various types of boilers, including the reactor core of light water reactors. This is a very complex type of boiling, since flow conditions change along the heated channel due to the increase of enthalpy and the resulting phase change. The boiling regimes may change from the nucleate subcooled and saturation boiling to evaporating film, and possibly to the film and mist-flow boiling. All the boiling regimes that can be encountered in heated channels are shown in FIGURE 4-9 and are discussed in more detail in the following sections.

Various expressions for the convective-boiling heat transfer have been developed, for both the subcooled and saturation nucleate boiling regimes. The most commonly used in practical calculations are described below.

4.5.1 Onset of Nucleate Boiling

The point in a boiling channel where the nucleate boiling first appears is called the Onset of Nucleate Boiling (ONB) point (see FIGURE 4-10). The location of this point determines the physical boundary between the single-phase forced convection and the nucleate boiling heat transfer regime in the channel.
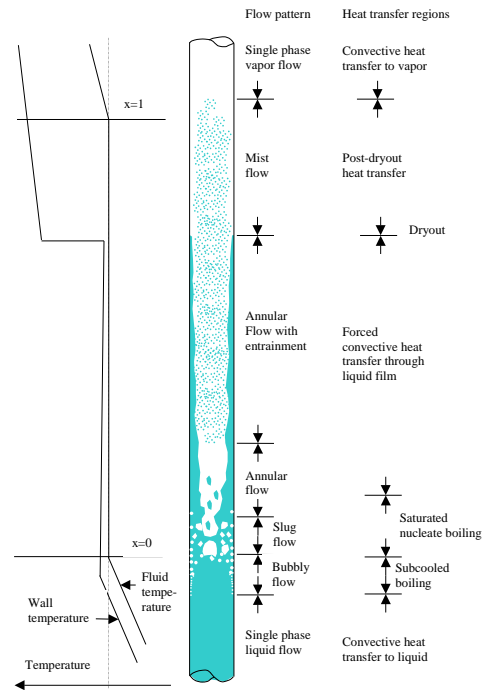
FIGURE 4-9. Two-phase flow and heat transfer regimes in a boiling channel.
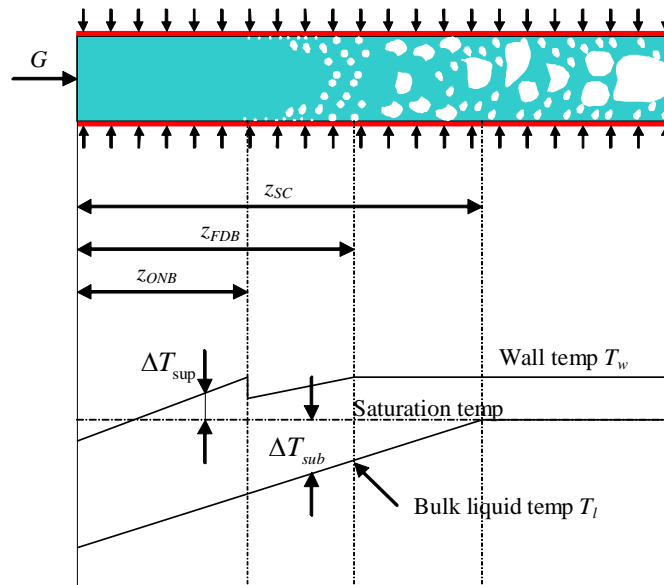
FIGURE 4-10. Wall and liquid temperature distributions in nucleate flow boiling.

The liquid temperature in a channel with a uniform heat flux distribution can be obtained from the energy balance and is as follows,

(4-108) $T_l(z) = T_{li} + \dfrac{q'' P_H z}{c_p GA}$.

The wall temperature can be obtained from the Newton's equation of cooling as,

(4-109) $T_w - T_l \equiv \Delta T_l = q''/h$.

Combining Eqs. (4-108) and (4-109) yields the following expression for the wall temperature,

(4-110) $T_w(z) = T_l(z) + \dfrac{q''}{h} = T_{li} + q''\left(\dfrac{P_H z}{c_p GA} + \dfrac{1}{h} \right)$.

It is convenient to introduce a so-called liquid subcooling defined as a difference of the liquid saturation temperature and the liquid bulk temperature. The liquid subcooling can be obtained from Eq. (4-108) as follows,

(4-111) $\Delta T_{sub} \equiv T_s - T_l = T_s - T_{li} - \dfrac{q'' P_H z}{c_p GA} = \Delta T_{subi} - \dfrac{q'' P_H z}{c_p GA}$.

Here ΔT_{subi} is the inlet subcooling of liquid. Another quantity of interest, which is often used in analysis of heated channels, is the wall superheat, defined as a difference between the wall temperature and the liquid saturation temperature. Wall superheat along the heated channel can be obtained from Eq. (4-110) as,

(4-112) $\Delta T_{sup}(z) \equiv T_w(z) - T_s = -\Delta T_{subi} + q''\left(\dfrac{P_H z}{c_p GA} + \dfrac{1}{h} \right)$.

It is clear that no boiling will occur when $\Delta T_{sup} < 0$, since the wall temperature is below the saturation temperature. However, there is no clear and easy criterion to define such wall superheat at which the subcooled boiling will start. This quantity has been investigated by many researches.

Bowring proposed that at the ONB point the wall superheat calculated from single-phase flow expression, Eq. (4-111), is equal to wall superheat which result from a correlation for the subcooled nucleate boiling. That is, the Bowring's criterion is as follows[4-3],

(4-113) $\Delta T_{sup}\left(z_{ONB}\right)\big|_{single\ phase} = \Delta T_{sup}\left(z_{ONB}\right)\big|_{subcooled\ boiling}$.

Assuming that the subcooled boiling correlation is given in a general form as,

(4-114) $\Delta T_{sup} = \psi \left(q''\right)^n$,

and combining Eqs. (4-112) through (4-114) yields the following expression for the ONB point,

$$(4\text{-}115) \quad z_{ONB} = \frac{c_p G A}{P_H} \left[\frac{\psi (q'')^n + \Delta T_{subi}}{q''} - \frac{1}{h} \right].$$

Examples of correlations for subcooled nucleate boiling will be given in the following section.

4.5.2 Subcooled Nucleate Boiling

Subcooled boiling region is divided into two sub-regions: **partial subcooled boiling** and **fully-developed subcooled boiling** region. In the partial subcooled boiling region only few nucleation sites are active and a considerable portion of the heat is transferred by normal single-phase forced convection. When the wall temperature increases, the number of active sites also increases and the area for single-phase heat transfer decreases. As the wall temperature is increased further, the whole surface is covered by active nucleation sites and boiling starts to be fully-developed.

Bowring suggested the following heat flux partitioning in the partial boiling region[4-3],

$$(4\text{-}116) \quad q'' = q''_{spl} + q''_{scb},$$

where q'' is the total average surface heat flux, q''_{spl} is the average surface heat flux transferred by single-phase convection and q''_{scb} is the average surface heat flux transferred by bubble nucleation.

The single-phase convection part q''_{spl} can be calculated in the same way as in single-phase region. For the bubbly-nucleation part q''_{scb} Rohsenow proposed a correlation derived for the nucleate pool boiling[4-17],

$$(4\text{-}117) \quad q''_{scb} = \mu_f i_{fg} \left[\frac{g(\rho_f - \rho_g)}{\sigma} \right]^{0.5} \left[\frac{c_{pf} \Delta T_{sup}}{C_{sf} i_{fg}} \right]^{1/r} \Pr_f^{-s/r},$$

where $r = 0.33$ and $s = 1.0$ for water and 1.7 for other fluids. The constant C_{sf} may vary from one fluid-surface combination to another. For water on mechanically polished stainless steel, the coefficient is equal to 0.0132.

Experimental data indicate that there is a correlation between the heat flux at the onset of nucleate boiling and the heat flux at which boiling becomes fully developed. This correlation has been approximated by Forster and Grief as

$$(4\text{-}118) \quad q''_{FDB} = 1.4 q''_{ONB}$$

This observation leads to the following expression for the local subcooling at the fully developed boiling location, due to Bowring[4-3],

$$(4\text{-}119) \quad \Delta T_{sub}(z)_{FDB} = \frac{q''}{1.4h} - \psi \left(\frac{q''}{1.4 \cdot 10^6} \right)^n.$$

Several correlations for subcooled nucleate boiling have been published in the literature. One example is the **Jens and Lottes correlation**, developed for subcooled boiling of water flowing upwards in vertical electrically heated stainless steel or nickel tubes. The correlation for the wall temperature is as follows[4-13],

$$(4\text{-}120) \quad T_w = T_s + 25\left(\frac{q''}{10^6}\right)^{0.25} e^{-p/62}$$

It should be noted that this correlation is valid for water only and that it is dimensional: T is in [K], q'' is in [W m^{-2}] and p is absolute pressure in [bar].

More recently, **Thom *et al.*** reported that the wall superheat obtained from (4-120) was consistently under-predicted in comparison with their measurements. They proposed the following modified correlation[4-19],

$$(4\text{-}121) \quad T_w = T_s + 22.65\left(\frac{q''}{10^6}\right)^{0.5} e^{-p/87} \quad,$$

and all variables are dimensional in a similar manner as in the Jens-Lottes correlation.

4.5.3   Saturated Flow Boiling

Saturated flow boiling region occurs in fuel assemblies of BWRs where nearly complete vaporization of the coolant is desired. To avoid the high wall temperatures and/or the poor heat transfer associated with the saturated film-boiling regime, the vaporization must be accomplished at low superheat or low heat flux levels. When boiling is initiated, both nucleate boiling and liquid convection may be the active heat transfer mechanisms. The importance of the two mechanisms varies over the channel length. As vaporization occurs, void fraction rapidly increases causing flow acceleration and, as a result, an enhancement of the convective heat transfer.

The increasing void fraction and acceleration of flow causes changes in the flow pattern along the boiling channel. For vertical upward flow, the flow pattern changes from bubbly to slug, churn and the annular flow. Correspondingly, the heat transfer regime changes from nucleate flow boiling to evaporation of the liquid film in annular flow. Further, it is clear that, as vaporization continues, the thickness of the liquid film will decrease, reducing its thermal resistance and thereby enhancing the effectiveness of this mechanism. When the liquid film becomes very thin, the required superheat to transport the wall heat across the liquid film becomes so low that nucleation is completely suppressed, and the only heat transfer mechanism is the heat conduction through the liquid film.

It should be clear that prediction of the convective boiling heat transfer coefficient requires an approach that accommodates a transition from a nucleate-pool-boiling-like condition at low qualities to a nearly pure film evaporation condition at higher qualities.

For more advanced calculations, one of the most frequently used correlations for prediction of heat transfer coefficient in saturated flow boiling in nuclear applications is the **Chen correlation**[4-7]. The fundamental assumption is that the total heat transfer

coefficient is a superposition of two parts: a microscopic (nucleate boiling) contribution h_{mic} and a macroscopic (bulk convective) contribution h_{mac}:

(4-122) $h = h_{mic} + h_{mac}$

The bulk-convective contribution is evaluated using the correlation similar to the Dittus-Boelter equation,

(4-123) $h_{mac} = 0.023 \left(\dfrac{\lambda_f}{D_h} \right) \mathrm{Re}^{0.8} \, \mathrm{Pr}^{0.4} \cdot F$.

Here the liquid Reynolds number is defined as,

(4-124) $\mathrm{Re} = \dfrac{G(1-x)D_h}{\mu}$.

S is the so-called suppression factor evaluated as,

(4-125) $S = \left(1 + 2.56 \cdot 10^{-6} F^{1.463} \cdot \mathrm{Re}^{1.17} \right)^{-1}$,

where F is found as,

(4-126) $F = \begin{cases} 1 & X_{tt}^{-1} \leq 0.1 \\ 2.35 \left(0.213 + \dfrac{1}{X_{tt}} \right)^{0.736} & X_{tt}^{-1} > 0.1 \end{cases}$,

and the Martinelli parameter is given by

(4-127) $X_{tt} = \left(\dfrac{1-x}{x} \right)^{0.9} \left(\dfrac{\rho_g}{\rho_f} \right)^{0.5} \left(\dfrac{\mu_f}{\mu_g} \right)^{0.1}$.

The microscopic contribution (nucleate boiling) to the overall heat transfer coefficient is determined by applying a correction to the Forster-Zuber relation for the heat transfer coefficient for nucleate pool boiling[4-11],

(4-128) $h_{mic} = 0.00122 \left[\dfrac{\lambda_f^{0.79} c_{pf}^{0.45} \rho_f^{0.49}}{\sigma^{0.5} \mu_f^{0.29} i_{fg}^{0.24} \rho_g^{0.24}} \right] \Delta T_{\sup}^{0.24} \left(p_s(T_w) - p_f \right)^{0.75} \cdot S$.

The Chen correlation has to be applied as follows:

1. Given mass flux, fluid properties, local heat flux and quality and guessed wall superheat;
2. Find X_{tt} from (4-127),
3. Find Re from (4-124),
4. Find F from (4-126),
5. Find S from (4-125),

6. Find h_{mac} from (4-123),
7. Find h_{mic} from (4-128),
8. Find h from (4-122),
9. Find superheat as $\Delta T_{\text{sup}} = q'' / h$,
10. Repeat steps 7 through 9 until the convergence is achieved.

The algorithm has been implemented into the Scilab code as shown below.

COMPUTER PROGRAM: The following function has been implemented into the Scilab code to calculate the heat transfer coefficient from the Chen correlation. The script uses water property functions described in Appendix D.

```
function [htc,DTnew,iter] = HTC_Chen(varargin)
//
n = length(varargin); htc=[];
if n < 5 then
  disp('Function calculates heat transfer coefficient using the Chen
correlation');
  disp('Syntax:');
  disp('  [htc] = HTC_Chen(G,q2p,p,x,Dh)');
  disp('  where:');
  disp('  htc - heat transfer coefficient, W/m2K');
  disp('  G   - mass flux, kg/m^2/s');
  disp('  q2p - wall heat flux, W/m2');
  disp('  p   - pressure, bar');
  disp('  x   - quality, -');
  disp('  Dh  - hydraulic diameter, m');
else
  G=varargin(1); q2p=varargin(2);p=varargin(3); x=varargin(4);
  Dh=varargin(5);
  RHOL = rholsat(p);
  RHOV = rhovsat(p);
  VISL = vislsat(p);
  VISV = visvsat(p);
  CPL  = cplsat(p);
  CONL = conlsat(p);
  CONV = convsat(p);
  Tsat = tsat(p);
  SIG  = surften(p);
  HFG  = hfg(p);
//
  DTguess = 5;
  eps = 100;
  Xtt = ((1-x)/x)^0.9*(RHOV/RHOL)^0.5*(VISL/VISV)^0.1;
  Rel = G*(1-x)*Dh/VISL;
  if 1/Xtt <= 0.1
    F = 1;
  else
    F = 2.35*(0.213+1/Xtt)^0.736;
  end
  S = 1/(1+2.56e-6*F^1.463*Rel^1.17);
  Prl = CPL*VISL/CONL;
  hmac = 0.023*CONL*Rel^0.8*Prl^0.4*F/Dh;
  iter = 1;
  ConstHmic =
0.00122*CONL^0.79*CPL^0.45*RHOL^0.49*S/SIG^0.5/VISL^0.29/HFG^0.24/RHOV^0.24;
  while iter <=100 & eps>=0.01
    DTsup = DTguess;
    Tw   = Tsat + DTsup;
    PsTw = psat(Tw);
    hmic = ConstHmic*DTsup^(0.24)*((PsTw-p)*1e5)^(0.75);
    htc = hmic + hmac;
    DTnew = q2p/htc;
    DTguess = 0.85*DTnew + 0.15*DTsup;
    eps = abs(DTnew-DTsup);
    iter= iter+1;
  end
end
endfunction
```

4.5.4   Forced Convective Critical Heat Flux

The conditions at which the wall temperature rises and the heat transfer decreases sharply due to a change in the heat transfer mechanism are termed as the **Critical Heat Flux** (CHF) conditions. The nature of CHF, and thus the change of heat transfer mechanism, varies with the enthalpy of the fluid. At subcooled conditions and low qualities this transition corresponds to a change in boiling mechanism from nucleate to film boiling. For this reason the CHF condition for these circumstances is usually referred to as the **Departure from Nucleate Boiling** (DNB).

At saturated conditions, with moderate and high qualities, the flow pattern is almost invariably in an annular configuration. In these conditions the change of the heat transfer mechanism is associated with the evaporation and disappearance of the liquid film and the transition mechanism is termed as **dryout**. Once dryout occurs, the flow pattern changes to the liquid-deficient region, with a mixture of vapour and entrained droplets. It is worth noting that due to high vapour velocity the heat transport from heated wall to vapour and droplets is quite efficient, and the associated increase of wall temperature is not as dramatic as in the case of DNB.

The mechanisms responsible for the occurrence of CHF (DNB- and dryout-type) are not fully understood, even though a lot of effort has been devoted to this topic. Since no consistent theory of CHF is available, the predictions of CHF occurrence relay on correlations obtained from specific experimental data. LWR fuel vendors perform their own measurements of CHF in full-scale mock-ups of fuel assemblies. Based on the measured data, proprietary CHF correlations are developed. As a rule, such correlations are limited to the same geometry and the same working conditions as used in experiments.

Most research on CHF published in the open literature has been performed for upward flow boiling of water in uniformly heated tubes. The overall experimental effort in obtaining CHF data is enormous. It is estimated that several hundred thousand CHF data points have been obtained in different labs around the world. More than 200 correlations have been developed in order to correlate the data. Discussion of all such correlations is not possible; however, some examples will be described in this section.

One of the earliest correlations was given by Bowring, who proposed the following expression to evaluate the CHF condition[4-4]:

(4-129) $$q''_{cr} = \frac{A + D_h \cdot G \Delta i_{subi} / 4}{C + L} ,$$

where,

(4-130) $$A = \frac{0.579 F_{B1} D_h \cdot G \cdot i_{fg}}{1 + 0.0143 F_{B2} D_h^{1/2} G} ,$$

(4-131) $$C = \frac{0.077 F_{B3} D_h \cdot G}{1 + 0.347 F_{B4} (G/1356)^n} ,$$

Here D_h is the hydraulic diameter [m], G is the mass flux [kg m^{-2} s^{-1}], i_{fg} is the latent heat [J kg^{-1}], p is the pressure [Pa], Δi_{subi} is the inlet subcooling [J kg^{-1}] and L is the tube length [m]. The correlation parameters n, F_{B1}, F_{B2}, F_{B3} and F_{B4} are functions of pressure and are as follows,

$$(4\text{-}132) \quad n = 2.0 - 0.5 p_R ,$$

$$(4\text{-}133) \quad p_R = \frac{p}{6.895 \cdot 10^6} ,$$

$$(4\text{-}134) \quad F_{B1} = \begin{cases} \dfrac{p_R^{18.942} \exp[20.8(1 - p_R)] + 0.917}{1.917} & p_R \leq 1 \\[3mm] p_R^{-0.368} \exp[0.648(1 - p_R)] & p_R > 1 \end{cases} ,$$

$$(4\text{-}135) \quad \frac{F_{B1}}{F_{B2}} = \begin{cases} \dfrac{p_R^{1.316} \exp[2.444(1 - p_R)] + 0.309}{1.309} & p_R \leq 1 \\[3mm] p_R^{-0.448} \exp[0.245(1 - p_R)] & p_R > 1 \end{cases} ,$$

$$(4\text{-}136) \quad F_{B3} = \begin{cases} \dfrac{p_R^{17.023} \exp[16.658(1 - p_R)] + 0.667}{1.667} & p_R \leq 1 \\[3mm] p_R^{-0.219} & p_R > 1 \end{cases} ,$$

$$(4\text{-}137) \quad \frac{F_{B4}}{F_{B3}} = p_R^{1.649} .$$

The correlation is based on a fit to data in the ranges $136 < G < 18600$ [kg m^{-2} s^{-1}], $2 < p < 190$ [bar], $2 < D_h < 45$ [mm] and $0.15 < L < 3.7$ [m].

For upflow boiling of water in vertical tubes with constant heat flux, Levitan and Lantsman recommended the following correlation for the occurrence of DNB in 8-mm-diameter pipe[4-14]:

$$(4\text{-}138) \quad q''_{cr} = \left[10.3 - 7.8 \frac{p}{98} + 1.6 \left(\frac{p}{98}\right)^2 \right] \left(\frac{G}{1000}\right)^{1.2\{[0.25(p-98)/98]-x_e\}} e^{-1.5x_e} .$$

It is customary to specify the flow quality to determine the occurrence of dryout. Levitan and Lantsman recommended the following relation for predicting the critical quality in 8-mm pipes[4-14]:

$$(4\text{-}139) \quad x_{cr} = \left[0.39 + 1.57 \frac{p}{98} - 2.04 \left(\frac{p}{98}\right)^2 + 0.68 \left(\frac{p}{98}\right)^3 \right] \left(\frac{G}{1000}\right)^{-0.5} .$$

In these relations q''_{cr} is the critical heat flux [MW m^{-2}], p is the pressure [bar], G is the mass flux [kg m^{-2} s^{-1}] and x_e is the equilibrium quality. The correlation given by Eq. (4-138) is valid in ranges $29.4 < p < 196$ [bar] and $750 < G < 5000$ [kg m^{-2} s^{-1}] and is accurate within $\pm 15\%$. For correlation given by Eq. (4-139) the ranges are: $9.8 < p < 166.6$ [bar] and $750 < G < 3000$ [kg m^{-2} s^{-1}], and the accuracy of x_{cr} is within ± 0.05.

Both these correlations can be used for prediction of CHF in tubes with other diameters by using proper correction factors. The CHF value calculated from Eq. (4-138) can be used for other tube diameters if the following correction factor is applied:

$$(4\text{-}140) \quad q''_{cr} = q''_{cr}\big|_{8mm} \cdot \left(\frac{8}{D}\right)^{0.5} \quad ,$$

where D is the tube diameter in [mm] and $q''_{cr}\big|_{8mm}$ is the critical heat flux obtained from Eq. (4-138).

In a similar manner, the critical quality calculated from Eq. (4-139) can be used for other tube diameters with the following correction factor:

$$(4\text{-}141) \qquad x_{cr} = x_{cr}\big|_{8mm} \cdot \left(\frac{8}{D}\right)^{0.15} .$$

Here $x_{cr}\big|_{8mm}$ is the critical quality obtained from Eq. (4-139) and D is the tube diameter in [mm].

4.5.5   Film Boiling Heat Transfer

The film boiling heat transfer will prevail in a heated channel after the occurrence of DNB. The characteristic feature of the film boiling is the existence of a vapour film which is covering the heated wall and isolating fluid from the wall, as schematically shown in FIGURE 4-11. The film is generally not smooth but exhibits irregularity at random locations. Several investigators have linked these distortions of the water-vapour interface to the growth of waves due to the interface instability.

For laminar, conduction-dominant transport, the heat transfer coefficient through the vapour film is given as,

$$(4\text{-}142) \qquad h = \frac{\lambda_g}{\delta} .$$

Here δ is the vapour film thickness and λ_g is the vapour conductivity. The vapour film thickness can be obtained from a simple, one-dimensional model. Substituting the predicted film thickness to Eq. (4-142) yields,

$$(4\text{-}143) \qquad h = \left[\frac{\rho_g (\rho_f - \rho_g) g i_{fg} \lambda_g^3}{4(z - z_{DNB}) \mu_g (T_w - T_s)} \right]^{1/4} ,$$

where z_{DNB} is the axial location where DNB occurs and z is the axial distance.
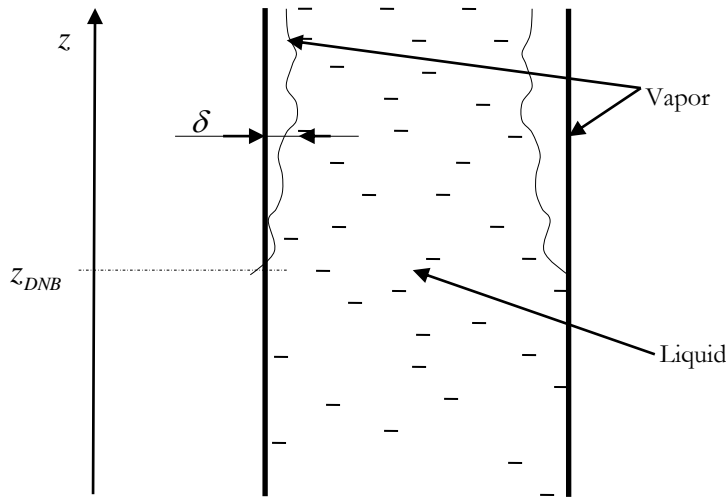
FIGURE 4-11. Schematic of film boiling heat transfer.

This simplified model, however, takes no account for the bubbles that rise with film and its accuracy is not very good.

Bromley[4-1] analysed film boiling heat transfer from horizontal pipes submerged in stagnant liquid and derived the following correlation for the heat transfer coefficient,

$$(4\text{-}144) \quad h = 0.62 \left[\frac{\lambda_g^3 \rho_g (\rho_f - \rho_g) g i'_{fg}}{\mu_g (T_w - T_s) D} \right]^{1/4} ,$$

where D is the pipe diameter and i'_{fg} is a modified latent heat to take into account the vapour superheat defined as,

$$(4\text{-}145) \quad i'_{fg} = i_{fg} \left[1 + 0.4 \frac{c_p (T_w - T_s)}{i_{fg}} \right]^2 .$$

Equation (4-144) takes into account the heat transfer due to conduction and convection only. If the wall temperature is high, the radiative heat transfer has to be taken into account as well, where

$$(4\text{-}146) \quad h_r = \frac{\Phi_{12} \sigma (T_w^4 - T_s^4)}{T_w - T_s} ,$$

is the radiative heat transfer coefficient and Φ_{12} is a correction factor to account for the geometry of the system and for the deviation of involved materials from the black body model. The combined heat transfer coefficient was given by Bromley as,

$$(4\text{-}147) \quad h_{tot} = h\left(\frac{h}{h_{tot}}\right)^{1/3} + h_r .$$

As can be seen the total heat transfer coefficient h_{tot} is not a simple sum of the two coefficients, since radiation is influencing the thickness of the vapour layer and thus is modifying the heat transfer coefficient obtained from Eq. (4-144).

The Bromley's model for film boiling from horizontal cylinder can be extended to other geometries by using the Helmholtz length scale instead of the pipe diameter in Eq. (4-144), where the Helmholtz-unstable wavelength is defined as,

$$(4\text{-}148) \quad \lambda_H = 16.24\left[\frac{\sigma^4\left(i'_{fg}\right)^3 \mu_g^5}{\rho_g\left(\rho_f - \rho_g\right)^5 g^5 \lambda_g^3 \left(T_w - T_s\right)^2}\right]^{1/2} .$$

4.5.6 Mist Flow Evaporation

Mist flow is a two-phase flow pattern when the flow quality is high and the liquid phase exists in the dispersed form only. Such flow pattern will occur in a heated channel when the flow quality exceeds the critical one; that is after the dryout occurs. Heat transfer regime that is associated with the mist flow is called mist flow evaporation or post-dryout (PDO) heat transfer. Several different heat transfer mechanisms may play role in mist flow evaporation:

1. Convective heat transfer from the wall to the vapour

2. Convective heat transfer from the vapour to the entrained droplets

3. Evaporation of droplets that collide with the wall and wet its surface

4. Evaporation of droplets that come to close proximity to the wall but do not wet the surface

5. Radiation heat transfer from the wall to the droplets

6. Radiation heat transfer from the wall to the vapour

7. Radiation heat transfer from vapour to droplets

Each of these mechanisms can be evaluated separately leading to a quite complex model. The heat exchange mechanisms in the mist-flow evaporation heat transfer are shown in FIGURE 4-12.
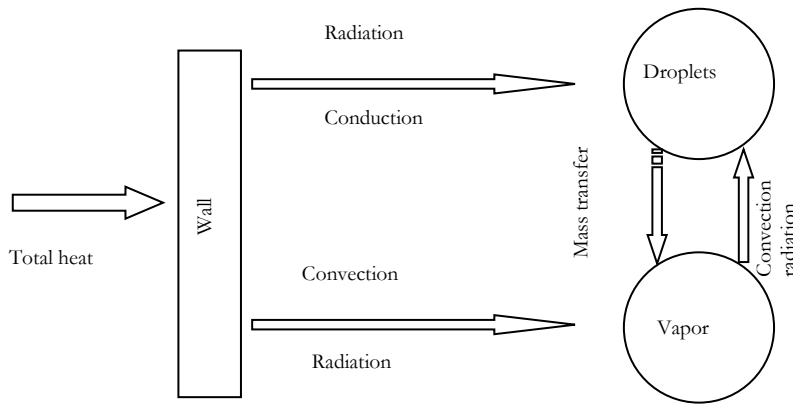
FIGURE 4-12. Heat exchange mechanisms in the mist-flow evaporation heat transfer.

Another, simplified approach is to correlate the heat transfer coefficient based on experimental data. Based on best fit to data, Groeneveld proposed the following correlation for heat transfer in the dispersed flow regime[4-12]:

$$(4\text{-}149) \quad Nu_g = \frac{hD}{\lambda_g} = a\left[\left(\frac{GD}{\mu_g}\right)\left(x + \frac{\rho_g}{\rho_f}(1-x)\right)\right]^b \Pr_{g,w}^c Y^d,$$

where,

$$(4\text{-}150) \quad Y = 1 - 0.1\left(\frac{\rho_f}{\rho_g} - 1\right)^{0.4}(1-x)^{0.4}.$$

Note that $\Pr_{g,w}$ is the vapour Prandtl number evaluated at the wall temperature and all other parameters are evaluated at the saturation temperature. Values of the constants a, b, c and d are provided for tubes and annuli only, see TABLE 4.2.

TABLE 4.2. Coefficients in the Groeneveld's correlation (Eq. (4-149)).

Geometry	a	b	c	d
Tubes	0.00109	0.989	1.41	-1.15
Annuli	0.0520	0.688	1.26	-1.06
Tubes and annuli	0.00327	0.901	1.32	-1.5

The validity of the correlation is limited to the following ranges: $2.5 < D < 25$ mm, $68 < p < 215$ bar, $700 < G < 5300$ [kg m^{-2} s^{-1}], $0.1 < x_e < 0.9$, $120 < q'' < 2100$ kW m^{-2}, $0.88 < \Pr_{g,w} < 2.21$, $0.706 < Y < 0.976$ and $6.6 \ 10^4 < \left(\frac{GD_h}{\mu_g}\right)\left(x_e + \frac{\rho_g}{\rho_f}(1-x_e)\right) < 1.3 \ 10^6$.

R E F E R E N C E S

[4-1]   Berenson, P.J., "Film boiling heat transfer from a horizontal surface," *J. Heat Transfer*, Vol. 83, p. 351, 1961.

[4-2]   Bird, R.B., Stewart, W.E. and Lightfoot, E.N., *Transport Phenomena*, Wiley, New York, 2002.

[4-3]   Bowring, R.W., "Physical model based on bubble detachment and calculation of steam voidage in the subcooled region of a heated channel", OECD Halden Reactor Project Report HPR-10, 1962.

[4-4]   Bowring, R.W., "A simple but accurate round tube uniform heat flux dryout correlation over the pressure range 0.7 – 17 MN/m2 (100 – 2500 psia), Br. Report AEEW-R789, Winfrith, U.K., 1972.

[4-5]   Bromley, L.A., *Chem. Eng. Progr.*, Vol. 46, p. 221, 1950.

[4-6]   Bui, T.D. and Dhir, V.K., "Film boiling heat transfer on an isothermal vertical surface", J. Heat Transfer, vol. 107, pp. 764-771, 1985.

[4-7]   Chen, J.C., "Correlation for boiling heat transfer to saturated fluids in convective flow", Ind. *Eng. Chem. Proc. Design and Dev.*, vol. 5, no. 3, pp. 322-339, 1966.

[4-8]   Colburn, A.P., *Trans. AIChE*, Vol. 29, p. 174, 1933.

[4-9]   Dihr, V.K. and Liaw, S.P., "Framework for a unified model for nucleate and transition pool boiling", *in Radiation, Phase Change Heat Transfer and Thermal Systems*, ASME HTD, vol. 81, pp. 51-58, 1987.

[4-10]   Dittus, F.W., Boelter, L. M. K., "University of California Publications in Engineering", Vol. 2, p. 433, Berkeley 1930.

[4-11]   Forster, H.K., Zuber, N.J., "Dynamics of Vapor Bubbles and Boiling Heat Transfer," Conference on Nuclear Engineering, Los Angeles, 1955.

[4-12]   Groeneveld, D.C., "Post-dryout heat transfer at reactor operating conditions", Report AECL-4513, 1973.

[4-13]   Jens, W.H and Lottes P.A., *Analysis of heat transfer, burnout, pressure drop and density data for high pressure water*, Rep. ANL-4627, 1951.

[4-14]   Levitan, L.L. and Lantsman, F.P., "Investigating burnout with flow of a steam-water in a round tube", *Thermal Eng.* (USSR), English trans., vol. 22, no. 1, pp. 102-105, 1975.

[4-15]   Lienhard, J.H. and Wong, P.T.Y., "The dominant unstable wave length and minimum heat flux during film boiling on a horizontal cylinder," *J. Heat Transfer*, Vol. 86, pp. 220-226, 1964.

[4-16]   Michiejev, M. A., *Principles of Heat Transfer* (in Russian), 2nd Ed. Moscow-Leningrad 1956.

[4-17]   Rohsenow, W.M., "A method of correlating heat transfer data for surface boiling of liquids", Trans. ASME, vol. 74, p. 969, 1952.

[4-18]   Sieder E.N., Tate G.E., *Ind. Eng. Chem.*, Vol. 28, p. 1429, 1936.

[4-19]   Thom, J.R.S. *et al.*, "Boiling in subcooled water in flow up heated tubes or annuli", Paper 6, Symp. Boiling Heat Transfer in Steam Generating Units and Heat Exchangers, Manchester, 15-16 Sept., 1965.

[4-20]   Zuber, N., "Hydrodynamic aspects of boiling heat transfer", AEC Report, AECU-4439, 1959.

EXERCISE 4-1. Heat is conducted through an infinite plate. What should be the minimum thickness of the plate if the required heat flux should not exceed 35 W/m² for the temperature difference on both sides of the plate equal to 40 K. The conductivity of the plate material is equal to 0.14 W.m⁻¹.K⁻¹.

EXERCISE 4-2. Heat is conducted through an infinite annulus with inner diameter equal to 10 mm and with the heat conductivity of the wall material equal to 5 W.m⁻¹.K⁻¹. The temperature difference between the inner and the outer wall is equal to $T_i - T_o = 2$ K, where T_i is the inner temperature and T_o is the outer temperature of the annulus wall. Calculate the wall thickness if the heat flux at the outer wall is equal to 10 kW.m⁻².

EXERCISE 4-3. An infinite plate is heated with internal heat sources with density q''' = 5 kW.m⁻³ and cooled on both sides in such a way, that temperature on one side is equal to 100 °C and on the other side of the plate is 80 °C. Find the location and value of the highest temperature in the plate. The plate thickness is 15 mm and the material conductivity is 3.5 W.m⁻¹.K⁻¹.

EXERCISE 4-4. An infinite cylinder with diameter d=10 mm is heated with uniformly distributed volumetric heat sources with density equal to q''' = 5 MW.m⁻³. Calculate the temperature at the centre line if the surface temperature is equal 250 °C and the material conductivity is 1.3 W.m⁻¹.K⁻¹. What will be the heat flux at the cylinder surface?

EXERCISE 4-5. An infinite annulus with inner and outer diameters equal to 8 and 10 mm, respectively is heated with uniformly distributed volumetric heat sources with density equal to q''' = 75 MW.m⁻³. The inner surface of the annulus wall is kept isolated and the outer surface is cooled in such a way that its temperature is kept constant and equal to 270 °C. Calculate the maximum temperature in the annulus, assuming that the wall material has the thermal conductivity equal to 3.5 W.m⁻¹.K⁻¹.

EXERCISE 4-6. Predict the location of the onset-of-nucleate-boiling point in a uniformly heated tube (8 mm internal diameter) with q'' = 0.5 MW m⁻² on the internal wall. The tube is cooled with water at 140 bars, inlet subcooling 70 K and mass flux 2000 kg m⁻² s⁻¹. Use Bowring's model for the onset of nucleate boiling and Jens-Lottes' correlation for subcooled boiling. Use saturated water properties at 140 bar pressure. What will be the difference in the location of the ONB point if Thom *et al.* model is used instead?

EXERCISE 4-7. For conditions as described in EXERCISE 4-6, find the location of the point where the fully-developed boiling starts.

EXERCISE 4-8. Subcooled water at p = 70 bar flows into a vertical round tube with uniformly heated wall with q''=200 kW m⁻² on the internal wall surface. The inlet subcooling is 40 K, the mass flux is 1200 kg m⁻² s⁻¹ and the tube internal diameter is D = 10 mm. Find the temperature distribution on the internal wall surface from the inlet to the point where the bulk water temperature is equal to the saturation temperature. Use saturated water properties at 70 bar pressure.

EXERCISE 4-9. Plot $q''_{crit}(z)$ using the Bowring's correlation and assuming steam-water flow at 70 bar in a pipe with D = 10 mm and length 3.5 m. The inlet subcooling is 10 K, total mass flux G = 1250 kg m⁻² s⁻¹.

EXERCISE 4-10. Using the Levitan and Lantsman correlation for dryout (4-139), plot x_{crit} as a function of pressure in a range 9.8 < p < 166.6 [bar] and using G as parameter with values G = 750, 1000, 1500 and 2000 [kg m⁻² s⁻¹] for boiling upflow of water in a uniformly heated, vertical tube with 8 mm internal diameter. Give the value of the pressure for which x_{crit} becomes maximum. Use this pressure to plot x_{crit} as a function of G.

EXERCISE 4-11. Calculate the heat transfer coefficient from the Groeneveld correlation (4-149) for steam-water flow in a vertical tube: D = 10 mm, G = 1200 kg m⁻² s⁻¹, p = 70 bar, heat flux q = 1.0 MW m⁻² at axial positions where x = 0.2, 0.4, 0.6 and 0.8. Check whether the validity ranges are satisfied.

5. Selected Applications

I n this chapter a few selected topics have been chosen to be covered in more detail. Compressible flows and critical single and two-phase flows are important in safety analyses of nuclear power plants. In particular, the results of analysis of a postulated Loss-of-Coolant accident have direct influence on the design solutions applied in nuclear power plants. Other safety-related topics considered in this chapter include the analysis of transients in pipelines. Such transients, called in earlier literature "water hammer", can cause significant damages in pipelines, unless proper design and operational measures are applied. The last section in this chapter is dealing with fluid-structure interactions (FSI) issues, such as stationary and transient reaction forces acting on solid walls. In recent years FSI gets more and more attention, since such interactions can cause premature failure of equipment in nuclear power plants.

5.1 Compressible Flows

5.1.1 Speed of Sound

Speed of sound is the speed of propagation of small pressure perturbations (vibrations) in an elastic medium. This speed varies with the medium and, for example, is higher in water than in air. Consider propagation of a sound wave of infinitesimal strength through an undisturbed medium, as shown in FIGURE 5-1.
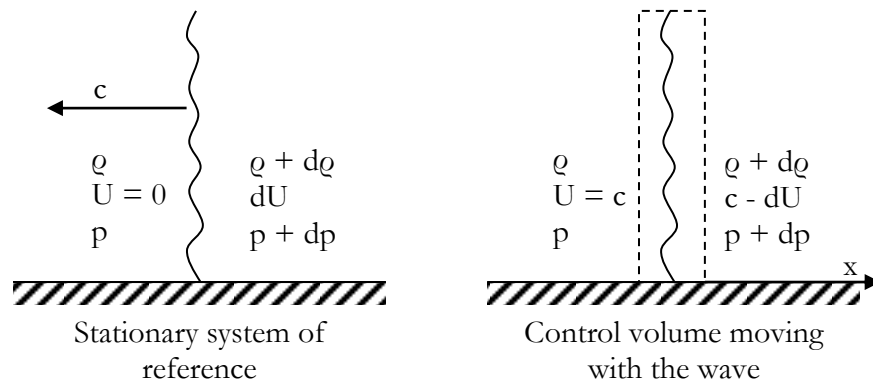
FIGURE 5-1. Propagation of a wave in an elastic medium.

The mass and momentum conservation equations formulated for the control volume moving with the wave are as follows,

$$(5\text{-}1) \qquad \rho c = (\rho + d\rho)(c - dU),$$

$$(5\text{-}2) \qquad p + c \cdot \rho c = p + dp + (c - dU) \cdot (\rho + d\rho)(c - dU).$$

Here U and dU are the mean velocity of the medium in front of the wave and its perturbation behind the wave, respectively. Similarly ϱ and p are the medium density and pressure, whereas $d\varrho$ and dp are their corresponding perturbations. Equation (5-1) yields,

$$(5\text{-}3) \qquad dU = \frac{d\rho}{\rho}c\,,$$

whereas Eq. (5-2) gives,

$$(5\text{-}4) \qquad dp = 2\rho c\, dU - c^2 d\rho\,.$$

Combining Eqs. (5-3) and (5-4) yields,

$$(5\text{-}5) \qquad c^2 = \frac{dp}{d\rho}\,,$$

or,

$$(5\text{-}6) \qquad c = \sqrt{\frac{dp}{d\rho}}\,.$$

Equation (5-6) gives a relationship for the speed of sound. In general, the speed of sound in any medium can be expressed as,

$$(5\text{-}7) \qquad c = \sqrt{\frac{C}{\rho}}\,,$$

where C is the stiffness coefficient of medium [Pa] and ρ is the density [kg·m^{-3}].

In a non-dispersive medium speed of sound is independent of the sound wave length. Air is a non-dispersive medium, whereas CO_2 is dispersive at ultrasonic frequencies (> 28 kHz).

Speed of sound in solids is given as,

$$(5\text{-}8) \qquad c = \sqrt{\frac{E}{\rho}}\,,$$

where E is Young's modulus and ρ is density.

In fluids the speed of sound is given by,

$$(5\text{-}9) \qquad c = \sqrt{\frac{K}{\rho}}\,,$$

where K is the **bulk modulus of elasticity**, defined as,

(5-10) $K = \dfrac{\partial p}{\partial \rho / \rho}$.

In liquids and gases acoustic waves are propagated in an adiabatic manner, that is, heat exchange does not take place. In such conditions, the following is valid for gases,

(5-11) $c = \sqrt{\dfrac{\kappa p}{\rho}} = \sqrt{\kappa R T}$.

Here $\kappa = c_p / c_v$, p is the mean pressure of gas and ϱ is the density, R is the gas constant and T is the temperature.
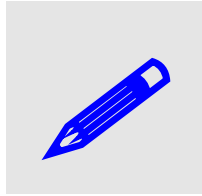
EXAMPLE 5-1. Calculate speed of sound in air at temperatures equal to -20 °C and +20 °C. SOLUTION: The heat capacity ratio and the gas constant for air are $\varkappa = 1.4$ and R = 287 J kg^{-1} K^{-1}, respectively. The speeds of sound are thus obtained as $c_1 = \sqrt{1.4 \cdot 287 \cdot (-20 + 273.15)} = 318.9 m/s$ and

$c_2 = \sqrt{1.4 \cdot 287 \cdot (20 + 273.15)} = 343.2 m/s$. As can be seen, the speed of sound increases with over 24 m/s when the air temperature increases from -20 to +20 °C.

The speed of sound is used as a reference value to express a speed of flow or of any object moving through a gaseous medium. The **Mach number** is defined as a ratio of the local object or flow speed U to the local speed of sound in the medium,

(5-12) $\mathrm{M} = \dfrac{U}{c}$.

5.1.2   Stationary Gas Flow in Channels

For adiabatic flow of gas in a channel, the energy equation is reduced to,

(5-13) $\dfrac{U^2}{2} + i = i_0$.

Here the energy dissipation terms are neglected. Assuming in addition that the flow is isentropic, the gas enthalpy can be expressed in terms of the temperature and pressure as,

(5-14) $i = \dfrac{\kappa}{\kappa - 1} R T = \dfrac{\kappa}{\kappa - 1} \dfrac{p}{\rho}$.

Equation (5-11) yields,

(5-15) $\dfrac{\kappa}{\kappa - 1} \dfrac{p}{\rho} = \dfrac{c^2}{\kappa - 1}$.

Combining Eqs. (5-13) through (5-15) yields,

(5-16) $$\frac{U^2}{2} + \frac{c^2}{\kappa-1} = \frac{c_0^2}{\kappa-1} .$$

Index "0" in Eqs. (5-13) and (5-16) refers to the stagnation conditions, when the flow velocity is zero, $U = 0$. Dividing both sides of the equation by c yields,

(5-17) $$\frac{U^2}{c^2} + \frac{2}{\kappa-1} = \frac{2}{\kappa-1}\frac{c_0^2}{c^2} \Rightarrow \frac{c}{c_0} = \frac{1}{\sqrt{1 + \frac{\kappa-1}{2}M^2}} .$$

The flow is **critical** when $M = 1$. All parameters pertinent to the critical conditions have index "*". Thus, the critical speed of sound is found from Eq. (5-16) as,

(5-18) $$c_* = c_0\sqrt{\frac{2}{\kappa+1}} .$$

Since $c = \sqrt{\kappa RT}$ and $c_0 = \sqrt{\kappa RT_0}$, Eq. (5-17) yields,

(5-19) $$\frac{T}{T_0} = \frac{1}{1 + \frac{\kappa-1}{2}M^2}$$

and

(5-20) $$\frac{T_*}{T_0} = \frac{2}{\kappa+1} .$$

Assuming an isentropic process for which,

(5-21) $$\frac{p^{\kappa-1}}{T^\kappa} = const, \quad \frac{T}{\rho^{\kappa-1}} = const ,$$

the critical pressure and density can be related to the stagnation values as follows,

(5-22) $$\frac{p_*}{p_0} = \left(\frac{2}{\kappa+1}\right)^{\frac{\kappa}{\kappa-1}}, \quad \frac{\rho_*}{\rho_0} = \left(\frac{2}{\kappa+1}\right)^{\frac{1}{\kappa-1}} .$$

The mass flow rate at any cross section in a channel can be calculated as,

(5-23) $$W = \rho UA = \rho A\sqrt{\frac{2}{\kappa-1}RT_0\left(1 - \frac{T}{T_0}\right)} .$$

Assuming the isentropic relationships (5-21) in Eq. (5-23), the mass flow rate can be calculated as follows,

$$(5\text{-}24) \quad W = A \frac{p_0}{\sqrt{T_0}} \sqrt{\frac{2\kappa}{R(\kappa-1)}} \sqrt{\left(\frac{p}{p_0}\right)^{\frac{2}{\kappa}} - \left(\frac{p}{p_0}\right)^{\frac{\kappa+1}{\kappa}}} \,.$$

This equation gives the mass flow rate through a duct in terms of the stagnation parameters and the local pressure. The expression suggests that for given stagnation conditions, the mass flow rate will increase with decreasing pressure p. This behaviour will however be limited to the point, when somewhere in the duct the flow velocity will reach the local speed of sound value, that is when M = 1. The duct cross-section where it first occurs is called the critical cross-section and the corresponding flow rate is the critical flow rate.

The **critical flow rate** can be found from the critical parameters as,

$$(5\text{-}25) \quad W_* = \rho_* U_* A_* = A_* \frac{p_0}{\sqrt{T_0}} \sqrt{\frac{\kappa}{R}} \sqrt{\left(\frac{2}{\kappa+1}\right)^{\frac{\kappa+1}{\kappa-1}}} \,.$$

It should be noted that the critical flow rate depends on the stagnation parameters only and the external pressure does not affect its value.
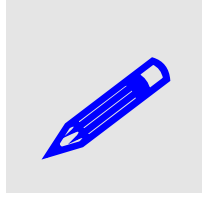
EXAMPLE 5-2. Two large volumes containing air are connected with each other by an ideal nozzle. Calculate the mass flow rate of air through the nozzle if the pressure and the temperature in one of the volumes is 2 MPa and 300 K, respectively, and the pressure in the other volume is 1.8 MPa. What should be the pressure in the second volume to obtain the maximum mass flow rate? Calculate the value of the maximum mass flow rate. SOLUTION: The mass flow rate through the nozzle can be calculated from Eq. (5-24) for sub-critical conditions and from Eq. (5-25) when flow is critical. The flow will be critical if the pressure in the second volume is less than the critical one, given by Eq. (5-22). This critical pressure is found as:

$$p_* = p_0 \left(\frac{2}{\kappa+1}\right)^{\frac{\kappa}{\kappa-1}} = 2 \left(\frac{2}{1.4+1}\right)^{\frac{1.4}{1.4-1}} = 1.056 \quad \text{MPa}$$

Thus the pressure in the second volume should be 1.056 MPa or less for flow to become the critical one. At given pressure the flow is under-critical and the mass flow rate can be found from Eq. (5-24):

$$W = A \frac{p_0}{\sqrt{T_0}} \sqrt{\frac{2\kappa}{R(\kappa-1)}} \sqrt{\left(\frac{p}{p_0}\right)^{\frac{2}{\kappa}} - \left(\frac{p}{p_0}\right)^{\frac{\kappa+1}{\kappa}}} = 10^{-4} \frac{2 \cdot 10^6}{\sqrt{300}} \sqrt{\frac{2 \cdot 1.4}{287(1.4-1)}} \sqrt{\left(\frac{1.8}{2}\right)^{\frac{2}{1.4}} - \left(\frac{1.8}{2}\right)^{\frac{1.4+1}{1.4}}} = 0.288 \text{kg/s}$$

When the pressure in the second volume becomes 1.056 MPa or less, the flow becomes critical and the air mass flow rate is found as,

$$W_* = A_* \frac{p_0}{\sqrt{T_0}} \sqrt{\frac{\kappa}{R}} \sqrt{\left(\frac{2}{\kappa+1}\right)^{\frac{\kappa+1}{\kappa-1}}} = 10^{-4} \frac{2 \cdot 10^6}{\sqrt{300}} \sqrt{\frac{1.4}{287}} \sqrt{\left(\frac{2}{1.4+1}\right)^{\frac{1.4+1}{1.4-1}}} = 0.467 \text{ kg/s}$$

Thus the mass flow rate would increase with about 50% if the pressure in the second volume was decreased below the critical value.

5.1.3 Discharge of Compressible Fluid from a Tank

In many engineering applications it is necessary to analyse the discharge of a compressible fluid from a tank with a finite volume through a small convergent nozzle. Due to the loss of fluid, the parameters in the tank are changing with time, influencing the conditions in the nozzle as well. Since the nozzle is small, it can be assumed that the conditions inside it are quasi steady-state. This assumption would not be correct for a large nozzle, in which the perturbations due to waves in the tank could not be ignored.

In nuclear engineering an important process is a **pressure vessel blowdown**, in which fluid is discharged from a tank. Blowdown can occur due to open-valve gas discharge from tanks or due to a ruptured pipe, which could lead to an uncontrolled fluid discharge from a pressure vessel. This type of accident is considered as one of the most severe ones in nuclear power plants, when blowdown of a reactor pressure vessel could occur during the Loss-of-Coolant Accident (LOCA), resulting from the rapture of a pipe in the reactor primary system.

Consider the case of adiabatic blowdown from a vessel containing perfect gas. The density change will be as,

$$(5\text{-}26) \qquad \frac{M}{V} = \rho = \rho_I \left(\frac{p}{p_I} \right)^{1/\kappa},$$

where subscript I designates the initial conditions.

Mass conservation equation for the ideal gas in the vessel is as follows,

$$W = -\frac{dM}{dt} \quad \Rightarrow \quad \left(\frac{p}{p_I} \right)^{(1-\kappa)/\kappa} \frac{d}{dt}\left(\frac{p}{p_I} \right) = -\frac{\kappa}{\rho_I} \frac{W}{V}.$$

Assuming that the critical flow prevails, the following differential equation for the pressure variation with time is obtained,

$$(5\text{-}27) \qquad \left(\frac{p}{p_I} \right)^{(1-3\kappa)/2\kappa} \frac{d}{dt}\left(\frac{p}{p_I} \right) = -\frac{\kappa}{\rho_I} \frac{A}{V} \sqrt{\kappa p_I \rho_I} \left(\frac{2}{\kappa+1} \right)^{\frac{\kappa+1}{2(\kappa-1)}}; \text{ at } t = 0,\ p/p_I = 1.$$

Solution of the above differential equation is as follows,

$$(5\text{-}28) \qquad \frac{p(t)}{p_I} = \left[1 + \left(\frac{\kappa-1}{2} \right)\left(\frac{2}{\kappa+1} \right)^{\frac{\kappa+1}{2(\kappa-1)}} \sqrt{\frac{\kappa p_I}{\rho_I}} \frac{A \cdot t}{V} \right]^{\frac{-2\kappa}{\kappa-1}}.$$

Combining Eq. (5-26) with (5-28) yields the mass of gas in the tank as a function of time during the critical discharge,

$$(5\text{-}29) \quad \frac{M(\tau)}{M_I} = \left[1 + \sqrt{\kappa} \left(\frac{\kappa - 1}{2} \right) \left(\frac{2}{\kappa + 1} \right)^{\frac{\kappa+1}{2(\kappa-1)}} \tau \right]^{\frac{-2}{\kappa-1}},$$

where,

$$(5\text{-}30) \quad \tau = \sqrt{\frac{p_I}{\rho_I}} \, \frac{A \cdot t}{V} = \frac{t}{\theta},$$

and

$$(5\text{-}31) \quad \theta = \frac{V}{A} \sqrt{\frac{\rho_I}{p_I}}.$$

M_I in Eq. (5-29) is the initial mass of the gas in the tank. The constant θ defined in Eq. (5-31) has a dimension of time and can be interpreted as a characteristic time constant of the tank during the critical discharge.

The time evolution of pressure in the tank given by Eq. (5-28) can be expressed in terms of the dimensionless discharge time τ as:

$$(5\text{-}32) \quad p(\tau) = p_I \left[1 + \sqrt{\kappa} \left(\frac{\kappa - 1}{2} \right) \left(\frac{2}{\kappa + 1} \right)^{\frac{\kappa+1}{2(\kappa-1)}} \tau \right]^{\frac{-2}{\kappa-1}}.$$

Obviously, the discharge flow from the tank to the ambient with pressure p_a will be critical as long as,

$$(5\text{-}33) \quad \frac{p_a}{p(\tau)} \le \left(\frac{2}{\kappa + 1} \right)^{\frac{\kappa}{\kappa-1}}.$$

Combining Eq. (5-32) with (5-33) yields the following expression for the non-dimensional critical discharge time,

$$(5\text{-}34) \quad \tau_{cr} = \frac{\left(\dfrac{p_I}{p_a} \right)^{\frac{\kappa-1}{2\kappa}} \left(\dfrac{2}{\kappa + 1} \right)^{\frac{1}{2}} - 1}{\sqrt{\kappa} \left(\dfrac{\kappa - 1}{2} \right) \left(\dfrac{2}{\kappa + 1} \right)^{\frac{\kappa+1}{2(\kappa-1)}}}.$$

It is interesting to note that the non-dimensional critical discharge time depends only on the type of gas and on the ratio of the initial pressure to the ambient pressure. In general, this relationship can be written as,

(5-35) $\quad \tau_{cr} = a + b \cdot \left(\dfrac{p_I}{p_a} \right)^c$,

where a, b and c are constants which are different for different gases, as specified in TABLE 5.1. This function is shown in FIGURE 5-2.

TABLE 5.1. Constants a, b and c in Eq. (5-35).

Constant	Monatomic gases ($\varkappa = 1.67$)	Diatomic gases ($\varkappa = 1.4$)	Triatomic gases ($\varkappa = 1.33$)
a	-4.108	-7.302	-9.010
b	3.555	6.666	8.348
c	0.201	0.143	0.124

EXAMPLE 5-3. Air is discharged to the surroundings from a vessel with volume $V = 10$ m³, with initial pressure $p_I = 15$ MPa and temperature $T_I = 300$ K through an orifice with a cross-section area $A = 10$ cm². Assuming the isentropic decompression of the air in the vessel, calculate the mass of the air that will be released from the vessel during the time when the discharge flow is critical. SOLUTION: for air the non-dimensional critical discharge time is given as:

$$\tau_{cr} = -7.302 + 6.666 \left(p_I / p_a \right)^{0.143} = -7.302 + 6.666 (15/0.101325)^{0.143} = 6.320$$

The initial mass of the air in the vessel is found as

$$M_I = V\rho_I = V \frac{p_I}{RT_I} = 10 \frac{15 \cdot 10^6}{287 \cdot 300} = 1742.16 \text{ kg}$$

At time τ_{cr} the mass of the air in the tank will be:

$$M(\tau) = M_I \left[1 + \sqrt{\varkappa} \left(\frac{\varkappa - 1}{2} \right) \left(\frac{2}{\varkappa + 1} \right)^{\frac{\varkappa+1}{2(\varkappa-1)}} \tau_{cr} \right]^{\frac{-2}{\varkappa-1}} = 1742.16 \left[1 + \sqrt{1.4} \left(\frac{1.4 - 1}{2} \right) \left(\frac{2}{1.4 + 1} \right)^{\frac{1.4+1}{2(1.4-1)}} 6.32 \right]^{\frac{-2}{1.4-1}} =$$

77.11 kg

Thus the mass of the released air during the critical discharge is 1665.05 kg.

Similar analysis can be performed for the under-critical discharge conditions. For that purpose the differential equation given by (5-21) has to be modified and the expression for the discharged mass flow rate that corresponds to the sub-critical flow should be used.
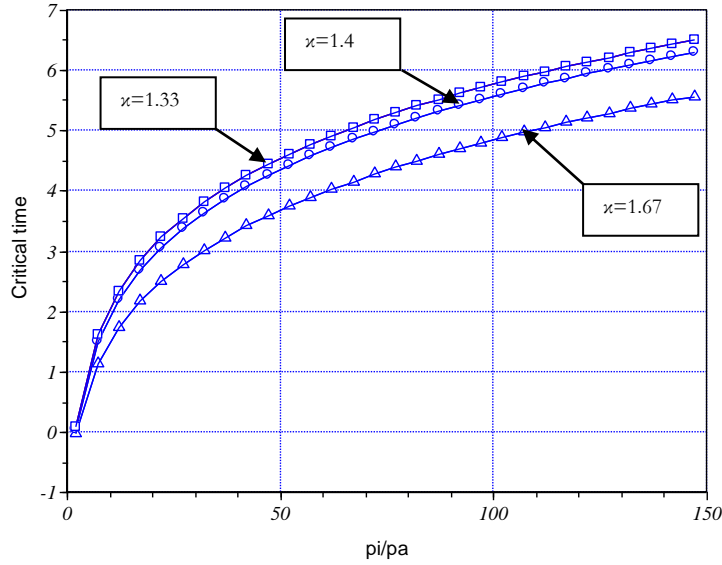
FIGURE 5-2. Dimensionless critical discharge time as a function of initial pressure for various gases.

5.1.4 Two-Phase Critical Flow

In single phase flows the critical flow occurs in locations where the flow velocity is equal to the local sound speed, that is where M = 1. In two-phase flows the situation is more complicated since the speed of sound cannot be uniquely determined. There may be actually more than one sound speed: one for each phase. Clearly, some modelling assumptions are necessary to determine the critical flow in two-phase flows.

One of the first and simplest models is based on the HEM formulation. The model is employing two fundamental assumptions: the velocities of the phases are equal and the phases are in the thermodynamic equilibrium. With these assumptions the mixture can be treated as a single fluid and the uniqueness of the speed of sound is preserved. Assuming an adiabatic flow, the mixture energy equation given by Eq. (5-13) can be written in terms of the mass flux as,

$$(5\text{-}36) \qquad \frac{G^2}{2\rho^2} + i = i_0 \,.$$

Further assuming isentropic flow, the mixture properties can be treated as a function of pressure only, and the equation becomes,

$$(5\text{-}37) \qquad G = \rho_h(p, s_0)\sqrt{2[i_0 - i(p, s_0)]} \,.$$

Here s_0 is the stagnation entropy.

The critical mass flux can be found as the maximum of the mass flux with respect to pressure,

$$\text{(5-38)} \quad \frac{dG}{dp} = \left(\frac{\partial \rho_h}{\partial p}\right)_s \sqrt{2(i_0 - i)} - \left(\frac{\partial i}{\partial p}\right)_s \Big/ \sqrt{2(i_0 - i)} = 0.$$

Solving this equation yields,

$$\text{(5-39)} \quad \sqrt{2(i_0 - i)}\Big|_* = \sqrt{\left(\frac{\partial i}{\partial p}\right)_s \Big/ \left(\frac{\partial \rho_h}{\partial p}\right)_s},$$

and substituting to Eq. (5-37) yields the critical mass flux as,

$$\text{(5-40)} \quad G\Big|_* = \rho_h(p_*, s_0) \sqrt{\left(\frac{\partial i}{\partial p}\right)_s \Big/ \left(\frac{\partial \rho_h}{\partial p}\right)_s}.$$

The homogeneous density and the partial derivatives are evaluated at the critical pressure in the nozzle, which is not known yet. Thus, an iterative solution is necessary. For practical applications, the following iterative process can be applied:

1. Guess the critical pressure in the nozzle $\tilde{p}_*$.

2. Since the flow is isentropic, the entropy at the nozzle is equal to the stagnation entropy and the quality at the nozzle can be found from the change of saturation entropy as $x = \left(s_0 - s_f(\tilde{p}_*)\right)/s_{fg}(\tilde{p}_*)$.

3. The enthalpy and the homogeneous density at the nozzle are found as $i = i_f(\tilde{p}_*) + x i_{fg}(\tilde{p}_*)$ and $\rho_h^{-1} = \rho_f^{-1}(\tilde{p}_*) + x\left[\rho_g^{-1}(\tilde{p}_*) - \rho_f^{-1}(\tilde{p}_*)\right]$

4. Calculate the mass flux from Eq. (5-37) and iterate through 1-4 until the maximum is found.

The model has been implemented into the Scilab code as shown below.
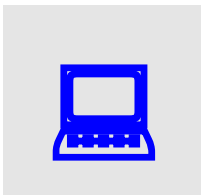
COMPUTER PROGRAM: This script contains a Scilab implementation of the Homogeneous Equilibrium Model of critical flow for water-steam mixture. The mixture pressure is given as `p0` parameter (currently equal to 70 bars). The script uses water property functions described in Appendix D.

```
// HEM critical flow of water-steam
// This script calculates the steam-water critical mass flow
// rate using HEM model
//
// Stagnation condition
//
p0 = 70; t0 = tsat(p0);
//
s0 = senvsat(p0); // saturated steam
h0 = hvsat(p0);
pgs = []; G = [];
err = 1.e6;        // Initial error
eps = 1;           // Required accuracy for mass flux (kg/m2/s)
iter = 0;
//
// calculate the mass flux for three different pressures
//
```

```
pr = [0.95 0.8 0.5];
pgs = p0*pr;   // vector with initial guess
// Define an inline function to calculate mass flux
deff('[G]=mflux(pgs,s0,h0)', ....
      ['x=(s0-senlsat(pgs))/(senvsat(pgs)-senlsat(pgs))';   ...
       'hmix=hlsat(pgs)+x*hfg(pgs)';  ...
       'rhom=1/(1/rholsat(pgs)+x/rhovsat(pgs))';  ...
       'G=rhom*sqrt(2*(h0-hmix))']);
//
for i=1:3; G(i)=mflux(pgs(i),s0,h0); end
while err > eps;
  A=[1 pr(1) pr(1)*pr(1);1 pr(2) pr(2)*pr(2);1 pr(3) pr(3)*pr(3)];
  Y=A\G;                    // Parabolic approximation for G=f(p)
  pr(4) = -Y(2)/2/Y(3);     // new pressure ratio guess at dG/dp=0
  G(4) = mflux(pr(4)*p0,s0,h0);   // New mass flux at dG/dp=0
  [Gn,id]=sort(G);          // Sort all values with largest first
  prn=pr(id);
  err = abs(Gn(1)-Gn(2));   // measure of error
  G=[]; G=Gn(1:3);          // reject the smallest mass flux
  pgs=[]; pr=[]; pr=prn(1:3);
  pgs=p0*pr;
  iter = iter + 1;
end

Gcr = G(1);    // Critical mass flux (kg/m2/s)
pcr = pgs(1);  // critical pressure (bar)
```

Using the HEM model for high pressure saturated water, the critical mass flux and the critical-to-stagnation pressure ratio can be calculated for various values of the stagnation pressures. The results are shown in FIGURE 5-3 and FIGURE 5-4, respectively.
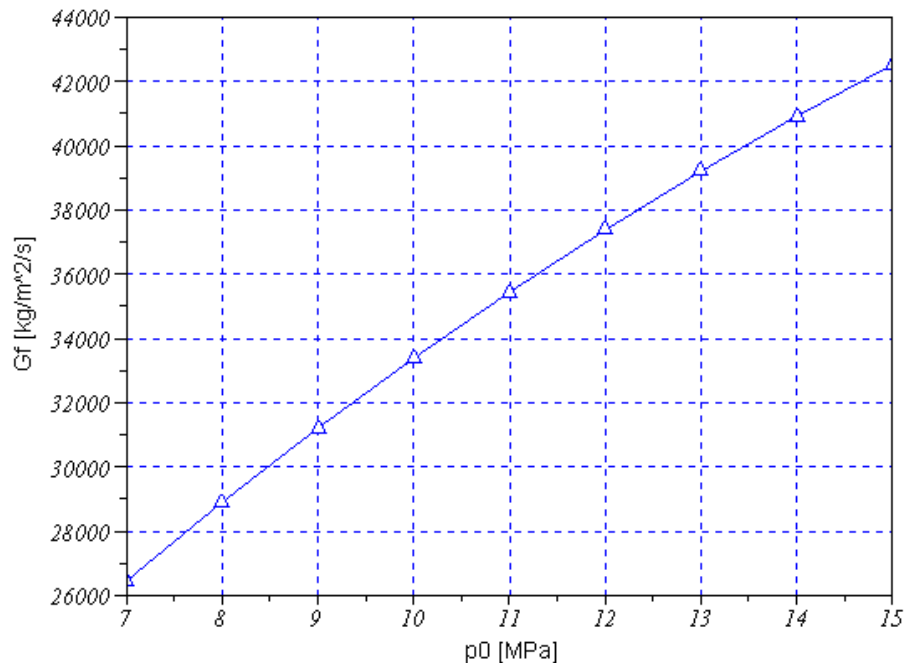
FIGURE 5-3. Critical mass flux of saturated water as a function of the stagnation pressure.
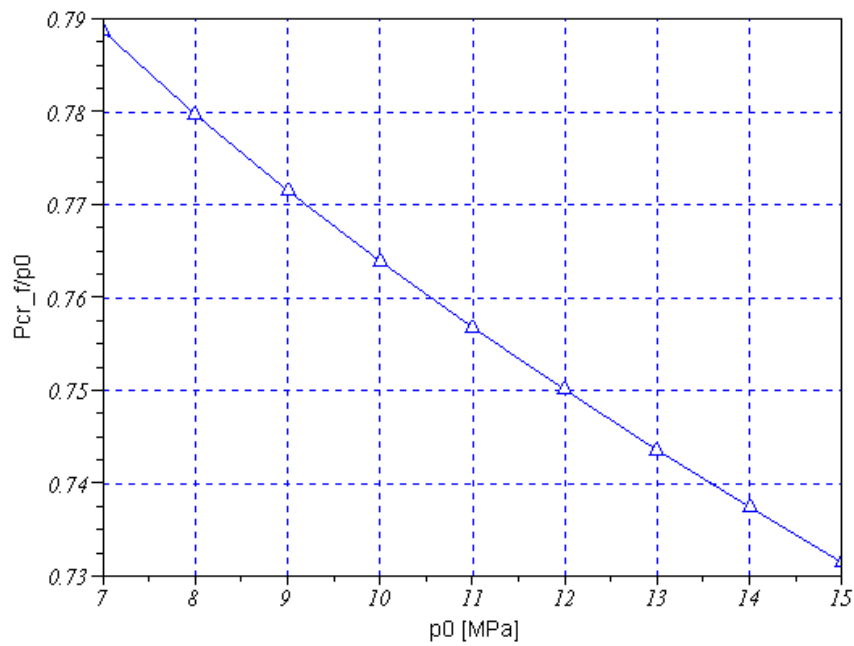
FIGURE 5-4. Critical-to-stagnation pressure ratio of saturated water as a function of the stagnation pressure.

If two-phase mixture of water and steam with quality x is considered, the critical mass flux and the critical-to-stagnation pressure ratio can be obtained from figures below.
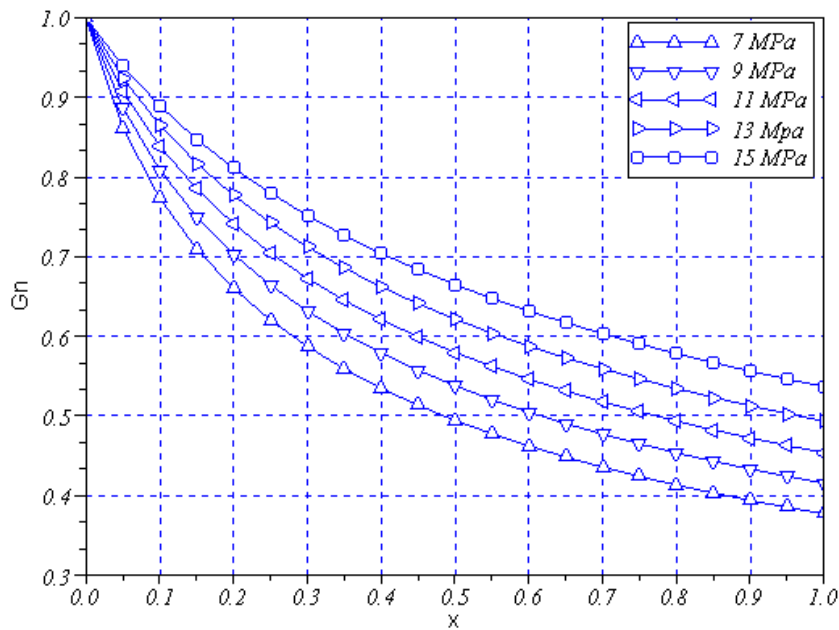
FIGURE 5-5. Ratio of mixture and saturated water critical mass flux as a function of quality x.
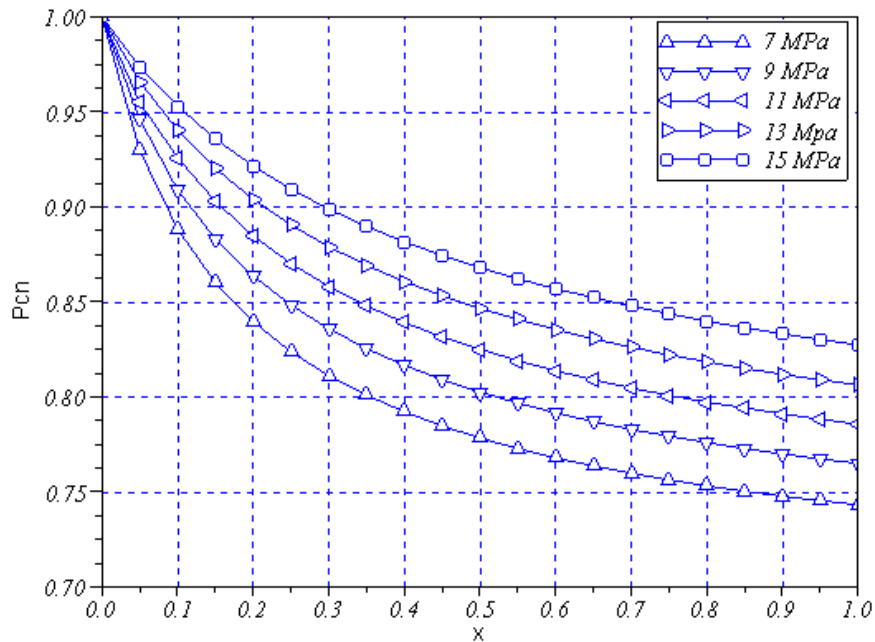
FIGURE 5-6. Ratio of mixture and saturated water critical pressure as a function of quality *x*.
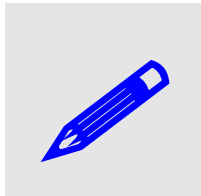
EXAMPLE 5-4. A pressure vessel is filled with a steam-water saturated mixture at 12 MPa pressure. The vessel has two nozzles: one located at the top and the other located at the bottom of the vessel. The nozzles are located in such a way that through the top nozzle only saturated steam is flowing, whereas through the bottom nozzle only saturated water is flowing. Calculate the mass flux and the critical pressure in each of the nozzles.

SOLUTION: Using FIGURE 5-3 the mass flux of saturated water at stagnation pressure 12 MPa is found equal to ~37500 kg/m².s. Using FIGURE 5-5 the critical mass flux of saturated vapour (p = 12 MPa and x = 1.0) is found as ~0.47*37500 = 17625 kg/m².s. Similarly, the critical pressure for saturated water is found from FIGURE 5-4 as ~0.75*12 = 9 MPa, whereas critical pressure for saturated steam is found from FIGURE 5-6 as ~0.80*9 = 7.2 MPa.

When both phases are far from the thermodynamic equilibrium, the HEM formulation cannot be applied. For such situations the **Homogeneous Frozen Flow model** is applicable. In this model it is assumed that:

- the velocities of the phases are equal,

- there is no heat or mass transfer between phases (phases are "frozen" at mass fractions existing at the stagnation conditions),

- the gas (or vapour) is modelled as perfect gas,

- the critical flow is defined from gas dynamics and determines the velocity.

Based on these assumptions, the critical mass flux is derived as,

$$(5\text{-}41) \quad G_* = \rho_* U_* = \frac{\left[2x_0 \frac{p_0}{\rho_{g0}} \left(\frac{\kappa}{\kappa + 1} \right) \right]^{1/2}}{\frac{(1 - x_0)}{\rho_{f0}} + \frac{x_0}{\rho_{g0}} \eta^{-1/\kappa}},$$

where,

$$(5\text{-}42) \quad \eta = \frac{p_*}{p_0} = \left(\frac{2}{\kappa + 1} \right)^{\frac{\kappa}{\kappa - 1}}.$$

The model is valid provided that the following inequality is satisfied,

$$(5\text{-}43) \quad \frac{1 - x_0}{\rho_{f0}} << \frac{x_0}{\rho_{g0}}.$$

Several prediction models for the critical two-phase flows have been published in the literature. Fauske carried out experiments with air-water and proposed the following model to calculate the critical flow,

$$(5\text{-}44) \quad G_* = \rho_m \sqrt{\left(\frac{\partial p}{\partial \rho_m} \right)_s},$$

where

$$\rho_m = \alpha \rho_g + (1 - \alpha) \rho_f,$$

$$\alpha = \frac{x}{x + \frac{\rho_g}{\rho_f} \cdot S \cdot (1 - x)},$$

$$S = 0.17 x^{0.18} \sqrt{\frac{\rho_f}{\rho_g}}.$$

Further, he assumed $x = const$, $\varrho_f = const$ and $\varrho_g = p/RT$.

Chisholm found good agreement with Fauske's experimental data if the critical flow is calculated as,

$$(5\text{-}45) \quad G_* = \sqrt{\frac{1.2 \rho_g p_{cr}}{x[x + (1 - x)/S^2]}},$$

where p_{cr} is the critical pressure in [Pa] and,

$$S = 1 + \left(4.46x^{0.18} - 1\right) \frac{\rho_f / \rho_g}{\left(\rho_f / \rho_g\right)_{p=1bar}}.$$

For the calculation of critical flow rates through tubes and nozzles with saturated liquid at inlet, Flinta et al. proposed the following correlation,

$$(5\text{-}46) \qquad G_* = 1400\left(p_s - 0.02\right)^{0.75},$$

where G_* is the critical mass flux in [kg.m^{-2}.s^{-1}] and p_s is the saturation pressure just upstream of the critical section in [bar].

5.2 Fluid-Structure Interactions

Fluid-structure interactions play important role in a safe operation of nuclear systems. Due to dynamic behaviour of fluids, they exert forces on submerged or surrounding structures.

The forces can be static; that is they do not change with time. These type of forces are encountered for example in fuel assemblies, where flowing coolant is exerting forces on the assembly structure, such as fuel rods, spacers or box walls. The magnitude of the forces must be known to avoid misplacements of the internal structures of the assembly.

Very often the forces exerted by fluid are time-dependent. The time-dependence can have either non-periodic or periodic character. The former may be created in a pipeline due to an external perturbation, such as activation of a pump or a sudden opening or closing of a valve. The later forces may be induced in a system due to periodicity in a flow, caused for example by detachments of vortices. If the frequency of the detachments coincides with the natural frequency of the structure, flow-induced vibrations may occur.

5.2.1 Static Reaction Forces

For open systems, that is for systems that have inlets and/or outlets, a general momentum conservation equation can be written as,

$$(5\text{-}47) \qquad \mathbf{F} = \frac{d}{dt}\int_V \rho\mathbf{v}dV + \int_A \mathbf{v}\rho\mathbf{v} \cdot d\mathbf{A}.$$

The first integral on the right-hand-side of the equation represents the storage of momentum in a system with volume V, filled with medium with density ρ and velocity $\mathbf{v}$. On the left-hand-side $\mathbf{F}$ represents the total force acting on the system, which typically includes contact forces such as due to pressure and shear, as well as body forces due to gravity. The second integral on the right hand side represents the momentum transport through inlets and outlets with total area A.

EXAMPLE 5-5. A free liquid jet with constant density, cross-section area and velocity moves over a vane as shown in the figure below. Calculate the reaction force exerted by liquid on the vane, assuming that the jet moves in the plane of the figure and neglecting friction and gravity forces.

SOLUTION: The pressure inside a free jet (not bounded by walls) is always the same as the ambient pressure. Thus both friction and pressure surface forces are equal to zero. Since gravity force is neglected and the case is steady-state, Eq. (5-47)

reduces to: $\mathbf{R} + \int\limits_A \mathbf{v}\rho\mathbf{v}\cdot d\mathbf{A} = 0$, where **R=-F** is the reaction force exerted by liquid on the vane.
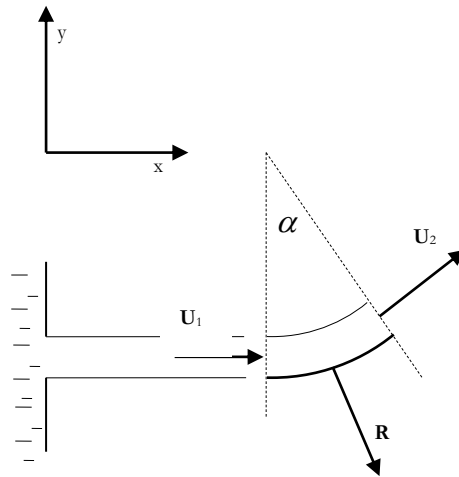
The components of the reaction force are readily obtained as:

$$R_x - \rho U_1^2 A_1 + \rho U_2^2 \cos\alpha A_2 = 0, \quad R_y + \rho U_2^2 \sin\alpha A_2 = 0.$$

Since $A_1 = A_2 = A$ and $U_1 = U_2 = U$, the total reaction force is obtained as:

$$R = \sqrt{R_x^2 + R_y^2} = \rho U^2 A \sqrt{2(1-\cos\alpha)}.$$

When flow in pipes is concerned, the pressure and velocity changes at inlets and outlets must be taken into account in Eq. (5-47). This aspect is taken into account in the following example.

EXAMPLE 5-6. Water at pressure 7 MPa, temperature 260 °C and mass flow rate W=30 kg.s^{-1} is flowing around a 75° bend, in which there is a contraction from 10 to 7.5 cm internal diameter. Calculate the force exerted on the bend assuming that the combined pressure loss due to friction and bend geometry is known and equal to 5 kPa. Neglect the gravity effects and assume constant water properties throughout the bend.

SOLUTION: The pressure difference between the inlet (section "1") and the outlet (section "2") can be found from the Bernoulli equation as follows,

$$\frac{\rho U_1^2}{2} + p_1 = \frac{\rho U_2^2}{2} + p_2 + \Delta p_{loss}$$

which yields the pressure difference,

$$p_1 - p_2 = \frac{\rho}{2}\left(U_2^2 - U_1^2\right) + \Delta p_{loss} = \frac{W^2}{2\rho A_1^2}\left[\left(\frac{A_1}{A_2}\right)^2 - 1\right] + \Delta p_{loss}$$

Substituting data and taking water density equal to 786.6 kg.m^{-3} yields,

$$p_1 - p_2 = \frac{30^2}{2\cdot 786.6\cdot 0.0078^2}\left[\left(\frac{10}{7.5}\right)^4 - 1\right] + 5000 = 25037\,\text{Pa}.$$

Applying Eq. (5-47) yields the following reaction components,

$$R_x - \rho U_1 A_1 U_1 + \rho U_2 A_2 U_2 \cos \alpha - p_1 A_1 + p_2 A_2 \cos \alpha = 0$$
$$R_y - \rho U_2 A_2 U_2 \sin \alpha - p_2 A_2 \sin \alpha = 0 \cdot$$

Both equations can be solved to obtain the reaction force R.

The dynamic form of Eq. (5-47) has to be used when calculating the reaction forces in a pipe with accelerating (or decelerating) fluid. This is typically the case when calculating the reaction forces during start-up of a pump connected to a pipeline.

5.2.2 Hydraulic Transients in Elastic Channels

Pressure fluctuations in closed channels (particularly in pipelines) have been investigated for many years since they may cause failures of various engineering systems. In the past the perturbations were frequently termed as **waterhammer**, oilhammer or steamhammer. Today, however, the term "hydraulic transients" is used more frequently.

Assume that liquid of density ρ is flowing in a rigid uniform pipe with local velocity U and pressure p, which are suddenly disturbed to $U + \lrcorner U$ and $p + \lrcorner p$, and the fluid density becomes $\varrho + \lrcorner \varrho$. FIGURE 5-7 depicts the propagation of the perturbation in both directions in the pipe with speeds relative to the pipe c_L in the left direction and c_R in the right direction.

Neglecting storage and friction terms, the momentum conservation equation formulated for control volumes surrounding each discontinuity are as follows,

$$W\Delta U = \begin{cases} -A\Delta p & \text{leftward} \\ A\Delta p & \text{rightward} \end{cases}$$
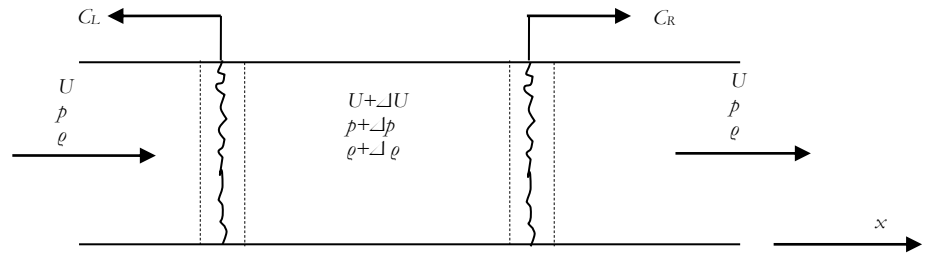
FIGURE 5-7. Propagation of a disturbance in a pipe.

Since the mass flow rates W in the left and right control volume are $\rho(c_L + U)A$ and $\rho(c_R - U)A$, respectively, the pressure disturbance is given as,

$$(5\text{-}48) \qquad \Delta p = \begin{cases} -\rho(c_L + U)\Delta U & \text{leftward} \\ \rho(c_R - U)\Delta U & \text{rightward} \end{cases} \cdot$$

Thus, if the velocity perturbation is known, the corresponding pressure perturbation can be found from Eq. (5-48), and vice versa.

Considering only the control volume moving to the right (in the positive x-direction) and assuming that $c_R = c$, the control volume mass balance is as follows,

$$\rho A(c - U) = (\rho + \Delta\rho)A(c - U - \Delta U).$$

Simplifying the equation and neglecting products of perturbations yields,

$$\Delta U = \Delta\rho \frac{c - U}{\rho}.$$

Since for most cases flow velocity is much smaller than the disturbance propagation speed, the relationship between the velocity and density perturbation can be written as follows,

$$(5\text{-}49) \qquad \Delta U = \Delta\rho \frac{c}{\rho}.$$

Combining Eq. (5-49) with (5-48) yields,

$$c^2 = \frac{\Delta p}{\Delta\rho} = \frac{\Delta p}{\Delta\rho/\rho}\frac{1}{\rho} = \frac{K}{\rho},$$

where,

$$(5\text{-}50) \qquad K = \frac{\Delta p}{\Delta\rho/\rho},$$

is the bulk modulus of elasticity of a fluid, and c is referred to as the **waterhammer or wave velocity**, and is calculated as,

$$(5\text{-}51) \qquad c = \sqrt{\frac{K}{\rho}}.$$

It should be recalled that the wave velocity in Eq. (5-51) is valid for flow of compressible fluid in a rigid pipe. The influence of pipe elasticity on the wave velocity will be discussed below.

> EXAMPLE 5-7. Water at pressure 7 MPa and temperature 260 °C is flowing at rate $W = 3000$ kg.s^{-1} in a pipe with diameter 0.5 m . Determine the pressure rise if the flow is instantaneously stopped at the downstream end by closing a valve. The water density is 786.6 kg.m^{-3} and the bulk modulus of elasticity K = 6.23•10^8.
> SOLUTION:
> $$A = \frac{\pi \cdot 0.5^2}{4} = 0.1963 \, \text{m}^2, \quad U = W/\rho A = 3000/786.6 \cdot 0.1963 = 19.4 \, \text{m} \cdot \text{s}^{-1}$$
> $$c = \sqrt{K/\rho} = \sqrt{6.23 \cdot 10^8/786.6} = 890 \, \text{m.s}^{-1}, \quad \Delta p = \rho c \Delta U = 786.6 \cdot 890 \cdot 19.4 = 13.6 \cdot 10^6 \, \text{Pa}.$$

When pipe walls are elastic, the dynamic pressure waves are propagating both in fluid and in the conduit walls. To investigate such phenomenon, it is necessary to take into consideration the transient behaviour of the conduit cross-section area. The transient,

one-dimensional continuity equation in a pipe with variable cross-section area can be written as follows,

$$(5\text{-}52) \qquad \frac{\partial(\rho A)}{\partial t} + \frac{\partial(\rho A U)}{\partial x} = 0.$$

Expanding the terms in parentheses yields,

$$A\frac{\partial \rho}{\partial t} + \rho\frac{\partial A}{\partial t} + AU\frac{\partial \rho}{\partial x} + \rho A\frac{\partial U}{\partial x} + \rho U\frac{\partial A}{\partial x} = 0.$$

Since total derivatives are given as,

$$\frac{\partial \rho}{\partial t} + U\frac{\partial \rho}{\partial x} = \frac{d\rho}{dt} \text{, and } \frac{\partial A}{\partial t} + U\frac{\partial A}{\partial x} = \frac{dA}{dt},$$

The continuity equation becomes,

$$A\frac{d\rho}{dt} + \rho A\frac{\partial U}{\partial x} + \rho\frac{dA}{dt} = 0,$$

or,

$$(5\text{-}53) \qquad \frac{1}{\rho}\frac{d\rho}{dt} + \frac{1}{A}\frac{dA}{dt} + \frac{\partial U}{\partial x} = 0.$$

At this point it is desirable to express the time derivative of the cross-section area in terms of pressure, since pressure changes will cause the changes of the cross-section area. Using the linear elasticity model for a circular pipe subject to internal pressure, the strain-stress relationship can be written as,

$$(5\text{-}54) \qquad \varepsilon = \frac{\sigma_2 - \nu\sigma_1}{E},$$

where,

$\quad\quad\quad \varepsilon \quad\quad$ - hoop strain,

$\quad\quad\quad \sigma_1 \quad\quad$ - axial stress,

$\quad\quad\quad \sigma_2 \quad\quad$ - hoop stress,

$\quad\quad\quad \nu \quad\quad$ - Poisson's ratio

$\quad\quad\quad E \quad\quad$ - Young's modulus.

If the pipeline has expansion joints throughout its length to relax the axial stresses, relationship (5-54) is simplified as,

(5-55) $\qquad \varepsilon = \dfrac{\sigma_2}{E}.$

The hoop stress in a thin-walled pipe having internal pressure p is,

$$\sigma_2 = \frac{pD}{2\delta}$$

where,

$\qquad D \qquad$ - pipe internal diameter,

$\qquad \delta \qquad$ - pipe wall thickness.

The time derivative of the hoop stress can be expresses as,

(5-56) $\qquad \dfrac{d\sigma_2}{dt} = \dfrac{d}{dt}\left(\dfrac{pD}{2\delta}\right) = \dfrac{p}{2\delta}\dfrac{dD}{dt} + \dfrac{D}{2\delta}\dfrac{dp}{dt}.$

Combining Eqs. (5-55) and (5-56) yields,

$$E\frac{d\varepsilon}{dt} = \frac{p}{2\delta}\frac{dD}{dt} + \frac{D}{2\delta}\frac{dp}{dt}.$$

Since,

(5-57) $\qquad \dfrac{dD}{dt} = D\dfrac{d\varepsilon}{dt},$

the time-derivative of the strain can be found as,

(5-58) $\qquad \dfrac{d\varepsilon}{dt} = \dfrac{\dfrac{D}{2\delta}\dfrac{dp}{dt}}{E - \dfrac{pD}{2\delta}}.$

It remains now to express the time derivative of the cross-section area in terms of the strain. It can be done as follows,

$$\frac{1}{A}\frac{dA}{dt} = \frac{1}{\dfrac{\pi D^2}{4}}\frac{d\left(\dfrac{\pi D^2}{4}\right)}{dt} = \frac{1}{D^2}2D\frac{dD}{dt} = 2\frac{d\varepsilon}{dt}.$$

Or, using Eq. (5-58),

$$(5\text{-}59) \quad \frac{1}{A}\frac{dA}{dt} = \frac{2D}{2\delta E - pD} \cdot \frac{dp}{dt} .$$

The first term in Eq. (5-53) can be expressed in terms of pressure time derivative as,

$$(5\text{-}60) \quad \frac{1}{\rho}\frac{d\rho}{dt} = \frac{1}{\rho}\frac{d\rho}{dp}\frac{dp}{dt} = \frac{1}{\rho}\frac{1}{\dfrac{dp}{d\rho}}\frac{dp}{dt} = \frac{1}{\dfrac{dp}{d\rho/\rho}}\frac{dp}{dt} = \frac{1}{K}\frac{dp}{dt} .$$

Combining Eqs. (5-53), (5-59) and (5-60) yields,

$$(5\text{-}61) \quad \left(\frac{1}{K} + \frac{2D}{2\delta E - pD}\right) \cdot \frac{dp}{dt} + \frac{\partial U}{\partial x} = 0 .$$

Defining,

$$(5\text{-}62) \quad \frac{1}{\left(\dfrac{1}{K} + \dfrac{2D}{2\delta E - pD}\right)\rho} = \frac{K}{\left(1 + \dfrac{K}{E}\dfrac{2D}{2\delta - pD/E}\right)\rho} = c^2 ,$$

and expanding the total derivative of pressure gives,

$$(5\text{-}63) \quad \frac{\partial p}{\partial t} + U\frac{\partial p}{\partial x} + \rho c^2 \frac{\partial U}{\partial x} = 0 .$$

This is the continuity equation for fluid flowing in an elastic conduit. As can be shown, c in Eq. (5-63) is the speed with which waves travel in an elastic conduit. The value given by Eq. (5-63) is valid for thin-walled pipes with expanding joints to relax the axial stresses. For other types of supports and conduits a proper expression for the wave speed must be used.

Halliwell[5-2] proposed the following general expression for the waterhammer wave speed,

$$(5\text{-}64) \quad c^2 = \frac{K}{\left(1 + \dfrac{K}{E}\psi\right)\rho} ,$$

where ψ depends on the type of conduit and supports. For most typical cases the parameter is as follows:

Rigid conduits,

$$\psi = 0 .$$

Thick-walled elastic pipe, anchored against longitudinal movement throughout its length,

$$(5\text{-}65) \quad \psi = 2(1+v)\left(\frac{R_o^2 + R_i^2}{R_o^2 - R_i^2} - \frac{2vR_i^2}{R_o^2 - R_i^2}\right).$$

Here:

v - Poisson's ratio

R_o, R_i - pipe outer and inner radius, respectively.

Thick-walled elastic pipe, with frequent expansion joints,

$$(5\text{-}66) \quad \psi = 2\left(\frac{R_o^2 + R_i^2}{R_o^2 - R_i^2} + v\right)$$

Thin-walled elastic pipe, anchored against longitudinal movements throughout its length,

$$(5\text{-}67) \quad \psi = \frac{D}{\delta}(1 - v^2),$$

where,

D - pipe inner diameter,

δ - wall thickness.

Thin-walled elastic pipe with frequent expansion joints,

$$(5\text{-}68) \quad \psi = \frac{2D}{2\delta - pD/E} \approx \frac{D}{\delta} \text{ (Since in most cases } 2\delta \gg pD/E \text{)}.$$

Eq. (5-63) cannot be solved since it contains two unknowns: pressure and flow velocity. To close the system, the momentum equation must be formulated as follows,

$$(5\text{-}69) \quad \frac{\partial U}{\partial t} + U\frac{\partial U}{\partial x} + \frac{1}{\rho}\frac{\partial p}{\partial x} + g\sin\theta + \frac{2C_f U|U|}{D} = 0,$$

where, in addition to recently mentioned variables,

g - acceleration of gravity

θ - inclination angle of the conduit

C_f - Fanning friction factor.

Equations (5-63) and (5-69) constitute a solvable system of equations, provided proper initial and boundary conditions are given. The equations can be written in a matrix form as follows,

$$(5\text{-}70) \qquad \frac{\partial \mathbf{y}}{\partial t} + \mathbf{b}\frac{\partial \mathbf{y}}{\partial x} = \mathbf{f}\,,$$

where,

$$(5\text{-}71) \qquad \mathbf{y} = \begin{bmatrix} p \\ U \end{bmatrix}, \qquad \mathbf{b} = \begin{bmatrix} U & \rho c^2 \\ \dfrac{1}{\rho} & U \end{bmatrix}, \qquad \mathbf{f} = \begin{bmatrix} 0 \\ -g\sin\theta - \dfrac{2C_f U|U|}{D} \end{bmatrix}.$$

The eigenvalues of matrix $\mathbf{b}$ determine the type of set of equations. The eigenvalues , λ , can be found from the characteristic equation as follows,

$$(5\text{-}72) \qquad \begin{vmatrix} U - \lambda & \rho c^2 \\ \dfrac{1}{\rho} & U - \lambda \end{vmatrix} = 0 \Rightarrow \lambda = U \pm c\,.$$

As can be seen both eigenvalues are real and distinct, thus Eq. (5-70) represents a set of hyperbolic partial differential equations that describes a phenomenon of the wave propagation.

Solution of the equations can be obtained using various numerical methods, for example the method of characteristics.
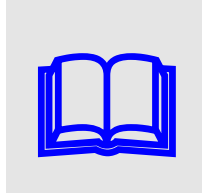
MORE READING: For interested readers books by Chaudhry (*Applied Hydraulic Transients*, 2nd edition, Van Nostrand Reinhold Company, New York, 1987) and Moody (*Introduction to Unsteady Thermofluid Mechanics*, John Wiley & Sons, New York, 1990) are recommended. The books are dealing with calculation of transients in conduits and the method of characteristics is one of the solution methods described in great detail.

The set of equations can be further simplified by dropping small terms, such as $U(\partial p/\partial x)$ and $U(\partial U/\partial x)$ as well as the gravity term, which disappears for horizontal pipelines. The resultant simplified set of equations is as follows,

$$(5\text{-}73) \qquad \frac{\partial p}{\partial t} + \rho c^2 \frac{\partial U}{\partial x} = 0,$$

$$(5\text{-}74) \qquad \frac{\partial U}{\partial t} + \frac{1}{\rho}\frac{\partial p}{\partial x} + \frac{2C_f U|U|}{D} = 0\,.$$

Further assuming negligible wall friction and uniform cross-section area of the channel, the equations can be combined, by eliminating either p or U,

$$\frac{\partial^2 p}{\partial t^2} + \rho c^2 \frac{\partial^2 U}{\partial x \partial t} = 0 \quad \text{and} \quad \frac{\partial^2 U}{\partial t \partial x} + \frac{1}{\rho}\frac{\partial^2 p}{\partial x^2} = 0,$$

yields,

$$(5\text{-}75) \quad \frac{\partial^2 p}{\partial t^2} - c^2 \frac{\partial^2 p}{\partial x^2} = 0,$$

or, if p is eliminated,

$$(5\text{-}76) \quad \frac{\partial^2 U}{\partial t^2} - c^2 \frac{\partial^2 U}{\partial x^2} = 0.$$

Eqs. (5-75) and (5-76) are linear hyperbolic partial differential equations describing the wave propagation phenomenon. A general solution of such equation can be sought in the following form (taking velocity as an example),

$$U = Ae^{\alpha t + \beta x}, \text{ with } \frac{\partial^2 U}{\partial t^2} = A\alpha^2 e^{\alpha t + \beta x} \text{ and } \frac{\partial^2 U}{\partial x^2} = A\beta^2 e^{\alpha t + \beta x}$$

where A, α, β are constants to be determined. Substituting into Eq. (5-76) yields,

$\alpha^2 - c^2 \beta^2 = 0$, and $\beta = \pm \dfrac{\alpha}{c}$. Thus, the general solution has the following form,

$$(5\text{-}77) \quad U = Ae^{\alpha(t \pm x/c)}.$$

Actually expression (5-77) represents two solutions: one for the "-" sign and the other for the "+" sign. Both solutions satisfy Eq. (5-76), and since the equation is linear, their sum satisfies the equation as well. Since many values of A and α will be obtained to satisfy the initial and boundary conditions, the general solution will be as follows,

$$(5\text{-}78) \quad U(x,t) = \sum_{n=0}^{\infty} A_n e^{\alpha_n(t+x/c)} + \sum_{n=0}^{\infty} A_n e^{\alpha_n(t-x/c)}.$$

The form of the general solution suggests that it can be written as,

$$(5\text{-}79) \quad U(x,t) = F_L(t + x/c) + F_R(t - x/c),$$

where F_L and F_R are arbitrary, twice differentiable functions.

Functions F_L and F_R have an interesting feature: they are constant along lines,

$t + x/c = const$, and $t - x/c = const$.

These lines are known as characteristics of the given differential equation.

5.2.3 Flow-Induced Vibrations

Unlike transients in elastic conduits considered in the previous section, flow induced vibrations may occur without any external perturbation, such as for example a closure of a valve or start-up of a pump. Such vibrations are induced by flow itself and are persistent, typically periodic, in time.

The most common cause of flow induced vibrations is vortex shedding in a flow past a submerged body. An example is a **von Kármán vortex street**, which is a repeating pattern of swirling vortices generated by the unsteady separation of flow over bluff bodies (see FIGURE 5-8).

For long circular cylinder the frequency of vortex shedding is given by the following empirical formula,

$$(5\text{-}80) \quad St = 0.198\left(1 - \frac{19.7}{Re}\right), \quad \text{for} \quad 250 < Re < 2 \cdot 10^5$$

where,

$$St = \frac{fD}{U} \qquad \text{- \textbf{Strouhal number}},$$

$$Re = \frac{UD}{\nu} \qquad \text{- Reynolds number},$$

f - vortex shedding frequency, 1/s,

D - cylinder diameter,

U - flow velocity,

ν - fluid viscosity.
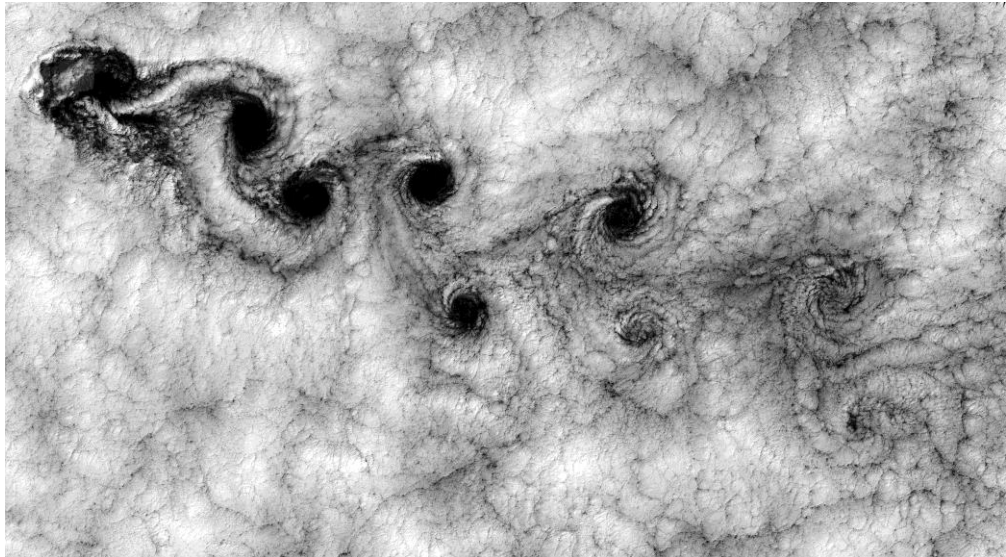
FIGURE 5-8. Von Karman vortex street off the Chilean cost near the Juan Fernandez Island (from Wikipedia Commons).

A simple example of a system that can be susceptible to flow-induced vibrations is shown in FIGURE 5-9.
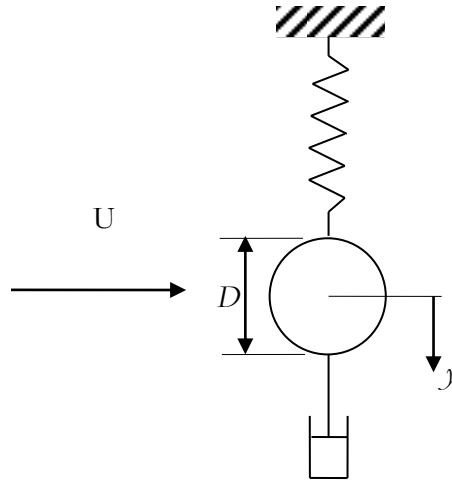
FIGURE 5-9. Oscillation of a cylinder.

A free-vibration system with mass m and spring constant k is governed by the following equation,

(5-81) $\qquad m\ddot{y} + \beta\dot{y} + ky = 0$, $\beta \geq 0$.

The motion will be periodic if $\beta < \beta_{cr}$ and aperiodic if $\beta > \beta_{cr}$, where the critical damping β_{cr} is given by,

(5-82) $\qquad \beta_{cr} = 2\sqrt{mk} = 2m\omega_0$.

Here $\omega_0 = \sqrt{k/m}$ is the frequency (radians per second) of the system without damping. Writing β as $\gamma\beta_{cr}$, the equation of motion can be written as,

(5-83) $\qquad \ddot{y} + \gamma\beta_{cr}\dot{y} + \omega_0^2 y = 0$.

The equation of motion of the cylinder in a flow is then,

(5-84) $\qquad \ddot{y} + \gamma\beta_{cr}\dot{y} + \omega_0^2 y = \dfrac{1}{m}F(t)$,

where $F(t)$ is the hydrodynamic force per unit length acting on the cylinder, and y is the transverse displacement. The lift force consists of the hydrodynamic force acting on the cylinder due to shedding of vortices and the added (or virtual) mass force of the fluid surrounding the cylinder. This force is equal to,

(5-85) $\qquad F_A = \rho\dfrac{\pi D^2}{4}\ddot{y} = m_A\ddot{y}$,

where ρ is the density of the fluid and m_A is referred to as the added (or virtual) mass.

The hydrodynamic lift force can be in general written as,

(5-86) $F_L = \dfrac{1}{2}\rho U^2 C_L D$,

where the force is expressed per unit length of the cylinder.

The lift force coefficient C_L excited by vortex shedding can be written in the complex for

(5-87) $C_L = C_{L0}e^{i\omega t}$,

where ω is the frequency (radians per second) of the vortices on each side of the cylinder.

Thus the equation of motion becomes,

(5-88) $\ddot{y} + \gamma\beta_{cr}\dot{y} + \omega_0^2 y = \dfrac{1}{2(m+m_A)}\rho U^2 D C_{L0}e^{i\omega t}$.

The solution to this equation can be found as,

(5-89) $y(t) = Ae^{i(\omega t-\varphi)}$.

Here,

(5-90) $A = \dfrac{\rho D C_{L0}}{2(m+m_A)\omega_0^2}\dfrac{U^2}{\left[\left(1-\Omega^2\right)^2+\left(2\gamma\Omega\right)^2\right]^{1/2}}$,

(5-91) $\Omega = \dfrac{\omega}{\omega_0} = \dfrac{\text{forcing frequency}}{\text{undumped natural frequency}}$,

(5-92) $\varphi = \arctan\left(\dfrac{2\gamma\Omega}{1-\Omega^2}\right)$.

This relatively simple analysis leads to an expression for the amplitude of oscillations given in terms of the velocity U. Plotting this relationship (see EXERCISE 5-5) reveals that the maximum amplitude is obtained when $\Omega \approx 1$, that is when the frequency of shedding vortices agrees with the natural frequency of the structure.

This simple criterion for resonance conditions was believed to be valid for many practically existing structures. However, recent results indicated that this is not always the case and the resonance (flow-induced vibrations) can occur even for shedding

frequencies that are far from the natural frequency. Below a more sophisticated analysis of flow-induced vibrations is shown.

If the submerged body is idealized as mass point connected to a spring, its motion to an external force **F**(t) is described by an ordinary differential equation as follows,

$$(5\text{-}93) \quad m\ddot{\mathbf{y}} + c\dot{\mathbf{y}} + k\mathbf{y} = \mathbf{F}(t),$$

where,

$\ddot{\mathbf{y}}, \dot{\mathbf{y}}, \mathbf{y}$ - body acceleration, velocity and displacement, respectively,

k - spring constant,

c - damping,

$\mathbf{F}(t)$ - fluid force.

When body oscillation frequency is coinciding with the periodic vortex wake mode, a good approximation to the force $F(t)$ and the response $y(t)$ is,

$$(5\text{-}94) \quad F(t) = |\mathbf{F}(t)| = F_0 \sin(\omega t + \phi),$$

$$(5\text{-}95) \quad y(t) = |\mathbf{y}(t)| = y_0 \sin(\omega t),$$

where,

$$\omega = 2\pi f, \text{ and } f \text{ is the body oscillation frequency.}$$

The response amplitude and frequency may be derived from Eqs. (5-93) through (5-95), where the influence of added mass (added mass is the mass of fluid that is accelerated with the cylinder) has to be taken into account. Khalak and Williamson (1999) obtained,

$$(5\text{-}96) \quad A^* = \frac{1}{4\pi^3} \frac{C_Y \sin\phi}{(m^* + C_A)\zeta} \left(\frac{U^*}{f^*}\right)^2 f^*$$

$$(5\text{-}97) \quad f^* = \sqrt{\frac{m^* + C_A}{m^* + C_{AE}}}$$

where,

C_A - potential added mass coefficient equal to 1,

$C_{AE} = \dfrac{1}{2\pi^3} \dfrac{C_Y \cos\phi}{A^*} \left(\dfrac{U^*}{f^*}\right)^2$ is an "effective" added mass coefficient

$$m^* = \frac{m}{\pi \rho D^2 L / 4} \qquad \text{- mass ratio,}$$

$$\varsigma = \frac{c}{2\sqrt{k(m + m_A)}} \qquad \text{- damping ratio,}$$

$$U^* = \frac{U}{f_N D} \qquad \text{- velocity ratio,}$$

$$A^* = \frac{y_0}{D} \qquad \text{- amplitude ratio,}$$

$$f^* = \frac{f}{f_N} \qquad \text{- frequency ratio,}$$

$$C_X = \frac{F_X}{\frac{1}{2}\rho U^2 DL} \qquad \text{- streamwise force coefficient,}$$

$$C_Y = \frac{F_Y}{\frac{1}{2}\rho U^2 DL} \qquad \text{- transverse force coefficient,}$$

$$f_N \qquad\qquad\qquad \text{- natural frequency in still water,}$$

$$f \qquad\qquad\qquad \text{- actual body oscillation frequency,}$$

$$m_A = C_A m_d \qquad \text{- added mass,}$$

$$m_d = \pi \rho D^2 L / 4 \qquad \text{- displaced mass of fluid,}$$

$$L \qquad\qquad\qquad \text{- cylinder length.}$$

The theory presented in this section is valid for an idealized case of a single cylinder submerged in fluid. For more complex cases with many submerged objects (such as nuclear fuel assembly with spacers) with arbitrary shapes, proper numerical approaches have to be used. Typical numerical scheme employs a coupled system of fluid-dynamic and structure dynamic codes, which solve simultaneously the two domains, which are coupled through the fluid-solid interface.

5.2.4　Conjugate Heat Transfer

Heat transfer between a solid body and an adjacent fluid is typically described with the boundary condition of the third kind, which states that the heat flux on the solid surface is proportional to the difference of the solid surface temperature, T_n, and the fluid characteristic temperature, T_∞, with a certain proportionality factor known as the heat transfer coefficient. This relationship, known as the Newton equation of cooling, can be written as,

(5-98) $q'' = h(T_w - T_\infty)$.

The heat transfer coefficient h can be determined both theoretically (e.g. by solving the boundary layer equations) and experimentally. In the theoretical analysis it is usually assumed that the conditions at the solid surface are known and are constant. Thanks to this assumption the analysis is radically simplified.

However, in many practical applications the wall temperature cannot be considered as constant. For example, in the vicinity of the critical heat flux a significant non-uniformity of the wall temperature can be expected due to the dramatic change of the heat transfer coefficient. In case of non-uniform and/or non-stationary distribution of the wall temperature, Eq. (5-98) is in general not valid. In such circumstances the heat transfer in fluid and the heat conduction in the solid have to be considered simultaneously, leading to the so-called conjugate-heat transfer problem.

A solution of the conjugate heat transfer problem is not a simple task since it requires a solution of sets of partial differential equations which have different forms in different regions. Once treated analytically, the most practical approach to solve the conjugate heat transfer problem is to introduce an unknown function on the solid-fluid interface that represents either the temperature or the heat flux. In that way the heat transfer problem can be separately solved in each of the domains. The unknown function is further established from the compatibility condition.

Once solving the problem of the convective heat transfer, boundary conditions of the third kind should be replaced with boundary conditions of the fourth kind,

(5-99) $-\lambda_f \nabla T_f \cdot \mathbf{n}_w \big|_w = -\lambda_s \nabla T \cdot \mathbf{n}_{ws} \big|_w + q''_w; \ \ T_f \big|_w = T_s \big|_w,$

where q''_w is a source of heat per unit surface area and $\mathbf{n}_w$ is a unit vector normal to the wall surface. The conjugation condition for convective heat transfer along a plate with thickness b and at location x along the plate can be evaluated from the following local conjugation number,

(5-100) $B_x = \dfrac{\lambda_f b}{\lambda_s x} \mathrm{Re}_x^n \mathrm{Pr}^m$.

Here Re_x is the flow Reynolds number based on the characteristic length x and Pr is the Prandtl number, whereas m and n are constants. If the value of the conjugation number is low, say,

(5-101) $B_x < B_{x,\min}$,

then there is no conjugation between the fluid and solid domains and the solutions in each of the domains can be found separately. The minimum value of the conjugation number, $B_{x,min}$ can be found from an approximate analysis and assuming the required accuracy of the solution. For example, accepting 5% error in prediction of the wall temperature during the laminar convective heat transfer to a flat plate, the conjugation number should not exceed 0.1, that is, $B_{x,min} = 0.1$.

An approximate solution of the laminar convective heat transfer to a plate yields,

$$(5\text{-}102) \quad N = \frac{Nu_x}{Nu_{x0}} = 1 + \left(\frac{13}{14}\right)^{1/3}\left[A + \varphi(x) - \left(\frac{14}{13}\right)^{1/3}\right],$$

where Nu_{x0} is the Nusselt number for the classical problem,

$$(5\text{-}103) \quad Nu_{x0} = \frac{3}{2}\frac{x}{\delta}\sqrt[3]{\frac{14}{13}\mathrm{Pr}},$$

Nu_x is the Nusselt number for the conjugate problem,

$$(5\text{-}104) \quad Nu_x = \frac{3}{2}\frac{x}{\delta}\mathrm{Pr}^{1/3}[A + \varphi(x)].$$

Here A is a constant and $\varphi(x)$ is a small-value function, such as $\varphi^2(x) \approx 0$.

A qualitative analysis suggests that for practical calculations the following relationship can be used,

$$(5\text{-}105) \quad N = 1 + C \cdot B^m,$$

where C and m are constants that need to be determined either from theory or from experiments.

5.2.5 Thermal Fatigue

Temperature oscillations that occur in fluids due to turbulent mixing of two streams with different temperatures may lead to the thermal fatigue in the adjacent solid body. This is due to a propagation of temperature waves, which, in turn, cause thermal stresses in the solid body.

Analytical solution of the temperature waves in half-infinite body is given as,

$$(5\text{-}106) \quad T(x,t) = T_{wm} + \Delta T_{wa}\,e^{-\sqrt{\frac{\omega}{2a}}x}\cos\left(\omega t - \sqrt{\frac{\omega}{2a}}x\right).$$

Here T_{wm} is the mean temperature of the body surface and ΔT_{wa} is the amplitude of oscillations; ω - is the frequency of oscillations, a is the thermal diffusivity, x is the distance from the body surface and t is time. The amplitudes of the temperature waves in stainless steel 316 ($a = 4.075\ 10^{-6}$ m^2/s) for various frequencies of temperature oscillations at the body surface are shown in FIGURE 5-10.

As can be seen, the wave amplitude decreases with the distance, however, the low-frequency waves have still substantial amplitude at a distance of 1 cm, whereas the high frequency waves are damped already at a few-millimetre distance from the body surface. This picture suggests that the low-frequency temperature oscillations are of

greater concern in terms of thermal fatigue, since they affect large portions of the solid body.

Thermal fatigue is of great concern in nuclear power plants. Until very recently it was believed that only the solid surface was affected by the temperature oscillations, leading to a so-called "elephant-skin" type of damage. The growth of possible cracks was believed to be arrested at 1 to 2 mm depth. However, the event in the Civeaux nuclear power plant in May 1998 indicated that a considerable crack (180 mm long and penetrating the whole thickness of the elbow wall) can appear during a relatively short period of time (less than 1500 hours), if some special conditions prevail. Analyses that followed the Civeaux event lead to a conclusion that mixing of two streams with large temperature difference may lead to low-frequency oscillations of wall temperatures, which may cause deep cracks. This indicates that transient fluid flow analyses are necessary to assess the risks of the occurrence of the thermal fatigue. Such analyses are very difficult and can be only performed using advanced CFD approaches.
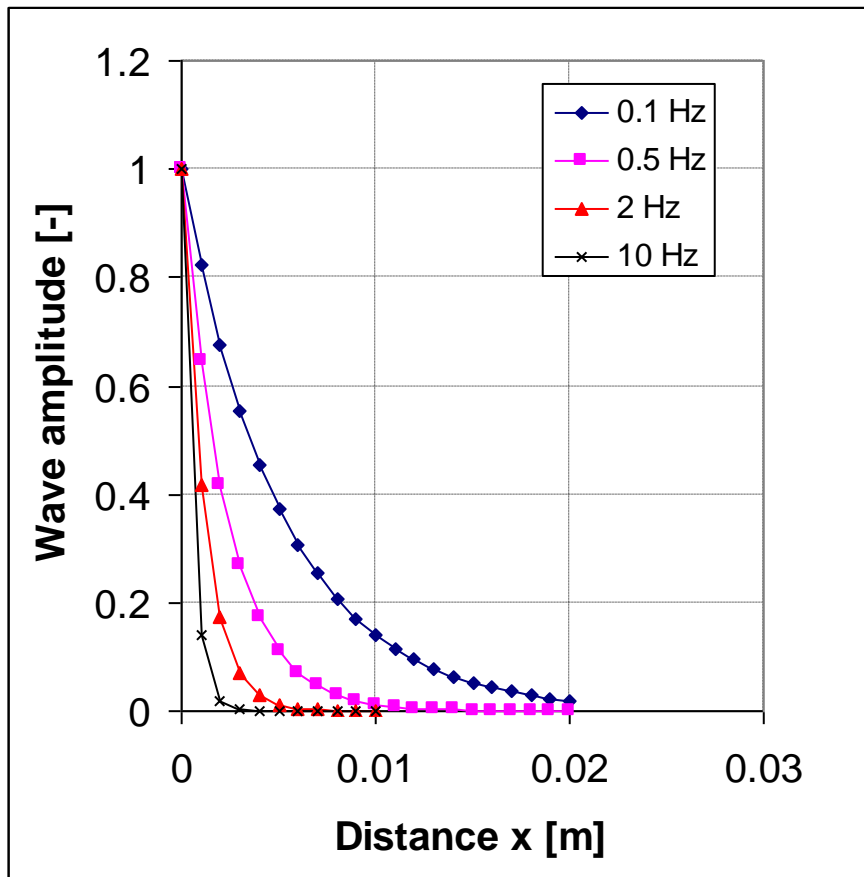
FIGURE 5-10. Temperature wave amplitude versus distance for various frequencies in stainless steel 316 ($a = 4.075 \cdot 10^{-6}$ m²/s).

5.3 Plant Components

The thermal-hydraulic behaviour of selected components of nuclear power plants is described in this section.

5.3.1 Pipelines and Valves

Pipelines and valves can be treated as insulated systems that do not perform any work. Applying the first principle of thermodynamics to such systems yields,

$$(5\text{-}107)\ \ I_2 - I_1 = Q_{1,2} - L_{t1,2} = 0\,.$$

Since at steady-state conditions the inflow and outflow mass flow rates are equal, the specific enthalpy of the fluid flowing through valves and pipelines is constant and the flow is isenthalpic.

Thus, working fluid that passes through valves and insulated pipelines preserves its enthalpy, irrespective of how big the pressure losses are.
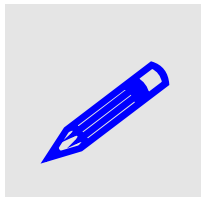
EXAMPLE 5-8. Calculate steam temperature and quality, if it passes through a valve with the total pressure drop equal to 0.1 MPa. Perform calculations for two cases: (a) upstream saturated steam is at pressure equal to 2.5 MPa; (b) upstream saturated steam is at pressure equal to 7 MPa. SOLUTION: Case (a): the upstream steam enthalpy is $i = 2802$ kJ/kg. The downstream temperature is found from tables using pressure 2.4 MPa and enthalpy equal to 2802 kJ/kg: $T_d = 221.95$ °C. Since the saturation temperature at the downstream pressure is equal to $T_s = 221.80$ °C, the steam is slightly superheated. The thermodynamic equilibrium quality is obtained as $x_e = (i\text{-}i_f)/i_{fg} = 1.000274$. Case (b): similar calculations indicate that the steam is wet. Its temperature is equal to the saturation temperature at 6.9 MPa equal to $T = 284.86$ °C, and its quality is equal to $x_e = 0.999145$

The above example shows that steam can be either superheated or get moisture due to pressure loss in valves or piping. The outcome depends on the upstream pressure and for pressures higher the approximately 3.5 MPa steam will become wet after isenthalpic pressure losses, whereas it will become superheated for lower pressures.

5.3.2 Heat Exchangers

The purpose of a heat exchanger is to transfer heat between two fluids without mixing. From the technical point of view, there are three most common heat exchanger designs: (a) co-current flow heat exchanges, (b) counter-current flow heat exchangers and (c) mixed flow heat exchangers. The three types of heat exchangers are schematically shown in FIGURE 5-11a-c.
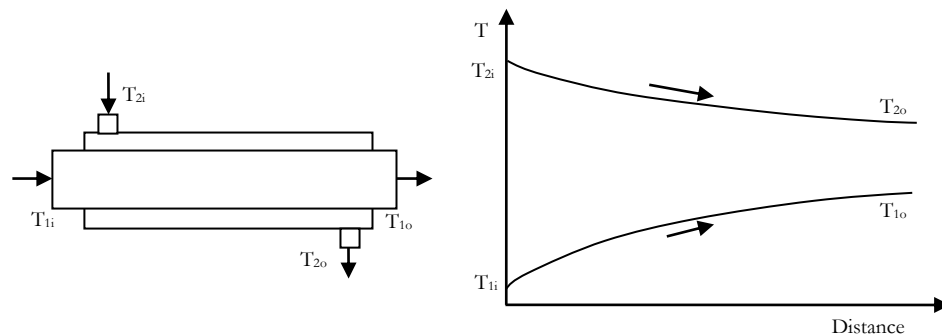
(a) Temperature distributions in co-current flow heat exchanger
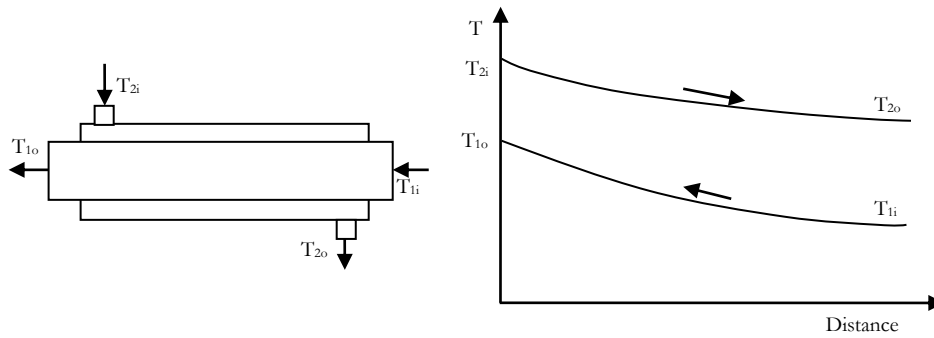
(b) Temperature distributions in counter-current flow heat exchanger
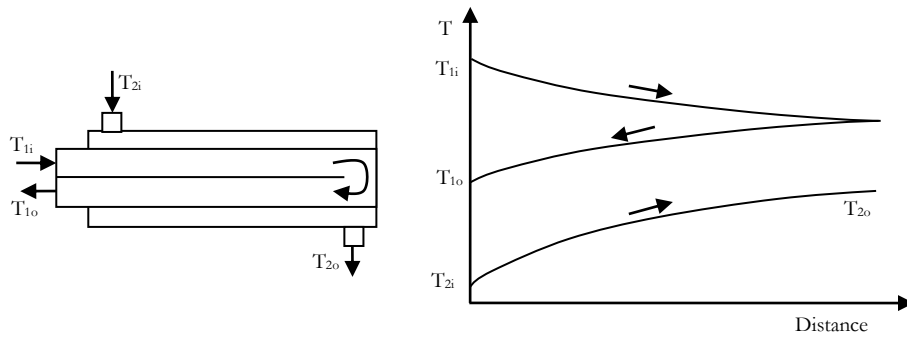
(c) Temperature distributions in the mixed flow heat exchanger.

FIGURE 5-11. Various types of heat exchangers.

Taking the co-current heat exchanger as an example, the total heat balance is as follows,

(5-108) $\quad q_{12} = W_1 c_{p1} \left(T_{1o} - T_{1i} \right) = -W_2 c_{p2} \left(T_{2o} - T_{2i} \right)$.

The total heat balance can be expressed in terms of the mean temperature difference as,

(5-109) $\quad q_{12} = h_O A \Delta T_m$.

Here h_O is the over-all heat transfer coefficient between fluids *1* and *2*, A is the total heat transfer area and ΔT_m is the mean temperature difference between fluids *1* and *2*.

The over-all heat transfer coefficient can be found from a consideration of stationary heat flow from one fluid, through the dividing wall, into the other fluid. Assuming that the dividing wall is a pipe with inner and the outer diameters d_i and d_o, respectively, the over-all heat transfer coefficient is as follows,

$$(5\text{-}110) \quad h_{Oi} = \cfrac{1}{\cfrac{1}{h_i} + \cfrac{d_i}{2\lambda}\ln\cfrac{d_o}{d_i} + \cfrac{d_i}{d_o}\cfrac{1}{h_o}} \;,$$

where h is the convective heat transfer coefficient and λ is the thermal conductivity of the wall material. Indices i and o refer to the inner and the outer pipe diameter (surface), respectively. The above formulation is valid when the reference heat transfer area is equal to the inner pipe surface area. Similar formulation of the over-all heat transfer coefficient with the reference heat transfer area equal to the pipe outer surface area is straightforward, however, care must be taken not to mixed the two formulations, since it will lead to computational errors.

The mean temperature difference in a heat exchanger can be obtained analytically, assuming constant fluid properties and heat transfer coefficients along the heat exchanger length. The energy balance for fluids 1 and 2 in a differential part of a heat exchanger can be written as follows,

$$(5\text{-}111) \quad -h_O dA(T_1 - T_2) = W_1 c_{p1} dT_1, \qquad h_O dA(T_1 - T_2) = W_2 c_{p2} dT_2 \,.$$

Combining the equations, yields,

$$(5\text{-}112) \quad -h_O\left(\frac{1}{W_1 c_{p1}} + \frac{1}{W_2 c_{p2}}\right) dA = \frac{d(T_2 - T_1)}{T_2 - T_1} \,.$$

Integration yields,

$$(5\text{-}113) \quad \ln\left(\frac{T_{2i} - T_{1i}}{T_{2o} - T_{1o}}\right) = h_O\left(\frac{1}{W_1 c_{p1}} + \frac{1}{W_2 c_{p2}}\right) A \,.$$

Combining Eqs. (5-113) and (5-108) yields,

$$(5\text{-}114) \quad q_{12} = h_O A \frac{(T_{2o} - T_{1o}) - (T_{2i} - T_{1i})}{\ln\dfrac{(T_{2o} - T_{1o})}{(T_{2i} - T_{1i})}} \,.$$

Comparing Eqs. (5-114) and (5-109) leads to the following expression for the mean temperature difference,

$$(5\text{-}115) \quad \Delta T_m = \frac{(T_{2o} - T_{1o}) - (T_{2i} - T_{1i})}{\ln\dfrac{(T_{2o} - T_{1o})}{(T_{2i} - T_{1i})}} \equiv \Delta T_{\ln} \,,$$

which is the logarithmic mean temperature difference. It can be shown that similar expressions are obtained for the mean temperature difference for the counter-current and mixed-flow heat exchangers.

A special type of heat exchanger is represented by a feedwater heater, which is used in power plants to preheat the feedwater returning to the reactor pressure vessel (BWR) or steam generators. Usage of feedwater pre-heaters increases the over-all thermal efficiency of the plant. It also reduces thermal shocks caused by low feedwater temperature returning to the steam generation unit.

In general there are two types of feedwater heaters: open and closed ones. A schematic of a closed, vertical shell-and-tube feedwater heater is shown in the figure below. The feedwater passes through the tubes and is heated by the steam extracted from the turbine. The condensate is next throttled to the feedwater pressure and mixed with it. The opened feedwater heater allows for direct mixing of the two streams, however, it required additional pumps to bring pressures of the streams to the same level.
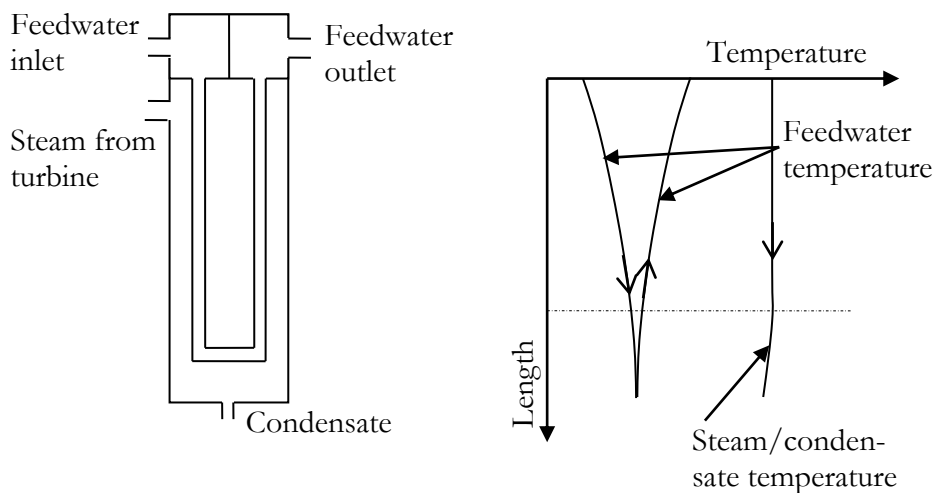
FIGURE 5-12. Schematics of a closed, vertical shell-and-tube feedwater heater.

5.3.3 Steam Generators

A steam generator is a special case of a heat exchanger in which water is evaporated to generate live steam. A typical U-tube steam generator is shown in FIGURE 5-13. The feedwater is distributed inside the downcomer by ring spargers and then is passing through the U-tube riser section. The vapour generated in the riser section is next separated from water in separators, and after passing through steam dryers, leaves the steam generator through the outlet nozzle. The saturated water leaving steam separators flows down and is mixed with feedwater in downcomer. Clearly, water particles circulate in the steam generator until they receive enough enthalpy to evaporate and leave through the outlet nozzle.
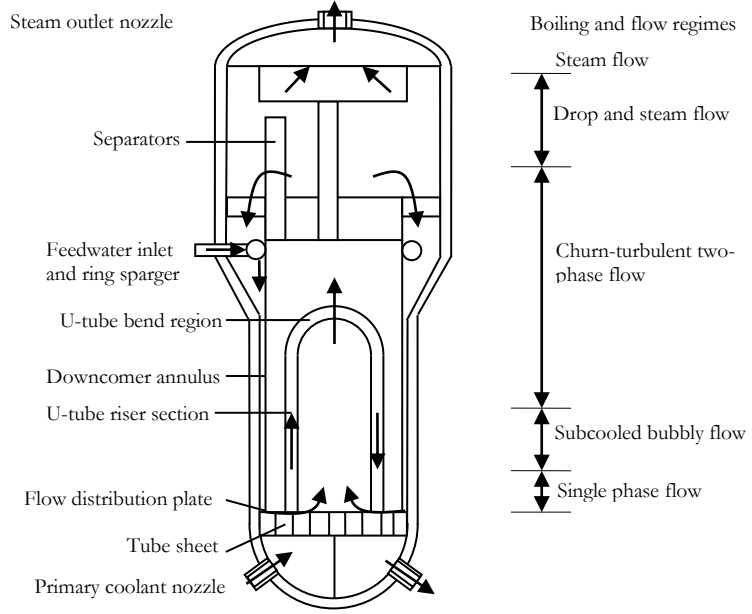
FIGURE 5-13. Steam generator.

The recirculation ratio, defined as,

$$(5\text{-}116) \quad R = \frac{W_D}{W_F},$$

describes the performance of a steam generator; here W_D is the total mass flow rate in the downcomer and W_F is the feedwater flow rate. The total mass flow rate in the downcomer is given as,

$$(5\text{-}117) \quad W_D = W_R + W_F,$$

where W_R is the recirculation mass flow rate.

The steam mass flow rate from the steam generator can be found from the energy balance as follows,

$$(5\text{-}118) \quad W_s(i_s - i_F) + q_{loss} = q_t = W_C(i_{co} - i_{ci}),$$

where W_s is the steam mass flow rate, i_s is the steam specific enthalpy, i_F is the feedwater specific enthalpy, W_C is the primary coolant mass flow rate, which has the specific enthalpy equal to i_{co} and i_{ci} at the outlet and the inlet from the steam generator, respectively. q_{loss} represents the energy losses in the steam generator and q_t is the total thermal power transferred from the primary loop to the steam generator. Since in steady-state the feedwater mass flow rate is equal to the steam mass flow rate, the recirculation ratio becomes,

$$(5\text{-}119) \quad R = \frac{W_D}{W_F} = \frac{W_D(i_s - i_F)}{W_C(i_{co} - i_{ci}) - q_{loss}}.$$

This equation cannot be used to calculate R, since W_D is not known and rather difficult to determine, as shown later on in this section. However, the equation states that the recirculation ratio increases with a decreasing product of mass flow rate and enthalpy drop of coolant. It means that if less heat is provided from the primary system, then more circulation of feedwater in the steam generator is required. It is worth noting that the smallest possible value of R is 1 and this corresponds to once-through evaporation of the feedwater in the steam generator ($W_D = W_F$). Practically, this parameter is approximately equal to 5 for the operation at full power, and it increases to about 30-40 when the power is reduced below 15% of the rated power.

EXAMPLE 5-9. Calculate the thermodynamic equilibrium quality of the two-phase mixture at the exit from the riser of a steam generator in which the recirculation ratio is equal to R. Assume that steam is saturated and neglect the thermal losses in the steam generator. SOLUTION: From the energy balance, the exit enthalpy in the riser is obtained as: $i_{RE} = (W_R i_R + W_s i_s)/(W_F + W_R)$. Since $W_R = W_D - W_F = W_F (R-1)$, the mixture enthalpy is obtained as,
$i_{RE} = [W_F(R-1)i_f + W_s i_s]/(RW_F) = [(R-1)i_f + i_s]/R$. Thus, the thermodynamic equilibrium quality is obtained as:

$$x_{\text{Re}} = \frac{\dfrac{(R-1)i_f + i_g}{R} - i_f}{i_{fg}} = \frac{1}{R}.$$

This result indicates that with increasing recirculation ratio, the thermodynamic equilibrium quality at the exit from the riser decreases. In particular, if the recirculation ratio is equal to 5, the mixture quality is equal to 20%, whereas $R = 1$ corresponds to situation when saturated vapour is leaving the riser, since then the equilibrium quality is equal to 100%.

In order to determine W_D it is necessary to consider pressure losses and energy changes on a path of a recirculating water particle. A schematic diagram of such a path is shown in FIGURE 5-14.

A water particle enters steam generator at point A and moves down in the downcomer. Next it passes the bundle entrance between points B and C and moves upward in the bundle. At the point of the onset of boiling it starts accelerating until it reaches point D. Finally it separates from steam particles between points D and A.

The total pressure drop along the path $ABCD$ is zero. Recognizing that it consists of four different parts, one can write,

(5-120) $\Delta p_{AB} + \Delta p_{BC} + \Delta p_{CD} + \Delta p_{DA} = 0$,

where:

Δp_{AB} - pressure drop in the downcomer,
Δp_{BC} - pressure drop at the entrance from downcomer to the bundle,
Δp_{CD} - pressure drop in the bundle,
Δp_{DA} - pressure drop in the steam separator and dryer.
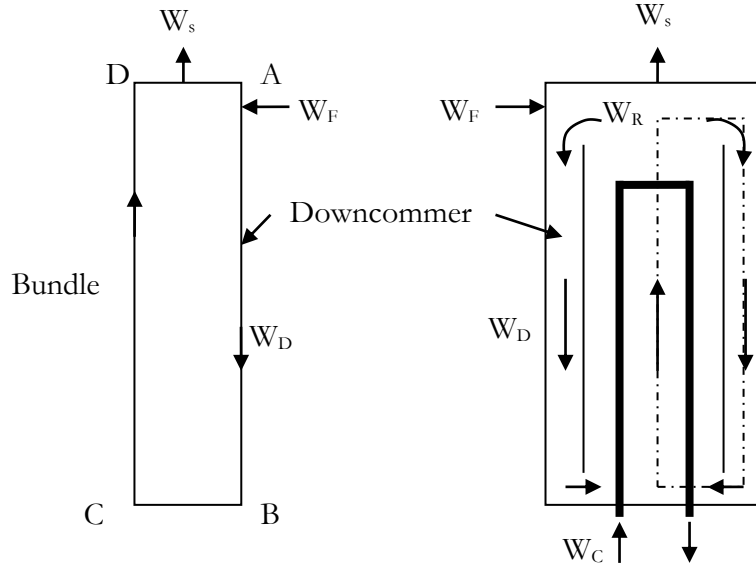
FIGURE 5-14. Schematic diagram of a recirculation flow path in a steam generator.

Assuming single-phase flow in the downcomer, the total pressure drop can be obtained as,

$$(5\text{-}121) \quad \Delta p_{AB} = H_D \rho g - C_f \frac{4H_D}{D_{hD}} \frac{W_D^2}{2\rho A_D^2},$$

where H_D, D_{hD} and A_D are downcomer height, hydraulic diameter and flow cross-section area, respectively; C_f is the Fanning friction factor, W_D is the mass flow rate in the downcomer and ρ is the water density.

The water entrance into the bundle is associated with a local pressure drop as follows,

$$(5\text{-}122) \quad \Delta p_{BC} = -\xi_{Bi} \frac{W_B^2}{2\rho A_B^2}.$$

Here W_B is the mass flow rate in the bundle (it is equal to the mass flow rate in the downcomer in the steady-state conditions), A_B is the flow cross-section area in the bundle and ξ_{Bi} is the local pressure loss coefficient at the bundle inlet.

The total pressure drop in the bundle consists of the single-phase flow part and the two-phase flow part. Assuming that the single-phase length is equal to H_{BSP}, the pressure drop in this part is obtained as,

$$(5\text{-}123) \quad \Delta p_{CDSP} = -H_{BSP} \rho g - \left(C_f \frac{4H_{BSP}}{D_{hB}} + \sum_i \xi_i \right) \frac{W_B^2}{2\rho A_B^2},$$

where D_{hB} and A_B are bundle hydraulic diameter and flow cross-section area, respectively; C_f is the Fanning friction factor, W_B is the mass flow rate in the

downcomer and ρ is the water density. If local obstacles (such as spacers) are present in the bundle, the local loss coefficients ξ_i should be specified.

In the two-phase flow part, the total pressure drop is found as,

$$(5\text{-}124) \quad \Delta p_{CDSP} = -r_4 H_{BTP} \rho g - \left(r_3 C_f \frac{4H_{BTP}}{D_{hB}} + 2r_2 + \sum_i \phi_{lo,i}^2 \xi_i \right) \frac{W_B^2}{2\rho A_B^2} .$$

Here H_{BTP} is the length of the two-phase flow part, r_2, r_3 and r_4 are integral two-phase flow multipliers, $\phi_{lo,i}^2$ are two-phase multipliers at locations, where local losses are given with loss coefficients ξ_i.

The pressure losses in the steam separators depend on their design details. As first approximation, the total pressure loss can be calculated as,

$$(5\text{-}125) \quad \Delta p_{DA} = -\xi_S \frac{W_B^2}{2\rho A_S^2},$$

where A_S is the reference flow area of the steam separator and ξ_S is the over-all pressure loss coefficient in the separator. Depending on the design details, this coefficient should include local and friction losses, as well as two-phase flow effects.

The equation for the total pressure drop in the flow path is as follows,

$$H_D \rho g - C_f \frac{4H_D}{D_{hD}} \frac{W_D^2}{2\rho A_D^2} - \xi_{Bi} \frac{W_B^2}{2\rho A_B^2} - H_{BSP} \rho g - \left(C_f \frac{4H_{BSP}}{D_{hB}} + \sum_i \xi_i \right) \frac{W_B^2}{2\rho A_B^2}$$
$$- r_4 H_{BTP} \rho g - \left(r_3 C_f \frac{4H_{BTP}}{D_{hB}} + 2r_2 + \sum_i \phi_{lo,i}^2 \xi_i \right) \frac{W_B^2}{2\rho A_B^2} - \xi_S \frac{W_B^2}{2\rho A_S^2} = 0$$

Since $W_D = W_B$ and $H_D = H_B = H_{BSP} + H_{BTP}$, the equation can be simplified and solved for W_D as follows,

$$(5\text{-}126) \quad H_{BTP} \rho g (1 - r_4) = \left[C_f \frac{4H_D}{D_{hD}} \frac{1}{A_D^2} + \frac{\xi_{Bi}}{A_B^2} + \left(C_f \frac{4H_{BSP}}{D_{hB}} + \sum_i \xi_i \right) \frac{1}{A_B^2} + \right.$$
$$\left. \left(r_3 C_f \frac{4H_{BTP}}{D_{hB}} + 2r_2 + \sum_i \phi_{lo,i}^2 \xi_i \right) \frac{1}{A_B^2} + \frac{\xi_S}{A_S^2} \right] \frac{W_D^2}{2\rho}$$

or

$$(5\text{-}127) \quad W_D = \rho \sqrt{\frac{2H_{BTP} g (1 - r_4)}{\Phi}},$$

where,

$$\text{(5-128)} \quad \Phi = \left[C_f \frac{4H_D}{D_{hD}} \frac{1}{A_D^2} + \frac{\xi_{Bi}}{A_B^2} + \left(C_f \frac{4H_{BSP}}{D_{hB}} + \sum_i \xi_i \right) \frac{1}{A_B^2} + \left(r_3 C_f \frac{4H_{BTP}}{D_{hB}} + 2r_2 + \sum_i \phi_{lo,i}^2 \xi_i \right) \frac{1}{A_B^2} + \frac{\xi_S}{A_S^2} \right] .$$

The length of the non-boiling part of the bundle can be obtained from a solution of the energy balance equations formulated for a differential length dH_B, as indicated in FIGURE 5-15.

The amount of heat exchanged between the coolant in the inlet leg and the feedwater in the shell can be calculated as,

$$\text{(5-129)} \quad dq_i = W_C c_{pC} dT_{Ci} = h \frac{1}{2} dA_B (T_B - T_{Ci}).$$

Here the first equation describes the change of coolant enthalpy over the differential length dH_B, whereas the second equation describes the convective heat transfer between coolant inside pipes (with temperature T_{Ci}) and the shell fluid (with temperature T_B). Similar heat balance over the outlet leg part is as follows,

$$\text{(5-130)} \quad dq_o = W_C c_{pC} dT_{Co} = h \frac{1}{2} dA_B (T_{Co} - T_B).$$

In the above equations it is assumed that the differential heat transfer area dA_B is equally distributed between the inlet and the outlet leg.
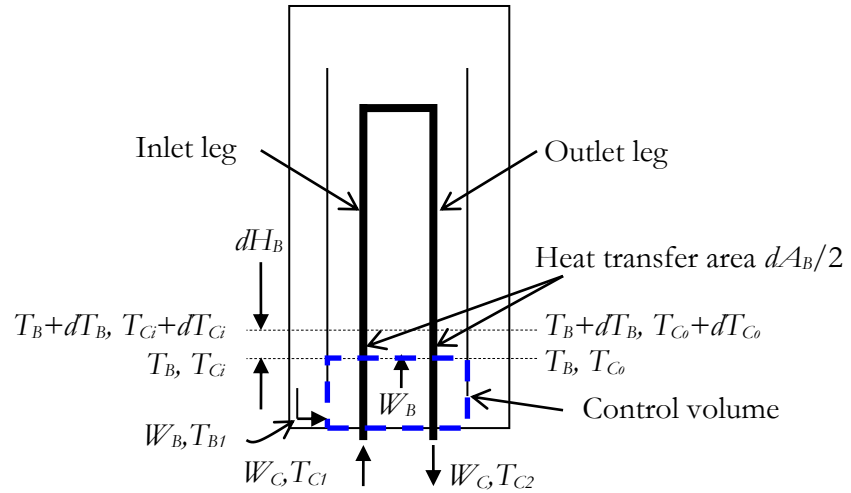
FIGURE 5-15. Principles of energy balance in the bundle part of a steam generator.

The corresponding energy balance for the shell fluid is as follows,

$$\text{(5-131)} \quad dq_i + dq_o = W_B c_{pB} dT_B = hdA_B \left[\frac{1}{2} (T_{Co} + T_{Ci}) - T_B \right].$$

Additional energy balance can be written for the control volume indicated in FIGURE 5-15,

(5-132) $\quad W_B c_{pB}\left(T_B - T_{B1}\right) = W_C c_{pC}\left(T_{Ci} - T_{C1}\right) + W_C c_{pC}\left(T_{C2} - T_{Co}\right),$

in which T_{B1} is the inlet temperature of the shell fluid and T_{C1}, T_{C2} are the inlet and outlet temperatures of coolant, respectively.

Let,

$$\xi = \frac{A_B h}{W_C c_{pC}} \qquad \text{and} \qquad S = \frac{W_C c_{pC}}{W_B c_{pB}}.$$

Using the above relations in the energy balance equations yield,

(5-133) $\quad \dfrac{dT_{Ci}}{d\xi} = \dfrac{1}{2}\left(T_B - T_{Ci}\right),$

(5-134) $\quad \dfrac{dT_{Co}}{d\xi} = \dfrac{1}{2}\left(T_{Co} - T_B\right),$

(5-135) $\quad \dfrac{1}{S}\dfrac{dT_B}{d\xi} = \dfrac{1}{2}\left(T_{Ci} + T_{Co}\right) - T_B,$

(5-136) $\quad \dfrac{1}{S}\left(T_B - T_{B1}\right) = \left(T_{Ci} - T_{Co}\right) + \left(T_{C2} - T_{C1}\right).$

Equation (5-135) can be differentiated as follows,

(5-137) $\quad \dfrac{1}{S}\dfrac{d^2 T_B}{d\xi^2} = \dfrac{1}{2}\left(\dfrac{dT_{Ci}}{d\xi} + \dfrac{dT_{Co}}{d\xi}\right) - \dfrac{dT_B}{d\xi},$

and combined with Eqs. (5-133) and (5-134) to yield,

(5-138) $\quad \dfrac{1}{S}\dfrac{d^2 T_B}{d\xi^2} = \dfrac{1}{4}\left(T_{Co} - T_{Ci}\right) - \dfrac{dT_B}{d\xi}.$

Combining Eqs. (5-136) with (5-138) results in the following ordinary differential equation,

(5-139) $\quad \dfrac{1}{S}\dfrac{d^2 T_B}{d\xi^2} = -\dfrac{dT_B}{d\xi} - \dfrac{1}{4S}\left(T_B - T_{B1}\right) + \dfrac{1}{4}\left(T_{C2} - T_{C1}\right).$

Substituting,

(5-140) $\theta = \dfrac{T_B - T_{B1}}{T_{C2} - T_{C1}}$,

the equation can be put in the following form,

(5-141) $\dfrac{d^2\theta}{d\xi^2} + S\dfrac{d\theta}{d\xi} - \dfrac{\theta}{4} = -\dfrac{S}{4}$.

The boundary conditions at $\xi = 0$ are as follows,

(5-142) $\theta = 0$, and $\left.\dfrac{d\theta}{d\xi}\right|_{\xi=0} = \dfrac{S}{2}\dfrac{T_{C1}+T_{C2}}{T_{C2}-T_{C1}} = K$.

Equation (5-141) can be solved by using a trial function,

$\Psi = \theta - S = Ae^{p\xi}$.

Substituting the trial function into Eq. (5-141) and applying the boundary conditions, the following solution is obtained,

(5-143) $\theta = \dfrac{K+p_2 S}{p_1 - p_2}e^{p_1\xi} - \dfrac{K+p_1 S}{p_1 - p_2}e^{p_2\xi} + S$.

Here,

$p_{1,2} = \dfrac{-S \mp \sqrt{S^2 + 1}}{2}$.

The boiling length in the bundle part of the steam generator can be found from Eq. (5-143) by taking,

$\theta = \theta_{sat} = \dfrac{T_{sat} - T_{B1}}{T_{C2} - T_{C1}}$.

Using Eq. (5-127), the mass flow rate in the downcomer can be found, which used in Eq. (5-119) gives the recirculation ratio of the feedwater in the steam generator.

5.3.4 Pumps

A pump is a device that increases the energy of a fluid by applying mechanical energy at the pump shaft. Pumps belong to the most important pieces of equipment in nuclear power plants, since they are often used for long-term cooling of nuclear reactor cores. In primary loops, the coolant circulation is provided by the Main Circulation Pumps (MCP). In early designs of BWR, main circulation pumps were located outside of the reactor pressure vessel. This type of design is schematically shown in FIGURE 5-16.
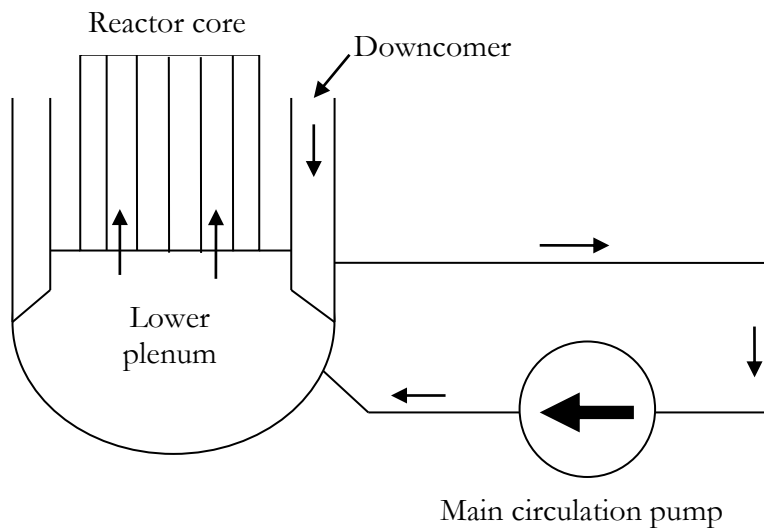
FIGURE 5-16. External main circulation pumps in early BWR design.

In modern BWR designs the pumps are located inside of the reactor pressure vessel. This design reduces the total length of the piping connected to the pressure vessel, reducing the probability of occurrence of a leakage or loss-of-coolant accident. Two major types of pumps are used: the centrifugal pumps and the jet pumps, as shown in FIGURE 5-17 and FIGURE 5-18.
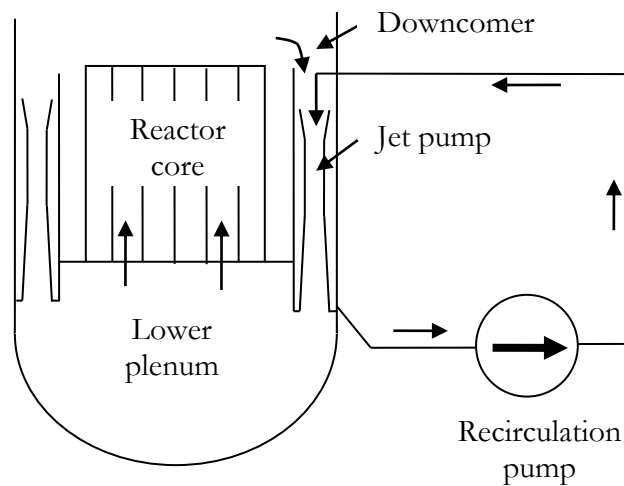
FIGURE 5-17. BWR with external recirculation and internal jet pumps.
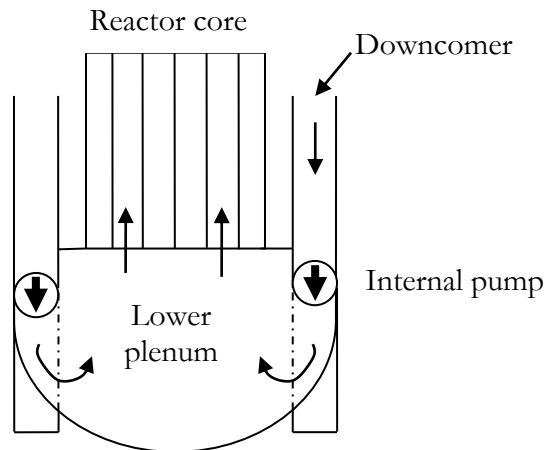
FIGURE 5-18. BWR with internal axial flow pumps.

Two types of pumps are most common in nuclear power plants and are presented in a more detail: the centrifugal pumps and the jet pumps.

Centrifugal pumps

The essential parts of the centrifugal pump are a rotating impeller and a case surrounding it. Depending on the liquid flow direction, three general categories are distinguished:

- radial flow pumps – in which the pressure is developed wholly by the centrifugal force

- mixed flow pumps – in which the pressure is developed partly by centrifugal force and partly by the lift of the vanes of the impeller on the liquid

- axial flow pumps – in which the pressure is developed by the propelling or lifting action of the vanes of the impeller on the liquid.

To select the proper pump for a particular application, it is necessary to know the characteristics of the pump and of the system in which it is used. Before further discussing pump characteristics, it is necessary to introduce the most important terms that are characterizing pumps.

Pumping Head (or shortly Head; symbol H) – this term stems from a particular form of the Bernoulli equation, given as,

$$(5\text{-}144) \quad \frac{p}{\rho g} + \frac{U^2}{2g} + z = H_t = const.$$

Each term in the above equation has dimensions of length, or head of flowing fluid. H_t is then termed the total head of the flow and it consists of the head due to local static pressure ($p/\rho g$), the head due to the local dynamic pressure ($U^2/2g$) and the

elevation head (z). The pumping head is thus equal to the pressure rise per unit weight: $H = \Delta p / \rho g$, and its dimension is length.

Pump Capacity (or Discharge; symbol Q) – is the volume rate of fluid discharged (dimensions: volume per unit time).

Rated or designed capacity (Q_R) – is the capacity at the maximum pump efficiency.

Pump efficiency (η) – is defined as the ratio of power delivered to the liquid divided by the input power, $\eta = N / N_{in}$. The power delivered to liquid can be obtained from the energy equation, and for the incompressible flow is given as $N = \rho g Q H$.

In nuclear reactors the **pumping power** is a substantial portion of the total reactor power and thus it must be taken into account in the over-all energy balance. If a pump is operating in a closed loop with the mass flow rate W and the total pressure drop in the loop is Δp, the total power delivered to the liquid (both reversible and irreversible) is,

$$(5\text{-}145) \quad N = \frac{\Delta p \cdot W}{\eta \cdot \rho} .$$

Typically the loop consists of channels with piecewise constant cross-section areas, for which the total pressure loss is given as (see Eq. (3-213)),

$$(5\text{-}146) \quad \Delta p = \left[\sum_k \left(\frac{4 L_k}{D_{h,k}} C_{f,k} \right) \frac{1}{A_k^2} + \sum_j \xi_j \frac{1}{A_{j,min}^2} + \frac{1}{A_2^2} - \frac{1}{A_1^2} \right] \frac{W^2}{2\rho} = \xi_{eff} \frac{W^2}{2\rho A_{ref}^2} .$$

Here ξ_{eff} is the effective loss coefficient calculated as,

$$\xi_{eff} = \sum_k \left(\frac{4 L_k}{D_{h,k}} C_{f,k} \right) \left(\frac{A_{ref}}{A_k} \right)^2 + \sum_j \xi_j \left(\frac{A_{ref}}{A_{j,min}} \right)^2 + \left(\frac{A_{ref}}{A_2} \right)^2 - \left(\frac{A_{ref}}{A_1} \right)^2 ,$$

were A_{ref} is an arbitrary chosen reference cross-section area of the channels in the loop. Combining Eq. (5-145) with (5-146), the total power delivered to the liquid by a pump operating in a loop is as follows,

$$(5\text{-}147) \quad N = \frac{\xi_{eff} \cdot W^3}{\eta \cdot 2\rho^2 A_{ref}^2} .$$

Pump inertia (I) – is the combined inertia of the pump rotating parts, motor and liquid in the pump impeller.

Pump rotational speed – either given as ω in rad/s, or as n, in revolves per minute, rpm. Obviously, $\omega = n \cdot 2\pi / 60$.

In practical analysis of a system with a pump it is necessary to know the relationship between the pump discharge and the pumping head. For a pump working with a constant speed, the discharge of the pump is a function of the rotational speed and the pumping head, $Q = f(H,n)$. In case of transient-state speed changes, the pump behaviour also depends on the net torque, T, and the pump inertia, I. In general, four variables (Q, H, n and T) have to be specified for the mathematical description of a pump. The relationships between these variables are called the pump characteristics or performance curves.

It is convenient to define non-dimensional pump variables, using their rated values,

$$(5\text{-}148) \quad \upsilon = \frac{Q}{Q_R}, \quad h = \frac{H}{H_R}, \quad \alpha = \frac{n}{n_R}, \quad \beta = \frac{T}{T_R}.$$

Here the subscript R denotes rated conditions. The pump operational mode is usually represented on the $\upsilon - \alpha$ plane, as shown in FIGURE 5-19.
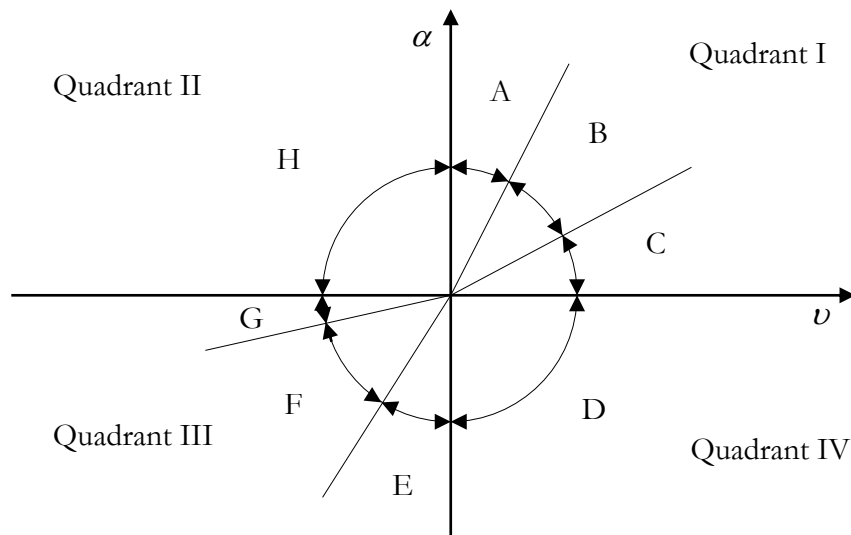
FIGURE 5-19. Quadrants and zones of pump operation.

TABLE 5.2. Definitions of quadrants and zones of pump operation.

Zone/ Quadrant	Definition	Sign				Reference picture in FIGURE 5-20.
		υ	α	h	β	
A/I	Normal pumping	+	+	+	+	(a)
B/I	Energy dissipation	+	+	-	+	(b)
C/I	Reverse turbine	+	+	-	-	(c)

D/IV	Energy dissipation	+	-	-	-	(d)
E/III-IV	Reverse rotation pumping	±	-	±	-	(e)
F/III	Energy dissipation	-	-	-	-	(f)
G/III	Normal turbining	-	-	+	+	(g)
H/II	Energy dissipation	-	+	+	+	(h)
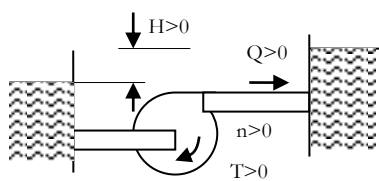
(a) Zone A – normal pumping
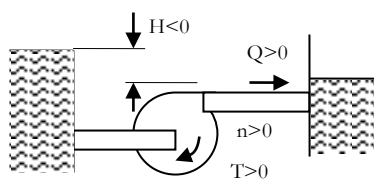
(b) Zone B – energy dissipation
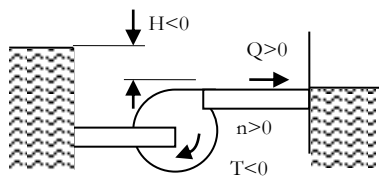
(c) Zone C – reverse turbine
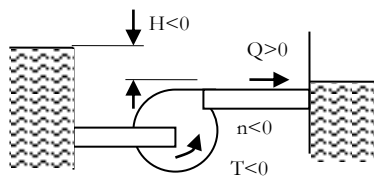
(d) Zone D – energy dissipation
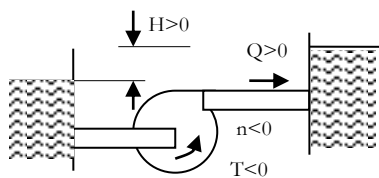
(e) Zone E – reverse rotation pumping
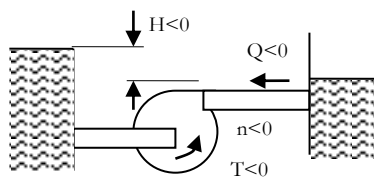
(f) Zone F – energy dissipation
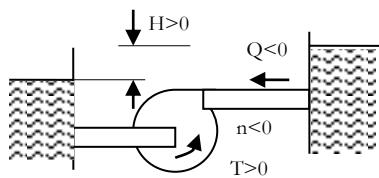
(g) Zone G – normal turbine
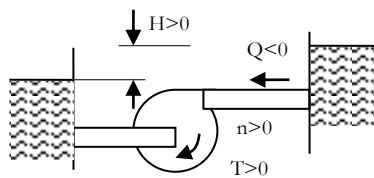
(h) Zone H – energy dissipation

FIGURE 5-20. Zones of pump operation.

For transient and abnormal operation of pumps their characteristics have to be specified in all four quadrants. However, for selecting a pump for a specific system, the

normal operation is considered and for that purpose knowledge of the pump characteristics in the first quadrant is sufficient.

Typical characteristics of the centrifugal pumps are shown in FIGURE 5-21. Three types of characteristics are shown: the rising characteristic, when initially the pumping height H increases with increasing discharge rate Q; the flat characteristic, when in a wide range of the discharge rate the pumping height remains constant; the falling characteristic, when for all range of discharge rate the pumping height is decreasing with increasing discharge rate.

The pump operating point is determined by superimposing the pump characteristics with the system curve, as shown in FIGURE 5-22. The system operation point coincides with the crossing point of the pump characteristic with the system curve. A well optimized system has the operating point which coincides with the point of the maximum pump efficiency.
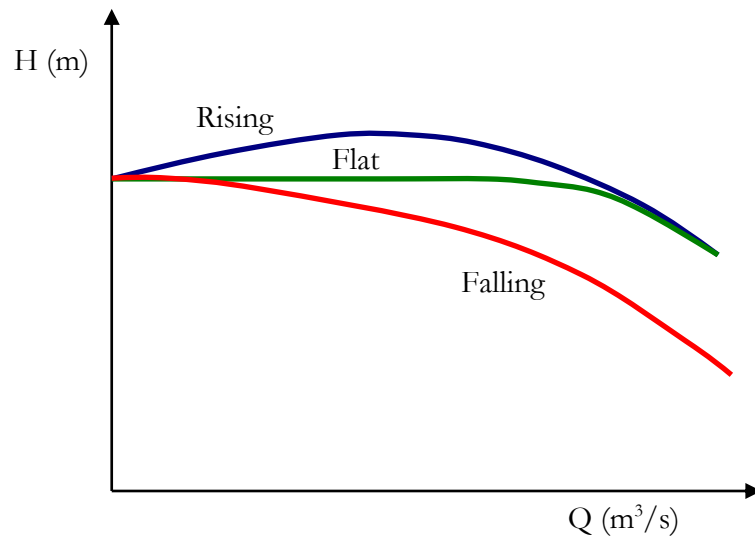
FIGURE 5-21. Pump characteristics.
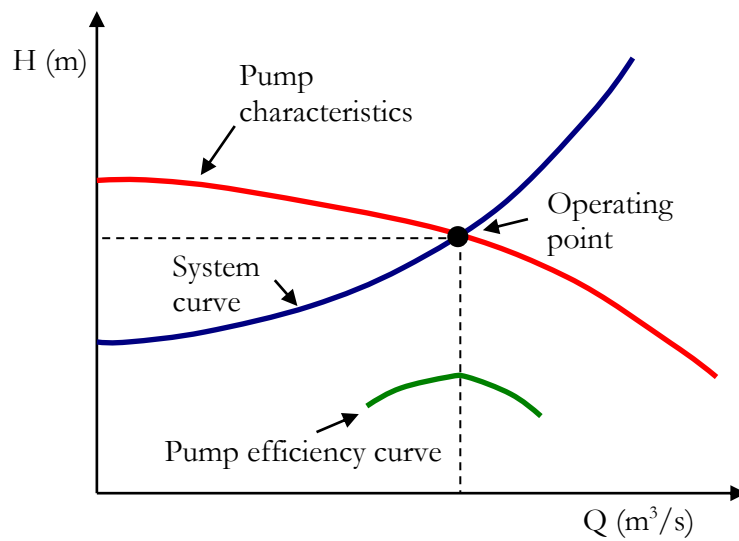
FIGURE 5-22. Pump operating point.
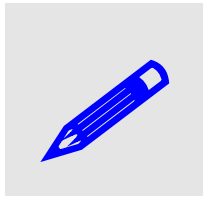
EXAMPLE 5-10. Find the operating point for a pumping system shown in FIGURE 5-23. Develop an algebraic expression for the general shape of the system curve $H = f(Q)$. Assume that the pump characteristics is given as $H = H_0 - AQ^2$ and that the pump rated capacity is $Q_R = 0.06$ m^3/s. Determine the required H_0 if $A = 2.5 \; 10^3 \; m/(m^3/s)$ and if the operating point is the point of the highest pump efficiency.
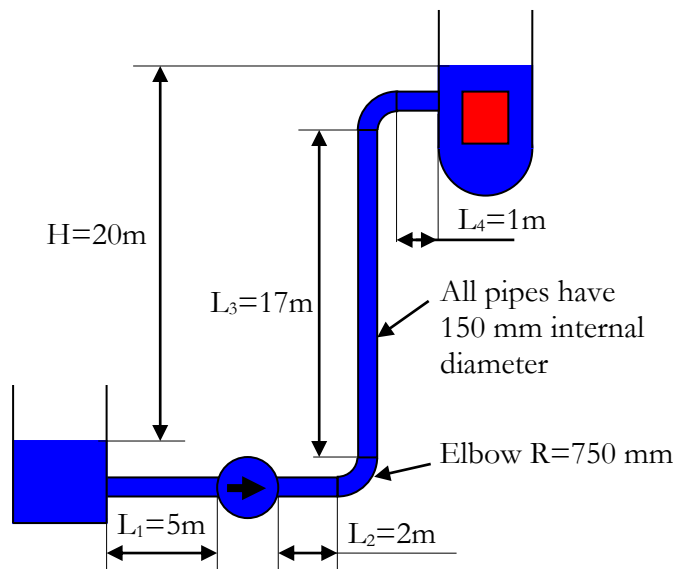
FIGURE 5-23. Schematic diagram of pumping system.

Hint: calculate and plot the system curve. Since the pump should work at highest efficiency, the volumetric flow in the system should be equal to Q_R. From the system curve find the corresponding H.

Jet pump

Jet pumps have several safety and economic advantages (such as robustness and practically no need for maintenance) which make them very attractive for nuclear applications. For reactor operational analysis it is necessary to know the **jet pump characteristics**, which describe the flow/pressure-drop relationship. The basic features of a jet pump can be investigated in a simple system shown in FIGURE 5-24.
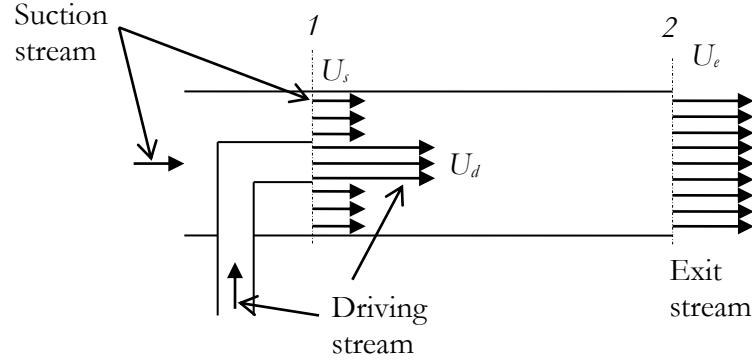
FIGURE 5-24. Schematic diagram of a jet pump.

Neglecting friction losses as well as assuming steady-state conditions and turbulent flow (velocity profiles at cross-sections *1* and *2* are assumed to be flat), the mass and momentum balances are as follows,

(5-149) $W_s + W_d = W_e$, or $\qquad \rho U_s A_s + \rho U_d A_d = \rho U_e A_e$,

(5-150) $U_d W_d + U_s W_s + p_1 A_1 = U_e W_e + p_e A_e$.

Here U, W, A and p are mean velocity, mass flow rate, cross-section area and pressure, respectively. Combining the two equations and noting that $A_1 = A_e = A$, yields,

(5-151) $p_e - p_1 = \dfrac{W_d(U_d - U_e) + W_s(U_s - U_e)}{A}$.

This is an expression for the pressure rise resulting from the mixing of the driving and the suction streams.

The performance of a jet pump is usually characterized by two dimensionless parameters μ and ν, defined as follow:

Flow ratio parameter

(5-152) $\mu = \dfrac{W_s}{W_d}$

Head ratio parameter

(5-153) $\quad v = \dfrac{\varphi_e - \varphi_s}{\varphi_{d1} - \varphi_e}$,

where,

(5-154) $\quad \phi = \dfrac{p}{\rho} + \dfrac{U^2}{2} + gz$,

corresponds to the specific energy of each stream. Thus, the head ratio v is defined as a ratio of the specific energy increase in the suction flow to the specific energy decrease of the driving flow.

It can be shown[5-4] that the μ-v relationship has the following general form,

(5-155) $\quad v = \dfrac{C - \dfrac{\mu^2}{2(1-R)^2}(1+\xi_s)}{-C + \dfrac{1}{2R^2}(1+\xi_d)}$,

where,

(5-156) $\quad R = \dfrac{A_d}{A}$,

is a ratio of the driving stream area to the mixing area (which is a sum of the suction and the driving stream areas). In addition,

(5-157) $\quad C = \dfrac{1}{R} + \dfrac{\mu^2}{1-R} - \dfrac{(\mu+1)^2}{2}$.

Parameters ξ_s and ξ_d in Eq. (5-155) represent local pressure loss coefficient at the suction and drive nozzles, respectively.

EXAMPLE 5-11. Calculate the jet pump head ratio parameter v if the flow ratio μ is equal to 1.5. Given: $R = 0.1589$, $\xi_s = 0.35$ and $\xi_d = 0.1$. SOLUTION: The constant C is obtained as: $C = 1/0.1589 + (1.5)^2/(1-0.1589)+(1.5+1)^2/2 = 12.093$. The pump head ratio is then calculated from Eq. (5-155) as $v = 1.026$.

5.3.5 Turbines Sets

A schematic of a turbine set is shown in FIGURE 5-25. Saturated steam from the steam generator (or from the reactor pressure vessel in BWR) is first expanded in the high pressure (HP) turbine to provide the shaft work output. The wet steam from the exit of the high pressure turbine is dried and superheated in the moisture separator reheater (MSR). In the next step, the superheated steam from the MSR is expanded in the low pressure (LP) turbine to provide additional shaft work output. Finally steam exhausting from the low pressure turbine is condensed in the condenser under

constant low pressure conditions and is pumped back to the steam generator or to the reactor pressure vessel.
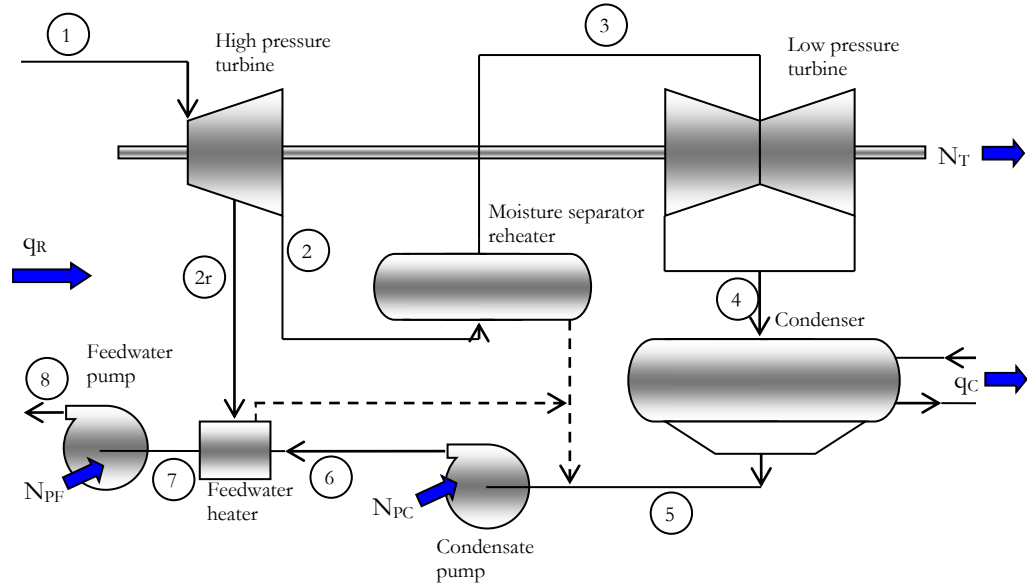
FIGURE 5-25. Schematics of a typical turbine set in nuclear power plant.

Turbines installed in nuclear power plants are slightly different from the turbines in the conventional systems. The main differences are as follows:

- Saturated or slightly superheated steam at the inlet to the high pressure turbine,

- Large exit volumes and consequently long blades in the exit part of low pressure turbine,

- reduced speed to 1500 rpm compared to 3000 rpm for the conventional systems.

The steam processes in the turbine set are shown on the *T-s* plane in FIGURE 5-26. The working fluid is continuously vaporized and condensed when circulating between the steam generator and the turbine. The label *1* corresponds to the saturated steam that enters the high pressure turbine. The steam exits from the high pressure turbine partly to the feedwater regenerator (stream with label *2r*, referred as bleeding) and the rest exits to the moisture separator reheater (stream with label *2*). Assuming that the inlet mass flow rate of steam to the turbine is W_1, the theoretical work N_t of the turbine is,

$$(5\text{-}158) \quad N_t = W_1\left(i_1 - i_{2r}\right) + \left(W_1 - W_r\right)\left(i_{2r} - i_{2s}\right) = W_1\left(i_1 - i_{2s}\right) - W_r\left(i_{2r} - i_{2s}\right)$$

Here i_{2r} is the enthalpy of the steam exiting to the feedwater reheater and W_r is its mass flow rate. The theoretical work of the turbine is calculated with an assumption that the steam is expanded in the turbine without losses; that is with constant entropy. This

would correspond to a process indicated with a straight vertical line between points *1* and *2s*. In reality there are internal losses in the turbine due to friction and leakages and the real process runs between points *1* and *2*, with a certain increase of the entropy. The internal power of the high pressure turbine can be calculated as,

$$(5\text{-}159)\quad N_i = W_1\left(i_1 - i_{2r}\right) + \left(W_1 - W_r\right)\left(i_{2r} - i_2\right) = W_1\left(i_1 - i_2\right) - W_r\left(i_{2r} - i_2\right).$$

The internal efficiency of a turbine is defined as,

$$(5\text{-}160)\quad \eta_i = \frac{N_i}{N_t}.$$

Substituting Eqs. (5-158) and (5-159) into (5-160) yields,

$$(5\text{-}161)\quad \eta_i = \frac{W_1\left(i_1 - i_2\right) - W_r\left(i_{2r} - i_2\right)}{W_1\left(i_1 - i_{2s}\right) - W_r\left(i_{2r} - i_{2s}\right)}.$$

For a turbine without bleeding, the internal efficiency is as follows,

$$(5\text{-}162)\quad \eta_i = \frac{\left(i_1 - i_2\right)}{\left(i_1 - i_{2s}\right)}.$$

The internal efficiency of a turbine decreases with increasing moisture in the steam. Since almost all turbines in nuclear power plants operate with saturated and wet steam, their efficiency is deteriorated in comparison with the turbines operating with dry steam. A simple estimate of the efficiency is given by the following equation,

$$(5\text{-}163)\quad \eta_{iw} = \eta_{id} \cdot x,$$

where x is the steam quality, η_{id} is the efficiency of the turbine working with dry steam and η_{iw} is the efficiency of the turbine working with wet steam.
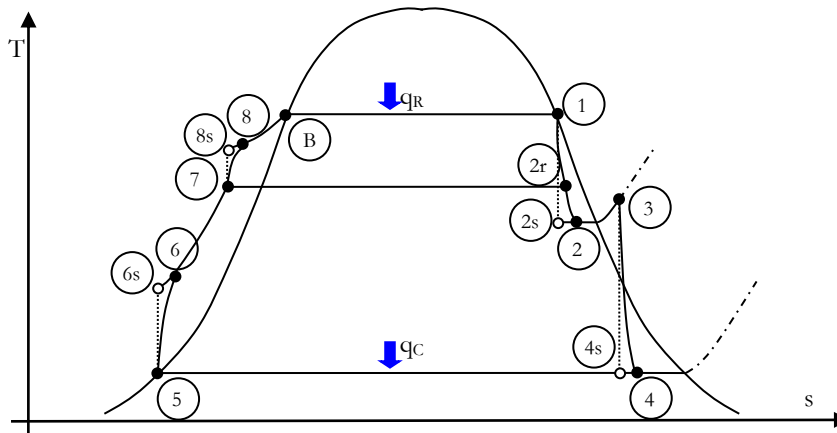
FIGURE 5-26. Steam cycles in a typical nuclear turbine set.

The power transmitted from a turbine to a generator is still reduced by mechanical losses in the turbine. The mechanical efficiency η_m of a turbine is defined as,

$$(5\text{-}164) \quad \eta_m = \frac{N_m}{N_i},$$

where N_m is the mechanical power transmitted from the turbine to the generator. The electrical power available at the generator bus depends on the turbine mechanical power and the generator efficiency, and can be calculated as,

$$(5\text{-}165) \quad N_e = \eta_g N_m.$$

Here N_e is the electrical power and η_g is the efficiency of the generator.

After leaving the high pressure turbine, wet steam is directed to the moisture separator reheater. Its function is to separate moisture from the steam and also to bring the steam to a superheat condition by heating.

After leaving the MSR, steam enters the low pressure turbine, where an additional shaft work is generated. The mechanical power of this turbine can be calculated in analogy to the high pressure turbine as,

$$(5\text{-}166) \quad N_{m2} = W_3 \left(i_3 - i_{4s} \right) \eta_{i2} \eta_{m2},$$

where N_{m2} is the mechanical power of the low pressure turbine, W_3 is the steam mass flow rate through the low pressure turbine, η_{i2} is the internal efficiency of the turbine, η_{m2} is the mechanical efficiency of the turbine, i_3 is the steam enthalpy at the inlet to the turbine and i_{4s} is the steam enthalpy at the exit from the turbine assuming an isentropic expansion of steam.

5.3.6 Steady-State Balance of Boiling Water Reactor

A schematic of a BWR is shown in FIGURE 5-27. It contains five major control volumes, representing the core, the upper plenum, the steam separators and dryers, the downcomer with the recirculation system and the lower plenum.

The over-all heat and mass balance equations of the reactor pressure vessel are as follows,

$$(5\text{-}167) \quad q_c + \left| N_p \right| + W_{fw} i_{fw} - W_s i_s + W_{cr} i_{cr} - W_{cl} i_{cl} - q_r = 0,$$

$$(5\text{-}168) \quad W_{fw} - W_s + W_{cr} - W_{cl} = 0,$$

where,

q_c – core thermal power,
N_p – recirculation pump power (negative if added to the system),
q_r – radiative power loss,

W_{fw} – feedwater flow rate,
W_s – steam flow rate,
W_{cr} – flow rate of the control rod drive system,
W_{cl} – flow rate to the cleaning system,
i_{fw} – feedwater specific enthalpy,
i_s – steam specific enthalpy,
i_{cl} – specific enthalpy of the cleaning water flow,
i_{cr} – specific enthalpy of the control rod drive system flow.
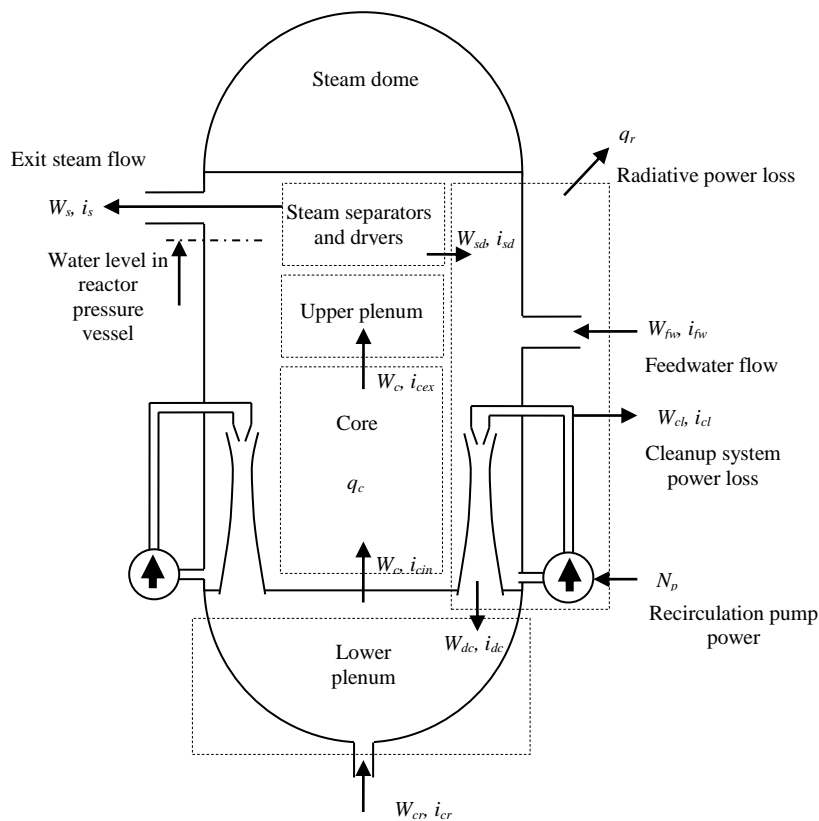
FIGURE 5-27. Thermal-hydraulic model of BWR.

The specific enthalpy of the steam leaving the reactor pressure vessel is slightly below the saturation value. This is due to imperfect separation in the steam separators, which is expressed by a so-called carryover fraction, F_{co}. Typical value of this factor is 0.001. Thus, the enthalpy of the steam at the exit from the reactor pressure vessel is as follows,

$$(5\text{-}169) \quad i_s = \left(1 - F_{co}\right)i_g + F_{co}i_f \,.$$

Here i_g and i_f are the saturated specific enthalpies of steam and water, respectively.

In a similar manner, the liquid leaving the steam separators has specific enthalpy slightly larger than the corresponding saturated value due to entrained small amounts of the vapour phase. This process is expressed with a so-called carryunder fraction, F_{cu}. Thus, the specific enthalpy of the stream leaving the separators-dryers, i_{sd}, is given as,

(5-170) $i_{sd} = (1 - F_{cu})i_f + F_{cu}i_g$.

A typical value of the carryunder fraction is 0.0025, but it may vary with water level in the reactor pressure vessel.

The mass balance in steam-separators and dryers yields,

(5-171) $W_{sd} = W_c - W_s$,

where W_{sd} is the mass flow rate of the returning stream to the downcomer from separators and dryers and W_c is the total coolant flow through the reactor core. The energy balance in the steam separators and dryers yields,

(5-172) $W_{sd}i_{sd} = W_c i_{cex} - W_s i_s$,

where i_{cex} is the mean specific enthalpy of the coolant leaving the reactor core.

The mass and energy balances for the downcomer are as follows,

(5-173) $W_{sd} + W_{fw} - W_{cl} - W_{dc} = 0$,

and,

(5-174) $W_{sd}i_{sd} + W_{fw}i_{fw} - W_{cl}i_{cl} - W_{dc}i_{dc} - q_r + |N_p| = 0$.

Here W_{dc} and i_{dc} are the mass flow rate and the specific enthalpy of the coolant flowing from the downcomer to the lower plenum, respectively.

In a similar way, the mass and conservation equations for the lower plenum can be written as,

(5-175) $W_{dc} + W_{cr} - W_c = 0$,

(5-176) $W_{dc}i_{dc} + W_{cr}i_{cr} - W_c i_{cin} = 0$,

where i_{cin} is the specific enthalpy of the coolant at the inlet to the reactor core.

Finally, for the reactor core, the following energy equation is valid,

(5-177) $W_c i_{cin} + q_c - W_c i_{cex} = 0$.

A typical engineering task is to calculate consistent initial flow and pressure distributions in the reactor pressure vessels. One example is to determine the steam dome pressure, when the core power is known and all other parameters have to be determined in a consistent manner. In general, the steam dome pressure is a function of the steam mass flow rate and for a BWR plant, the pressure is usually given as,

(5-178) $p_d = p_0 + p_1 \upsilon + p_2 \upsilon^2 ,$

where coefficients p_0, p_1 and p_2 are known from the fitting to the plant data and $\upsilon = W_s / W_{sR}$ is a ratio of the actual steam mass flow to the rated one. To use the energy balances in the pressure vessel, it is necessary to know enthalpies, which depend on the system pressure. Clearly, the balance equations have to be solved iteratively with Eq. (5-178) to converge. Typically convergence is obtained when pressure changes between two consecutive iterations become acceptably small.

If the feedwater temperature - rather than dome pressure - is unknown, a similar equation to Eq. (5-178) is used for the feedwater temperature in terms of the steam flow ratio $\upsilon = W_s / W_{sR}$. The solution is sought in an iterative manner, until the temperature difference between two consecutive iterations becomes acceptably small.

In the simplest case (and often as an initial guess) it can be assumed that the pressure is constant in the whole reactor pressure vessel. Eqs. (5-167) through (5-177) constitute then a system of eleven independent equations that can be solved for eleven unknowns. It can be further recognized that the global mass balance of the secondary system requires that the feedwater flow and the steam flow are equal to each other, thus,

(5-179) $W_{fw} = W_s .$

Equation (5-168) yields,

(5-180) $W_{cr} = W_{cl} .$

This equation implies that at the steady-state condition, the control-rod water flow and the cleaning water flow are equal to each other. Further, if the connection of the cleaning water system is as indicated in FIGURE 5-27, it is reasonable to assume that,

(5-181) $i_{cl} \approx i_{dc} .$

From the over-all mass and energy balance for the BWR pressure vessel the steam flow rate from the reactor is obtained as follows:

(5-182) $W_s = \dfrac{q_c - q_r + |N_p| + W_{cl}(i_{cr} - i_{cl})}{(i_s - i_{fw})} .$

It should be noted that this equation cannot be used to calculate the steam mass flow rate from the reactor, since the enthalpy of the cleaning water is not known. In simplified calculations, however, the term $W_{cl}(i_{cr} - i_{cl})$ is usually neglected. In addition, the pumping power and the heat losses are considered as approximately equal to each other, and the over-all energy balance yields the steam mass flow rate as follows,

(5-183) $W_s \cong \dfrac{q_c}{\left(i_s - i_{fw}\right)}$.

A more accurate method to predict the reactor equilibrium parameters is described in what follows. The return flow from steam-separators and dryers is obtained from Eq. (5-171) and the core exit enthalpy is found from Eq. (5-172) as,

(5-184) $i_{cex} = \dfrac{W_{sd} i_{sd} + W_s i_s}{W_c}$.

The core inlet enthalpy can be calculated from Eq. (5-177) as follows,

(5-185) $i_{cin} = i_{cex} - \dfrac{q_c}{W_c}$.

Finally, the mass flow rate from the downcomer to the lower plenum is found from Eq. (5-175) as,

(5-186) $W_{dc} = W_c - W_{cr}$,

and the enthalpy of coolant entering the lower plenum from the downcomer can be obtained from (5-176) as follows,

(5-187) $i_{dc} = \dfrac{W_c i_{cin} - W_{cr} i_{cr}}{W_{dc}}$.

Substituting Eqs. (5-184) through (5-187) into Eq. (5-182) yields,

(5-188) $W_s = \dfrac{W_c\left(q_c - q_r\right) + q_r W_{cl} + W_c\left(W_{cr} i_{cr} - W_{cl} i_{sd}\right) + \left|N_p\right|\left(W_c - W_{cl}\right)}{W_c\left(i_{fw} - i_s\right) + W_{cl}\left(i_{sd} - i_{fw}\right)}$.

Equation (5-188) gives an exact expression for calculation of the steam mass flow rate from the reactor pressure vessel in terms of parameters which are usually known or are the required operational set points, such as for example the mass flow rate through the core and the total thermal power of the reactor. Once the steam mass flow rate is calculated, other operational variables, such as the core inlet and outlet specific enthalpies, can be found.

 Figures below show the variation of selected performance parameters in function of the core total mass flow rate, assuming that all other parameters (such as e.g. the reactor power) are constant. This type of a BWR reactor operation is conducted at the end of a fuel cycle during the stretch-out period.

FIGURE 5-28 indicates that when increasing the coolant mass flow rate through the reactor core at a constant power, the mean coolant quality at the core exit decreases quite significantly. This means that the thermal margins are improved in the reactor. At

the same time, as results from FIGURE 5-29, the inlet coolant subcooling is decreasing as well.
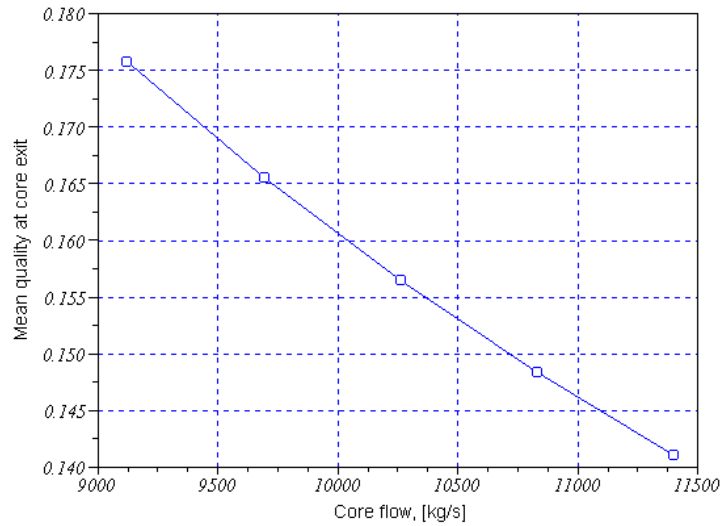
FIGURE 5-28. Mean quality at core exit as a function of core flow. Assumed data: p = 7 MPa, q_c = 3000 MWt, q_r = 0.1% q_c, $|N_p|$ = 3.23 MW, t_{fw} = 215 °C, W_{cr} = 65 kg/s, T_{cr} = 60 °C, F_{co} = 0.001, F_{cu} = 0.0025.
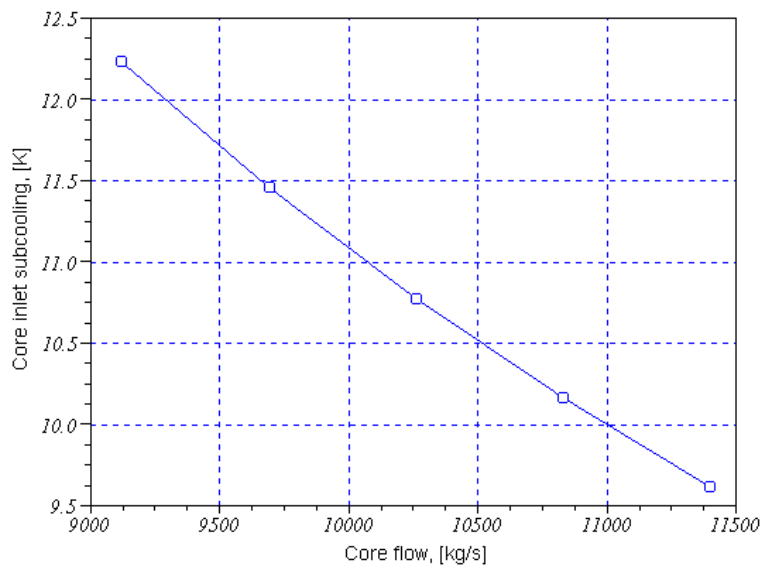
FIGURE 5-29. Core inlet subcooling as a function of core flow. Assumed data: p = 7 MPa, q_c = 3000 MWt, q_r = 0.1% q_c, $|N_p|$ = 3.23 MW, t_{fw} = 215 °C, W_{cr} = 65 kg/s, T_{cr} = 60 °C, F_{co} = 0.001, F_{cu} = 0.0025.
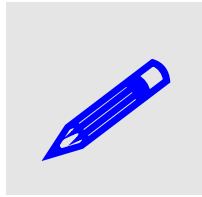
EXAMPLE 5-12. Calculate the mean coolant quality at the exit from the BWR core, the coolant subcooling at the core inlet and the steam flow rate from the pressure vessel at steady-state assuming the following data: $p = 7$ MPa, $q_c = 3000$ MWt, $q_r = 0.1\%$ q_c, $P_p = 3.23$ MW, $T_{fw} = 215$ °C, $W_{cr} = 65$ kg/s, $T_{cr} = 60$ °C, $F_{co} = 0.001$, $F_{cu} = 0.0025$ and $W_c = 11000$ kg/s. SOLUTION: for pressure $p = 7$ MPa, the saturation enthalpies for the liquid and vapour are 1267.4 kJ/kg and 2772.6 kJ/kg, respectively. The enthalpy of steam leaving the reactor pressure vessel is thus $1267.4*0.001+2772.6*0.999 = 2771.1$ kJ/kg. Feedwater enthalpy is found from tables as i(p=7 MPa, T=215°C) = 922.2 kJ/kg. In a similar manner, the enthalpy of water returning from the steam-separators and dryers is found as $1267.4*0.9975+2772.6*0.0025 = 1271.2$ kJ/kg. Substituting data to Eq. (5-188), the steam flow rate is obtained as $W_s = 1585.4$ kg/s. From Eq. (5-184) the core exit enthalpy is equal to 1487.4 kJ/kg, which corresponds to a thermodynamic equilibrium quality equal to 0.146. The enthalpy at the core inlet is obtained from Eq. (5-185) and is equal to 1214.4 kJ/kg. From the water property tables, the coolant temperature is found as T(p=7 MPa, i=1214.4 kJ/kg) = 275.8 °C which corresponds to 10 K inlet subcooling.

REFERENCES

[5-1]   Chaudhry, M.H., *Applied Hydraulic Transients*, 2nd edition, Van Nostrand Reinhold Company, New York, 1987.

[5-2]   Halliwell, A.R., "Velocity of a Waterhammer Wave in an Elastic Pipe," *J. Hydraulics Div. Am. Soc. Civil Engrs.*, vol. 89, No. HY4, pp. 1-21, 1963.

[5-3]   Khalak, A. and Williamson, C.H.K., "Motion, forces and model transitions in vortex induced vibrations at low mass damping," *J. Fluids Struct.*, vol. 13, pp. 813-851, 1999.

[5-4]   Liao, L-Y., "Study and application of boiling water reactor jet pump characteristics," *Nucl. Eng. Des.*, vol. 132, pp. 339-350, 1992.

[5-5]   Moody, F.J., *Introduction to Unsteady Thermofluid Mechanics*, John Wiley & Sons, New York, 1990.

[5-6]   White, F. M., *Viscous Fluid Flow*, McGraw-Hill Inc., 1991, ISBN 0-07-069712-4

EXERCISES

EXERCISE 5-1. Calculate the sound speed and the Mach number for an air stream flowing out from a tank with the velocity equal to a half of the maximum outflow velocity. The air temperature in the tank is equal to 150 °C.

EXERCISE 5-2. Calculate the mass flow rate of air flowing through the de Laval nozzle if the area of the outlet cross section is equal to $A_o = 10$ cm², the stagnation pressure $p_0 = 1.3 \cdot 10^5$ Pa, stagnation temperature $T_0 = 288$ K and the ambient pressure $p_a = 1.03 \cdot 10^5$ Pa.

EXERCISE 5-3. Compute the velocity of waterhammer waves in a 1 m diameter steel pipeline having a wall thickness of 25 mm if: (a) the pipeline is anchored at the upstream end, (b) the pipeline has expansion joints throughout its length.

EXERCISE 5-4. A long wire is hanging in an open air. Calculate the frequency of the vortex detachment from the wire if the wind is blowing with velocity 15 m/s in the direction perpendicular to the wire length. The wire diameter is 5 mm and the air temperature is 0 °C.

EXERCISE 5-5. Calculate and plot the amplitude of oscillations of a pipeline with $D = 1$ m and $\omega_0 = 15.7$ rad/sec as a function of wind speed U.

Appendix A – Selected Constants and Data

Constants:

NAME	VALUE
Universal ideal gas constant	$B = 8.31447$ J/mol.K
Boltzman's constant	$k = B/N_A = 1.38065 \cdot 10^{-23}$ J/K
Planck's constant	$h = 6.62461 \cdot 10^{-34}$ J/K
Speed of light in vacuum	$c = 2.99792 \cdot 10^8$ m/s
Avogadro's number	$N_A = 6.02214 \cdot 10^{23}$ 1/mol
Stefan-Boltzmann constant	$\sigma = 5.67040 \cdot 10^{-8}$ W/m^2.K^4
Molar volume of an ideal gas (T=273.15 K, p = 101325 Pa)	$V_m = 22.4140 \cdot 10^{-3}$ m^3/mol
Wien displacement law constant	$b = 2.89777 \cdot 10^{-3}$ m.K
Standard acceleration	$g = 9.80665$ m/s^2

Data of selected gases:

Gas	Molar mass, M, [kg/mol]	Specific gas constant, R, [J/kg.K]	Specific heat, c_p at 273.15 K, [J/kg.K]	$\kappa = \dfrac{c_p}{c_v}$
Air	28.96	287	1022.7	1.40
CO_2	44.01	189	825	1.30
H_2	2.0156	4121.8	14235	1.41

H$_2$O (vapour)	18	462	5354[1]	1.33
He	4.002	2079	5234	1.66
N$_2$	28.016	296.7	1043	1.40
O$_2$	32	259.8	913	1.4

[1] At 7 MPa and saturation condition

Appendix B – Selected Special Functions

The **Bessel differential equation** is given as follows:

$$x^2 \frac{d^2 y}{dx^2} + x \frac{dy}{dx} + \left(x^2 - n^2\right)y = 0, \quad n \geq 0. \tag{B-1}$$

A general solution of this equation can be found as,

$$y(x) = C_1 J_n(x) + C_2 Y_n(x) \quad , \tag{B-2}$$

where $J_n(x)$ is the **Bessel function of the first kind** and n-th order:

$$J_n(x) = \left(\frac{x}{2}\right)^n \sum_{k=1}^{\infty} \frac{(-1)^k \left(\frac{x}{2}\right)^{2k}}{k!\,(n+k)!} \quad , \tag{B-3}$$

and $Y_n(x)$ is the **Bessel function of the second kind** (called also the Neumann function) and n-th order, given as,

$$Y_n(x) = \frac{J_n(x)\cos n\pi - J_{-n}(x)}{\sin n\pi} \quad . \tag{B-4}$$

For small x, the functions have asymptotic values described as follows:

$$J_n(x) \approx \frac{1}{2^n n!} x^n, \qquad Y_n(x) \approx 2^{n-1}(n-1)!\,x^{-n}, \quad n \neq 0. \tag{B-5}$$

In particular,

$$Y_0(x) \cong \frac{2}{\pi}\left(\ln x - 0.11593\right), \qquad Y_1(x) \cong \frac{2}{\pi x}. \tag{B-5a}$$

Useful expansions of Bessel functions valid for small x are as follows:

$$J_0(x) = 1 - \frac{x^2}{2^2 (1!)^2} + \frac{x^4}{2^4 (2!)^2} - \frac{x^6}{2^6 (3!)^2} + \ldots, \tag{B-5b}$$

$$J_1(x) = \frac{x}{2 \cdot 0! \cdot 1!} - \frac{x^3}{2^3 \cdot 1! \cdot 2!} + \frac{x^5}{2^5 \cdot 2! \cdot 3!} - \dots \qquad \text{(B-5c)}$$

For large x the functions are approximately described with:

$$J_n(x) \approx \sqrt{\frac{2}{\pi x}} \cos\left(x - \frac{\pi}{4} - \frac{n\pi}{2}\right), \quad Y_n(x) = \sqrt{\frac{\pi}{2x}} e^{-x} \quad . \qquad \text{(B-6)}$$

In particular, for $x > 15$ the following approximations are valid:

$$J_0(x) \approx \sqrt{\frac{2}{\pi x}}\left[\cos\left(x - \frac{\pi}{4}\right) + \frac{1}{8x}\sin\left(x - \frac{\pi}{4}\right)\right], \text{ error} < 0.0001 \qquad \text{(B-6a)}$$

$$J_1(x) \approx \sqrt{\frac{2}{\pi x}}\left[\sin\left(x - \frac{3\pi}{4}\right) - \frac{3}{8x}\cos\left(x - \frac{3\pi}{4}\right)\right], \text{ error} < 0.0001 \qquad \text{(B-6b)}$$

Derivatives of the Bessel functions of the first and second kind are calculated as follows,

$$\frac{dZ_n(\alpha x)}{dx} = \alpha Z_{n-1}(\alpha x) - \frac{n}{x}Z_n(\alpha x), \quad Z = J, Y \qquad . \qquad \text{(B-7)}$$

In particular,

$$\frac{dJ_0(\alpha x)}{dx} = -\alpha J_1(\alpha x), \quad \frac{dY_0(\alpha x)}{dx} = -\alpha Y_1(\alpha x). \qquad \text{(B-7a)}$$

Selected useful integrals of the Bessel functions are as follows,

$$\int xZ_0(x)dx = xZ_1(x) + C, \quad \int Z_1(x)dx = -Z_0(x) + C. \qquad \text{(B-8)}$$

In particular,

$$\int xJ_0(\alpha x)dx = \frac{x}{\alpha}J_1(\alpha x) + C, \quad \int xY_0(\alpha x)dx = \frac{x}{\alpha}Y_1(\alpha x) + C. \qquad \text{(B-8a)}$$

The plots of the Bessel function of the first and second kind and of the zero and first order ($n = 0$ and $n = 1$) are shown in Figures B-1 and B-2 below.

FIGURE B-1. Bessel functions of the first kind $J_0(x)$ and $J_1(x)$.

Zeros of $J_0(x)$:

$x_1 = 2.4048$, $x_2 = 5.5201$, $x_3 = 8.6537$, $x_4 = 11.7915$, $x_5 = 14.9309$.

Zeros of $J_1(x)$:

$x_1 = 3.8317$, $x_2 = 7.0156$, $x_3 = 10.1735$, $x_4 = 13.3237$, $x_5 = 16.4706$.
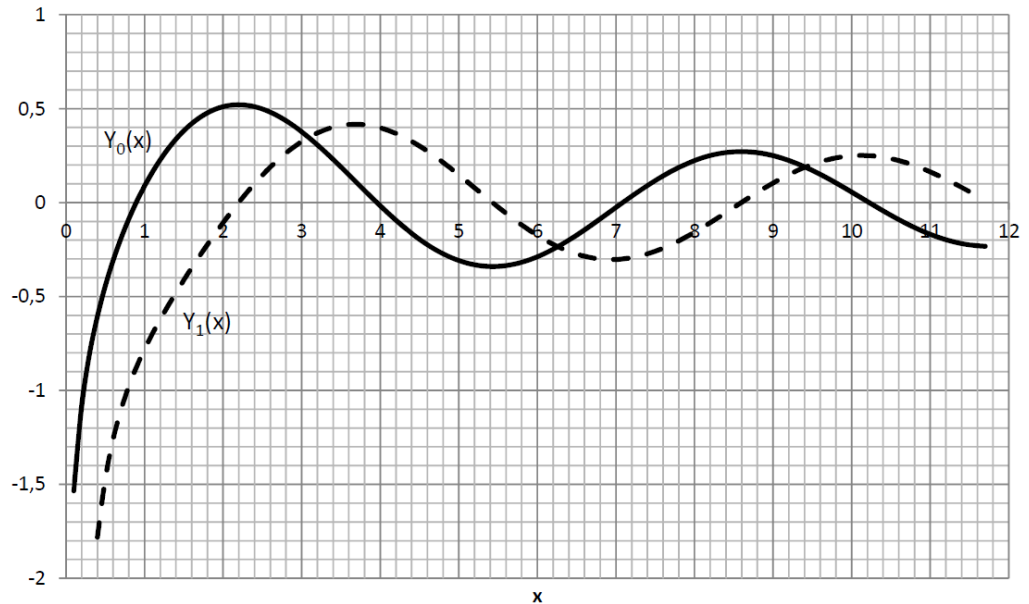
FIGURE B-2. Bessel functions of the second kind $Y_0(x)$ and $Y_1(x)$.

Zeros of $Y_0(x)$:

$x_1 = 0.8936$, $x_2 = 3.9577$, $x_3 = 7.0861$, $x_4 = 10.2223$, $x_5 = 13.3611$.

<u>Zeros of $Y_1(x)$:</u>

$x_1 = 2.1971$, $x_2 = 5.4297$, $x_3 = 8.5960$, $x_4 = 11.7492$, $x_5 = 14.8974$.

The **modified Bessel differential equation** is given as:

$$x^2 \frac{d^2 y}{dx^2} + x \frac{dy}{dx} - \left(x^2 + n^2 \right) y = 0, \quad n \geq 0. \tag{B-9}$$

A general solution of this equation is as follows,

$$y(x) = C_1' I_n(x) + C_2' K_n(x) \quad, \tag{B-10}$$

where $I_n(x)$ is the **modified Bessel function of the first kind** and n-th order:

$$I_n(x) = i^{-n} J_n(ix) = i^n J_n(-ix) \quad, \tag{B-11}$$

and $K_n(x)$ is the **modified Bessel function of the second kind** (called also the modified Henkel function) and n-th order:

$$K_n(x) = \frac{\pi}{2} i^{n+1} \left[J_n(ix) + i Y_n(ix) \right]. \tag{B-12}$$

$I_n(x)$ and $K_n(x)$ are real monotonic functions for $n = 0, \pm 1, \pm 2, \ldots$ and real x.

Expansions of the modified Bessel functions of the first kind valid for small x are as follows:

$$I_0(x) = 1 + \frac{x^2}{2^2 (1!)^2} + \frac{x^4}{2^4 (2!)^2} + \frac{x^6}{2^6 (3!)^2} + \ldots \quad, \tag{B-11a}$$

$$I_1(x) = \frac{x}{2 \cdot 0! \, 1!} + \frac{x^3}{2^3 \cdot 1! \, 2!} + \frac{x^5}{2^5 \cdot 2! \, 3!} + \ldots \quad. \tag{B-11b}$$

Asymptotic approximations of the modified Bessel functions of the second kind valid for small x are given as:

$$K_0(x) \cong -\left(\ln x - 0.11593 \right), \tag{B-12a}$$

$$K_1(x) \cong \frac{1}{x} \quad. \tag{B-12b}$$

Asymptotic expansions of the modified Bessel functions valid for large x are as follows:

$$I_0(x) = \frac{e^x}{\sqrt{2\pi x}} \left(1 + \frac{1}{8x} + \ldots \right) \quad, \tag{B-11c}$$

$$I_1(x) = \frac{e^x}{\sqrt{2\pi x}}\left(1 - \frac{3}{8x} + \ldots\right) \quad , \tag{B-11d}$$

$$K_0(x) = \sqrt{\frac{\pi}{2x}}\, e^{-x}\left(1 - \frac{1}{8x} + \ldots\right), \tag{B-12c}$$

$$K_1(x) = \sqrt{\frac{\pi}{2x}}\, e^{-x}\left(1 + \frac{3}{8x} + \ldots\right). \tag{B-12d}$$

Derivatives of the modified Bessel functions of the first and second kind are calculated as,

$$\frac{dI_0(\alpha x)}{dx} = \alpha I_1(\alpha x), \qquad \frac{dK_0(\alpha x)}{dx} = -\alpha K_1(\alpha x). \tag{B-13}$$

Selected useful integrals of the modified Bessel functions are as follows:

$$\int x I_0(\alpha x)\,dx = \frac{x}{\alpha} I_1(\alpha x) + C, \quad \int x K_0(\alpha x)\,dx = -\frac{x}{\alpha} K_1(\alpha x) + C. \tag{B-14}$$

The plots of the modified Bessel function of the first and second kind and of the zero and first order ($n = 0$ and $n = 1$) are shown in Figures B-3 and B-4 below.
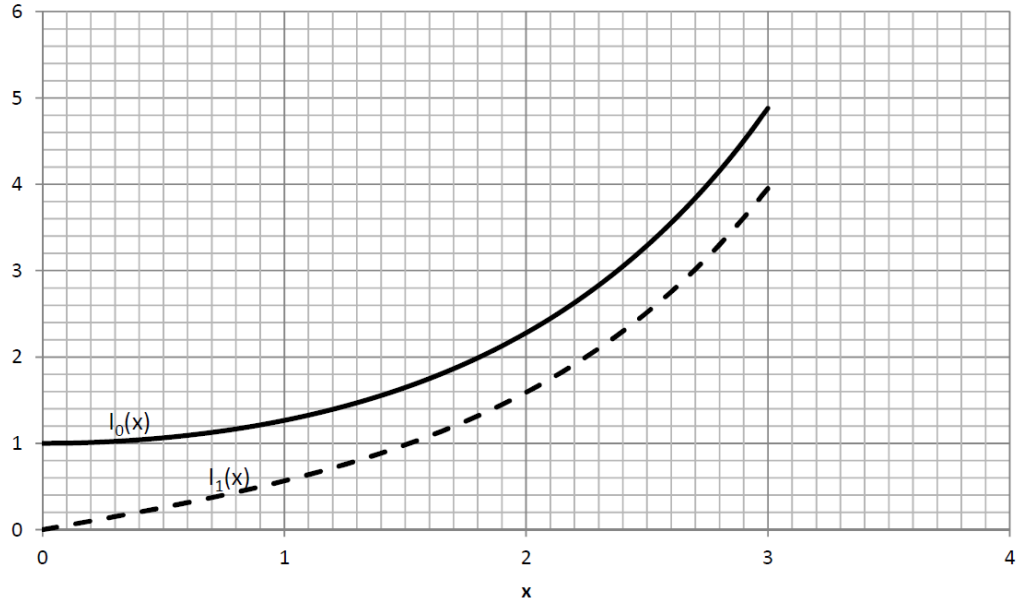
FIGURE B-3. Modified Bessel functions of the first kind $I_0(x)$ and $I_1(x)$.
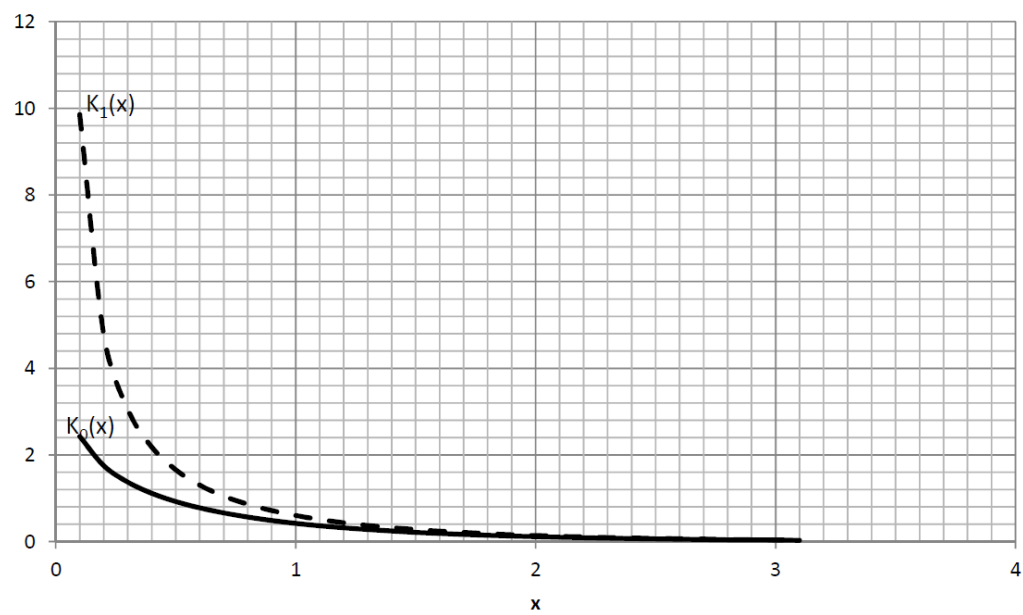
FIGURE B-4. Modified Bessel functions of the second kind $K_0(x)$ and $K_1(x)$.

Appendix C – Dimensionless Numbers

DIMENSIONLESS GROUP	DEFINITION
Biot number	$\mathrm{Bi} = \dfrac{hL}{\lambda_s}$
Fourier number	$\mathrm{Fo} = \dfrac{at}{L^2}$
Grashof number	$\mathrm{Gr} = \dfrac{g\beta\Delta T H^3}{\nu^2}$
Mach number	$\mathrm{Ma} = \dfrac{U}{c}$
Nusselt number	$\mathrm{Nu} = \dfrac{hL}{\lambda_f}$
Péclet number	$\mathrm{Pe} = \dfrac{UL}{a} = \mathrm{Pr}\cdot\mathrm{Re}$
Prandtl number	$\mathrm{Pr} = \dfrac{\nu}{a} = \dfrac{\mu c_p}{\lambda_f}$
Reynolds number	$\mathrm{Re} = \dfrac{UL}{\nu}$
Stanton number	$\mathrm{St} = \dfrac{h}{\rho c_p U} = \dfrac{\mathrm{Nu}}{\mathrm{Re}\cdot\mathrm{Pr}}$

L – characteristic length, H – characteristic height, U – velocity, a – diffusivity, t – time, c_p – specific heat, h – heat transfer coefficient, ρ - density, λ - thermal conductivity, ν - kinematic viscosity, β - thermal expansion coefficient.

Subscripts: $()_f$ – fluid, $()_s$ – solid.

Appendix D - Selected Steam-Water Data

Steam-water properties at saturation for pressure p = 7 MPa (t_{sat} = 285.83 °C)

Phase	Density	Viscosity	Enthalpy	Conductivity	Spec. heat
	[kg m^{-3}]	[Pa s]	[J kg^{-1}]	[W m^{-1} K^{-1}]	[J kg^{-1} K^{-1}]
Water	739.724	9.12488 10^{-5}	1267660	0.571881	5402.48
Steam	36.525	1.89601 10^{-5}	2772630	0.0629146	5356.59

Steam-water properties at saturation for pressure p = 15.5 MPa (t_{sat} = 344.79 °C)

Phase	Density	Viscosity	Enthalpy	Conductivity	Spec. heat
	[kg m^{-3}]	[Pa s]	[J kg^{-1}]	[W m^{-1} K^{-1}]	[J kg^{-1} K^{-1}]
Water	594.38	6.83274 10^{-5}	1629880	0.458470	8949.98
Steam	101.93	2.31084 10^{-5}	2596120	0.121361	14000.6

Steam-water properties can be calculated with the following Scilab functions, based on XSteam functions (www.x-eng.com) and available for download from http://www.sh2701.blogspot.se. The Scilab software can be obtained freely from http://www.scilab.org.

FUNCTION DESCRIPTION	**CALL SYNTAX**
Thermal conductivity of saturated water, [W/m.K]	conlsat(p)
Thermal conductivity of saturated vapour, [W/m.K]	convsat(p)
Specific heat of saturated water, [J/kg.K]	cplsat(p)
Specific heat of saturated vapour, [J/kg.K]	cpvsat(p)

Thermal conductivity of subcooled water, [W/m.K]	`conliq(p,T)`
Thermal conductivity of superheated vapour, [W/m.K]	`convap(p,T)`
Specific heat of subcooled water, [J/kg.K]	`cpliq(p,T)`
Specific heat of superheated vapour, [J/kg.K]	`cpvap(p,T)`
Latent heat, [J/kg]	`hfg(p)`
Specific enthalpy of saturated water, [J/kg]	`hlsat(p)`
Specific enthalpy of saturated vapour, [J/kg]	`hvsat(p)`
Specific enthalpy of subcooled water, [J/kg]	`hliq(p,T)`
Specific enthalpy of superheated vapour, [J/kg]	`hvap(p,T)`
Density of saturated water, [kg/m^3]	`rholsat(p)`
Density of saturated vapour, [kg/m^3]	`rhovsat(p)`
Density of subcooled water, [kg/m^3]	`rholiq(p,T)`
Density of superheated vapour, [kg/m^3]	`rhovap(p,T)`
Dynamic viscosity of saturated water, [Pa.s]	`vislsat(p)`
Dynamic viscosity of saturated vapour, [Pa.s]	`visvsat(p)`
Dynamic viscosity of subcooled water, [Pa.s]	`visliq(p,T)`
Dynamic viscosity of superheated vapour, [Pa.s]	`visvap(p,T)`
Surface tension, [N/m]	`surften(p)`
Saturated temperature, [°C]	`tsat(p)`
Saturated pressure, [bar]	`psat(T)`

p – pressure [bar], T – temperature [°C].

Appendix E – Scilab Thermal-Hydraulic Library

Thermal-hydraulic calculations can be performed with the following Scilab functions, available for download from http://www.sh2701.blogspot.se. The Scilab software can be obtained freely from http://www.scilab.org.

FUNCTION DESCRIPTION	CALL FORMATS

Fanning friction factor using the Blasius correlation.
 	
 Two calling formats are available, with the following input parameters:
 	
 Re – Reynolds number
 	
 or:
 	
 G – mass flux, [kg/m^2.s]
 	
 Dh – hydraulic diameter, [m]
 	
 vis – dynamic viscosity, [Pa.s]
	`Cf_Blasius(Re)`
	
	 `Cf_Blasius(G,Dh,vis)`

Fanning friction factor using the Filonenko correlation.
 	
 Two calling formats are available, with the following input parameters:
 	
 Re – Reynolds number
 	
 or:
 	
 G – mass flux, [kg/m^2.s]
 	
 Dh – hydraulic diameter, [m]
 	
 vis – dynamic viscosity, [Pa.s]
	`Cf_Filonenko(Re)`
	
	 `Cf_Filonenko(G,Dh,vis)`

Fanning friction factor using the Haaland correlation.
 	
Two calling formats are available, with the following input parameters:
 	
Re – Reynolds number
 	
or:
 	
G – mass flux, [kg/m^2.s]
 	
Dh – hydraulic diameter, [m]
 	
vis – dynamic viscosity, [Pa.s]
	`Cf_Haaland(Re)`
	
	`Cf_ Haaland (G,Dh,vis)`

Heat transfer coefficient using the Dittus-Boelter correlation.
 	
Two calling formats are available, with the following input parameters:
 	
Re – Reynolds number
 	
Pr – Prandtl number
 	
or:
 	
G – mass flux, [kg/m^2.s]
 	
Dh – hydraulic diameter, [m]
 	
vis – dynamic viscosity, [Pa.s]
 	
con – thermal conductivity, [W/m.K]
 	
cp – specific heat, [J/kg.K]
	`Nu=HTC_DittusBoelter(Re, Pr)`
	
	`htc=HTC_DittusBoelter(G, Dh,vis,con,cp)`
	
	Nu – Nusselt number
	
	htc – heat transfer coefficient, [W/m^2.K]

Heat transfer coefficient using the Chen correlation. One calling format is available, with the following input parameters: G – mass flux, [kg/m^2.s] q2p – heat flux, [W/m^2] p – pressure, [bar] x – equilibrium quality	`htc=HTC_Chen(G,q2p,p,x, Dh)` htc – heat transfer coefficient, [W/m^2.K]

Dh – hydraulic diameter, [m]	

Heat transfer coefficient using the Gnielinski correlation.
 	
Two calling formats are available, with the following input parameters:
 	
Re – Reynolds number
 	
Pr – Prandtl number
 	
Cf – Fanning friction factor
 	
or:
 	
G – mass flux, [kg/m^2.s]
 	
Dh – hydraulic diameter, [m]
 	
vis – dynamic viscosity, [Pa.s]
 	
con – thermal conductivity, [W/m.K]
 	
cp – specific heat, [J/kg.K]
 	
Cf – fanning friction factor
	`Nu=HTC_Gnielinski(Re,`
	`Pr,Cf)`
	
	`htc=HTC_Gnielinski(G,`
	`Dh,vis,con,cp,Cf)`
	
	Nu – Nusselt number
	
	htc – heat transfer coefficient, [W/m^2.K]

Heat transfer coefficient using the Jackson correlation.
 	
Two calling formats are available, with the following input parameters:
 	
Re – Reynolds number
 	
Pr – Prandtl number
 	
cp – bulk specific heat, [J/kg.K]
 	
rho – bulk density, [kg/m^3]
 	
h – bulk enthalpy, [J/kg]
 	
t – bulk temperature, [°C]
 	
tw – wall temperature, [°C]
 	
p – pressure, [bar]
 	
or:
	`Nu=HTC_Jackson(Re,`
	`Pr,cp,rho,h,t,tw,p)`
	
	`htc=HTC_Jackson(G,`
	`Dh,vis,con,cp,rho,h,t,tw,`
	`p)`
	
	Nu – Nusselt number
	
	htc – heat transfer coefficient, [W/m^2.K]

G – mass flux, [kg/m².s] Dh – hydraulic diameter, [m] vis – dynamic viscosity, [Pa.s] con – thermal conductivity, [W/m.K] The rest of the parameters have the same meaning as in the first call format.	

Heat transfer coefficient using the Petukhov-Kirillov correlation.
 	
Two calling formats are available, with the following input parameters:
 	
Re – Reynolds number
 	
Pr – Prandtl number
 	
Cf – Fanning friction factor
 	
or:
 	
G – mass flux, [kg/m².s]
 	
Dh – hydraulic diameter, [m]
 	
vis – dynamic viscosity, [Pa.s]
 	
con – thermal conductivity, [W/m.K]
 	
cp – specific heat, [J/kg.K]
	`Nu = HTC_PetukhovKirillov(Re, Pr, Cf)`
	
	`htc=HTC_PetukhovKirillov( G, Dh,vis,con,cp,)`
	
	Nu – Nusselt number
	
	htc – heat transfer coefficient, [W/m².K]

Wall temperature in subcooled boiling using the Jens-Lottes correlation.
 	
Two calling formats are available, with the following input parameter:
 	
q2p – wall heat flux, [W/m²]
 	
p – pressure, [bar]
 	
or:
 	
q2p – wall heat flux, [W/m²]
 	
p – pressure, [bar]
 	
Tsat – saturation temperature, [°C]
	`Tw = TW_JensLottes(q2p,p)`
	
	`Tw = TW_JensLottes(q2p,p,Tsat)`

Wall temperature in subcooled boiling using the Thom correlation.
 	
Two calling formats are available, with the following input parameter:
 	
q2p – wall heat flux, $[W/m^2]$
 	
p – pressure, [bar]
 	
or:
 	
q2p – wall heat flux, $[W/m^2]$
 	
p – pressure, [bar]
 	
Tsat – saturation temperature, [°C]
	`Tw = TW_Thom(q2p,p)`
	
	`Tw = TW_Thom(q2p,p,Tsat)`

Specific enthalpy distribution in a heated channel. Input parameters: z – axial coordinate, [m] Axs – channel cross-section area at z-locations, $[m^2]$ Ph – heated perimeter, [m] hin – inlet specific enthalpy, [J/kg] G – mass flux, $[kg/m^2.s]$ q2p – heat flux, $[W/m^2]$	`h=EnergyEquation1D(z,Axs, Ph,hin,G,q2p)` h – specific enthalpy distribution in channel
Pressure distribution in a channel. Input parameters: z – axial coordinate, [m] Dh – channel hydraulic diameter, [m] G – mass flux, $[kg/m^2.s]$ pin – inlet pressure, [Pa] rho – bulk fluid density, $[kg/m^3]$ vis – bulk fluid dynamic viscosity, [Pa.s]	`[p]=MomentumEquation1D(z, Dh,G,pin,rho,vis,Cf,gvec)` p – pressure distribution in a channel, [Pa]

Cf – Fanning friction factor gvec – gravity vector projected on the channel axis, [m/s^2]	
Pressure and specific enthalpy distribution in a heated channel with single-phase flow. Input parameters: z – axial coordinate, [m] Axs – channel cross-section area, [m^2] Pw – wetted perimeter, [m] Ph – heated perimeter, [m] pin – inlet pressure, [Pa] Gin – inlet mass flux, [kg/m^2.s] tin – inlet temperature, [°C] twin – wall temperature at inlet, [°C] q2p – heat flux, [W/m^2] gvec – gravity vector projected on the channel axis, [m/s^2] htc_opt – heat transfer coefficient option ; string ('DittusBoelter', or 'PetukhovKirillov', or 'Jackson') Cf_opt – friction factor option; string ('Haaland' or 'Blasius')	`[h,p]=ChannelSolver(z,Axs,Pw,Ph,pin,Gin,tin,twin,q2p,gvec,htc_opt,Cf_opt)` `h` – specific enthalpy `p` – pressure distribution in a channel, [Pa]

INDEX

.